

Characterization of the Anti-inflammatory Activity of Enones Based on the Evaluation of Their Heme Oxygenase-1 and Inducible NO Synthase Activity

Dissertation

zur Erlangung des Doktorgrades der Naturwissenschaften

Dr. rer. nat.

an der Fakultät der Chemie und Pharmazie

der Universität Regensburg



vorgelegt von

Hannelore-Maria Rücker

aus

Timisoara, Rumänien

Regensburg 2014

Promotionsgesuch eingereicht am: 05.03.2014

Diese Arbeit wurde angeleitet von PD Dr. Sabine Amslinger.

Content

1	Introduction	1
1.1	α,β-Unsaturated carbonyl compounds and inflammation.....	1
1.2	Heme oxygenase-1 (HO-1)	5
1.2.1	Activity and induction of HO-1	5
1.2.2	HO-1 as therapeutic target.....	6
1.2.3	Techniques for measuring HO-1 activity.....	6
1.2.4	Development of a HO-1 activity assay	8
1.3	The activity of inducible nitric oxide synthase (iNOS)	11
1.3.1	The nitrite (Griess) assay.....	12
1.4	The oxygen radical absorbance capacity-(ORAC)-fluorescein assay	12
1.5	Anti-inflammatory activity of a diverse group of α,β-unsaturated carbonyl compounds and polyphenols.....	14
1.6	Reactivity and biological activity of natural and synthetic chalcones.....	18
1.6.1	Reactivity of chalcones.....	18
1.6.2	Reactivity assessment of chalcones by a kinetic thiol assay	20
1.6.3	Biological activity of chalcones.....	20
1.7	α-X-Modified enones as a different approach in fine-tuning their Michael acceptor reactivity and biological activity	23
1.7.1	α -X-Modification in 2',3,4,4'-tetramethoxychalcones (α -X-TMCHs).....	23
1.7.2	Limno-CP and its α -X-Limno-CP derivatives	25
1.8	The anti-inflammatory activity of both enantiomers of arteludovicinolide A	26
1.9	Enzyme-triggered CO-releasing molecules (ET-CORMs)	27
1.10	Aim of this study	29
2	Materials and Methods.....	30
2.1	Materials.....	30
2.1.1	Cell lines.....	30
2.1.2	Cell culture media, buffers and reagents for cell culture.....	30

2.1.3	Antibodies, proteins and enzymes	31
2.1.4	Kits.....	31
2.1.5	Chemicals and reagents	31
2.1.6	Synthesis of compounds.....	33
2.1.7	Buffers and solutions.....	34
2.1.8	Equipment.....	37
2.1.9	Consumables	39
2.2	Methods.....	40
2.2.1	Cell culture	40
2.2.2	Dilution of test compounds	40
2.2.3	Viability assay (MTT assay)	41
2.2.4	Viability assay with lipopolysaccharide (MTT-LPS assay)	42
2.2.5	Nitrite assay (Griess assay).....	43
2.2.6	Activity assay for heme oxygenase-1 (HO-1)	44
2.2.7	Western blot analysis	51
2.2.8	ORAC-fluorescein assay	53
2.2.9	Statistical analysis.....	54
3	Results and Discussion.....	55
3.1	Heme oxygenase-1 (HO-1) activity assay	55
3.1.1	Development and optimization of the HO-1 activity assay.....	55
3.1.2	Time course of HO-1 protein expression and HO-1 activity in RAW264.7 macrophages exposed to chalcone DHDMCH.....	65
3.1.3	Inhibition of HO-1 activity in DHDMCH or LPS stimulated RAW264.7 macrophages by SnPPIX.....	68
3.1.4	Heme oxygenase-1 activity in human dendritic cells (DC)	69
3.2	Screening of natural products and drugs towards their HO-1 activity in RAW264.7 macrophages	71
3.2.1	Influence of natural products and drugs on the viability of RAW264.7 macrophages	71

3.2.2	Effect of natural products as well as the two drugs oltipraz and dexamethasone on HO-1 activity in RAW264.7 macrophages.....	73
3.2.3	Effect of natural products and dexamethasone on the HO-1 protein expression in RAW264.7 macrophages.....	77
3.3	Characterization of chalcones towards their anti-inflammatory, antioxidative and cytoprotective activity.....	79
3.3.1	Effect of chalcones on the viability of RAW264.7 macrophages.....	79
3.3.2	Influence of chalcones on HO-1 activity and HO-1 protein expression	81
3.3.3	Effect of chalcones on nitrite production	84
3.3.4	Antioxidant capacity of chalcones.....	86
3.3.5	Structure-activity relationship (SAR) of hydroxy- and methoxychalcones	88
3.4	Characterization of α-X-TMCHs towards their anti-inflammatory, antioxidative and cytoprotective activity	92
3.4.1	Effect of α -X-TMCHs on the viability of RAW264.7 macrophages	92
3.4.2	Influence of α -X-TMCHs on HO-1 activity and HO-1 protein expression.....	95
3.4.3	Effect of α -X-TMCHs on nitrite production.....	97
3.4.4	Conclusion.....	100
3.5	Characterization of α-X-Limno-CP derivatives (5-aryl-3(2<i>H</i>)-furanones) towards their anti-inflammatory and antioxidative activity.....	102
3.5.1	Effect of α -X-Limno-CPs on cell viability and nitrite production of RAW264.7 macrophages	102
3.5.2	Antioxidant capacity of α -X-Limno-CPs	105
3.5.3	Conclusion.....	106
3.6	Characterization of both enantiomers of arteludovicinolide A towards their anti-inflammatory activity.....	108
3.6.1	Influence on the viability and nitrite production of RAW264.7 macrophages.....	108
3.6.2	Influence of both enantiomers of arteludovicinolide A on the heme oxygenase-1 (HO-1) activity in murine macrophages RAW264.7	109
3.6.3	Summary.....	110
3.7	The anti-inflammatory activity of iron dienylphosphate tricarbonyl complexes as enzyme-triggered CO-releasing molecules (ET-CORMs)	111

3.8	Characterization of further compounds towards their cytotoxic, antioxidative and anti-inflammatory activity.....	116
3.8.1	Cytotoxic activity of two γ -butyrolactone derivatives on the human colon cancer cell line HT-29.....	116
3.8.2	Biological activity of different sesquiterpene lactone derivatives, γ -butyrolactones and 4-substituted cyclopentenones	116
3.8.3	Biological activity of chalcone-analogs	121
4	Summary.....	122
5	References.....	125

ABBREVIATIONS

2'-HOC	2'-Hydroxychalcone
AAPH	2,2'-Azobis(2-methylpropionamidine) dihydrochloride
AP-1	Activator protein 1
APS	Ammonium persulfate
ARE	Antioxidant response element
AUC	Area under curve
BARD	Bardoxolone methyl
BR	Bilirubin
BSA	Bovine serum albumin
BV	Biliverdin
BVR	Biliverdin reductase
CDDO	2-Cyano-3,12-dioxooleana-1,9(11)-dien-28-oic acid, bardoxolone
CH	Chalcone, (1,3-diphenylprop-2-en-1-one)
CO	Carbon monoxide
CORMs	CO releasing molecules
COX	Cyclooxygenase
DC	Dendritic cells
DHDMCH	2',4'-Dihydroxy-3,4-dimethoxychalcone
DMEM	Dulbecco's modified eagle's medium
DMSO	Dimethyl sulfoxide
DPPH	2,2-Diphenyl-1-picrylhydrazyl
EDTA	Ethylenediaminetetraacetic acid
ELISA	Enzyme-linked immunosorbent assay
eNOS	Endothelial NO-synthase
ET-CORMs	Enzyme-triggered CO-releasing molecules
FCS	Fetal calf serum

GSH	Glutathione
GST	Glutathione S-transferase
HEI-OC1 cells	House ear institute-organ of corti 1 cells
HO	Heme oxygenase
HPLC	High performance liquid chromatography
HTMCH	2'-Hydroxy-3,4',4-trimethoxychalcone
HUVEC	Human umbilical vein endothelial cells
ICAM-1	Intercellular adhesion molecule-1
IFN- γ	Interferon- γ
IKK	I κ B kinase
IL	Interleukin
iNOS	Inducible NO-synthase
IP-10	Interferon γ -induced protein 10
ISL	Isoliquiritigenin
I κ B	Inhibitor of NF- κ B
Keap1	Kelch-like ECH-associated protein 1
LC-MS	Liquid chromatography–mass spectrometry
LPS	Lipopolysaccharide
MA	Michael acceptor
MAPK	Mitogen-activated protein kinase
MCE	Monocyclic cyanoenone
MTT	3-[4,5-Dimethylthiazol-2-yl]-2,5-diphenyl-tetrazoliumbromide
NADPH	β -Nicotinamide adenine dinucleotide phosphate
NEA	Non essential amino acid
NED	N-(1-naphthyl)ethylenediamine
Nfr2	Nuclear factor erythroid 2 related factor 2
NF- κ B	Nuclear factor κ B

nNOS	Neuronal NO-synthase
NO	Nitric oxide
NQO1	NAD(P)H:quinine oxidoreductase 1
ns	Not significant
OPD	<i>ortho</i> -Phenylenediamine dihydrochloride
ORAC	Oxygen radical absorbance capacity
PBS	Phosphate buffered saline
PEGF	Platelet-derived growth factor
ROS	Reactive oxygen species
RP-HPLC	Reversed phase high performance liquid chromatography
rpm	Revolutions per minute
RPMI 1640 medium	Roswell Park Memorial Institute 1640 medium
RT	Room temperature
RTQ-PCR	Real-time quantitative polymerase chain reaction
SAR	Structure-activity relationship
SDS	Sodium dodecyl sulfate
SERS	Surface enhanced Raman scattering
TEMED	N,N,N',N'-Tetramethylethylenediamine
TGF-1 β	Transforming growth factor-1 β
THMCH	2',3,4'-Trihydroxy-4-methoxychalcone
TMCH	2',3,4,4'-Tetramethoxychalcone
TNF- α	Tumor necrosis factor- α
T-PBS	Tween 20-phosphate buffered saline
TRIS	Tris(hydroxymethyl)aminomethane
VEGF	Vascular endothelial growth factor

1 Introduction

1.1 α,β -Unsaturated carbonyl compounds and inflammation

α,β -Unsaturated carbonyl compounds possessing a Michael acceptor functionality represent a prominent class of biologically and pharmacologically active electrophiles amongst the vast number of electrophilic compounds with numerous biological targets.¹ Of great importance are thiol-regulated signal transduction pathways essential for the cellular redox homeostasis and cell protection. Especially under pathological conditions involving chronic inflammation, atherosclerosis, diabetes, liver, lung and brain injury, kidney disease and cancer, these particular redox-sensitive and cytoprotective signaling cascades are promising targets of therapeutic drugs.² Already in the late 1980's Talalay *et al.* reported that the beneficial biological activity of chemoprotective agents is directly connected to their Michael acceptor activity.³ On one hand, α,β -unsaturated carbonyl compounds possess a distinct Michael acceptor reactivity by which they can react with nucleophilic sulfhydryl groups of sensor cysteins on key signaling proteins. On the other hand the α,β -unsaturated carbonyl moiety itself as well as additional groups, i.e. phenolic hydroxyls can react as radical scavengers or antioxidants due to their pronounced reduction potential (Figure 1).⁴

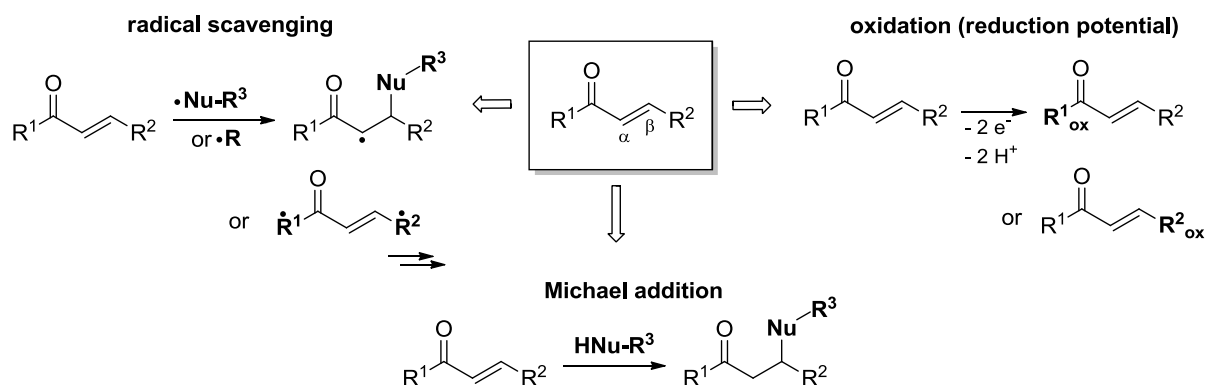


Figure 1. Reactivities of α,β -unsaturated carbonyl compounds.

The electrophilic nature of the α,β -unsaturated carbonyl unit enables many natural products, which possess this functionality to act as powerful antioxidant, anti-inflammatory, neurochemoprotective and cancer chemopreventive agents. A high drug design potential emerges from the class of Michael acceptors because they can selectively address certain cellular targets in fairly complex signaling pathways, due to a distinct and moderate electrophilic behavior. Prominent α,β -unsaturated compounds, where their Michael acceptor reactivity was shown to be closely related to their biological potency, comprise phytochemicals such as the food polyphenols curcumin, butein and isoliquiritigenin (ISL), endogenous inducers like the cyclopentenone pro-

taglandin 15-deoxy- $\Delta^{12,14}$ -prostaglandin J₂ (15d-PGJ₂)⁵ and the highly potent pentacyclic triterpenoids (CDDOs) as well as the monocyclic cyanoenone (MCE) relatives⁶⁻⁹ (Figure 2).

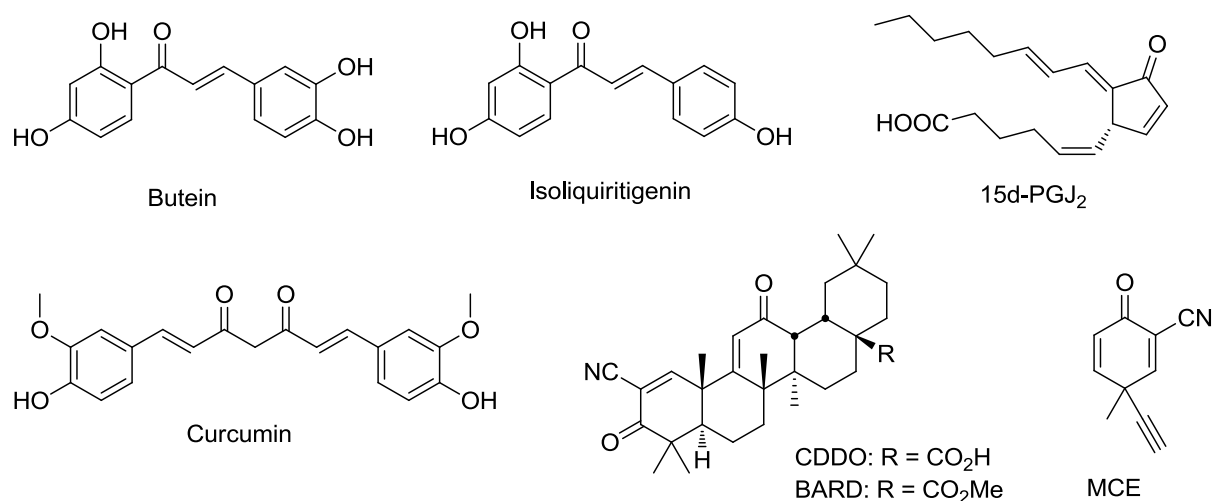


Figure 2. Structures of prominent α,β -unsaturated compounds as biological active Michael acceptors. 15d-PGJ₂, 15-deoxy- $\Delta^{12,14}$ -prostaglandin J₂; CDDO, bardoxolone; BARD, bardoxolone methyl; MCE, monocyclic cyanoenone.

α,β -Unsaturated carbonyl compounds can act as redox active agents by directly neutralizing reactive oxygen species (ROS) such as the superoxide radical ($O_2^{\bullet-}$), hydroxyl radical ($\bullet OH$) and hydrogen peroxide (H_2O_2) produced as a consequence of unbalanced biochemical processes in the body (e.g. in the mitochondria or under chronic inflammation) or as a result of increased exposure to xenobiotics, thus reinstalling redox homeostasis.² A more important reactivity of the α,β -unsaturated carbonyl compounds is their ability to modulate certain sulfhydryl groups on cysteine-dependent signaling pathways. Two major signaling pathways can be targeted by α,β -unsaturated carbonyl compounds particularly leading to beneficial effects: the inflammatory signaling pathway regulated by the transcriptional factor NF- κ B and the redox-sensitive and anti-inflammatory Keap1/Nrf2/ARE signaling system.

The transcriptional factor Nrf2 (NF-E2 related factor 2) is a member of the cap'n collar family of basic leucine transcription factors. Under basal conditions Nrf2 is sequestered in the cytosol as an inactive complex with Keap1 (Kelch-like ECH-associated protein 1). Electrophiles and other inducers can modify critical surface SH groups of cysteines (e.g. Cys151, Cys273 and Cys288) of Keap1 covalently or by oxidation.¹⁰ This leads to a conformational change in Keap1, thereby allowing Nrf2 to stabilize and accumulate in the nucleus. Here, the Nrf2-dependent gene expression is triggered by binding of Nrf2 to the antioxidant response element ARE on the 5' upstream DNA sequence. The phase II proteins encoded by the Nrf2/ARE-regulated genes are detoxifying proteins and enzymes controlling the redox status of the cell, possessing direct antioxidant activity and synthesizing endogenous reducing agents such as glutathione (GSH), regulators of apop-

tos, cell cycle and differentiation, heat shock proteins, regulators of immune response and inflammation and enzymes involved in cellular metabolism¹¹⁻¹² (Figure 3).

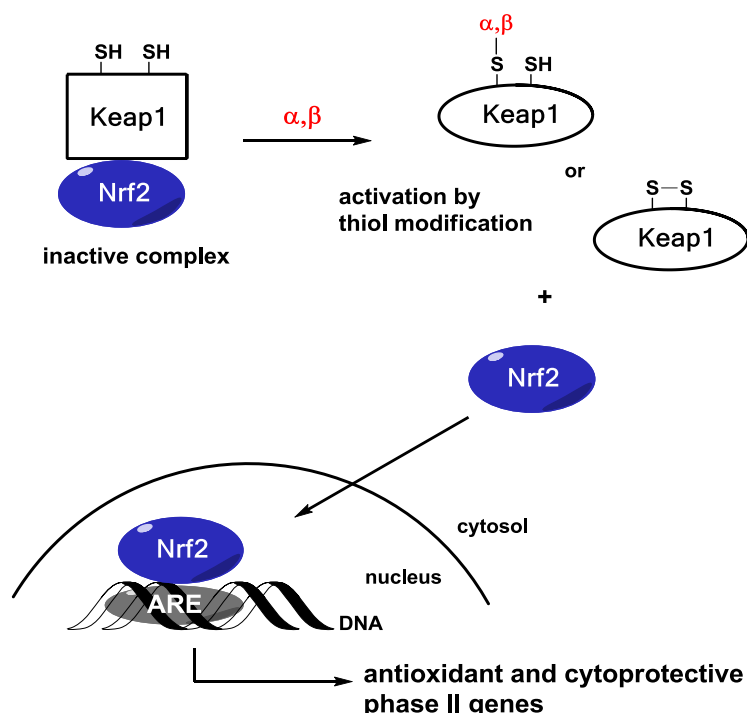


Figure 3. The molecular mechanism of the redox-sensitive Keap1/Nrf2/ARE signaling pathway. Under basal conditions Nrf2 is inactivated by the chaperon protein Keap1 in the cytosol. α,β -Unsaturated carbonyl compounds (α,β) can modify certain SH groups of cysteines of Keap1 covalently or by oxidation. This leads to a conformational change in Keap1, which dissociates from Nrf2. The free form of Nrf2 translocates into the nucleus where it binds to the antioxidant response element (ARE) on the DNA and triggers the expression of anti-inflammatory and cytoprotective proteins.

The Keap1/Nrf2/ARE system acts as a master switch¹³ in the cellular redox stress response and mediates the cytoprotective signaling, especially by the induction of NAD(P)H:quinine oxidoreductase 1 (NQO1), glutathione S-transferase (GST) and heme oxygenase-1 (HO-1). Due to its sensing mechanisms activated by a wide range of electrophiles and antioxidants of natural or synthetic origin, the Keap1/Nrf2/ARE system is raised to a promising target against the development of several diseases, such as cancer, diabetes, neurodegenerative and cardiovascular disorders involving inflammation and oxidative stress.¹⁴⁻¹⁷

The nuclear factor-kappa B (NF- κ B) is a major and ubiquitous transcription factor implicated in the immune and inflammatory responses through the regulation of genes encoding pro-inflammatory cytokines (IL-1 β , IFN- γ , TNF- α), adhesion molecules (ICAM-1), chemokines (IP-10, IL-8), growth factors (PEGF, VEGF) and inducible enzymes such as cyclooxygenase 2 (COX-2) and inducible nitric oxide synthase (iNOS). It consists of homo- and heterodimers of the Rel protein family (RelA (p65), RelB, cRel, p50 and p52) and is kept inactive in the cytosol through an association with an inhibitory protein of the I κ B family (inhibitor of NF- κ B). Following cell stimulation, NF- κ B is released, accumulating within the nucleus, binding to the 5' downstream κ B promoter region on the DNA and inducing the transcription of inflammatory genes. The activa-

tion of NF- κ B is mediated by the I κ B kinase (IKK) complex, causing the phosphorylation of I κ B followed by a proteasomal degradation. Electrophiles like α,β -unsaturated carbonyl compounds can inhibit the NF- κ B pathway by reacting with specific SH groups of the cysteine residues of IKK, thus abolishing the NF- κ B activation. Alternatively, they can directly modulate SH groups of cysteines of the NF- κ B subunits, suppressing the DNA binding activity of the transcriptional factor and causing a down regulation of the protein expression of inflammatory proteins and cytokines (Figure 4).

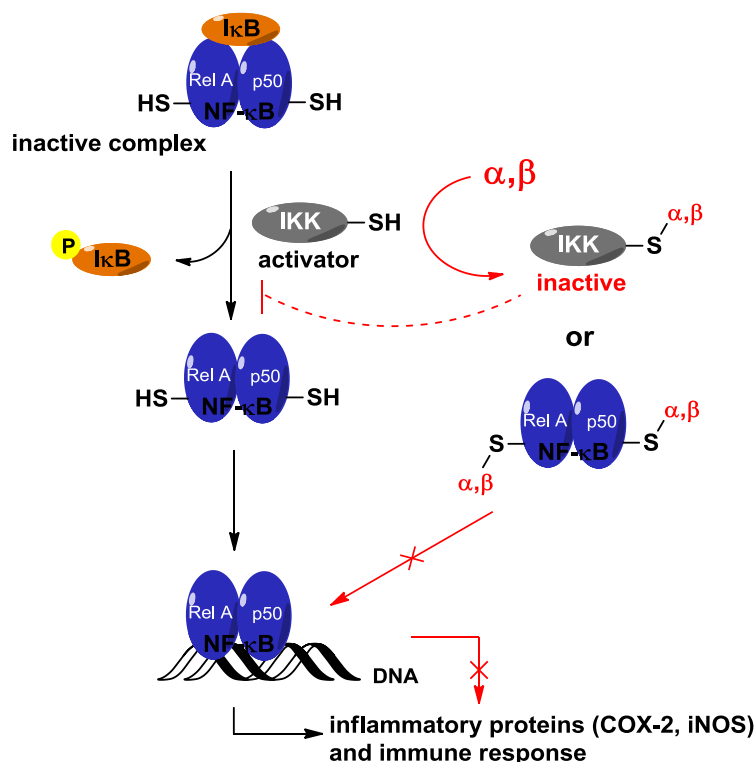


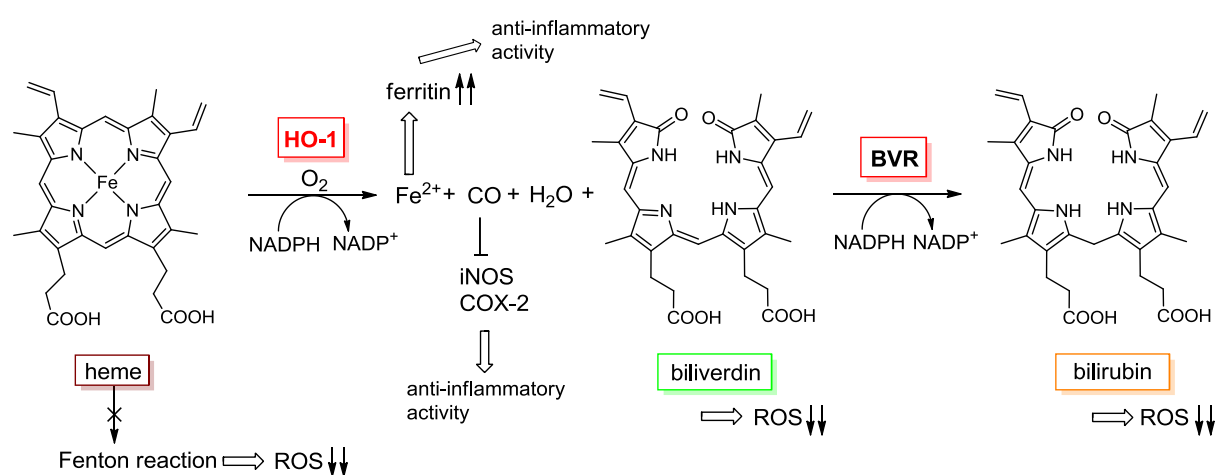
Figure 4. Inhibition of the inflammatory NF- κ B signaling pathway by electrophiles. NF- κ B is kept inactive through an association with the inhibitor I κ B. The activation of NF- κ B is mediated by the I κ B kinase (IKK) complex, causing the phosphorylation of I κ B. Subsequently, NF- κ B is released and binds to the κ B promoter region on the DNA inducing the transcription of inflammatory genes. α,β -Unsaturated carbonyl compounds (α,β) can react with SH groups of the cysteines of IKK, thus abolishing the NF- κ B activation. Alternatively, the DNA binding of the active NF- κ B can be inhibited, which leads to a suppression of the protein expression of inflammatory proteins and a reduced immune response.

The NF- κ B pathway was shown to be activated by a wide range of stimuli including inflammatory cytokines (TNF- α), endotoxins (lipopolysaccharide, bacteria, viruses), growth factors (TGF- β), reactive oxygen species (ROS), therapeutic drugs (Taxol, acetylsalicylic acid), environmental hazards (heavy metals, cigarette smoke) and several chemical agents. Although NF- κ B is essential for normal T and B cell development in the cellular defense system and in the expression of stress response proteins (COX-2, iNOS), its dysfunction leads to various diseases such as atherosclerosis, multiple sclerosis, Alzheimer's disease, inflammatory bowel disease, neuropathological and renal diseases, asthma, diabetes and cancer. The inhibition of the NF- κ B pathway is therefore regarded as a potential therapeutic approach in inflammation and cancer.¹⁸⁻²¹

1.2 Heme oxygenase-1 (HO-1)

1.2.1 Activity and induction of HO-1

Heme oxygenase-1 (HO-1) is a redox sensitive, inducible stress protein converting heme to CO, Fe²⁺ and biliverdin (BV), which is further reduced to bilirubin (BR) by biliverdin reductase (BVR). These products are particularly important for the overall chemopreventive, chemoprotective and anti-inflammatory activities of HO-1 (Scheme 1). Biliverdin and bilirubin act as radical scavengers through their conjugated π -system that leads to a decrease of reactive oxygen species, ROS. CO is an inhibitor of proinflammatory heme-containing proteins such as inducible NO synthase (iNOS) or cyclooxygenase-2 (COX-2) and the released iron (II) ion can induce the anti-inflammatory protein ferritin. Finally, the breakdown of free heme itself can reduce oxidative damage, since heme acts as a promoter in the Fenton reaction.²²⁻²⁵



Scheme 1. Heme degradation catalyzed by heme oxygenase-1 (HO-1) and biliverdin reductase (BVR) together with the resulting cytoprotective, anti-inflammatory and antioxidative effects.

As a member of the cytoprotective phase II enzymes the transcription of HO-1 is mainly regulated by the Keap1/Nrf2/ARE signaling pathway.¹² Amongst other stimuli of HO-1 induction such as UV light, heavy metals, oxidative stress,²⁶ especially electrophiles like α,β -unsaturated carbonyl compounds can react with nucleophilic sulfhydryl groups of the Nrf2-complexing chaperon Keap1.²⁷⁻²⁸ Thereby the Nrf2 regulated antioxidant-responsive element (ARE) is activated which leads to a transcriptional induction of HO-1 (Figure 3). Other regulatory mechanisms of HO-1 gene induction have been discussed, such as the MAPK (mitogen-activated protein kinases) signaling pathway,²⁹ several kinases²⁴ and transcriptional factors, such as NF- κ B and AP-1 (activator protein 1).³⁰⁻³¹ However, the specific MAPK and/or other kinases involved in the HO-1 induction appear to vary in an inducer- and cell-specific fashion.

1.2.2 HO-1 as therapeutic target

The upregulation of heme oxygenase-1 has proved to be a useful tool to fight inflammation. The potent cytoprotective effects of HO-1 have been associated with therapeutic benefits in various pathological conditions such as systematic inflammation in response to infections (sepsis), asthma, oxidative lung injury (hyperoxia) and cardiovascular injury (hypertension, atherosclerosis) as well as organ transplantation, ischemia and reperfusion.³² Moreover, evidence that oxidative stress leads to chronic inflammation in HO-1 deficient mice³³⁻³⁴ and to an inflammatory syndrome³⁵ in the first reported human to lack of HO-1 enzyme activity, supports the fact that the induction of HO-1 serves as an adaptive mechanism to protect against oxidative damage. In this respect, the development of anti-inflammatory, antioxidant and cytoprotective drugs based on their induction of HO-1 activity is a promising approach.

1.2.3 Techniques for measuring HO-1 activity

HO-1 activity has been measured using several techniques. HO assays that use gas chromatography of carbon monoxide have been described.³⁶⁻³⁷ However, the most common HO-1 activity assay relies on the formation of bilirubin, which is in comparison to biliverdin the more stable downstream product. Since its formation from biliverdin by BVR is a lot faster than the initial HO-1 reaction, the amount of bilirubin per time corresponds directly to the HO-1 activity, as long as there is enough active BVR present. Another enzymatically active form of heme oxygenases, namely HO-2 is constitutively expressed and present only in very low amounts in most cell types, except for brain, liver, spleen and the testis.³⁸ Thus, the determination of bilirubin has to be considered as the sum of HO-1 and HO-2 activity, which is expressed as the overall HO activity.

The amount of bilirubin can be determined by quite a range of methods such as direct spectrophotometric quantification at 468 nm³⁹ or the difference in absorbance at 464 to 530 nm ($\epsilon_{464-530} = 40 \text{ mM}^{-1} \text{ cm}^{-1}$),⁴⁰ using the specific radioactivity of ¹⁴C-bilirubin,⁴¹ quantification by HPLC,⁴²⁻⁴³ different fluorescence-based techniques,⁴⁴⁻⁴⁹ SERS Raman spectroscopy,⁵⁰ LC-MS/MS quantification with ¹³C-labeled bilirubin as tracer⁵¹ or by ELISA with specific anti-bilirubin antibodies.⁵² Moreover, particularly when serum samples are analyzed, bilirubin is derivatized by diazotization-based methods prior to its quantification,⁵³ oxidation by bilirubin oxidase⁵⁴ or a formation bilirubin-zinc complexes was utilized.⁵⁵

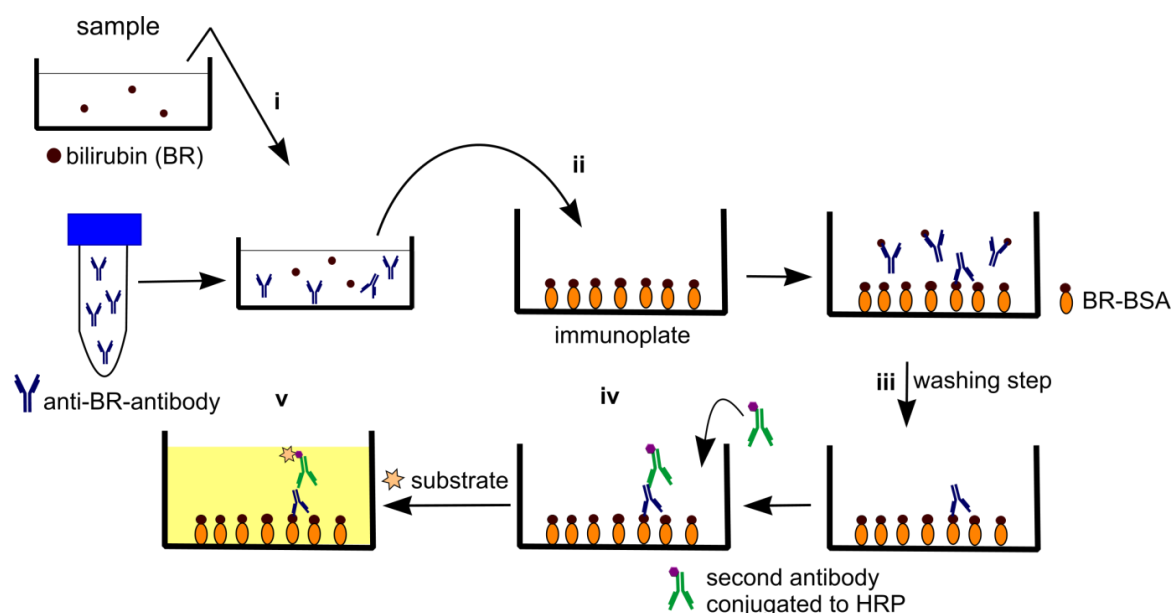
In a heme oxygenase activity assay the bilirubin is formed in situ from the active protein, which originates from stimulated cell cultures or tissues of interest. By employing microsomal fractions (100,000 g centrifugation precipitate) the amount of the membrane-bound proteins HO-1 and HO-2 was elevated compared to the “normal” 20,000 g supernatant in tissue fractions,^{42, 56-57} but a disadvantage of this method is that it cannot be scaled down to a microplate level on the centrifugation step. Variations of the HO-1 activity assay can be found throughout the literature, and many rely on the formation and the extraction/solubilization of bilirubin. Its solubility is

greatly enhanced in organic solvents, therefore mostly a chloroform extraction is used together with a spectrophotometric quantification⁵⁸⁻⁵⁹ or EtOH:DMSO 95:5 is added prior to an HPLC quantification.⁴³ Based on the originally developed HO assay concept by Tenhunen,⁵⁶ the typical assay components added to the 18,000 g supernatant are hemin, a NADPH-generating system⁶⁰ containing NADPH, glucose-6-phosphate, glucose-6-phosphate dehydrogenase and rat liver cytosol prepared from a 100,000 g supernatant as a source of biliverdin reductase⁶¹⁻⁶² in buffer, pH 7.4. HO activity was measured by this method in different cell types, including porcine^{58, 63} or bovine aortic endothelial cells,⁶⁴⁻⁶⁶ astrocytes,⁶⁷ porcine renal epithelial proximal tubule cells and rat kidney epithelial cells⁶⁸ as well as murine macrophages RAW264.7.⁶⁹⁻⁷⁰

Despite these many examples, the extraction methods cannot easily be transformed into a plate assay. This makes them less attractive when many samples have to be analyzed at a time and a wider screening is targeted. One possibility to overcome this shortcoming is to 'extract' and analyze bilirubin at the same time by using the specific monoclonal anti-bilirubin antibody 24G7.⁷¹

1.2.3.1 An-ELISA for bilirubin quantification

The group of Izumi *et al.* developed an enzyme-linked immunosorbent assay (ELISA), using the anti-bilirubin antibody 24G7 and a second HRP-conjugated rabbit anti-mouse antibody to determine unconjugated and conjugated bilirubin and also bilirubin derivatives. They could measure 10^{-7} - 10^{-5} mol L⁻¹ of unconjugated and conjugated bilirubin in human serum samples. The assay results gave a good correlation coefficient (CC = 0.86) compared with the HPLC results.⁷²



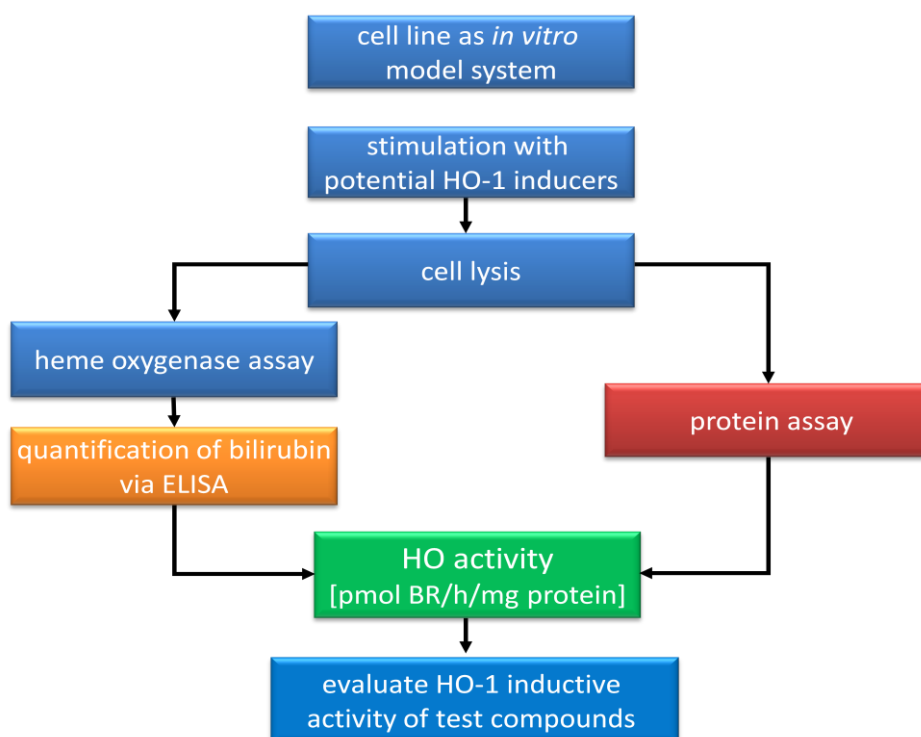
Scheme 2. The bilirubin-ELISA procedure. (i) Samples containing bilirubin are incubated with an excess of specific anti-bilirubin antibody. (ii) The mixture is transferred to an immunoplate coated with a bilirubin-BSA conjugate (BR-BSA). (iii) Free, unbound anti-bilirubin antibodies are washed from the plate. (iv) A second HRP-conjugated antibody is added and allowed to bind to the anti-bilirubin antibody. (v) The HRP enzyme substrate is added to quantify the anti-bilirubin antibody bound to the immunoplate.

The bilirubin-ELISA is built as a non-competitive, indirect assay (Scheme 11). The sample containing bilirubin (BR) is incubated with an excess of the specific anti-bilirubin antibody. The free unbound anti-bilirubin antibody is captured on an immunoplate coated with the bilirubin-BSA (BR-BSA)-conjugate and detected with a second horse radish peroxidase (HRP)-conjugated antibody. After adding the substrate solution containing *ortho*-phenylenediamine dihydrochloride (OPD) and H₂O₂, the reaction is stopped with H₂SO₄ and the absorbance of the yellow product can be measured at 492 nm. The intensity of the absorbance is proportional to the amount of anti-bilirubin antibody bound to the immunoplate, which is inversely proportional to the amount of bilirubin in the sample.

The anti-bilirubin monoclonal antibody 24G7 was used in immunohistochemistry to study bilirubin IX α accumulation in atherosclerotic lesions of rabbit foam cells⁷³ and the involvement of HO-1 activity in neuronal survival of kainate model rats.⁷⁴ The ELISA method was used to measure an increased bilirubin level in cerebrospinal fluid in Alzheimer's disease,⁷⁵ to assess the antioxidant activity of serum and urinary bilirubin oxidative metabolites⁷⁶ and to examine the HO-1 activity in oxidant-induced injury in cultured human airway epithelial cells.⁷⁷

1.2.4 Development of a HO-1 activity assay

Because of the lack of a high throughput method to determine HO-1 activity to screen many potential new HO-1 inducers, which could be used as lead structures for drug development, a simple and reliable cell line-based assay is needed. This can be achieved by developing a HO-1 activity assay, which can be used in a microtiter plate setting, applicable on non-microsomal fractions of cell lysates by combining the HO enzymatic reaction with the ELISA method determining the produced bilirubin in the sample. The purpose of the HO-1 activity assay is to screen for HO-1 activity inducers *in vitro* in a feasible way by using a 96-well plate format for all steps of the assay, including cell culture, cell sample preparation, HO enzymatic reaction, protein determination and bilirubin quantification via ELISA. A concept of the HO-1 activity assay is shown in Scheme 3. As an *in vitro* model system, cells are cultured in a 96-well plate and incubated with the potential HO-1 inducers. Cell lysis is then performed in the same microtiter plate by using a mild and efficient cell lysis buffer containing a protease inhibitor cocktail and a detergent in order to solubilize and stabilize the target proteins from degradation. Without further centrifugation step, the obtained whole cell lysate is transferred to a new microtiter plate and incubated with the HO enzyme reaction mixture consisting of hemin, biliverdin reductase (BVR) and NADPH. The final product of the HO and the BVR reaction, bilirubin, is then quantified by ELISA using the specific anti-bilirubin antibody 24G7 and a second HRP-conjugated antibody for detection.



Scheme 3. Concept of the HO-1 activity assay to screen for new HO-1 inducers *in vitro*.

Finally, the total protein amount in the whole cell lysate is determined using a protein assay kit. Bilirubin amounts in samples are calculated from a bilirubin calibration curve carried out on each plate and HO activity is expressed as pmol bilirubin h⁻¹ mg⁻¹ total protein. For HO-1 activity determination, the HO activity of the cells stimulated with the test compound is compared to control cells incubated only with culture medium and expressed as x-fold HO-1 activity of control.

1.2.4.1 Preliminary optimizations of the HO-1 activity assay

First optimizations of the HO-1 activity assay were started in the diploma thesis (Hannelore Rücker, Universität Regensburg, October 2009)⁷⁸ and were continued and further developed in the present work.

As an *in vitro* model system, the human colon cancer cell line HT-29 was used to develop the HO-1 activity assay. For this purpose HT-29 cells (1 · 10⁵ cells/well) were incubated in a 96-well plate with potential HO-1 inducers in several concentrations for a maximum of 24 h and control cells were treated with culture medium alone. The cell lysis was performed in the 96-well plate and included two steps: i) cells were incubated with a concentrated lysis buffer (40 mM TRIS-HCl, pH 7.4, 250 mM sucrose, 10 mM EDTA, 100 mM NaCl, 1% (v/v) SDS detergent, 4% protease inhibitor cocktail) on an orbital plate shaker for 15 min at 4 °C and ii) diluted with lysis buffer (without detergent and protease inhibitor) to a final detergent concentration of 0.05% in the cell lysate sample. Low concentrations of detergent in the lysis buffer (<0.1%) gave poor cell lysis

results. More importantly, higher concentrations of detergent (>0.05%) interfered with the protein detection when using the Bradford protein assay to give false positive results.

For determining the HO activity, the whole cell lysates (10 µg protein/well) were incubated for 1 h at 37 °C with the HO reaction mixture containing 25 µM hemin, 3 mM NADPH, 100 µg guinea pig liver cytosol extract prepared by ultracentrifugation as a source of biliverdin reductase in TRIS-HCl-sucrose buffer, pH 7.4. HO assay components based on the HPLC assay method developed by Ryter *et al.*⁴³ The enzymatic reaction was stopped with a 1 M HCl aqueous solution and pH was then adjusted to 7.4 with 1.2 M NaOH aqueous solution. Here several stop solutions and procedures were screened and the HCl/NaOH procedure was found to be the best solution. Bilirubin standard solutions prepared in TRIS-HCl-sucrose buffer, pH 7.4 were added after the incubation step to the HO reaction mixture containing only whole cell lysate and the liver cytosol extract. The bilirubin in the standards and the samples was then quantified with the ELISA method described by Izumi *et al.*, which was slightly modified.⁵² Samples were incubated with the specific anti-bilirubin antibody (0.571 µg mL⁻¹) and then the mixture was transferred on an immunoplate coated with a bilirubin-BSA conjugate (3.5 µg mL⁻¹). Both parameters, the anti-bilirubin antibody and bilirubin-BSA conjugate concentration were optimized. Next, the bound anti-bilirubin antibody on the immunoplate was incubated with a second HRP-conjugated antibody (0.2 µg mL⁻¹) and then detected by adding the substrate OPD and H₂O₂. The reaction was terminated by a 3 M H₂SO₄ solution and absorbance was measured at 492 nm. Unknown bilirubin concentration in the samples was calculated by using the linear regression curve generated from the bilirubin standards (5-50 · 10⁻⁹ M bilirubin) on each plate. Finally, the protein amount in the whole cell lysate was determined using the Bradford protein assay. HO activity was expressed as pmol bilirubin h⁻¹ mg⁻¹ total protein.

First results with the HO-1 activity assay were promising, but insufficient stimulation of HT-29 with known HO-1 inducer compounds and a poor reproducibility of data were persistent. Therefore, further troubleshooting and optimization of the HO-1 activity assay was aimed.

Crucial for the assay is the cell lysis step which requires a more feasible one step procedure in the 96-well plate format by using a mild but sufficient detergent in the lysis buffer. Components of the lysis buffer, especially the detergent should not interfere with the protein detection or the ELISA. The use of a detergent compatible protein assay kit can avoid this problem and be also suitable for detecting small amounts of protein in the sample. Components of the HO enzymatic reaction and the reaction buffer should be suitable and sufficient to estimate the HO activity in the whole cell sample. The HO-1 activity assay should be applicable on different cell lines as *in vitro* model systems, as long as they are adherent. Also, the preparation of the test compound solutions for their incubation with the cells should be simplified to avoid compound precipitation in the cell culture medium.

1.3 The activity of inducible nitric oxide synthase (iNOS)

Nitric oxide (NO) is an ubiquitous key signaling molecule implicated in neurotransmission,⁷⁹ vasodilatation⁸⁰ and regulation of the immune system.⁸¹ NO is produced by three isoforms of NO synthase, which are: endothelial NOS (eNOS), inducible NOS (iNOS), and neuronal NOS (nNOS). All isoforms contain heme as a prosthetic group and catalyze the reaction of L-arginine to L-citrulline using O₂ and NADPH.⁸² The catalytic activity of the inducible NO-synthase is given in Figure 5.

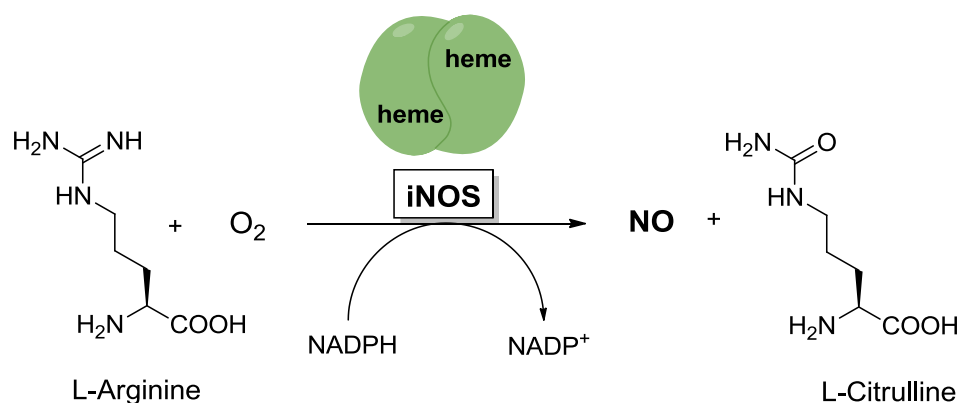


Figure 5. The enzymatic activity of the inducible nitric oxide synthase (iNOS). The amino acid L-arginine is converted to L-citrulline by the active iNOS dimer with heme as the prosthetic group, using oxygen and NADPH to produce NO.

The function of the iNOS enzyme depends on its expression level, which is regulated by the proinflammatory NF- κ B signaling pathway (Figure 4). iNOS, when induced in macrophages, generates large amounts of NO that has cytostatic or cytotoxic effects on parasitic or tumor target cells. This is caused by the high affinity of NO to protein-bound iron, thus inhibiting the catalytic centers of iron-sulfur cluster-dependent enzymes involved in mitochondrial electron transport, DNA replication (ribonucleotide reductase) or in the citric acid cycle (acotinase). Furthermore, NO and peroxynitrites (ONOO⁻), yielding from the reaction with superoxide radicals (O₂^{•-}) can directly interfere with the DNA of target cells and cause strand breaks and fragmentation. High levels of NO produced by activated macrophages may not only be toxic to parasites or tumor cells, but may also harm healthy cells, contributing to the pathophysiology of inflammatory diseases and septic shock. In inflammation, hypertension and atherosclerosis increased reactive nitrogen species (NO, ONOO⁻) induce tyrosine nitration, oxidation of SH groups of cysteins and lipid peroxidation. Targeting nitrosative stress may represent a therapeutic potential in pathologies like Alzheimer's disease or cancer.⁸³⁻⁸⁴ The activity of iNOS can be inhibited on the transcriptional level by inactivating the NF- κ B pathway, where i.e. α,β -unsaturated carbonyl compounds can react with key SH groups of cysteine residues of IKK or NF- κ B and suppress the protein expression of iNOS and other proinflammatory enzymes as displayed in Figure 4. The pre-

vention of the overproduction of NO through control of regulatory pathways may assist in the treatment of NO-mediated disorders without changing the physiological levels of NO.⁸⁵

1.3.1 The nitrite (Griess) assay

The potential anti-inflammatory activity of α,β -unsaturated carbonyl compounds or other compounds can be assessed by their ability to inhibit the iNOS activity causing a suppression in the NO production. iNOS activity can be determined by the quantification of nitrite, the more stable oxidation product of nitric oxide, using the Griess reaction in the so called nitrite assay.⁸⁶ In the murine macrophage cell line RAW264.7, the NO synthesis can be induced by lipopolysaccharide (LPS), a bacterial wall constitute.⁸⁷

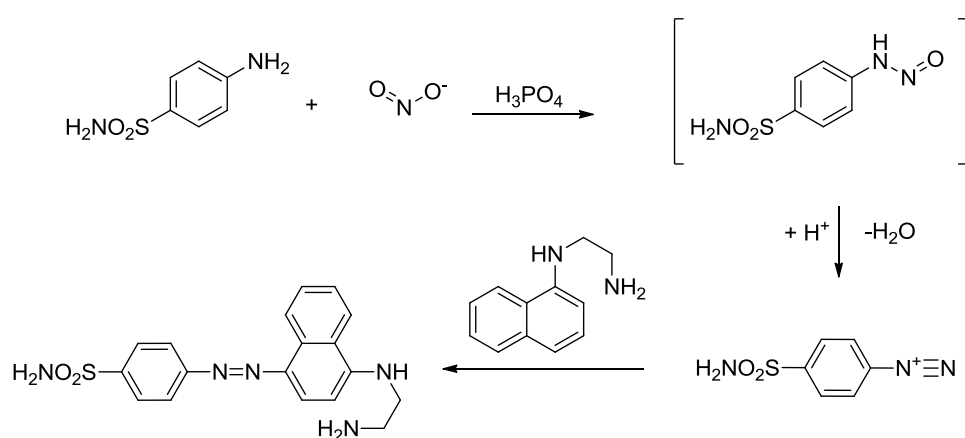


Figure 6. The Griess reaction is used to quantify the nitrite derived from the NO production in RAW264.7 macrophages stimulated with lipopolysaccharide (LPS) in the nitrite assay. Under acidic conditions nitrite reacts with the amino group of sulfanilamide to form the diazonium cation, which couples to N-(1-naphthyl)ethylenediamine (NED) in *para*-position to form the azo dye.

Nitric oxide which oxidizes to nitrite and accumulates in the cell culture medium is quantified by the Griess reaction, which is a diazotization reaction followed by an azo coupling using sulfanilamide, N-(1-naphthyl)ethylenediamine (NED) and phosphoric acid (Figure 6). Under acidic conditions the nitrite in the cell culture medium reacts with the amino group of sulfanilamide to form the diazonium cation, which couples to NED in *para*-position to form the corresponding azo dye, which absorbance can be measured at 560 nm. The NO production is quantified in LPS-stimulated macrophages in the presence or absence of a test compound. Consequently, a potential inhibition of the NO production by the compound estimates its anti-inflammatory activity.

1.4 The oxygen radical absorbance capacity-(ORAC)-fluorescein assay

The radical scavenging activity of antioxidants can be determined by the cell free oxygen radical absorbance capacity-(ORAC)-fluorescein method generating peroxy radicals from AAPH (2,2'-azobis(2-methylpropionamidine) dihydro-chloride) as a free radical initiator and using fluorescein as a fluorescent probe.⁸⁸ The protecting effect of an antioxidant, reacting as radical scaven-

ger can be quantified by assessing the area under the fluorescence decay curve (AUC) of the sample compared to the blank, in which no antioxidant is present (Figure 7).

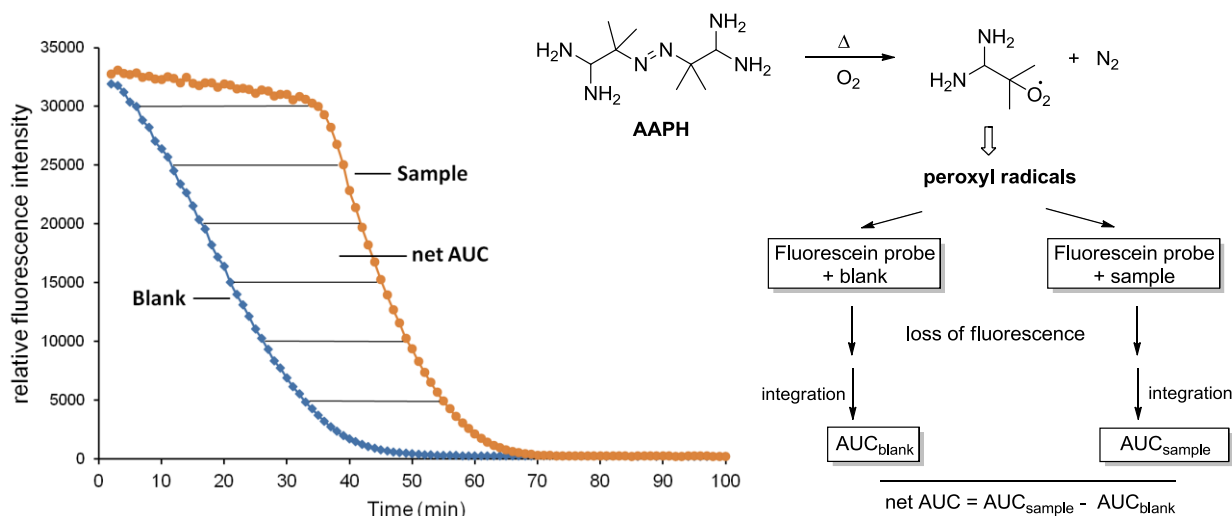


Figure 7. ORAC-fluorescein assay. The fluorescence decay from the reaction of radicals generated from AAPH with fluorescein in the absence (blank) or presence of an antioxidant (sample) is measured over time. The net area under the fluorescence decay curve (net AUC) determines the antioxidant capacity of the test compound.

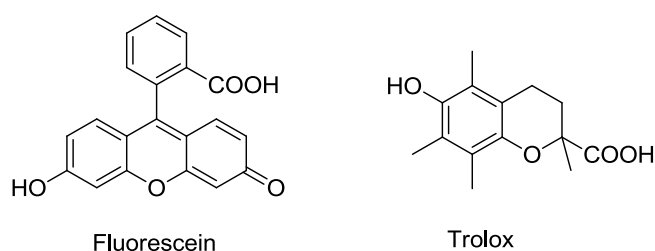


Figure 8. Structures of fluorescein used as fluorescence probe and Trolox, a standard antioxidant in the ORAC-fluorescein assay.

From the curves (relative fluorescence intensity versus time) the area under the fluorescence decay curve (AUC) is calculated as

$$AUC = 1 + \sum_{i=1}^{i=100} f_i/f_0$$

Equation 1

where f_0 is the initial fluorescence reading at 0 min and f_i is the fluorescence reading at time i . The net AUC corresponding to a sample is calculated by subtracting the AUC corresponding to the blank. Linear regression equations between net AUC and antioxidant concentration are determined for all the samples and ORAC values are compared to Trolox, a water-soluble vitamin E (α -tocopherol) derivative (Figure 8). The final ORAC values are expressed as Trolox equivalents by using the standard curve determined for each assay.

1.5 Anti-inflammatory activity of a diverse group of α,β -unsaturated carbonyl compounds and polyphenols

A structurally diverse group of natural products and synthetic compounds were investigated for their HO-1 induction behavior using the ELISA-based HO-1 activity assay in the model cell line RAW264.7. Known Nrf2 inducers possessing the α,β -unsaturated carbonyl moiety¹¹ together with polyphenols which are also a prominent class of inducers of cytoprotective proteins¹⁶ were focused on for the screening. The following pharmacologically interesting compounds were examined (Figure 9.): the chalcones cardamonin,⁸⁹⁻⁹¹ flavokawain A⁹² and xanthohumol,⁹³⁻⁹⁵ the flavonoids (-)-epicatechin,⁹⁶⁻⁹⁷ kaempferol⁹⁸⁻¹⁰¹ and quercetin,¹⁰²⁻¹⁰³ three cinnamic acid derivatives caffeic acid,¹⁰⁴⁻¹⁰⁵ chlorogenic acid^{104, 106-107} and CAPE,¹⁰⁸⁻¹¹¹ the isothiocyanate sulforaphane^{28, 112-114} and the disulfide oltipraz,¹¹⁵⁻¹¹⁷ curcumin¹¹⁸ and 3-hydroxycoumarin,^{27, 119} the sesquiterpene zerumbone,¹²⁰⁻¹²¹ rosolic acid,⁶⁶ dexamethasone,^{89, 122} a synthetic glucocorticoid, and two compounds lacking the α,β -unsaturated carbonyl moiety resveratrol¹²³⁻¹²⁴ and carnosol,¹²⁵⁻¹²⁶ a diterpene with a catechol unit.

The mechanism by which these compounds lead to a HO-1 induction is commonly by activating the Keap1/Nrf2/ARE pathway. Although the Nrf2 inducers are from distinct chemical classes, comprising diphenols, quinones, Michael acceptors and isothiocyanate, all have in common that they are electrophiles and can covalently modify thiol groups on Keap1 by alkylation or oxidation. The activation of the transcriptional factor Nrf2 that binds to the ARE and promotes the phase II protein expression, is mediated by a direct reaction with thiol groups of the suppressor protein Keap1 as shown for sulforaphane,¹²⁷ zerumbone¹²⁸ and xanthohumol.¹²⁹ Certainly, there are also other indirect mechanisms, which lead to activation of the Nrf2/ARE pathway and thus to HO-1 induction, involving the activation of kinase pathways which phosphorylates Nrf2 and Keap1. The involvement of protein kinase in Nrf2 activation was suggested for resveratrol,¹³⁰ curcumin¹³¹ and carnosol.¹³²

A HO-1 induction on mRNA, protein or enzyme activity levels were shown for most of the biologically active compounds in different cell and tissue types, summarized in Table 1. No HO-1 induction tests have been described for 3-hydroxycoumarin, oltipraz, cardamonin and flavokawain A. Since the HO-1 inductive activity is known for some compounds, the screening aimed also at the establishment and validation of the ELISA-based HO-1 activity assay as a simple and reliable screening method for HO-1 activity.

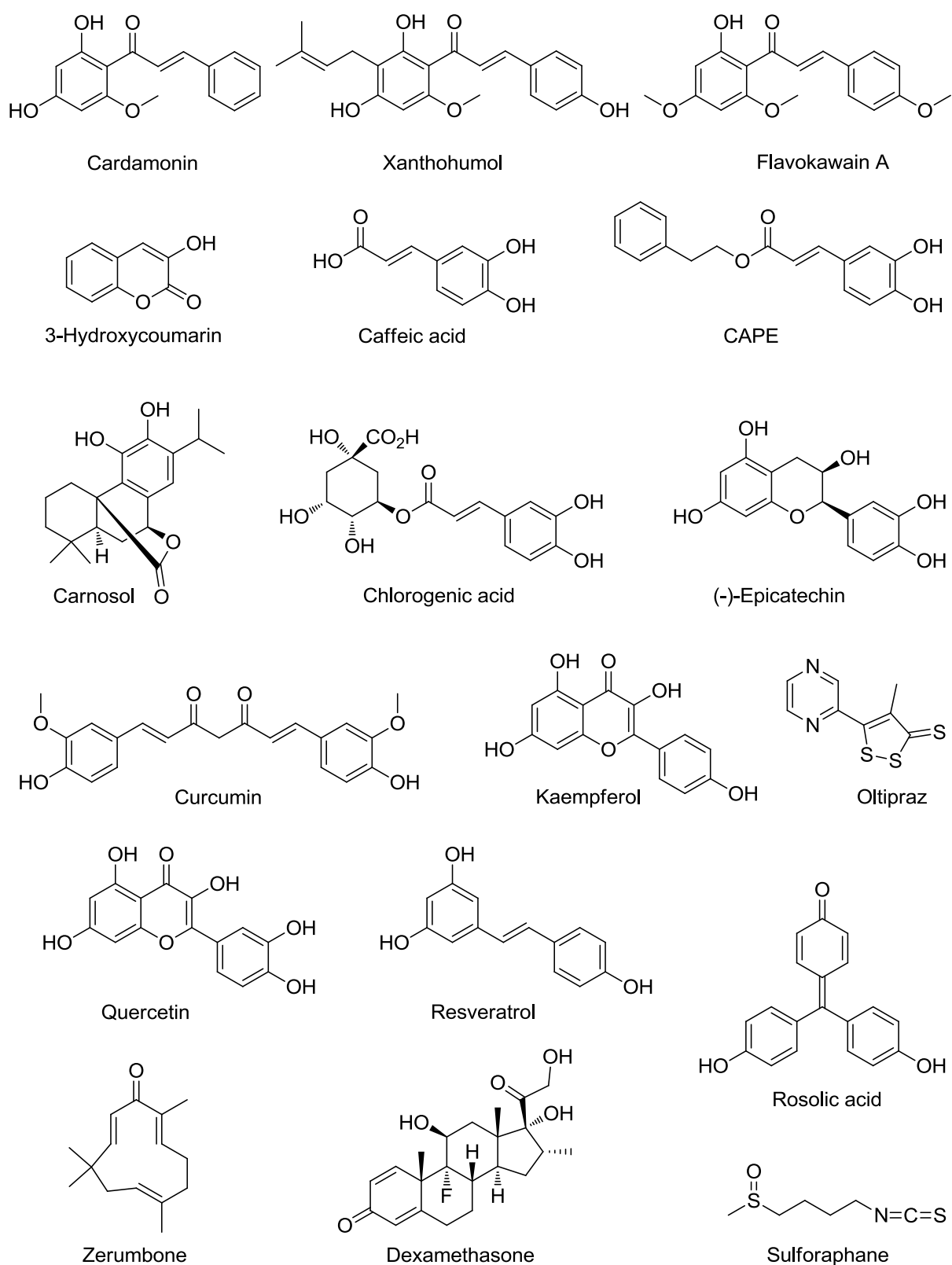


Figure 9. Structures of biologically active natural compounds and synthetic drugs screened in the ELISA-based HO-1 activity assay.

Table 1. HO-1 inducer activity of natural products and synthetic drugs.

Compound (Dose)	Mechanism of HO-1 induction	Model cells or mammalian	Ref.
Xanthohumol			
2-10 μ M	induction of HO-1 mRNA and HO-1 protein level in normal hepatocytes (THLE-2) by activation of Nrf2; no HO-1 induction was observed in carcinoma hepatocytes HepG2	human hepatocytes, THLE-2 and HepG2	133
CAPE			
15-50 μ M	increase of HO-1 protein expression and HO-1 activity	DI TNC1 rat astrocytes	67
5-30 μ M	increase of HO-1 protein expression and HO-1 activity by binding of Nrf2 to ARE	LLC-PK ₁ renal epithelial cells	68
20 μ M	HO-1 mRNA and protein expression induction	HUVEC, human vascular endothelium cells	134
Carnosol			
10 μ M	increase of HO-1 mRNA and protein expression by binding of Nrf2 to ARE, activation of ERK, p38 MAPK and JNK	PC12 rat pheochromocytoma	135
(-)-Epicatechin			
50 μ M	induction of HO-1 and Nrf2 protein expression	ARPE-19 human retinal pigment epithelial cells	136
Curcumin			
15-50 μ M	increase of HO-1 protein expression and HO-1 activity	DI TNC1 rat astrocytes	67
5-30 μ M	increase of HO-1 protein expression and HO-1 activity by binding of Nrf2 to ARE	LLC-PK ₁ renal epithelial cells	68
5-15 μ M	increase of HO-1 mRNA, HO-1 protein expression and HO-1 activity	bovine aortic endothelial cells	65
200 mg kg ⁻¹	HO-1 expression and activity in liver, DNA binding of Nrf2-ARE in liver	male Albino rats	137
15 μ M	increase of HO-1 mRNA expression by binding of Nrf2 to ARE, activation of PKC- δ and p38 MAPK	THP-1 human monocytes	131
Kaempferol			
100 μ M	increase of HO-1 mRNA and protein expression	RAW264.7 murine macrophages	138
10-100 μ M	increase of HO-1 mRNA expression	RAW264.7 murine macrophages	139
10 μ M	induction of HO-1 protein expression by activation of Nrf2 and JNK	HEI-OC1, auditory mice cells	140
Quercetin			
100 μ M	increase of HO-1 mRNA and protein expression	RAW264.7 murine macrophages	138

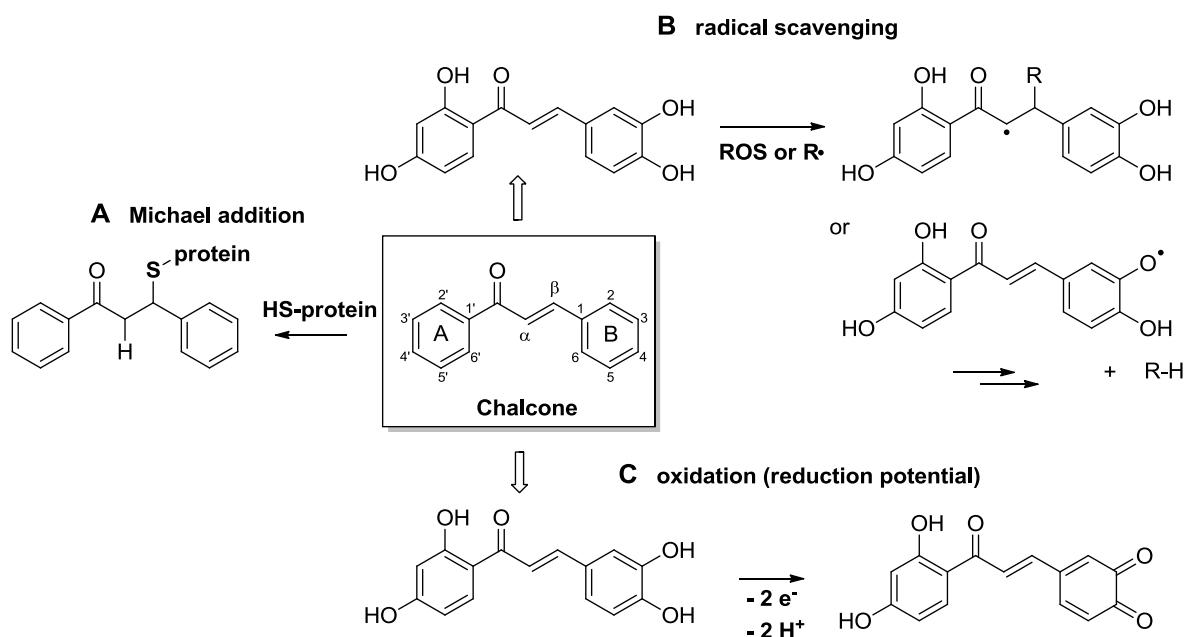
Compound (Dose)	Mechanism of HO-1 induction	Model cells or mammalian	Ref.
30 μ M	increase of HO-1 protein expression	microglial BV2 cells	141
100 μ M	induction of HO-1 activity and Nrf2 activation	EtOH-treated human hepatocytes isolated from liver cancer patients	142
50 μ M	induction of HO-1 and Nrf2 activation	ARPE-19 human retinal pigment epithelial cells	136
Resveratrol			
15 μ M	induction of HO-1 mRNA and protein expression by activation of Nrf2/ARE and ERK	PC12 rat pheochromocytoma	130
1-10 μ M	induction of HO-1 mRNA and protein expression via NF- κ B activation	human aortic smooth muscle cells	143
5-100 μ M	increase of HO-1 protein expression	cortical neuronal mice cells	144
5-100 μ M	increase of HO-1 mRNA, no induction of HO-1 protein expression, reduction of HO-1 activity	DI TNC1 rat astrocytes	145-146
Rosolic acid			
15 μ M	induction of HO-1 protein expression and HO-1 activity	bovine aortic endothelial cells	66
Zerumbone			
1-25 μ M	induction of HO-1 expression and activation of Nrf2/ARE	RL34 rat liver epithelial cells	147
10 μ M	induction of HO-1 mRNA and protein expression by a Nrf2/ARE dependent pathway	JB6 Cl41 mouse epidermal cells and mouse skin from female hairless mice	128
Sulforaphane			
0.1 μ M	induction of HO-1 protein expression	rat aortic smooth muscle cells	148
20 μ M	induction of HO-1 protein expression and activation of Nrf2/ARE	HepG2 human hepatocytes	149
Dexamethasone			
5 μ M	induction of HO-2 mRNA, protein expression and HO activity, no HO-1 mRNA induction observed	HeLa, human cervix cancer cells	150
0.5-50 μ g mL ⁻¹	suppression of HO-1 mRNA in cytokine-stimulated cells	rat astroglial cells	151
1 μ g mL ⁻¹	no induction of HO-1 activity	GT1-7 hypothalamic neurons	152
1.2 mg kg ⁻¹	suppression of HO-1 protein expression and HO-1 activity in LPS stimulated macrophages	alveolar macrophages of chronic bronchitis model rats	153

Compound (Dose)	Mechanism of HO-1 induction	Model cells or mammalian	Ref.
Caffeic acid			
20 μM	no HO-1 induction observed	HUVEC, human vascular endothelium cells	134
150 μM	no HO-1 mRNA induction	bovine aortic endothelial cells	154
Chlorogenic acid			
150 μM	no HO-1 mRNA induction	bovine aortic endothelial cells	154

1.6 Reactivity and biological activity of natural and synthetic chalcones

1.6.1 Reactivity of chalcones

Chalcones (1,3-diphenylprop-2-en-1-ones) are a diverse group of naturally occurring plant metabolites that can be regarded as open-chain flavonoids, where the two aromatic rings are bridged by an α,β -unsaturated carbonyl moiety possessing a Michael acceptor reactivity. Chalcones can be regarded as bifunctional antioxidants: i) they possess a distinct Michael acceptor reactivity, due to the α,β -unsaturated carbonyl moiety, allowing them to interact with reactive SH-groups on “sensor” proteins involved in cytoprotective and also in inflammatory signaling pathways, (Scheme 4, pathway A) and ii) the α,β -unsaturated carbonyl moiety itself and additional phenolic hydroxy groups on the aromatic rings can react as radical scavengers (Scheme 4, pathway B) or antioxidants due to their reduction potential (Scheme 4, pathway C).^{4, 155-156}



Scheme 4. General structure and reactivities of chalcones.

Several structural and electronic characteristics of chalcones influence the reactivity of the Michael acceptor moiety and thus the potential biological activity of chalcones. Aromatic OH-groups display a positive resonance effect (+M effect), due to the free electron pairs on the oxygen atom, which contributes to the conjugated aromatic π -electron system and further to the α,β -unsaturated carbonyl moiety of the chalcone. However, when deprotonated, hydroxylates are present in the chalcone, which is to a certain degree possible under physiological conditions (pK_A (phenol) = 10). In this case the strong resonance effect is pushing electrons into the conjugated π -electron system of the chalcone resulting in a more electron rich α,β -unsaturated carbonyl unit, which leads to a reduced electrophilic character and therefore to a weaker Michael acceptor reactivity towards nucleophiles. If methoxy groups are present on the aromatic rings of the chalcone, the resonance effect is weaker compared to hydroxylates, due to the alkylation. The position of the hydroxy and methoxy groups on the aromatic ring plays an important role and can influence the reactivity of chalcones in a tremendous way. As proven in several studies,^{27, 66, 157} the 2'-hydroxy group is essential for the Michael acceptor reactivity of chalcones, due to the intramolecular H-bond which activates the carbonyl group. Furthermore, the H-bond of the 2'-OH group contributes to a stabilized conjugation in the π -system. Generally, a replacement of a more electron donating OH group by a methoxy in the A- or B-ring restores the reactivity of the chalcone. Moreover, since the double bond of the Michael acceptor functionality can be referred to as a push-pull double bond, an exchange in the B-ring restores more reactivity compared to a similar exchange in the A-ring. Methoxy groups in 3 or 4-position on the B-ring and 4'-position on the A-ring can contribute to a stabilization of the conjugated π -system. A loss in reactivity can occur when OMe groups are present in 2 or 6-position on both rings, due to steric hindrance, which can hamper the nucleophilic attack on the β -position of the α,β -unsaturated carbonyl moiety or destabilize the conjugation of the π -system.

2'-Hydroxychalcones can readily isomerize to flavanones through an intramolecular Michael addition, leading to a loss of the functional group and thus altering the reactivity of the chalcone under biological conditions. This important effect was recently investigated by the group of Pauli under several biological conditions typical for cell-based assay systems using the chalcone isoliquiritigenin (ISL).¹⁵⁸ Also significant for the reactivity and thus biological activity of chalcones acting as a Michael acceptors is the stability of the thiol adduct. Here, electron donating groups like OMe, can decrease the acidity of the α -hydrogen, slowing down the retro-Michael reaction. A balanced activation of the Michael acceptor unit and stabilization of the resulting adduct is therefore crucial for the overall reactivity of chalcones.¹⁵⁷

1.6.2 Reactivity assessment of chalcones by a kinetic thiol assay

In order to predict the biological activity of electrophiles based on thiol-mediated regulation processes, a kinetic assay for the assessment of the second rate constant k_2 in thia-Michael additions was developed in our group. The chemical reactivity of hydroxy-alkoxychalcones was recently determined using the kinetic thiol assay for the thia-Michael addition reactions with the S-nucleophile cysteamine (Figure 10).¹⁵⁹

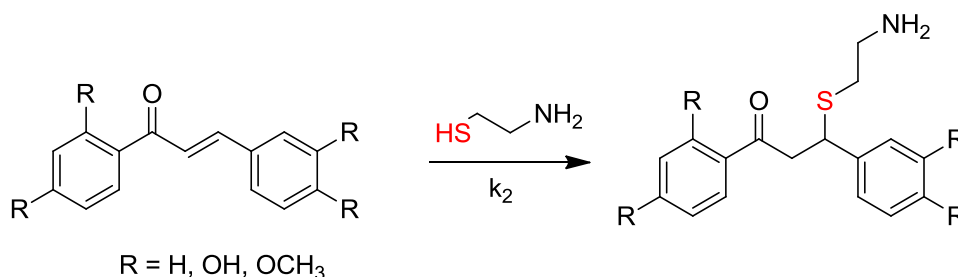


Figure 10. Michael addition reaction of natural and synthetic chalcones with the S-nucleophile cysteamine. k_2 is the second order rate constant of the addition reaction.

Reactions were carried out in 100 mM TRIS-HCl pH 7.4, 2 mM EDTA/ethylene glycol 20:80, 25 °C under pseudo-first order conditions at concentrations of 40 μ M for chalcones and 12 to 500 fold cysteamine. The calculated thia-Michael addition reaction rate was displayed as k_2 value in $M^{-1} s^{-1}$. Hydroxy- and methoxychalcones gave quite different reactivities in the Michael additions of thiols, with k_2 values in the range of 5.08 - 0.193 $M^{-1} s^{-1}$, displaying an overall good electrophilicity. The results showed that a 2'-OH group on the A-ring is essential for the reactivity of the chalcones. Not only electronic effects, but also steric effects can influence the Michael acceptor reactivity. One aspect is the conformation of the conjugated system determined by the dihedral angle between the two aromatic rings, which is in turn influenced by the substituents present on the aromatic rings of the chalcone. A fairly flat chalcone (as shown by X-ray structures) displays generally a higher reactivity, due to a stabilized conjugation of the π -system compared to a chalcone where the aromatic rings are twisted.

1.6.3 Biological activity of chalcones

In the present study, the plant chalcones isoliquiritigenin (ISL), butein, calythropsin, 2',3,4'-trihydroxy-4-methoxychalcone (THMCH) and 2',4'-dihydroxy-3,4-dimethoxychalcone (DMDHCH) and the synthetic chalcones 2'-hydroxychalcone, chalcone, 2'-hydroxy-3,4,4'-trimethoxychalcone (HTMCH) and 2',3,4,4'-tetramethoxychalcone (TMCH) were selected (Figure 11) to investigate their anti-inflammatory and antioxidative activity in RAW264.7 murine macrophages.

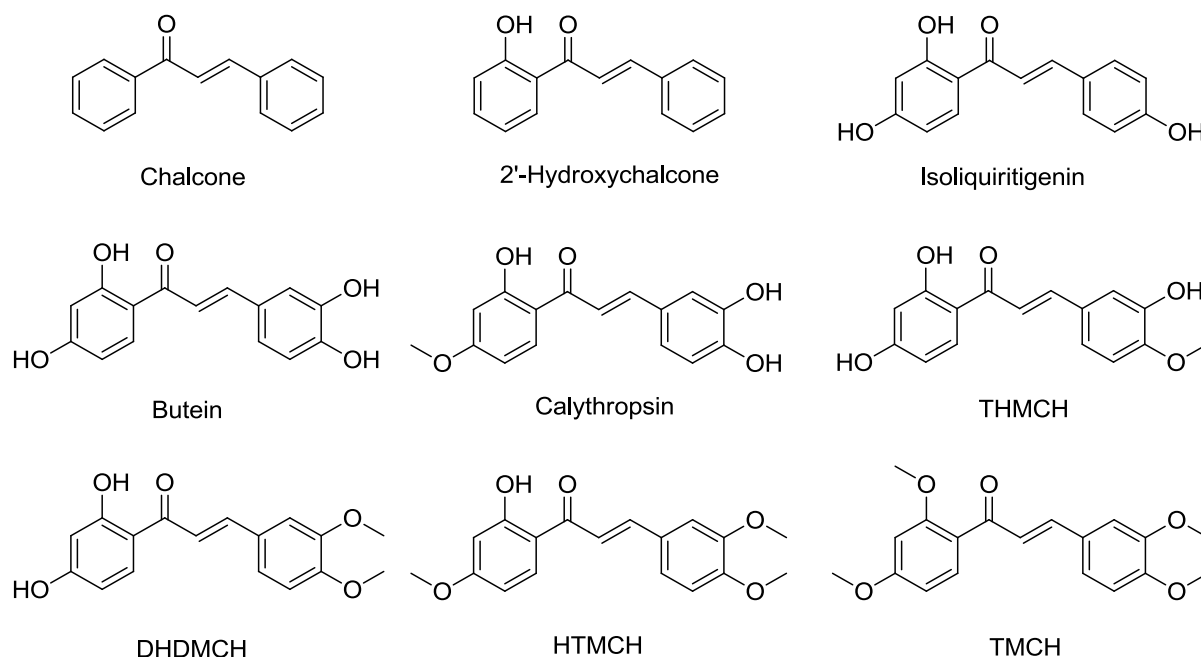


Figure 11. Structures of natural and synthetic chalcones investigated in this study towards their *in vitro* anti-inflammatory and antioxidative activity.

Synthetic and natural hydroxy- and methoxychalcones are of particular interest as they display a wide range of biological properties and exert diverse pharmacological activities including anti-inflammatory, antifungal, antibacterial, antiviral, antimitotic, antitumor, antituberculosis and antimalarial.¹⁶⁰ The importance of chalcones as pharmacologically active compounds is closely connected to their Michael acceptor reactivity and antioxidant potential, by which they can address and affect multiple targets in the cell. By addition to reactive thiol groups on the surface of sensor proteins or transcriptional factors, chalcones can trigger the anti-inflammatory and cytoprotective Keap1/Nrf2/ARE signaling pathway and on the other side inhibit the pro-inflammatory pathway regulated by NF- κ B.¹⁶¹ In case of the synthetic chalcone 3,3',4,4',5,5'-hexamethoxychalcone, a Nrf2-dependent HO-1 induction as well as a NF- κ B down regulation was shown.¹⁶² The anti-inflammatory chalcone butein was found to be an inhibitor of IKK by direct binding on its cysteine residue 179, through which it blocks NF- κ B and NF- κ B-regulated gene products.¹⁶³ Lee *et al.* reported the inhibitory effect of butein on NO production, iNOS gene expression and NF- κ B activity in LPS-stimulated murine macrophages RAW264.7 cells.¹⁶⁴ Studies have also shown that butein induces HO-1 mRNA and protein expression in rat liver cells¹⁶⁵ and that it prevents oxidative damage in human dental pulp cells by inducing HO-1 protein expression and activity via a Nrf2 dependent pathway.¹⁶⁶ The radical scavenging properties of butein was investigated towards DPPH and ABTS radicals.¹⁶⁷ Chalcone exerts its anti-inflammatory activity by inhibiting the activation of NF- κ B and inducing the HO-1 protein expression, which is accompanied by an up regulated level of Nrf2 in the nucleus and an increased ARE activity in bovine aortic endothelial cells. Furthermore, the overall cytoprotective activity of

chalcone may be mediated through a direct modification of cysteine thiol groups on target proteins and regulated by the intracellular GSH level.¹⁶⁸ The chemopreventive activity of chalcone was shown by its inhibitory effect against pulmonary and mammary carcinogenesis when given after carcinogen administration to female rats.¹⁶⁹ 2'-Hydroxychalcone was found to induce HO-1 protein expression as well as enzyme activity in RAW264.7 cells⁶⁹ and bovine aortic endothelial cells.⁶⁶ Additionally, 2'-hydroxychalcone promoted its anti-inflammatory activity in RAW264.7 cells by reducing iNOS expression, NO production and TNF- α release.⁶⁹ Isoliquiritigenin (ISL), a plant constituent from *Dalbergia odorifera* (Leguminosae) and *Glycyrrhiza uralensis* (licorice), has been reported to possess estrogenic,¹⁷⁰ neuroprotective,¹⁷¹ hepatoprotective,¹⁷² anticancer¹⁷³⁻¹⁷⁵ and anti-inflammatory activity.¹⁷⁶⁻¹⁷⁷ Furthermore an induction of HO-1 expression was reported in RAW264.7 macrophages¹⁷⁸ and rat hepatic stellate cells.¹⁷⁹ ISL is a major inducer of quinone reductase and activates the ARE.¹⁸⁰ The antioxidant and chemoprotective actions of ISL was shown in cerebral ischemia model rats, where ISL treatment protected against depletion of antioxidant proteins (superoxide dismutase, catalase and glutathione peroxidase) caused by free radical formation.¹⁸¹ The chalcone calythropsin, firstly isolated from *Calythropsis aurea* was found to possess weak antimitotic activity due to its cytotoxic effect.¹⁸² Furthermore, calythropsin extracted from *Faramaea salicifolia* displayed cytotoxicity against several human cancer cell lines.¹⁸³ DHDMCH and THMCH are abundant in *Iryanthera polyneura* (Myristicaceae) and were isolated 1979 from the trunk of the tree. It is known that Maku Indians of South America use crushed leaves from this tree to treat infected wounds and cuts.¹⁸⁴ The chalcone THMCH revealed a moderate cytotoxicity against several human tumor cell lines, especially against Jurkat cells and was also found to exert an impressive antiproliferative activity against the Jurkat cell cycle.¹⁸⁵ No anti-inflammatory activity was reported for the naturally occurring calythropsin, DHDMCH and THMCH.

Chalcones possess an unique capability to address certain cysteine residues, which qualify them as a valuable tool to modulate biological activity. Several natural and synthetic hydroxy- and methoxychalcones were characterized towards their anti-inflammatory and antioxidative activity, demonstrated by their induction of HO-1 activity and inhibition of NO production in RAW264.7 macrophages and also by their radical scavenging capacity in the ORAC assay. A structure-activity relationship can be assessed, due to the diverse substitution pattern of hydroxy and methoxy groups in 2',3,4,4'-positions of the two aromatic rings, influencing not only the Michael acceptor reactivity but also the overall anti-inflammatory and antioxidative property of the chalcone. Furthermore, the chemical reactivity of the chalcones determined by the kinetic thiol assay in thia-Michael additions¹⁵⁹ was compared to their estimated biological activity.

1.7 α -X-Modified enones as a different approach in fine-tuning their Michael acceptor reactivity and biological activity

A promising approach using α,β -unsaturated compounds for the development of new potent cytoprotective, chemopreventive and anti-inflammatory drugs is to systematically modify the α -position of the α,β -unsaturated carbonyl moiety thus influencing the Michael acceptor reactivity and the biological activity. Examples of such α -modifications leading to a fine-tuned biological activity are found within the class of pentacyclic triterpenoids CDDO¹⁸⁶⁻¹⁸⁷ and also among the chalcones.¹⁸⁸

1.7.1 α -X-Modification in 2',3,4,4'-tetramethoxychalcones (α -X-TMCHs)

In order to manipulate the reactivity of chalcones either a change directly at the Michael system or on the aromatic rings, as seen in the chapter before, can be made. The approach of modifying the α -position of the α,β -unsaturated carbonyl system is a promising concept, because it should lead to a direct and straightforward influence on its reactivity.⁴ Modified chalcones in α -position and their biological studies are known for chalcones with X = halogen,¹⁸⁸⁻¹⁸⁹ aromatic,¹⁹⁰⁻¹⁹¹ alkyl,^{189, 192-193} COOEt,¹⁸⁸ COOH,¹⁹⁴ CN¹⁸⁸ and alkoxy.¹⁹³ But there is no fine-tuning-of-reactivity-approach, particularly on a chalcone scaffold, which investigates a clear influence of different α -X-substituents on the activity in different biological settings. The natural product-like 2',3,4,4'-tetramethoxychalcone, TMCH was chosen as a scaffold for a diverse library of α -X-TMCHs, possessing no free hydroxy groups, so that possible oxidative pathways altering the biological response can be excluded. The α -X-TMCHs used in this work were synthesized in our group by Nafisah Al-Rifai. As shown in Figure 12, thirteen distinct substituents were introduced in the α -position of the Michael system along with the α -H-TMCH, where the chalcones were obtained as two different double bond isomers. The synthetic approach of the chalcones together with their chemical reactivity and their biological evaluation were published recently.¹⁹⁵

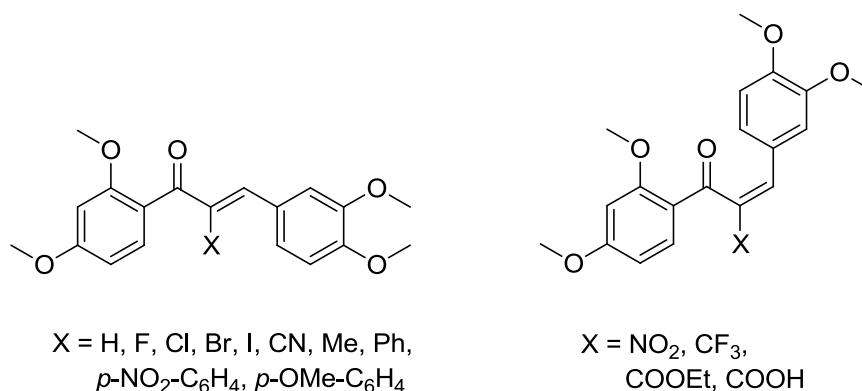
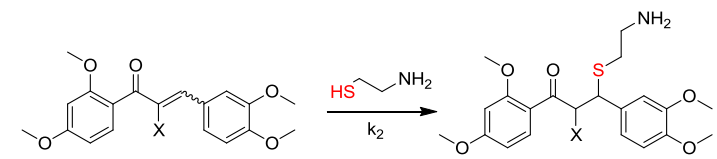


Figure 12. Structures of α -X-TMCHs tested for their *in vitro* anti-inflammatory and antioxidative activity.

For a broad range of reactivity, different electron withdrawing and electron donating substituents for the α -position were chosen. The more electron withdrawing groups like CN, NO₂, CF₃ or

halogens should increase the electrophilicity of the chalcones, whereas the Ph and Me groups should deactivate the Michael acceptor system towards nucleophiles. The Michael acceptor activity of the α -X-TMCHs was tested in our group by Nafisah Al-Rifai and Sabine Amslinger via the thiol assay (see chapter 1.6.2). The reaction constants k_2 of the thia-Michael additions to cysteamine and thus the electrophilic potential of the α -X-TMCHs are displayed in Table 2. As expected, the more electron withdrawing groups CN, NO₂, CF₃, Br and Cl are increasing the reactivity, in the case of α -CN-TMCH even in a tremendous way, namely more than 6 orders of magnitude when compared with α -COOH-TMCH, the chalcone with the lowest observed reactivity. The Me and Ph group along with the COOH group, which is supposed to be deprotonated under physiological conditions, reduced the activity compared to α -H-TMCH. Interestingly, the most electron negative halogen, α -F-TMCH, acts deactivating on the Michael acceptor reactivity, suggesting that in this case the resonance effect overrules the inductive effect of the halogen.

Table 2. Results of the kinetic measurements of α -X-TMCHs with cysteamine determined in our group.¹⁹⁵

		
α -X-chalcone	k_2 [^a] [M ⁻¹ s ⁻¹]	Rel. rate[^b]
CN	5750 \pm 130	1,600,000
NO ₂	749 \pm 9.0	200,000
CF ₃	17.1 \pm 1.8	4,600
Br	2.89 \pm 0.08	780
Cl	1.65 \pm 0.02	450
<i>p</i> -NO ₂ -C ₆ H ₄	0.293 \pm 0.025	79
I	0.282 \pm 0.015	76
COOEt	0.281 \pm 0.029	76
H	0.193 \pm 0.019	52
F	0.0168 \pm 0.00035	4.5
<i>p</i> -OMe-C ₆ H ₄	0.00856 \pm 0.0013	2.3
Me	0.00750 \pm 0.00039	2.0
Ph	0.00669 \pm 0.00029	1.8
COOH	0.00371 \pm 0.000060	1.0

[a] Reactions were carried out in 100 mM TRIS-HCl pH 7.4, 2 mM EDTA/ethylene glycol 20:80, 25 °C under pseudo-first order conditions at concentrations of 40 μ M for chalcones (80 μ M for NO₂ and CF₃) together with 12 to 500 fold cysteamine; [b] k_2 relative to k_2 (COOH).

Steric effects can also play a crucial role in the reactivity of the chalcones, overcompensating the electronic effects of the α -substituents. This can be observed for the less reactive α -I-TMCH compared to α -Br-TMCH or α -Cl-TMCH, for example, where the bulky iodo-substituent forces the

carbonyl group and the A ring of the chalcone out of the plane, leading to a reduced conjugation of the π -electron system as seen in the corresponding X-ray structure.¹⁹⁵ The quite distinct electrophilicity of α -X-TMCHs as shown in the kinetic assay makes them to excellent structures for a biological evaluation. Therefore, based on these results, the α -X-TMCHs were investigated for their ability to induce the anti-inflammatory and cytoprotective enzyme HO-1 on protein and activity level, using the HO-1 activity assay and Western blot analysis. On the other hand, their ability to inhibit the pro-inflammatory protein iNOS and thus the production of NO was tested via the Griess assay in the murine macrophage cell line RAW264.7. The cytotoxic concentrations of the compounds tested first in the MTT assay were excluded in the activity assays.

1.7.2 Limno-CP and its α -X-Limno-CP derivatives

Limnophila geoffrayi is a plant used in the traditional medicine of Thailand for detoxification.¹⁹⁶ Inspired by the plant ingredient limnophilaspiroketone, the model compound Limno-CP was chosen as a scaffold for a library of α -modified derivatives (α -X-Limno-CPs, Figure 13). It is known that 3(2H)-furanones display a rather weak Michael acceptor activity,¹⁹⁷ which makes them an ideal skeleton to start modifications from. Different substituents were introduced in the α -position of the 3(2H)-furanone unit in order to systematically influence the potential Michael acceptor based biological activity of these compounds.¹⁹⁸

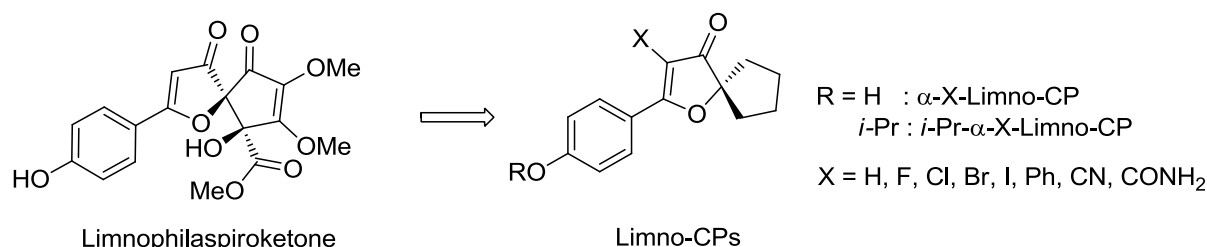


Figure 13. Model compounds α -X-Limno CPs derived from limnophilaspiroketone.

The α -X-Limno-CPs were synthesized by Simon Lindner in our group.¹⁹⁹ Two sets of compounds were prepared, one bearing the isopropyl protected phenolic group (*i*-Pr- α -X-Limno-CP) and the second set with the free phenolic group (α -X-Limno-CP). It could be demonstrated that the α -modifications have a significant effect on the ¹³C NMR chemical shifts of the β -carbon as the reactive center of the Michael system, comprising chemical shifts of 184 ppm for α -H Limno-CP up to 167 ppm for α -F-Limno-CP and down to 185 ppm for α -CN-Limno-CP.¹⁹⁸ Based on the ¹³C NMR chemical shifts the Limno-CP derivatives have been considered as moderate Michael acceptors, which could be useful in addressing reactive SH groups on specific protein targets. Additionally, a potential antioxidative activity can be addressed to the phenolic group on the enone unit. Therefore the α -X-Limno-CP compounds were tested towards their anti-inflammatory activity in the Griess assay and their antioxidant capacity in the ORAC-fluorescein assay.

1.8 The anti-inflammatory activity of both enantiomers of arteludovicinolide A

Artemisia (Asteraceae) are widely abundant plants playing a special role in the Chinese folk medicine.²⁰⁰ First isolated in 1991 from the aerial parts of *Artemisia ludoviciana*,²⁰¹ the sesquiterpene lactone arteludovicinolide A displays anti-inflammatory activity, demonstrated by the inhibition of NO production in LPS activated RAW264.7 macrophages.²⁰² One important structural feature of the natural product is the α -methylene group on the lactone unit, which is part of one of the two Michael acceptor moieties present in the compound. The second Michael acceptor functionality is part of the cyclopentenone ring and was found to play an important role in the biological activity of such sesquiterpenes.²⁰³ The electrophilicity and thus the reactivity towards SH-nucleophiles of these two Michael acceptor units is to a certain degree restricted, due to: i) the sterical hindrance of the methyl group in β -position of the α,β -unsaturated carbonyl compound on the cyclopropanone ring, and ii) the ester group on the lactone ring deactivating the potential Michael acceptor activity. However, the free *exo*-methylene group should favor the attack of a nucleophile on the β -position. Taken together, all these special structural features may contribute to a distinct biological activity of these sesquiterpenes.

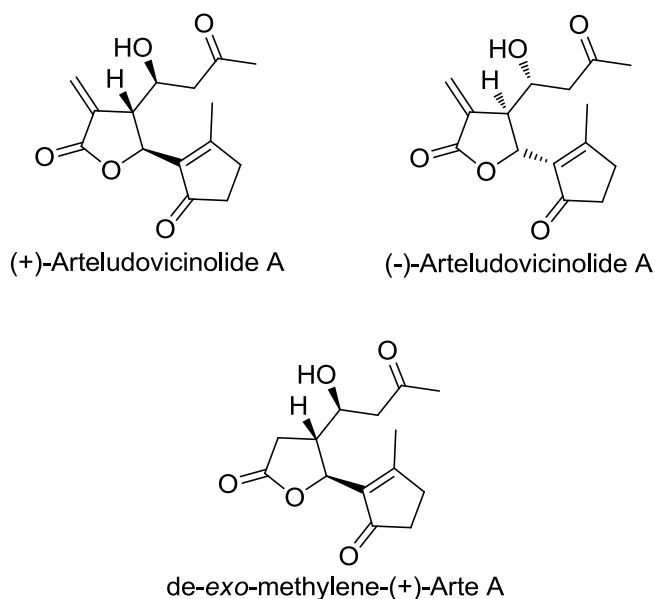


Figure 14. Structures of both enantiomers of arteludovicinolide A and a derivative lacking the *exo*-methylene group of the lactone ring, which were tested for their anti-inflammatory activity in murine macrophages RAW264.7.

The naturally occurring (+)-arteludovicinolide A, along with the synthetic (-)-enantiomer and a derivative of the former, lacking the *exo*-methylene group on the lactone ring, de-*exo*-methylene-(+)-arte A (Figure 14) were synthesized by Andreas Kreuzer (research group of O. Reiser, Universität Regensburg)²⁰⁴ and investigated in this work towards their cytotoxic and anti-inflammatory activity in murine macrophages RAW264.7. The synthesis of compounds together with their biological investigations were published recently.²⁰⁵

1.9 Enzyme-triggered CO-releasing molecules (ET-CORMs)

Carbon monoxide (CO) is an important biological signaling molecule and is envisioned as a therapeutic agent because it exerts cytoprotection, vasodilatory and anti-inflammatory properties.²⁰⁶ CO can influence the activity of the proinflammatory enzyme inducible NO-synthase (iNOS). On the transcriptional level, CO can inhibit the activation of the transcription factor NF- κ B and thus the protein expression of iNOS.⁸⁵ On the protein level, CO can block the formation of the active iNOS dimer²⁰⁷ or bind to the iron on the heme prosthetic group of iNOS and inhibit its catalytic activity to produce NO (Figure 15).²⁰⁸

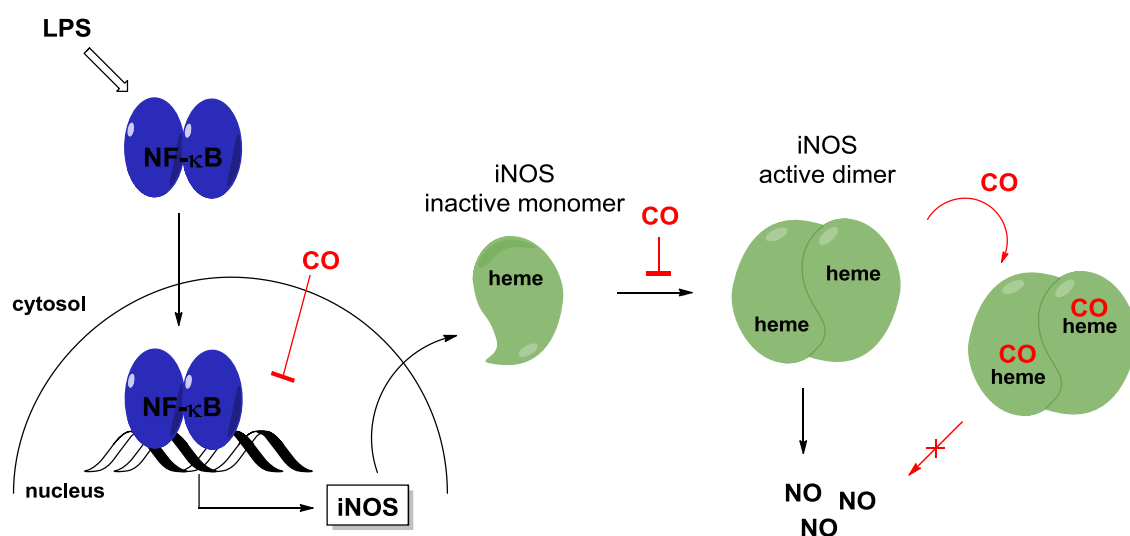
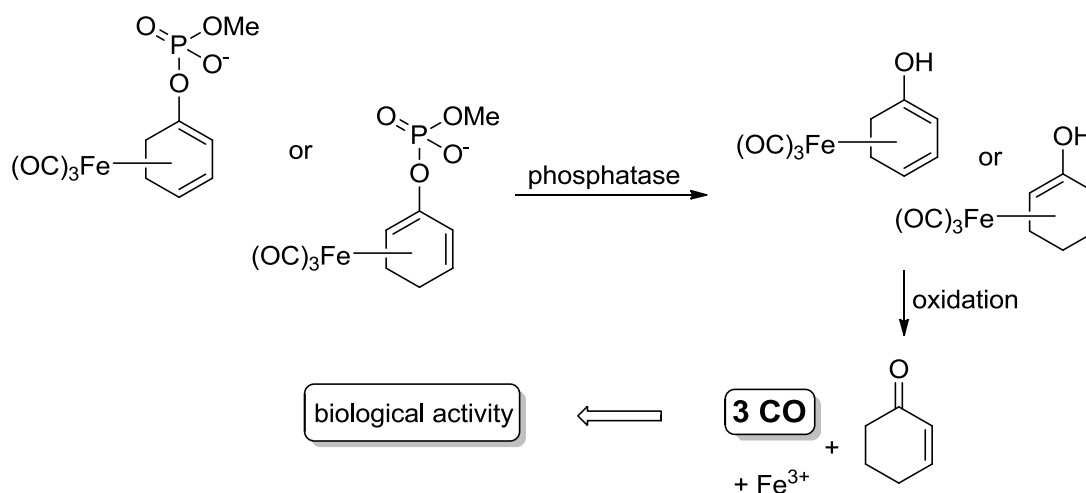


Figure 15. Potential regulation of CO of transcription and protein activity of inducible NO-synthase (iNOS). Activation of transcriptional factor NF- κ B can be induced by lipopolysaccharide (LPS).

The use of gaseous CO is however risky and limited, due to its low bioavailability, its high affinity to hemoglobin causing hypoxia and the inhibition of the mitochondrial electron transport chain resulting in a breakdown of the energy supply. To overcome these problems a new strategy was developed, using CO releasing molecules (CORMs) that ensure a controlled delivery of CO directly to the tissue.²⁰⁹ The first generation of CORMs comprised transition-metal carbonyl complexes, while many efforts were made concerning the stability, the water solubility and the CO-release under physiological conditions, for a possible application of CORMs in medicine.²¹⁰ Together with the group of H.-G. Schmalz (Universität zu Köln) a new concept was established for enzyme-triggered CO-releasing molecules (ET-CORMs) based on acyloxydiene-Fe(CO)₃ complexes, (Figure 17), which were characterized towards their toxicity and inhibition on NO production by Birgit Kraus (research group of J. Heilmann, Universität Regensburg) and Sabine Amslinger.²¹¹⁻²¹² Further modifications towards water soluble phosphorester-based ET-CORMs were accomplished.²¹³ The idea is that upon enzymatic ester cleavage in the cell, the obtained (hydroxycyclohexadiene)Fe(CO)₃ complexes subsequently decompose under oxidative conditions to give the enone ligand, an Fe³⁺ ion and three CO molecules (Scheme 5).



Scheme 5. Proposed mechanism of action displayed by phosphorester-based enzyme-triggered CO-releasing molecules (ET-CORMs).²¹³ The phosphatase-catalyzed cleavage of the phosphorester gives the (hydroxy-cyclohexadiene)Fe(CO)₃ complexes as intermediates, which decompose under oxidative conditions to the enone ligand, a Fe³⁺ ion and three CO molecules.

As part of a collaboration with the group of H.-G. Schmalz, the biological activity of two ET-CORMs, *rac*-**17** and *rac*-**18**, (Figure 16), which displayed a reasonable water solubility and were able to release CO on activation by different acid phosphatases, was investigated in the murine macrophage cell line RAW264.7 towards their toxicity and inhibition of LPS induced NO production.

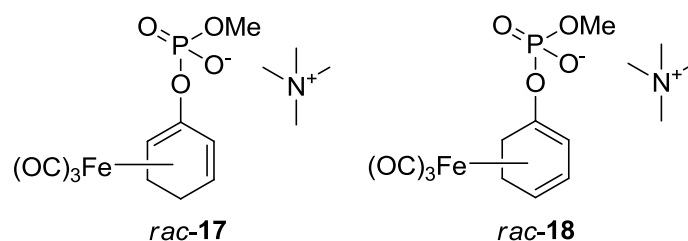


Figure 16. Structures of phosphorester-based ET-CORMs tested towards their anti-inflammatory activity.

The enzyme-triggered decomposition of ET-CORMs releases not only CO and free iron (III) ions but also the cycloenone ligand, which can further decompose and exert an anti-inflammatory activity or even higher cytotoxicity. Consequently, the overall biological activity of ET-CORMs may not only be contributed to the release of CO alone but also to the decomposition products or a combination of both. In our recent study, the possible degradation product 2-cyclohexenone, obtained upon decomposition of acyloxycyclohexadiene-Fe(CO)₃ was shown to strongly contribute to the overall activity of the monoester complexes of ET-CORMs, demonstrated by a significant inhibition of NO production of 2-cyclohexenone in RAW264.7 macrophages.²¹²

In order to investigate an influence of the possible degradation products on the biological response of ET-CORMs, some more phenolic and cyclohexanone derivatives **1-5** (Figure 17) were tested towards their toxicity and inhibition of NO production.

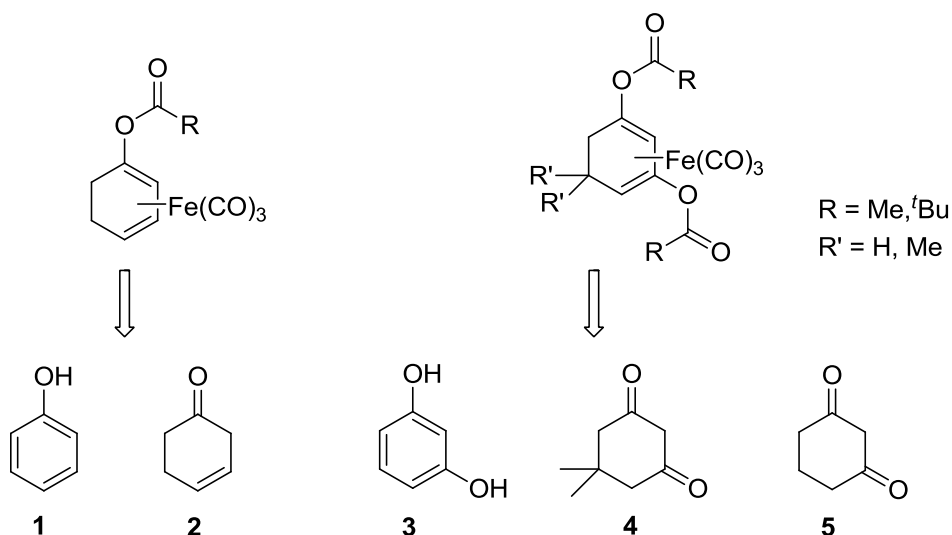


Figure 17. Structures of possible decomposition products (1-5) of mono- or diesters of acyloxydiene-Fe(CO)₃ complexes of potential ET-CORMs.

Also a possible involvement of the free ions Fe²⁺ and Fe³⁺ on the biological activity of ET-CORMs was tested, since it was shown that Fe³⁺ inhibited NOS activity in LPS-treated murine macrophages J774A.1 by controlling its nuclear transcription²¹⁴ and that Fe²⁺ ions reduce NO in patients suffering from ACE inhibitor-induced cough.²¹⁵

1.10 Aim of this study

This work is aimed to characterize and evaluate several natural and synthetic α,β -unsaturated carbonyl compounds towards their anti-inflammatory and antioxidant properties *in vitro*. Using the murine macrophage cell line RAW264.7, a reliable and sensitive ELISA-based HO-1 activity assay was established in order to screen for new anti-inflammatory and cytoprotective HO-1 activity inducers, useful as lead structures for drug development. The concept of modulating the Michael acceptor reactivity by introducing different substituents in α -position of the α,β -unsaturated carbonyl moiety in model compounds leading to a fine-tuned biological activity was assessed in different biological settings including: i) their inductive effect on the HO-1 activity determined by the established HO-1 activity assay, ii) their inhibitory effect on the NO production in RAW264.7 macrophages stimulated with LPS and measured by the Griess assay and iii) their antioxidant capacity and radical scavenging properties using the cell-free ORAC-fluorescein assay.

2 Materials and Methods

2.1 Materials

2.1.1 Cell lines

For this study the murine macrophage cell line RAW264.7 was used, a kind gift from T. Grune (Humboldt Universität Berlin). The cell line was established from murine tumors induced with Abelson leukemia virus.²¹⁶ A second cell line used in this work was the human colon cancer cell line HT-29, firstly isolated from primary colorectal adenocarcinoma tumor cells in 1964.²¹⁷ Samples of dendritic cells (DC) derived from human monocytes obtained from blood samples of healthy donors were kindly provided by the Department of Internal Medicine III, Universitätsklinikum Regensburg.

2.1.2 Cell culture media, buffers and reagents for cell culture

All cell culture media and reagents were purchased from Biochrom AG, Berlin unless otherwise described.

media/buffer/reagent	comment
RPMI 1640 medium	with phenol red, w/o L-glutamine w/o phenol red, w/o L-glutamine
DMEM	1.0 g mL ⁻¹ D-glucose
Sodium pyruvate	100 mM
Non-essential amino acids	100 x
Trypsin/EDTA solution	10 x in PBS
L-glutamine	200 mM
FCS Superior	heat inactivated: 30 min at 56 °C
PBS	Sigma, Steinheim

The following fully supplemented culture media were used for cell culture and all cell-based assays including the preparation of the final concentrations of test compounds.

RPMI cell culture medium with 10% FCS and 2 mM L-glutamine	500 mL RPMI with phenol red, 50 mL FCS, heat inactivated, 5 mL L-glutamine
Colorless RPMI cell culture medium with 10% FCS and 2 mM L-glutamine	500 mL RPMI without phenol red, 50 mL FCS, heat inactivated, 5 mL L-glutamine
DMEM cell culture medium	500 mL DMEM, 50 mL FCS, heat inactivated, 5 mL sodium pyruvate, 5 mL non-essential amino acids

2.1.3 Antibodies, proteins and enzymes

Anti-bilirubin antibody, 24G7, 1 mg mL ⁻¹	Shino-Test, Kanagawa, Japan
HRP-conjugated anti-mouse antibody, 2 mg mL ⁻¹	Rockland, Gilbertsville, PA, USA
Anti-HO-1 antibody, mouse, monoclonal, 1 mg mL ⁻¹	StressMarq, Victoria, Canada
Anti- α -tubulin antibody, mouse, monoclonal, clone DM1A, Cat.No. IMG-80196	IMGENEX, San Diego, CA, USA
Biliverdin reductase (BVR), recombinant rat protein, 1 mg mL ⁻¹ , 180 nmol min ⁻¹ mg ⁻¹	Stressgen, assay designs, Ann Arbor, MI, USA
Protease inhibitor cocktail, complete tablets	Roche, Mannheim
BSA, Cohn Fraction V, pH 5	Biomol, Hamburg

2.1.4 Kits

Detergent compatible protein assay	BioRad, Munich
Super Signal West Dura Extended Duration Substrate	Thermo Scientific, Rockford, IL, USA

2.1.5 Chemicals and reagents

(-)-Epicatechin	AppliChem, Darmstadt
1,4-Dithiothreitol	Merck, Darmstadt
2,2'-Azobis(2-methylpropionamidine) dihydrochloride (AAPH)	Acros Organics, Geel, Belgium
2-Mercaptoethanol	Serva, Heidelberg
3-[4,5-Dimethylthiazol-2-yl]-2,5-diphenyltetrazolium bromide (MTT)	Sigma-Aldrich, Steinheim
3-Hydroxycoumarin	Sigma-Aldrich, Steinheim
Ammonium persulfate	Merck, Darmstadt
Bilirubin-IX α	Frontier Scientific, Carnforth, UK
Brij 97	Sigma, Steinheim
Bromophenol Blue	Merck, Darmstadt
Caffeic acid	Acros Organics, Geel, Belgium
Caffeic acid phenethyl ester (CAPE)	Roth, Karlsruhe
Cardamonin	Calibochem (Merck Group), Darmstadt

Carnosol	Cayman Chemical, Ann Arbor, MI, USA
Chlorogenic acid	Cayman Chemical, Ann Arbor, MI, USA
Citric acid monohydrate	Merck, Darmstadt
Coomassie brilliant blue G-250	Biomol, Hamburg
Dexamethasone	Sigma-Aldrich, Steinheim
Disodiumhydrogenphosphate dihydrate	Merck, Darmstadt
Disodiumhydrogenphosphate monohydrate	Merck, Darmstadt
DMSO	Merck, Darmstadt
EDTA-Na ₂ x 2 H ₂ O (Titrplex)	Merck, Darmstadt
Ethanol, p.a.	J.T.Baker, Deventer, Holland
Fluorescein	Sigma-Aldrich (Fluka), Steinheim
FeCl ₂ , anhydrous	Sigma-Aldrich, Steinheim
FeCl ₃ , anhydrous	Sigma-Aldrich, Steinheim
Gelatin from cold water fish skin	Sigma-Aldrich, Steinheim
Glycerin	VWR (Prolabo), Fontenay-sous-Bois, France
Glycine	Merck, Darmstadt
H ₂ O ₂ solution, 30% in water	Merck, Darmstadt
Hemin	Sigma-Aldrich (Fluka), Steinheim
Kaempferol	Calbochem (Merck Group), Darmstadt
Lipopolysaccharides (LPS from <i>Escherichia coli</i> 055:B4)	Sigma-Aldrich, Steinheim
Low fat milk powder	Saliter, Obergünzburg
Methanol	Merck, Darmstadt
N-(1-Naphtyl)ethylenediamine dihydro-chloride (NED)	Sigma-Aldrich (Fluka), Steinheim
N,N,N,N-Tetramethylethylenediamine (TEMED)	Sigma-Aldrich, Steinheim
NADPH	Biomol, Hamburg
Nonidet P-40 (NP 40)	Sigma-Aldrich (Fluka, BioChemika), Steinheim
Oltipraz	Sigma-Aldrich, Steinheim

<i>ortho</i> -Phenylenediamine dihydrochloride (OPD)	Acros Organics, Geel, Belgien
Phosphoric acid, 85%	Fluka, Buchs, Switzerland
Potassium chloride	Merck, Darmstadt
Potassium hydrogen phosphate	Merck, Darmstadt
Precision Plus Protein Standards	Bio Rad, Munich
Quercetin	Cayman Chemical, Ann Arbor, MI, USA
Resveratrol	Cayman Chemical, Ann Arbor, MI, USA
Rotiphorese Gel 30 (acrylamind-bisacrylamide-mix)	Roth, Karlsruhe
Sodium deoxycholate	Merck, Darmstadt
Sodium salicylate	Merck, Darmstadt
Sodiumdihydrogenphosphate monohydrate	Merck, Darmstadt
Sodiumdodecylsulfate (SDS)	Sigma-Aldrich, Steinheim
Sucrose	Sigma-Aldrich, Steinheim
Sulfanilamide	Merck, Darmstadt
Sulforaphane	Sigma-Aldrich, Steinheim
Sodium nitrite	Merck, Darmstadt
Tin protoporphyrin IX (SnPPiX)	Frontier Scientific, Carnforth, UK
Tris-(hydroxymethyl)-aminomethane (TRIS)	Merck, Darmstadt
Triton X-100	Merck, Darmstadt
Trolox, 97%	Acros Organics, Geel, Belgium
Tween-20	Merck, Hohenbrunn
Xanthohumol	Roth, Karlsruhe
Zerumbone	Sigma-Aldrich, Steinheim

2.1.6 Synthesis of compounds

The following compounds investigated in this work were synthesized in our working group (Universität Regensburg). The α -X-Limno-CP derivatives (5-aryl-3(2*H*)-furanones) were prepared by Simon Lindner. The α -X-tetramethoxychalcones, HTMCH, TMCH and flavokawain A were synthesized by Nafisah Al-Rifai. The bilirubin-BSA conjugate and the chalcones ISL, DHDMCH, THMCH and butein were prepared by Sabine Amslinger. Calythropsin was prepared

by Paul Baumeister. 2'-Hydroxychalcone was synthesized by Killian Wörmann. Further test compounds were kindly provided by members of other groups as part of several collaborations. The following compounds were provided by different group members of O. Reiser. Both enantiomers of arteludovicinolide A and the derivative de-*exo*-methylene-(+)-arte A were synthesized by Andreas Kreuzer. The γ -butyrolactone derivatives, GBL-**1** and GBL-**2** were synthesized by Mohd Tajudin Mohd Ali, diethylaminomethyl-GBL and α -methylene-GBL by Sabrina Fürst. A xanthatin derivative **AB-1** was synthesized by Andreas Bergmann. **MS-342 F9-F18**, a guaianolide derivative was synthesized by Michael Schwarz. 4-Hydroxy-2-cyclopentenone was synthesized by Peter Kreitmeier and eight cyclopentenone derivatives **KU 1-KU 8** were synthesized by Kathrin Ulbrich. Four chalcone analogs, **MS-C-01**, **SU-F-01**, **SU-C-02** and **SU-CT-03** were synthesized by Mihai Surducun, a visiting PhD student in the group of B. König (Universität Regensburg). The ET-CORMs *rac*-**17** and *rac*-**18** were synthesized and the compounds **1-5** were provided by Steffen Romanski, group member of H.-G. Schmalz (Universität zu Köln).

2.1.7 Buffers and solutions

All buffers and solutions were prepared with ultrapure water, filtered over a nitrate cellulose filter (0.45 nm) and degassed for 10 min in the ultrasound bath.

2.1.7.1 Cell lysis

Lysis buffer stock solution (2x), pH 8.0	80 mM TRIS-HCl, 500 mM sucrose, 4 mM EDTA, 274 mM NaCl, 20% (v/v) glycerin, stored at 4 °C
TRIS-HCl buffer stock solution, pH 7.4	500 mM in H ₂ O, stored at 4 °C
Sucrose stock solution	2 M in H ₂ O, stored at room temperature
EDTA stock solution	125 mM in H ₂ O, stored at room temperature
NaCl stock solution	1 M in H ₂ O, stored at room temperature
Triton X-100, 10% (v/v)	1 mL detergent, ad 10 mL H ₂ O, stock solution stored at room temperature protected from light
Nonidet P-40, 10% (v/v)	
Sodium deoxycholate, 10% (v/v)	
Brij 97, 10% (v/v)	
SDS, 10% (v/v)	
Complete protease inhibitor cocktail (25x, Roche)	dissolve 1 tablet in 2 mL H ₂ O, stored at 4 °C, stable for 1-2 weeks
Lysis buffer, pH 7.4	40 mM TRIS-HCl, 250 mM sucrose, 2 mM EDTA, 137 mM NaCl, 10% (v/v) glycerin, 0.1% Triton X-100, 4% (v/v) complete protease inhibitor cocktail, stored at 4 °C

2.1.7.2 Protein assay

BSA stock solution	2 mg mL ⁻¹ in BSA buffer, stored at 4 °C
BSA buffer	150 mM NaCl, 0.05% NaN ₃ , stored at 4 °C
Bradford reagent	100 mg coomassie brilliant blue G-250, 100 mL 85% phosphoric acid, 50 mL ethanol, ad 1 L H ₂ O, dissolved over night in the dark at 4 °C and filtered twice over round cellulose filters, stored in brown flaks at 4 °C

2.1.7.3 HO enzymatic reaction

TRIS-HCl/sucrose buffer, pH 7.4	40 mM TRIS-HCl, 250 mM sucrose, stored at room temperature
NADPH stock solution	15 mM in H ₂ O, prepared freshly, kept at 4 °C
Hemin stock solution	250 µM in DMSO, 100 µL aliquots stored at -20 °C
BVR enzyme solution	1 ng mL ⁻¹ in BVR buffer, 100 µL aliquots stored at -20 °C
BVR buffer	50 mM TRIS-HCl, pH 8.0 ,1 mM EDTA, 5 mM DTT, stored at 4 °C
Bilirubin stock solution	10 mM in DMSO, prepared freshly
NaOH	1 M in H ₂ O, stored at room temperature
HCl	1 M in H ₂ O, stored at room temperature

2.1.7.4 ELISA for bilirubin quantification

PBS, pH 7.4	8.0 g NaCl, 0.20 g KCl, 1.44 g Na ₂ HPO ₄ , 0.24 g KH ₂ PO ₄ , ad 1 L H ₂ O, stored at 4 °C
Bilirubin-BSA conjugate	0.71 mg mL ⁻¹ in PBS, 200 µL aliquots stored at -20 °C
Coating solution	0.035 µg mL ⁻¹ bilirubin-BSA conjugate in PBS
Wash buffer (T-PBS)	0.1% (v/v) Tween-20 in PBS, pH 7.4, stored at room temperature
Blocking solution, 3% G-PBS	3.33 g gelatin, ad 50 mL PBS, pH 7.4, stored at 4 °C
1% G-PBS	1.11 g gelatin, ad 50 mL PBS, pH 7.4 , stored at 4 °C
1. Antibody solution	0.571 µg mL ⁻¹ anti-bilirubin antibody, 0.5 mM sodium salicylate in 1% G-PBS solution,

	prepared freshly
2. Antibody solution	0.2 $\mu\text{g mL}^{-1}$ HRP-conjugated anti-mouse antibody in 1% G-PBS solution, prepared freshly
Citrate buffer, pH 5.0	48.6 mM citric acid monohydrate, 102.8 mM $\text{Na}_2\text{HPO}_4 \times \text{H}_2\text{O}$, stored at room temperature
Substrate solution	0.4 mg mL^{-1} OPD, 0.4 $\mu\text{L mL}^{-1}$ H_2O_2 (30%) in citrate buffer, pH 5.0, prepared freshly
Stop solution	3 M H_2SO_4
2.1.7.5 Liver cytosol extract preparation	
Saline	0.9% (w/v) NaCl in H_2O
TRIS-HCl/sucrose buffer	20 mM TRIS-HCl, 250 mM sucrose, pH 7.4
2.1.7.6 ORAC-fluorescein assay	
Phosphate buffer, 75 mM, pH 7.4	solution A: 75 mM Na_2HPO_4 , solution B: 75 mM NaH_2PO_4 , ad solution B to A to adjust to pH 7.4, stored at 4 °C
Fluorescein stock solutions	500 μM in phosphate buffer, 75 mM, pH 7.4, dissolved using an ultrasound bath, stored at 4 °C protected from light 500 nM in phosphate buffer, 75 mM, pH 7.4, prepared freshly
Trolox stock solutions	8 mM in phosphate buffer, 75 mM, pH 7.4, stored at 4 °C 800 μM in phosphate buffer, 75 mM, pH 7.4, prepared freshly
AAPH	40 mM in phosphate buffer, 75 mM, pH 7.4, prepared freshly
2.1.7.7 Nitrite detection with Griess	
Griess reagent	20 mg NED, 200 mg sulfanilamide, 70 μL H_3PO_4 (85%), ad 20 mL H_2O , dissolve in water bath, prepared freshly, stored in the dark
Nitrite standard	1 mM NaNO_2 in cell culture media without phenol red, stored at 4 °C
LPS stock solution	200 $\mu\text{g mL}^{-1}$ in PBS, stored at 4 °C
2.1.7.8 MTT assay	
MTT reagent	4 mg mL^{-1} in PBS, stored at 4 °C

SDS solution, 10% (w/v)	50 g SDS, ad 500 mL H ₂ O, stored at room temperature
LPS stock solution	200 µg mL ⁻¹ in PBS, stored at 4 °C
2.1.7.9 Western blot	
Electrophoresis buffer (1x), pH 8.3	3.03 g TRIS, 14.4 g glycine, 1.0 g SDS, ad 1 L H ₂ O, stored at 4 °C
Transfer buffer (1x), pH 8.3	3.03 g TRIS, 14.4 g glycine, 20% (v/v) methanol, ad 1 L H ₂ O, stored at 4 °C
Separating gel buffer (4x), pH 8.8	90.9 g TRIS, 2.0 g SDS, ad 500 mL H ₂ O, stored at room temperature
Stacking gel buffer (2x), pH 6.8	15.14 g TRIS, 1.0 g SDS, ad 500 mL H ₂ O, stored at room temperature
Sample buffer (3x), pH 6.8	727 mg TRIS, 5.0 g SDS, 30.0 g glycine, 10.0 g sucrose, 3.0 g β-mercaptoethanol, 0.5 g bromophenol blue, ad 100 mL H ₂ O, stored at room temperature
Wash buffer (1x), pH 7.4	2.48 g TRIS, 8.77 g NaCl, 0.05% Tween 20, ad 1 L H ₂ O, stored at 4 °C
Low-fat milk solution (1%)	1.25 g low-fat milk dry powder, 125 mL wash buffer (1x), prepared freshly
Low-fat milk solution (5%)	1.25 g low-fat milk dry powder, 25 mL wash buffer (1x), prepared freshly
APS solution (10%)	0.05 g ammonium persulfate, 500 mL H ₂ O, prepared freshly and kept at 4 °C
Separating gel (SDS-PAGE)	12 % (w/v) acrylamide, 375 mM TRIS-HCl pH 8.8, 0.1% (w/v) SDS, 0.1% (w/v) APS, 0.1% TEMED
Stacking gel (SDS-PAGE)	5% acrylamide, 125 mM TRIS-HCl pH 6.8, 0.1% (w/v) SDS, 0.1% (w/v) APS and 0.1% TEMED

2.1.8 Equipment

Analytical balance	SI-234, Denver Instruments, Göttingen Sartorius research, R160P, Sartorius, Göttingen
Autoclave	Typ 23, Melag, Berlin
Block heater	Techne Dri-Block DB-3D, Thermo Dux, Gesellschaft für Laborgeräte mbH, Wertheim

Cell culture microscope	Olympus CKX41-SF, Olympus, Hamburg
Centrifuges	Sigma 1-14, rotor 152-G, Sigma, Osterode Megafuge 1.0 R with rotor 2705, Heraeus Sepatech, Osterode Jouan BR4i multifunction centrifuge with rotor AB 1.14, Thermo Electron Corporation, Saint-Herblain, France Ultracentrifuge TGA 45, Kontron Instruments with rotor TFT 6513, reduced to 54.000 rpm, Zürich, Switzerland
Drying oven	AL01-03-100, 115 L, Advantage Lab, Schilde, Belgium
Electrophoresis and western blotting unit	Mini-Protean Tetra Handcast System, BioRad, Munich
Hot plate magnetic stirrer	IKA-RCT basic, safety control, IKA-Werke, Staufen
Incubator	New Brunswick Scientific, Nütringen
Laminar airflow cabinet	Clan LAF, ClausDamm, Fredensborg, Denmark
Luminescent image analyzer	LAS 3000 Fujifilm Intelligent Dark Box, Fuji Photo Film (Europe) GmbH, Düsseldorf Software: Image Reader LAS 3000, Fujifilm, Stamford, IL, USA
Microtiter plate reader	Multiskan Spectrum, Thermo, Vantaa, Finland
Neubauer cell counting chamber	Marienfeld, Landau-Königshofen
pH meter	WTW-inoLab pH level 1 with a SenTix-Mic-glas electrode, WTW, Weilheim
Platform shaker	Rocking platform shaker, VWR Collection, VWR, Darmstadt Vibrating platform shaker, Titramax 100, Hiedolph, Schwabach
Ultrapure water purification system	Milli-Q UF Plus, Millipore. Schwalbach with membrane from membranPure, Bodenheim
Ultrasound bath	Brandelin Sonorex Super RK 255-H, Brandelin Electronic GmbH & Co. KG, Berlin
Ultraturex	B. Braun, Melsungen AG, Melsungen
Vacuum pump	ME 2C, Vaccubrand GmbH, Wertheim

Vortex shaker	IKA-Vortex Genius 3, IKA-Werke, Staufen IKA-Lab Dancer, IKA-Werke, Staufen
Water bath	WBU 45 Memmert, Schwabach
2.1.9 Consumables	
Centrifuge tubes, 15/50 mL	sterile, for cell culture, Greiner Bio-One, Frickenhausen, TPP, Trasadingen, Switzerland non-sterile, 15 mL, Roth, Karlsruhe sterile, 50 ml, VWR , Darmstadt
Serological pipettes, 5/10/25 mL	sterile, for cell culture, Greiner Bio-One, Frickenhausen, TPP, Trasadingen, Switzerland
Cell culture flasks, 25/75/150 cm ²	Greiner Bio-One, Frickenhausen, TPP, Trasadingen, Switzerland
Cell scraper M	TPP, Trasadingen, Switzerland
Microplates	
6-well plates	for cell culture, Becton Dickinson Labware, Le Pont De Claix, France, TPP, Trasadingen, Switzerland
96-well plates	for cell culture, TPP, Trasadingen, Switzerland non-steril, non-treated surface, pureGrade, BRAND, Wertheim for ORAC assay, F-bottom, GreinerBio-One, Frickenhausen ELISA immunoplates, Nunc, Roskilde, Denmark
Centrifuge tubes, 1.5/2 mL	Eppendorf, Hamburg, Roth, Karlsruhe
Cellulose nitrite filter	pore size 0.45 µm, Satorius Stedim, Göttingen
PVDF membrane	pore size 0.45 µm, Millipore, Billerica, MA, USA
pH test stripes	pH fix test stripes, pH 1-14, Roth, Karlsruhe
Nitrocellulose membrane	pore size 0.55 µm, Bio-Rad, Munich
Whatman blotting paper	1.0 mm, Roth, Karlsruhe
Filter paper circles	Ø 185 mm, Scheicher & Schuell, Dassel

2.2 Methods

2.2.1 Cell culture

Murine macrophage cells RAW264.7 were cultured in RPMI 1640 medium with phenol red supplemented with 10% (v/v) heat inactivated fetal calf serum (FCS) and 2 mM glutamine at 37 °C in humidified air containing 5% CO₂. The adherent cells were split three times a week before reaching confluence. For splitting the culture medium was removed, 10 mL of fresh medium was added and cells were scraped off the flask bottom. The cell suspension was diluted 1:20 or 1:10 with 20 mL of fresh culture medium in the same culture flask. Every week the cells were split in a new flask.

The human colon cancer cells HT-29 were grown in DMEM supplemented with 10% (v/v) heat inactivated fetal calf serum (FCS), 1% (v/v) non-essential amino acids and 1% (v/v) sodium pyruvate. Cells were cultured at 37 °C in humidified air containing 5% CO₂. The adherent cells were split once a week before reaching confluence. Every second to third day the cell culture media was changed. For splitting, the culture medium was removed, cells were washed with 10 mL of PBS and 2 mL of a trypsin/EDTA solution was added. The adherent cells were then incubated for 5 min at 37 °C in order to detach them from the bottom of the cell culture flask. The trypsinization was stopped by the addition of 6 mL of fresh DMEM and the cell suspension was centrifuged at 700 rpm for 5 min at RT. The cell pellet was resuspended in 5 mL of fresh DMEM and the cell suspension was diluted 1:10 with 10 mL of fresh culture medium in a new culture flask.

2.2.1.1 Cell counting

The cell number in the cell suspension was determined as cells/mL, by using a cell counting chamber. Dead cells were stained with a 0.4 mg mL⁻¹ trypan blue solution in PBS and were excluded from counting.

2.2.1.2 Cell sample preparation

Cells were seeded out on 96-well plates for cell viability or protein activity assays (HO-1 or Griess assay) at different cell concentrations in 150 µL of medium/well and allowed to attach for 24 h. For western blot analysis 3 × 10⁶ RAW264.7 cells/well in 5 mL of medium were placed in 6-well plates and allow to attach for 24 h. After removing the culture medium, cells were incubated with the test compounds diluted in culture media in several concentrations for different incubation times, maximum for 24 h.

2.2.2 Dilution of test compounds

Stock solutions of test compounds (100 mM) were prepared in DMSO and stored at -20 °C. Final test concentrations of compounds were freshly prepared by diluting the stock solution in fully supplemented culture medium. The final concentration of DMSO in the medium was below 0.1%.

At this concentration the solvent had no effect on the cell viability of RAW264.7 or HT-29 cells or other tested activity compared to control cells. The SnPPIX stock solution (10 mM) was prepared freshly in a 0.10 mM aqueous solution of NaOH and diluted in culture medium to yield the test concentration. The ET-CORMs, FeCl₂, FeCl₃ and compounds **1-5** (potential decomposition products of ET-CORMs) were diluted in ethanol and stock solutions were prepared at 40 and 400 mM. Test concentrations were freshly prepared by diluting the stock solution in culture medium. The final concentration of ethanol in the medium was below 0.25%. At this concentration the solvent had no effect on the cell viability of RAW264.7 cells or other tested activity compared to control cells.

2.2.3 Viability assay (MTT assay)

To exclude cytotoxicity of test compounds, a cell viability assay was performed. Cell viability was evaluated by determining the mitochondrial function of living cells on the basis of their ability to reduce the yellow tetrazolium salt MTT (3-[4,5-dimethylthiazol-2-yl]-2,5-diphenyltetrazolium bromide) into a violet formazan dye by mitochondrial reductases.²¹⁸

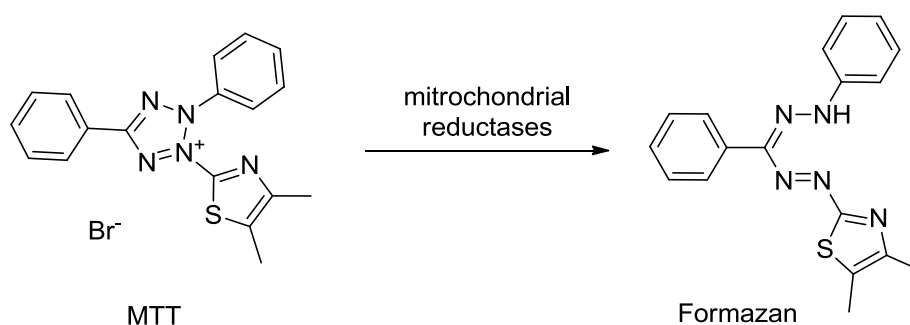


Figure 18. The reduction reaction of the tetrazolium salt MTT to a formazan dye, is catalyzed by mitochondrial reductases only in living cells and is therefore used to assess cytotoxicity.

Cells (RAW264.7: 5000/well and HT-29: 20,000/well) were plated into 96-well plates and allowed to attach for 24 h. The total assay volume was 100 μ L. Control cells were incubated only with culture medium with or without DMSO or EtOH, according to the solvent used in the stock solution. The test compounds were added to wells in several concentrations and incubated for 20 h (Scheme 6). Then, 10 μ L of 4 mg mL⁻¹ MTT in PBS were added to each well. After 4 h the culture medium was removed and 100 μ L of a 10% SDS solution were put in each well to solubilize the formazan product. The absorbance was measured at 560 nm with a microplate reader (Multiskan Spectrum Photometer) after 24 h incubation in darkness at room temperature. Cell viability was expressed as percent compared to control cells incubated only with medium.

	1	2	3	4	5	6	7	8	9	10	11	12
A		100			100			100				
B		75			75			75			control cells	
C		50	test compound 1		50	test compound 2		50	test compound 3			
D		25	[μM]		25	[μM]		25	[μM]			
E		10			10			10				
F		5			5			5			solvent control	
G		1			1			1				
H		0.5			0.5			0.5				
5,000 RAW264.7 cells or 20,000 HT-29 cells/well in 100 μL medium												

Scheme 6. Pipetting scheme for a 96-well plate used in the MTT-cytotoxicity assay. Columns 1 and 12 were filled with medium alone, the wells between column 2 and 11 were plated with cells as indicated: control cells were incubated with medium alone; stimulated cells were incubated with the test compounds in medium in several concentrations; solvent control cells were incubated with medium supplemented with the highest solvent concentration used in the assay.

2.2.4 Viability assay with lipopolysaccharide (MTT-LPS assay)

RAW264.7 cells were seeded in 96-well plates at a density of 5000 per well, cultured for 24 h, and then incubated for 20 h with RPMI medium without phenol red supplemented with test compounds in presence and absence of 10 ng mL⁻¹ of LPS (lipopolysaccharide). Controls received only culture medium (without phenol red), with or without DMSO or EtOH, according to the solvent used in the stock solution, both in presence and absence of 10 ng mL⁻¹ of LPS (Scheme 7). Total assay volume was 100 μL. Afterwards, 10 μL of a MTT solution (4 mg mL⁻¹ in PBS) were added to each well, and cells were incubated for another 4 h at 37 °C. Subsequently, the culture medium was removed from wells and 100 μL of a 10% SDS solution was added, and formazan was allowed to dissolve overnight. The absorbance was determined at 560 nm with a Multiskan Spectrum Photometer. Cell viability was expressed as percent compared to control cells incubated only with medium.

	1	2	3	4	5	6	7	8	9	10	11	12
A												
B		control cells	solvent control	100	75	50	25	10	5	1	0.5	
C		w/o LPS	w/o LPS			test compound [μ M]			w/o LPS			
D												
E												
F		control cells	solvent control	100	75	50	25	10	5	1	0.5	
G		with LPS	with LPS			test compound [μ M]			with LPS			
H												
5,000 RAW264.7 cells/well in 100 mL RPMI culture medium												

Scheme 7. Pipetting scheme for a 96-well plate used in the MTT-LPS assay. Columns 1 and 12 were filled with medium alone, the wells between column 2 and 11 were plated with 5000 RAW264.7 cells/well: control cells were incubated with medium alone; stimulated cells were incubated with different concentrations of the test compound in medium; solvent control cells were incubated with medium supplemented with the highest solvent concentration used in the assay. In row A to D cells were incubated without LPS, the cells in row E to H were incubated in the presence of 10 ng mL⁻¹ of LPS.

2.2.5 Nitrite assay (Griess assay)

The produced NO that accumulated as nitrite in the culture medium was quantified using the Griess reaction. RAW264.7 macrophages (8×10^4 cells/well) were plated in 96-well plates and allowed to attach for 24 h.

	1	2	3	4	5	6	7	8	9	10	11	12
A												
B		control cells	solvent control	100	75	50	25	10	5	1	0.5	
C		w/o LPS	w/o LPS			test compound [μ M]			w/o LPS			
D												
E												
F		control cells	solvent control	100	75	50	25	10	5	1	0.5	
G		with LPS	with LPS			test compound [μ M]			with LPS			
H												
80,000 RAW264.7 cells/well in 100 mL RPMI culture medium												

Scheme 8. Pipetting scheme for a 96-well plate used in the Griess nitrite assay. Columns 1 and 12 were filled with medium alone, the wells between column 2 and 11 were plated with 80,000 RAW264.7 cells/well: control cells were incubated with medium alone; stimulated cells were incubated with different concentrations of the test compound in medium; solvent control cells were incubated with medium supplemented with the highest solvent concentration used in the assay. In row A to D cells were incubated without LPS, the cells in row E to H were incubated in the presence of 10 ng mL⁻¹ of LPS.

Afterwards, 100 μL of fresh RPMI culture medium without phenol red supplemented with test compounds in presence and absence of 10 ng mL^{-1} LPS were added to the cells. Controls received only culture medium (without phenol red) with or without DMSO or EtOH, according to the solvent used in the stock solution, both in presence and absence of 10 ng mL^{-1} of LPS (Scheme 8). The cells were incubated for 24 h. 50 μL of culture medium was mixed with 50 μL of Griess reagent and incubated for 15 min at room temperature. The absorbance was measured at 560 nm with a Multiskan Spectrum Photometer and nitrite concentrations were calculated from a standard curve established with serial dilutions (0/5.0/10/25/50 μM) of NaNO_2 in RPMI culture medium without phenol red. Nitrite production was expressed as percent compared to control cells incubated only with medium in presence of 10 ng mL^{-1} LPS.

2.2.6 Activity assay for heme oxygenase-1 (HO-1)

2.2.6.1 Stimulation of RAW264.7 macrophages

For the HO-1 activity assay RAW264.7 cells (8×10^4 cells/well) were plated in 96-well plates, allowed to attach for 24 h and exposed to test compounds in various concentrations for 3 to 24 h. The total assay volume was 100 μL . Control cells were incubated with culture medium alone. (Scheme 9) After removing the culture medium, cells were washed with PBS (150 μL /well) and 96-well plates were stored at -80°C until utilized for the HO-1 assay.

	1	2	3	4	5	6	7	8	9	10	11	12
A								25				
B		control cells for bilirubin standards						10	compound 2			
C								5	[μM]		control cells	
D								1				
E					25			25				
F					10	compound 1		10	compound 3		solvent control	
G					5	[μM]		5	[μM]			
H					1			1				
80,000 RAW264.7 cells/well in 100 μL RPMI culture medium												

Scheme 9. Pipetting scheme for a 96-well plate with cell culture samples used in the HO-1 assay. Columns 1 and 12 were filled with medium alone, the wells between column 2 and 11 were plated with 80,000 cells/well: control cells were incubated with medium alone; stimulated cells were incubated with the test compounds in medium; solvent control cells were incubated with medium supplemented with the highest solvent concentration used in the assay.

2.2.6.2 Cell lysis

For cell lysis 150 μL of ice cold lysis buffer (40 mM TRIS-HCl, 250 mM sucrose, 137 mM NaCl, 10% (v/v) glycerin, 2 mM EDTA, 0.1% (v/v) Triton X-100 detergent, protease inhibitor cocktail from Roche, pH 7.4) was added to each well and the 96-well plate was placed on an orbital plate shaker and allowed to shake for 15 min at 4 $^{\circ}\text{C}$.

2.2.6.3 Determination of protein concentration

To avoid detergent interference the total protein concentrations in the cell lysate were determined using the Bio-Rad Detergent Compatible Protein Assay kit which is based on the Lowry assay.²¹⁹ Briefly, 5 μL of sample were mixed with 25 μL of a alkaline copper tartrate solution supplemented with a SDS solution and 200 μL of the Folin reagent and incubated for 30 min at room temperature according to the manufacturer instructions. The absorbance was read at 750 nm with a Multiskan Spectrum Photometer. Protein standards were prepared from a 2.0 mg mL^{-1} BSA standard solution by serial dilutions in lysis buffer (1.0/0.5/0.25/0.125/0 mg mL^{-1} BSA).

2.2.6.4 HO enzymatic activity

90 μL of the collected whole cell lysates were placed in a 96-well plate together with 10 μL of bilirubin standards solutions or the HO reaction mixture. Scheme 10 shows a typical 96-well sample plate used for the HO activity assay.

	1	2	3	4	5	6	7	8	9	10	11	12
A			0			250						
B			0.5			500					control cells	
C			1	control cells		1000					+ HO-reaction mixture	
D			2.5	+ 'bilirubin standards'		2500						
E			5	[nM]								
F			10				stimulated cells + HO reaction mixture				solvent control	
G			50								+ HO-reaction mixture	
H			100									
	90 μL of whole cell lysate + 10 μL of 'bilirubin standards' or HO reaction mixture											

Scheme 10. Pipetting scheme for a 96-well plate used in the HO activity assay. 90 μL of whole cell lysate was transferred on the plate between column 2 and 11 and incubated with 10 μL of the HO reaction mixture or 'bilirubin standards' for 1 h at 37 $^{\circ}\text{C}$. Lysates from control cells were incubated with 'bilirubin standards' and from stimulated cells, control cells and solvent control cells were incubated the HO reaction mixture.

Bilirubin (BR) standards were prepared in TRIS-HCl/sucrose buffer in several concentrations to give a final concentration in the well of 0.5-2500 $\cdot 10^{-9}$ M BR in 120 μL . 10 μL of 'bilirubin stand-

ards' were added to 90 μL of whole cell lysate from unstimulated control cells. For 'zero control' (B_0 value) 10 μL of TRIS-HCl/sucrose buffer were added to 90 μL of whole cell lysate of unstimulated control cells. Finally, 10 μL of the HO reaction mixture (Table 3) were added to 90 μL of the whole cell lysates from controls and samples. The assay volume was 100 μL . A pipette summary for each HO-1 assay sample is shown in Table 4.

Table 3. Components of the HO reaction mixture.

volume/ μL	assay component	final concentration in 100 μL reaction mixture
0.75	267 mM TRIS-HCl, pH 7.4	40 mM
1.25	1.2 M sucrose	250 mM
2.0	15 mM NADPH	300 μM
1.0	1.0 ng μL^{-1} BVR	0.01 ng μL^{-1}
1.0	250 μM hemin	2.5 μM
4.0	TRIS-HCl/sucrose buffer, pH 7.4	40/250 mM
90	whole cell lysate (10-30 μg protein)	

The reaction was performed at 37 $^{\circ}\text{C}$ in the dark for 1 h and terminated by the addition of 10 μL aqueous 1 M HCl. The plate was placed 5 min on ice and the pH was adjusted to 7.4 with 10 μL of aqueous 1 M NaOH. The total assay volume was 120 μL .

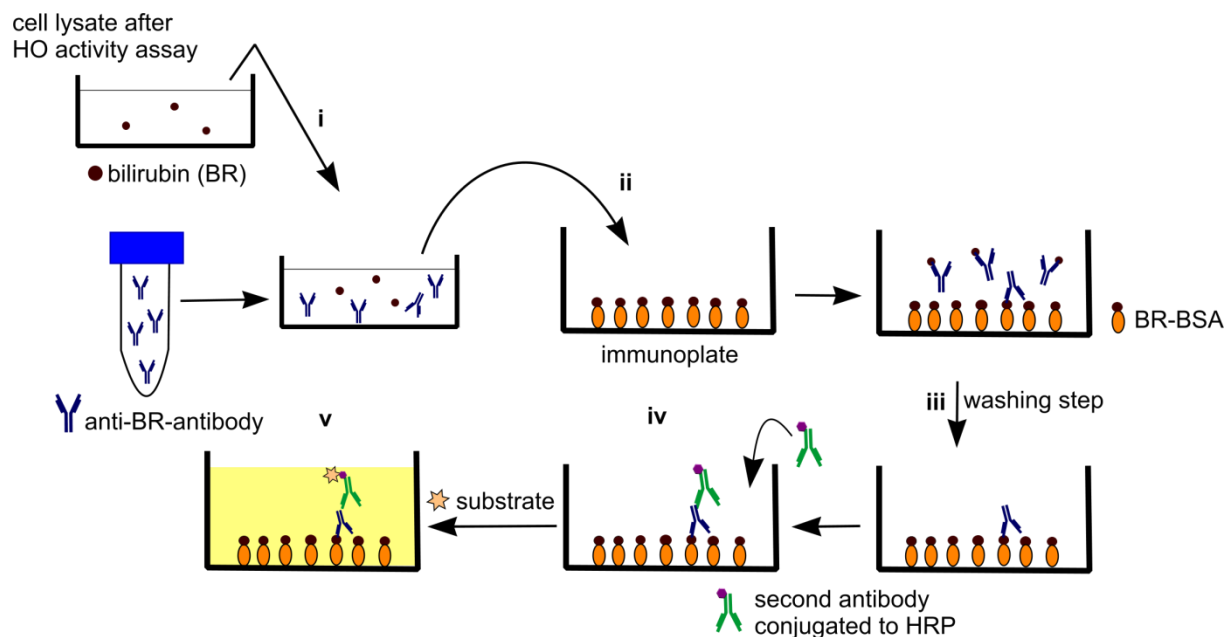
Table 4. Pipetting summary for the HO activity assay.

well	whole cell lysate		TRIS-HCl/sucrose buffer	bilirubin standards	HO reaction mixture
	unstimulated	stimulated			
'zero control' (B_0)	+	-	+	-	-
'bilirubin standards'	+	-	-	+	-
sample	-	+	-	-	+
control sample	+	-	-	-	+
solvent control	+	-	-	-	+

2.2.6.5 ELISA

The amount of bilirubin was quantified by the ELISA method described by Izumi *et al.*⁵² The bilirubin-ELISA is built as a non-competitive, indirect assay (Scheme 11). The HO reaction mixture containing the formed bilirubin (BR) was incubated with an excess of the specific anti-bilirubin antibody. The free unbound anti-bilirubin antibody was captured on an immunoplate coated

with the bilirubin-BSA (BR-BSA)-conjugate and detected with a second horse radish peroxidase (HRP)-conjugated antibody.



Scheme 11. The bilirubin-ELISA procedure. (i) Samples from the HO activity assay containing bilirubin were incubated with an excess of specific anti-bilirubin antibody. (ii) Mixture was transferred to an immunoplate coated with a bilirubin-BSA conjugate (BR-BSA). (iii) Free, unbound anti-bilirubin antibodies were washed from the plate. (iv) A second HRP-conjugated antibody was added and allowed to bind to the anti-bilirubin antibody. (v) The HRP enzyme substrate was added to detect the anti-bilirubin antibody bound to the immunoplate.

After adding the substrate solution containing *ortho*-phenylenediamine dihydrochloride (OPD) and H_2O_2 , the reaction was stopped with H_2SO_4 and the absorbance of the yellow product was measured at 492 nm. The intensity of the absorbance is proportional to the amount of anti-bilirubin antibody bound to the immunoplate, which is inversely proportional to the amount of bilirubin in the HO reaction mixture.

Procedure

1. An ELISA immunoplate was coated with 100 μ L/well of bilirubin-BSA conjugate in PBS (0.35 μ g protein/well) over night at 4 $^{\circ}$ C.
2. 100 μ L of the samples from the HO reaction mixture (stimulated and unstimulated cells, 'zero control' and 'bilirubin standards') were incubated with 100 μ L of anti-bilirubin antibody in 1% G-PBS (0.571 μ g mL⁻¹) on a 96-well plate for 2 h at 37 $^{\circ}$ C.
3. Meanwhile, the immunoplate coated with the bilirubin-BSA conjugate was washed three times with T-PBS and blocked with 200 μ L/well of 3% G-PBS for 1 h at room temperature in the dark.
4. The blocked immunoplate was washed three times with T-PBS.
5. 100 μ L of the anti-BR antibody mixture from step 2. were transferred to the blocked immunoplate and incubated for 30 min at 37 $^{\circ}$ C.

6. The immunoplate was washed three times with T-PBS.
7. 100 µL/well of the second antibody (HRP-conjugated anti-mouse antibody from goat, 0.2 µg mL⁻¹) in 1% G-PBS were added and incubated for 30 min at 37 °C.
8. The immunoplate was washed six times with T-PBS.
9. 100 µL/well of the freshly prepared substrate solution (0.40 g mL⁻¹ OPD and 0.4 µL mL⁻¹ 30% H₂O₂ in citrate buffer, pH 5.0) were added and incubated in the dark for 5 min at room temperature.
10. The peroxidase reaction was terminated by the addition of 50 µL/well of 3 M H₂SO₄.
11. The absorbance was measured at 492 nm in a microplate reader (Multiskan Spectrum Photometer).

2.2.6.6 Analysis of the ELISA

Because the amount of bilirubin is determined by quantifying the anti-bilirubin antibodies, which did not bind to the bilirubin in the sample, the intensity of the signal is indirect proportional to the bilirubin concentration. A sigmoidal calibration curve was plotted as the ratio of B/B₀ (B = mean absorbance for each 'bilirubin standard', B₀ = mean absorbance for 'zero control') against the bilirubin concentrations expressed as lg(x) (x = bilirubin concentration of standard) and data was fitted to a four parameter logistic equation. After normalization of the sample as B/B₀ (B = mean absorbance for each 'sample', B₀ = mean absorbance for 'zero control') unknown concentrations of samples (control cells and stimulated cells, here lysates incubated with HO-1 reaction mixture) were determined using curve fit equation 1.²²⁰

$$y = A_1 + \frac{(A_2 - A_1)}{1 + \left(\frac{x}{x_0}\right)^p}$$

Equation 2.

A₁, A₂, x₀, p: parameters of the four-parameter logistic model, with

A₁ = expected response at zero dose of bilirubin

p = slope factor

x₀ = IC₅₀, i.e., concentration of bilirubin with an expected response exactly halfway between A₁ and A₂

A₂ = expected response for infinite bilirubin concentration

y = B/B₀

B = mean absorbance for 'bilirubin standard' or 'sample'

B₀ = mean absorbance for 'zero control'

The HO activity in whole cell lysates was calculated as picomoles bilirubin produced per hour per milligram of total protein and the data was expressed as fold HO-1 activity compared to control cells. For more details section 3.1.1, Table 9 .

2.2.6.7 Bilirubin quantification via ELISA with HT-29 cells

HT-29 cells (1×10^5 cells/well) were plated in 96-well plates, allowed to attach for 24 h and incubated for another 24 h. The total assay volume was 150 μ L. After removing the culture media, cells were washed with PBS (150 μ L/well) and 96-well plates were stored at -80°C until utilized. For cell lysis 150 μ L of ice cold lysis buffer (40 mM TRIS-HCl, pH 7.4, 250 mM sucrose, 137 mM NaCl, 10% (v/v) glycerin, 2 mM EDTA, 0.1-1% (v/v) detergent, protease inhibitor cocktail from Roche) was added to each well and the 96-well plate was placed on an orbital plate shaker and allowed to shake for 30 min at 4°C . 90 μ L of the collected whole cell lysate was placed in a 96-well plate and 10 μ L of bilirubin standards was added. Bilirubin standards were prepared in TRIS-HCl/sucrose buffer in several concentrations ($5\text{-}50\cdot 10^{-9}$ M BR). The assay volume was 100 μ L. The reaction was performed at 37°C in the dark for 1 h and terminated by the addition of 10 μ L aqueous 1.0 M HCl. The plate was placed 5 min on ice and the pH was adjusted to 7.4 with 10 μ L of aqueous 1.1 M NaOH. The total assay volume was 120 μ L. The amount of bilirubin was quantified by the ELISA method described above in chapter 2.2.6.5. A linear bilirubin calibration curve was plotted as the ratio of B (B = mean absorbance for each 'bilirubin standard') against the bilirubin concentrations expressed as $\lg(x)$ (x = bilirubin concentration of standard) and unknown bilirubin concentration in samples was determined by linear regression analysis.

2.2.6.8 Liver cytosol extract preparation

Biliverdin reductase (BVR) is an important additive to the HO/BVR enzymatic reaction mixture of the HO activity assay, in order to assure a full conversion of the produced biliverdin to bilirubin. As a BVR source a cytosol extract gained by ultracentrifugation of guinea pig liver homogenates was used. The guinea pig liver was kindly provided by Sigurd Elz (Lehrstuhl Pharmazeutische Chemie I, Universität Regensburg). The guinea pig liver was separated, stored in ice cold saline and homogenized in 60 mL of ice cold buffer of 20 mM TRIS-HCl and 250 mM sucrose, pH 7.4 by using an ultraturex equipment (\varnothing 30 cm, B. Braun, Melsungen AG). The obtained homogenate was centrifuged for 30 min at 4000 rpm, 4°C . After removing the lipid layer the supernatant was transferred to ultracentrifuge tubes and centrifuged for 1 h at 40,000 rpm (ultracentrifuge TGA 45, Kontron Instruments with rotor TFT 6513, Zürich, Switzerland), 4°C . The lipid layer was removed again, and the supernatant which was the cytosolic liver fraction was aliquoted and stored at -20°C .

The protein concentration of the liver extract was determined by the Bradford method.²²¹ Briefly, liver extracts were diluted 1:100 and 1:250 in 20 mM TRIS-HCl, 250 mM sucrose buffer, pH 7.4. On a 96-well plate 12 μ L of the sample dilutions were incubated with 238 μ L of the Bradford reagent for 5 min at room temperature and absorption was measured at 595 nm. The mean values were calculated from three parallels. Protein concentrations were determined by a linear regression curve prepared from BSA standard concentrations (1/0.75/0.5/0.25/0.125/0.0625

and 0 mg mL⁻¹) in 20 mM TRIS-HCl, 250 mM sucrose buffer, pH 7.4. The protein concentration of the liver cytosol extract was 32.7 ± 2.7 mg mL⁻¹.

2.2.6.9 Determination of HO activity in liver cytosol extracts

For the HO/BVR enzymatic reaction 3 µL of liver cytosol (0.098 µg) was incubated with 3 mM NADPH and 25 µM hemin in lysis buffer (40 mM TRIS-HCl, pH 7.4, 250 mM sucrose, 10 mM EDTA, 100 mM NaCl, 0.05% (w/v) SDS detergent, 4% protease inhibitor cocktail). As control the liver cytosol was assayed in lysis buffer alone. Assay volume was 100 µL. The reaction mixture was incubated for 1 h at 37 °C and stopped with 10 µL of aqueous 1.0 M HCl. The pH was adjusted to 7.4 with 10 µL of aqueous 1.2 M NaOH. The total assay volume was 120 µL. For bilirubin standards several concentrations of bilirubin were prepared in TRIS-HCl/sucrose buffer added to the lysis buffer to give the final concentrations of 5-75·10⁻⁹ M. The amount of bilirubin in samples was quantified by the ELISA method described above in chapter 2.2.6.5. A linear bilirubin calibration curve was plotted as the ratio of B (B = mean absorbance for each 'bilirubin standard') against the bilirubin concentrations expressed as lg(x) (x = bilirubin concentration of standard) and unknown bilirubin concentration in samples was determined by linear regression analysis.

2.2.6.10 HO-1 activity assay with dendritic cells (DC)

Dendritic cells (DC) were kindly provided by the Department of Internal Medicine III, University Hospital of Regensburg. DC were generated from freshly isolated human monocytes as described previously.²²² After 7 days, DC maturation was induced by 100 ng mL⁻¹ of LPS in the presence or absence of the tetramethoxychalcone α-CF₃-TMC (0.5 and 1 µM) in order to analyze the effect of chalcones on HO-1 activity. Plates were stored at -80 °C until utilized for the HO-1 assay. For cell lysis 100 µL of ice cold lysis buffer (40 mM TRIS-HCl, 250 mM sucrose, 137 mM NaCl, 10% (v/v) glycerin, 2 mM EDTA, 0.1% (v/v) Triton X-100 detergent, protease inhibitor cocktail from Roche, pH 7.4) was added to each well and the 96-well plate was placed on an orbital plate shaker and allowed to shake for 15 min at 4 °C. The HO enzymatic reaction was performed as described above with a slight modification. 90 µL of the collected whole cell lysate from cell samples was placed in a 96-well plate and 10 µL of the HO reaction mixture was added.

Table 5. Pipetting summary for the HO activity assay with dendritic cells.

well	whole cell lysate			TRIS-HCl/sucrose buffer	bilirubin standards	HO reaction mixture
	unstimulated	stimulated	lysis buffer			
'zero control' (B ₀)	-	-	+	+	-	-
bilirubin standards	-	-	+	-	+	-
sample	-	+	-	-	-	+
control sample	+	-	-	-	-	+

Bilirubin standards were prepared in TRIS-HCl/sucrose buffer in several concentrations ($1\text{-}2500\cdot 10^{-9}$ M BR) and 10 μL of 'bilirubin standards' were added to 90 μL of lysis buffer. For 'zero control' (B_0 value) 10 μL of TRIS-HCl/sucrose buffer were added to 90 μL of lysis buffer (Table 5). The assay volume was 100 μL . The reaction was performed at 37 $^{\circ}\text{C}$ in the dark for 1 h and terminated by the addition of 10 μL aqueous 1 M HCl. The plate was placed 5 min on ice and the pH was adjusted to 7.4 with 10 μL of aqueous 1 M NaOH. The total assay volume was 120 μL . The amount of bilirubin was determined by the ELISA method described above. For the quantification of the bilirubin a sigmoidal calibration curve was plotted as the ratio of B/B_0 (B = mean absorbance for each 'bilirubin standard', B_0 = mean absorbance for 'zero control') against the bilirubin concentrations expressed as $\lg(x)$ (x = bilirubin concentration of standard). The data was fitted to a four parameter logistic equation (Equation 2) and unknown concentrations of samples were determined: the basal bilirubin level in the cell lysate of untreated control cells together with the HO activity in control cells and stimulated cells in presence of LPS. The HO-1 activity was estimated by comparing the HO activity of treated cells to control cells.

2.2.6.11 Inhibition of HO activity in RAW264.7 macrophages by SnPPIX

As a negative control for the HO-1 assay, the HO-1 activity was measured in RAW264.7 cells treated with 10 μM of the chalcone DHDMCH and 10 ng mL^{-1} of LPS for 24 h in the presence of 5 or 10 μM of SnPPIX, an inhibitor of HO-1 activity. The SnPPIX stock solution (10 mM) was freshly prepared in a 0.10 mM aqueous solution of NaOH and diluted in culture medium to the corresponding test concentrations. HO-1 activity in stimulated RAW264.7 cells was determined under standards assay conditions as described in

2.2.7 Western blot analysis

2.2.7.1 Sample preparation

RAW264.7 cells (3×10^6 cell/well) were plated in 6-well plates and allowed to attach for 24 h. The cells were then incubated with different concentrations of test compounds for 3 to 24 h prior to cell harvesting, in total for 24 h. The assay volume was 4 mL/well and 2 wells per test compound were used. Control cells were incubated with culture medium alone. After removing the culture medium cells were washed with PBS (5 mL/well), detached from the plate in 1 mL PSB/well using a cell scraper and pelleted by centrifugation for 5 min at 14,000 rpm and 4 $^{\circ}\text{C}$. The cell pellet was stored at -80 $^{\circ}\text{C}$ until used for western blotting.

For cell lysis 400 μL of ice cold lysis buffer (40 mM TRIS-HCl, 250 mM sucrose, 137 mM NaCl, 10% (v/v) glycerin, 2 mM EDTA, 0.1% (v/v) Triton X-100 detergent, protease inhibitor cocktail from Roche, pH 7.4) were added to the cell pellet and incubated for 30 min at 4 $^{\circ}\text{C}$. Subsequently, the lysates were centrifuged (14,000 rpm, 15 min, 4 $^{\circ}\text{C}$) and the protein amount of the supernatant determined by the DC Protein Assay (see section 2.2.6.3).

2.2.7.2 SDS-PAGE

From each supernatant 33 µg of protein were heated to 95 °C for 4 min in sample buffer and separated by SDS-polyacrylamide gel electrophoresis (SDS-PAGE) using the electrophoresis unit Mini-Protean Tetra Handcast System (BioRad). The discontinuous system consisted of a lower separating 12%-acrylamide gel and an upper stacking gel containing 5% acrylamide. Gels were run for 1 h at 200 V in electrophoresis buffer. Molecular weights of the different proteins were estimated using protein markers (Precision Plus Protein Standards, Bio Rad) of known molecular weight.

2.2.7.3 Blotting

The separated proteins in the gel were transferred to a nitrocellulose or PVDF membrane. The gel together with the membrane were placed in the transfer cell (Mini-Protean Tetra Handcast System, BioRad) filled with transfer buffer between two piles of three blotting papers (Whatman, 1.0 mm, Roth). The transfer was performed for 1 h at 130 V.

2.2.7.4 Protein detection

To avoid unspecific binding of the antibodies, the membrane was blocked with a 5% (w/v) low fat milk solution for 1 h on a rocking platform shaker at RT. Two membrane stripes were cut out according to the molecular weight of the relevant protein bands, the target protein HO-1 (32 kDa) and the loading control α -tubulin (57 kDa). The specific primary antibodies were diluted to an adequate working concentration in a 1% (w/v) low fat milk solution (1 µg mL⁻¹ anti-HO-1 antibody or anti- α -tubulin antibody (1:500)) and incubated with the membrane stripes on a rocking platform shaker for 1 h at RT or over night at 4 °C. Afterwards, the secondary HRP-conjugated anti-mouse antibody (0.2 µg mL⁻¹ in a 1% (w/v) low fat milk solution) was incubated with the membrane for 30 min at RT on a rocking platform shaker. The membrane was washed in 1% (w/v) low fat milk solution for three times 5 min on a rocking platform shaker. A last washing step was performed with 1 x washing buffer for 10 min at RT. The immunoreactive bands were detected with a chemiluminescence reagent kit (Thermo Scientific, Rockford USA) and visualized with a luminescent image analyser (LAS 3000, Fujifilm, Düsseldorf). Relative density of protein bands was analyzed by the Multi Gauge 3.0 software (Fujifilm Life science, Tokyo, Japan) and the relative intensity of HO-1 protein expression was calculated as the ratio of α -tubulin to HO-1 protein and data was expressed as fold of control.

Technical assistance for the gelelectrophoresis, western blotting and protein detection was supplied by Dita Fritsch (group of Sabine Amslinger, Universität Regensburg).

2.2.8 ORAC-fluorescein assay

The radical scavenging activity of test compounds was determined by the cell free oxygen radical absorbance capacity-(ORAC)-fluorescein method generating peroxy radicals from AAPH (2,2'-azobis(2-methylpropionamidine) dihydro chloride) as a free radical initiator and using fluorescein as a fluorescent probe. The assay was carried out in a flat bottom 96-well plate (Greiner Bio-One) in 75 mM phosphate buffer (pH 7.4) and the final assay volume was 200 μ L. Stock solutions of the test compounds (100 mM) were prepared in DMSO. All dilution steps of the assay components were performed in phosphate buffer (75 mM, pH 7.4) to reach the final assay concentrations. The final DMSO concentration for the test compounds in phosphate buffer was below 0.01% (v/v). At this concentration the solvent had no effect on the fluorescence decay of fluorescein compared to the blank. A typical 96-well plate pipetting scheme for the ORAC-fluorescein assay is shown in Scheme 12.

	1	2	3	4	5	6	7	8	9	10	11	12
A	PB	PB				Trolox	[μ M]				solvent control	PB
B			1	2	3	4	5	6	7	8		
C												
D												
E	PB		compound 1			[μ M]		compound 2			[μ M]	PB
F		0.5	1	4	7	10	0.5	1	4	7	10	
G												
H												
with 300 nM fluorescein and 12 mM AAPH/well in 75 mM phosphate buffer, pH 7.4												

Scheme 12. Pipetting scheme for a 96-well plate used in the ORAC-fluorescein assay. Trolox calibration standards (1-8 μ M), 2 test compounds (0.5-10 μ M), 0.01% DMSO as solvent control and phosphate buffer (PB, 75 mM, pH 7.4) as blank together with fluorescein (300 nM) and AAPH (40 mM) were carried out in quadruplicates.

Several calibration solutions of Trolox (1-8 μ M), test compound samples (0.5-10 μ M), solvent control (0.01% DMSO) and phosphate buffer as blank (75 mM, pH 7.4) were carried out on each plate. Table 6 gives the assay components and their final concentration in the assay. Solutions of Trolox (20 μ L/well, 1-8 μ M), test compounds (20 μ L/well, 0.5-10 μ M), solvent control (0.01% DMSO) and phosphate buffer as blank (20 μ L/well) together with fluorescein (120 μ L/well, 300 nM) were incubated for 15 min at 37 $^{\circ}$ C. AAPH (60 μ L/well, 12 mM) was added rapidly to the reaction mixture and the fluorescence was recorded every 60 seconds for 100-300 min at 37 $^{\circ}$ C (λ_{ex} 485 nm, λ_{em} 535 nm) in a Tecan plate reader (XFluor4 software version V 4).

Table 6. Components of the ORAC-fluorescein assay for the Trolox standards.

	assay component (in 75 mM phosphate buffer, pH 7.4)	volume [μ L]/well	final concentration (in 200 μ L assay volume)
i.	10-80 μ M Trolox	20	1-8 μ M
or	5-100 μ M test compound	20	0.5-10 μ M
or	0.1% DMSO (solvent control)	20	0.01%
or	75 mM phosphate buffer (blank)	20	75 mM
ii.	500 nM fluorescein	120	300 nM
iii.	40 mM AAPH	60	12 mM

Raw data was exported to an Excel sheet for further calculations. ORAC values were calculated as described by Davalos *et al.*⁸⁸ Each data point was first normalized by multiplying it by the factor $\text{fluorescence}_{\text{blank}, t=0} / \text{fluorescence}_{\text{sample}, t=0}$. and the fluorescence decay curves were plotted as relative fluorescence intensity versus time. From the normalized curves, the area under the fluorescence decay curve (AUC) was calculated as

$$\text{AUC} = 1 + \sum_{i=1}^{i=100} f_i/f_0$$

Equation 3

where f_0 is the initial fluorescence reading at 0 min and f_i is the fluorescence reading at time i . The net AUC corresponding to a sample was calculated by subtracting the AUC corresponding to the blank. Linear regression equations between net AUC and antioxidant concentration were calculated for all the samples. ORAC values were expressed as Trolox equivalents by using the standard curve calculated for each assay. Final results were in μ mol of Trolox equivalent/ μ mol of test compound.

2.2.9 Statistical analysis

Data is presented as the mean \pm SD of at least 3 independent experiments carried out in triplicates for HO and MTT assays and in quadruplicates for ORAC, MTT-LPS and NO assays. Significances: ***, $p < 0.001$; **, $p < 0.01$; *, $p < 0.05$ versus control. Comparison between groups was made using two-sided paired Student's t test. A p value < 0.05 was considered statistically significant. Calculations were performed using Microsoft Office Excel 2007 and Origin 8 SR4 (Origin Lab Corporation 1991-2008). IC₅₀ values were calculated with the Excel sheet ED50plus v1.0, (M.H. Vargas, Mexico).

3 Results and Discussion

3.1 Heme oxygenase-1 (HO-1) activity assay

Based on the HO enzymatic activity assay and the quantification of bilirubin by an indirect ELISA method a combined concept for the HO-1 activity assay was developed. A microtiterplate assay format was designed for all steps of the HO-1 assay, including cell culture, stimulation with potential HO-1 inducers, cell lysis, HO enzymatic activity assay and ELISA-based bilirubin quantification. The present work is based on assay optimizations made previously in the diploma thesis (Hannelore Rücker, Universität Regensburg, October 2009).⁷⁸ Some ELISA parameters were successfully optimized in the diploma thesis, such as the concentration of the bilirubin-BSA conjugate for coating the immunoplate and the amount of the anti-bilirubin antibody or the second HRP-conjugated antibody, and were used without no further optimization in this work as described in Materials and Methods. Further HO-1 assay parameters such as the cell line, the cell sample preparation, the parameters for the HO enzymatic reaction and the range of the bilirubin standard concentrations were developed and optimized in the present work.

3.1.1 Development and optimization of the HO-1 activity assay

3.1.1.1 Cell lines

The cell line HT-29 was used as an *in vitro* model to develop the HO-1 assay and was replaced by the murine macrophage cell line RAW264.7, which is known to show inducible HO-1 activity.^{70, 162} The RAW264.7 cell line has been used in the Griess assay to assess the anti-inflammatory activity of natural products such as polyphenols, by determining their influence on the proinflammatory pathway that involves NF- κ B and thus the induction of iNOS, COX-2 and TNF- α . Thereby, the inhibitory effect of tested compounds is assessed, by determining the NO production in RAW264.7 stimulated with lipopolysaccharides (LPS). An advantage of the RAW264.7 cell line is the fast rate of growth of 3 days, allowing a higher screening efficiency for compounds, compared to the human cell line HT-29 which reaches cell confluence after one week. Some HO-1 assay parameters optimized with the cell line HT-29 as indicated below, were also used in the optimization of the HO-1 assay with RAW264.7 cells.

3.1.1.2 Optimization of the cell lysis

The lysis buffer was found to be a crucial parameter for the HO-1 assay development. As an intracellular membrane protein, a sufficient amount of soluble HO-1 protein is present when a whole cell lysate is prepared. With an increased total protein amount in the whole cell lysate a higher HO-1 protein content is assumed. The optimization of a suitable lysis buffer for the cell lysis started with the addition of the ionic detergent SDS (1.0% v/v). But, high concentrations of

SDS in the lysis buffer were not recommended due to the risk of protein denaturation during cell lysis. Therefore a mild but sufficient detergent in the lysis buffer was necessary.

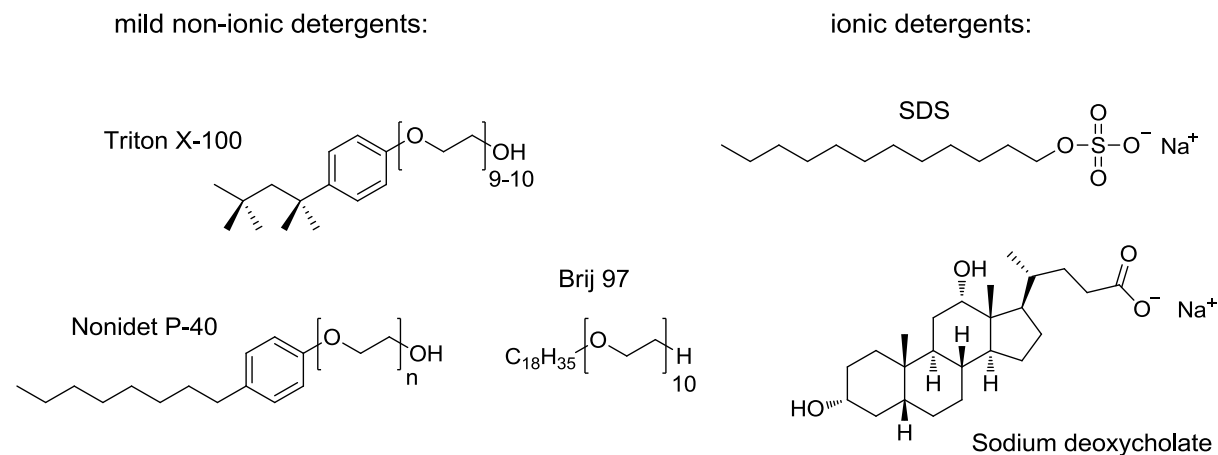


Figure 19. Structures of non-ionic and ionic detergents used to optimize the lysis buffer in the cell lysis.

For this purpose the non-ionic detergents Nonidet P-40, Triton X-100 and Brij 97 (Figure 19) were screened for their efficiency in the cell lysis of HT-29 cells in the 96-well plate and the results are summarized in Figure 20.

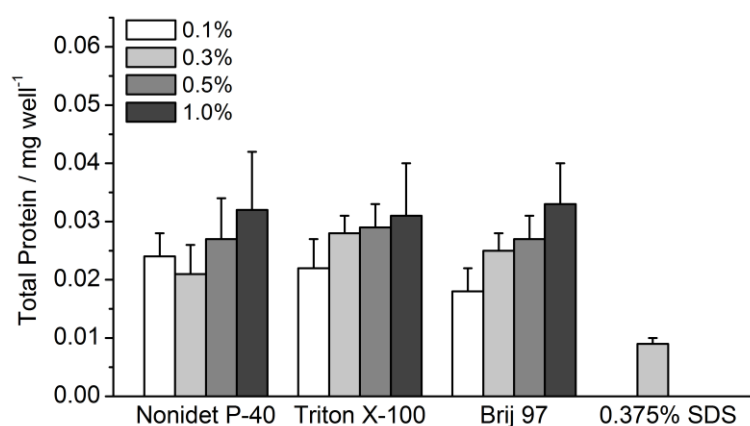


Figure 20. Influence of different detergent concentrations in the lysis buffer on the cell lysis of HT-29 cells. Cell lysis of HT-29 was performed with lysis buffer 2 (LB2, see Table 7) in case of the detergents Nonidet P-40, Triton X-100 and Brij 97 and compared to the cell lysis performed with 0.375% SDS in lysis buffer as described in Material and Methods. Protein amounts were determined with the detergent compatible protein assay (Bio-Rad) as described in Material and Methods.

HT-29 cells were incubated with the lysis buffer 2 (Table 7) containing the detergents Nonidet P-40, Triton X-100 and Brij 97 in the concentration range of 0.1 to 1.0% (w/v) for 1 h at 4 °C on an orbital plate shaker. The total protein content of the obtained whole cell lysate was determined by the detergent compatible protein assay (Bio-Rad) as described in Material and Methods, section 2.2.6.3.

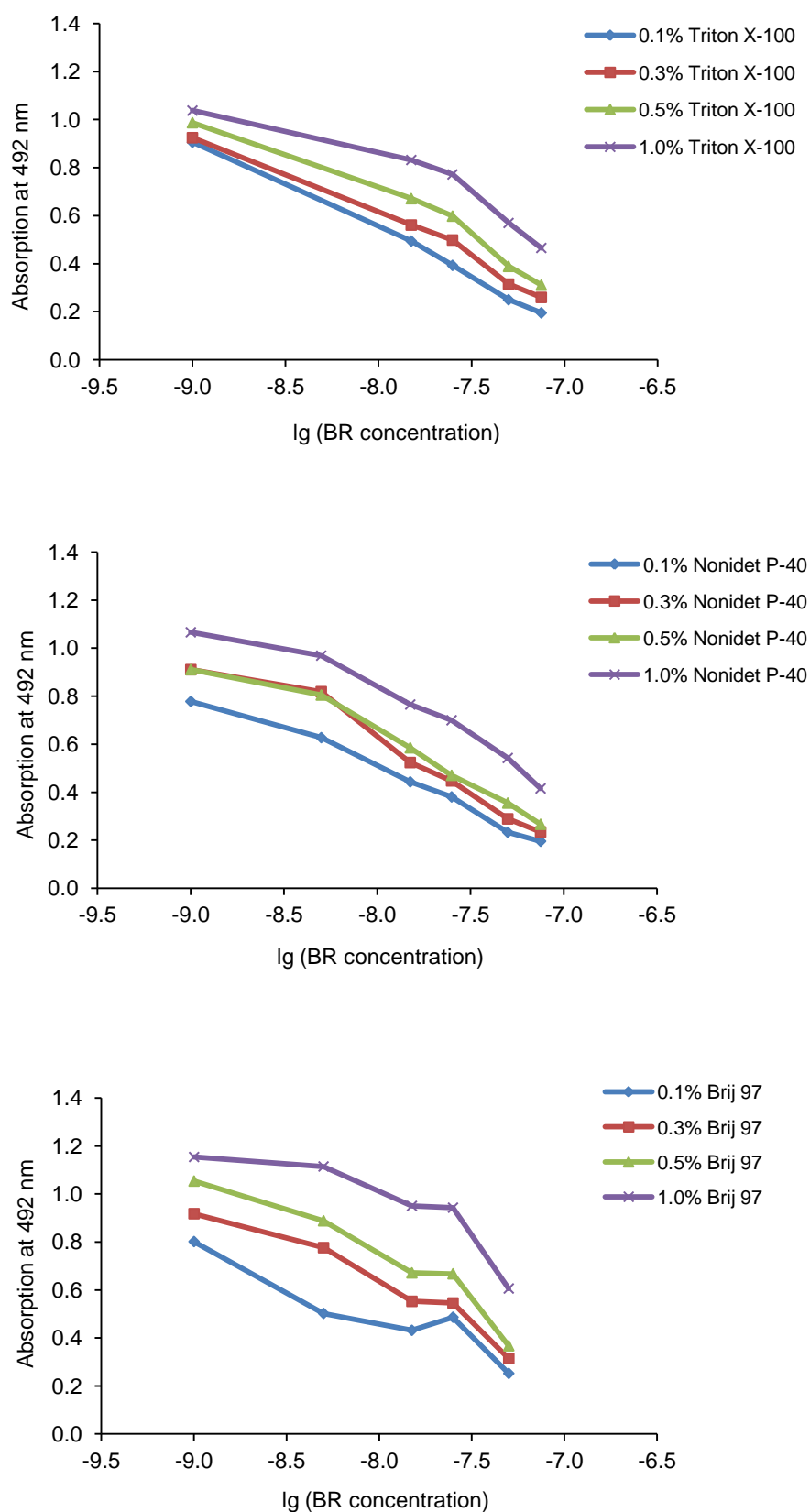


Figure 21. Influence of increasing detergent concentrations in the lysis buffer on the absorption signal. $5\text{-}50 \cdot 10^{-9}$ M of bilirubin (BR) were added to the lysis buffer (LB2, see Table 7) in presence of different concentrations of detergent as indicated and bilirubin content was detected via ELISA. A representative data set is shown. A lower signal indicates higher bilirubin amounts, due to the indirect ELISA method.

Additionally, cell lysis with HT-29 cells was performed with lysis buffer (40 mM TRIS-HCl, pH 7.4, 250 mM sucrose, 10 mM EDTA, 100 mM NaCl, 4% protease inhibitor cocktail) containing 0.375% of SDS, a slightly changed procedure to the method used in the diploma thesis, in order to compare the efficiency of SDS to the mild detergents in the lysis buffer. As shown in Figure 20 with an increased detergent concentration in the lysis buffer a higher protein content in cell lysate could be determined. Moreover, the overall protein content in the whole cell lysate obtained with the mild, non-ionic detergents Nonidet P-40, Triton X-100 and Brij 97 was higher (18-33 µg protein/well) compared to the protein content of the lysis buffer with 0.375% SDS (9.0 µg protein/well), suggesting a more efficient cell lysis when using a non-ionic detergent.

Next, a possible interference of an increased detergent concentration in the lysis buffer with the detection of bilirubin in the sample was investigated and results are depicted in Figure 21. Known bilirubin concentrations were added to lysis buffer 2 (Table 7) containing several detergent concentrations as indicated and bilirubin was detected via ELISA.

An increase in the absorbance signal was observed in presence of increased detergent concentrations in the lysis buffer as depicted in Figure 21. A similar behavior was observed for all tested detergents Triton X-100, Nonidet P-40 and Brij 97. Since the absorption signal was indirect proportional to the detected bilirubin (BR) in the sample, the results suggest an inhibition of the bilirubin detection by an increasing amount of detergent in the lysis buffer. High concentrations of detergent in the lysis buffer can interfere with the epitope-antibody interactions in the ELISA and inhibit the binding of the anti-bilirubin antibody 24G7 to bilirubin. These results suggest that the ELISA procedure tolerates a detergent concentration of 0.1% (w/v) in the lysis buffer. At a concentration of 0.1% of detergent in the lysis buffer cell lysis performed well, see Figure 20. Therefore, a final detergent concentration of 0.1% in the lysis buffer is a good compromise between cell lysis and ELISA tolerance.

Table 7. Contents of different lysis buffers, pH 7.4 screened for the optimization of the HO-1 activity assay.

lysis buffer 1 (LB1)	lysis buffer 2 (LB2)	modified RIPA buffer	Brij 97 buffer
137 mM NaCl	137 mM NaCl	150 mM NaCl	150 mM NaCl
40 mM TRIS-HCl	40 mM TRIS-HCl	50 mM TRIS-HCl	10 mM TRIS-HCl
250 mM sucrose	250 mM sucrose	0.05% Nonidet P-40	2 mM EDTA
2 mM EDTA	2 mM EDTA	0.25% sodium deoxycholate	0.0875% Brij 97
10% glycerine	10% glycerine	0.05% SDS	0.0125% Nonidet P-40
0.1% Triton X-100	0.1% Triton X-100	4% complete protease inhibitor cocktail (Roche)	4% complete protease inhibitor cocktail (Roche)
0.25% sodium deoxycholate	4% complete protease inhibitor cocktail (Roche)	4% complete protease inhibitor cocktail (Roche)	
4% complete protease inhibitor cocktail (Roche)			

In order to further improve the lysis buffer system, several lysis buffers containing different detergents at concentrations not higher than 0.1% were investigated. Whole cell lysates of HT-29 cells were prepared, incubated with known bilirubin concentrations and analyzed via ELISA as shown in Figure 22. Here the non-ionic detergents Brij 97, Triton X-100 and Nonidet P-40 or the ionic detergents SDS and sodium deoxycholate were compared in the different lysis buffer systems (Table 7). The highest amount of added bilirubin to the sample was detected with lysis buffer 2 containing only 0.1% of Triton X-100, which was shown by a low absorption signal. A high absorption level and thus a low detection of bilirubin in the sample was observed in the presence of the modified RIPA buffer and the Brij buffer, suggesting an inhibitory effect of the detergents present in the buffers. In some cases precipitation in the whole cell lysate was observed during the enzymatic HO reaction step, when the lysis buffer 1 and RIPA which contained sodium deoxycholate were used.

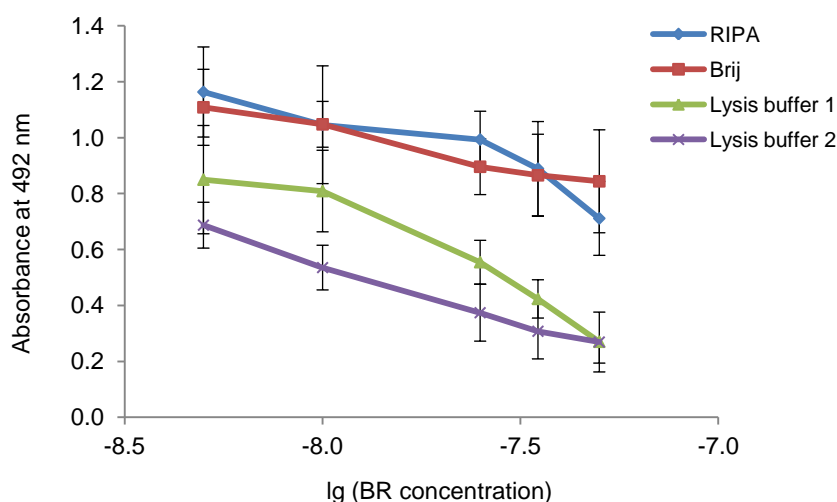


Figure 22. Influence of different lysis buffers on the detection of bilirubin ($5\text{-}50 \cdot 10^{-9}$ M) measured in whole cell lysates of HT-29 cells via ELISA. Data represents the mean of 3 independent experiments carried out in triplicates.

Based on the results and the observations made, lysis buffer 2 was found to be the optimal lysis buffer system in the cell lysis of HT-29 cells. Furthermore, no significant difference in the total protein amount of the whole cell lysate of HT-29 cells was obtained upon cell lysis with the different lysis buffers (Table 7). Taken together, lysis buffer 2 containing 0.1% of Triton X-100 gave the best results concerning the cell lysis and the compatibility with the bilirubin detection via ELISA in the obtained whole cell lysate.

Cell lysis with the cell line RAW264.7 was also performed with lysis buffer 2 containing 0.1% of Triton X-100 and gave good results. The cell lysis incubation time of 1 h at 4 °C could be reduced to 15 min at 4 °C without decreasing the amount of total protein in the whole cell lysate. After changing the model cell line for the HO-1 assay from HT-29 to RAW264.7 lysis buffer 2 (Table 7) was used routinely in the cell lysis of RAW264.7 (see section 2.2.6.2) and is mentioned in the

following as lysis buffer. The average total protein content in whole cell lysates of RAW264.7 control cells incubated for 24 h was 0.284 ± 0.067 mg mL⁻¹, corresponding to 25.6 µg per sample.

3.1.1.3 Optimization of the HO enzymatic reaction conditions

pH

The lysis buffer and thus the obtained whole cell lysate serves as reaction mixture for the HO/BVR enzymatic reaction. A constant pH of 7.4 of the lysis buffer solution throughout the assay is required. The physiological pH of 7.4 is in the maximum activity range of HO⁵⁶ and is also tolerated for biliverdin reductase (BVR) despite the non-optimal pH conditions for this enzyme. BVR shows a pH optimum at 8.5-8.7 and requires NADPH as cofactor.²²³ It was crucial to find conditions for the cell lysis and the HO/BVR reaction that are compatible with the highly sensitive bilirubin-ELISA quantification.

The protease inhibitor cocktail is a necessary additive to the lysis buffer, ensuring the stability of enzymes due to protein degradation mechanisms activated when cells are lysed. For the HO-1 activity assay a convenient protease inhibitor cocktail in tablet form (Roche, Mannheim) was used, from which 25-fold stock solutions were prepared in water as recommended by the manufacturer to give a pH of 7.0. In a control experiment the pH of the lysis buffer solution was measured using pH test stripes (Roth, Karlsruhe) to ensure the necessary pH of 7.4 during the HO-1 assay steps. The results are summarized in Table 8. Addition of the protease inhibitor cocktail to the freshly prepared lysis buffer (entry 1) decreased unexpectedly the pH of the buffer substantially from 7.4 to suboptimal reaction conditions for HO and BVR (pH 5.5). Raising the pH of the lysis buffer stock solution to pH 7.8 or 8.0 gave for the ready to use lysis buffer in the cell lysis the intended pH of 7.4 (entry 1, columns 4 and 5). With an increased pH of 7.8 or 8.0 of the lysis buffer stock solution, the pH of the reaction mixture remained also stable during the HO/BVR reaction (entry 2, columns 4 and 5).

Table 8. pH measurements in the lysis buffer solution and the whole cell lysates of RAW264.7 cells during the HO-1 assay. Stock solutions of the lysis buffer were prepared with pH 7.4, 7.8 and 8.0 and after addition of protease inhibitor (1st entry). Cell lysis was performed as described in Materials and Methods (2.2.6.2). The pH of the yielding whole cell lysate was then determined in every step of the HO-1 assay as indicated (entry 2-4) using pH test stripes.

Entry	HO-1 activity assay condition	pH of lysis buffer stock solution		
		7.4	7.8	8.0
1	lysis buffer ready to use for cell lysis (+ protease inhibitor cocktail)	5.5	7.4	7.4
2	HO/BVR enzyme assay in whole cell lysate	5.5	7.4	7.4
3	stop of reaction with 1 M HCl	1.0	1.0	1.0
	and pH readjustment with 1 M NaOH	7.4	7.4	7.4
4	ELISA (incubation with anti-BR antibody)	7.4	7.4	7.4

The suboptimal HO/BVR reaction conditions of pH 5.5 could also be observed when the HO activity was determined in RAW264.7 cells using the lysis stock solution with an initial pH of 7.4 for the HO-1 assay (Figure 23). RAW264.7 cells were stimulated with 10 μ M of curcumin for 24 h and HO activity was measured via ELISA. Lysis buffer stock solutions with an initial pH of 7.4, 7.8 and 8.0 were used to prepare lysis buffer the ready to use for cell lysis; HO reaction and ELISA was performed as described in Material and Methods. The amount of bilirubin was determined using a linear regression analysis of the bilirubin standard curve ($5\text{--}50 \cdot 10^{-9}$ M) measured in lysis buffer. Figure 23 shows an increase of HO enzymatic activity due to an increase of the pH of the lysis buffer used to prepare the whole cell lysate, suggesting an improvement of the reaction condition for both enzymes, HO and BVR.

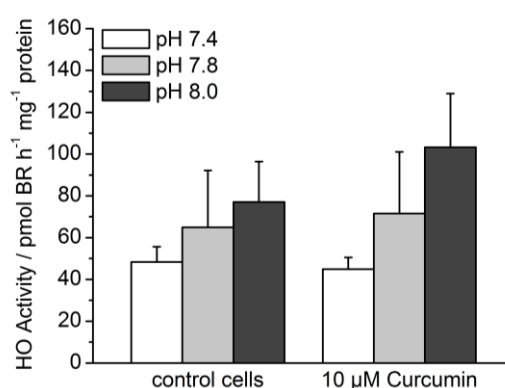


Figure 23. Influence of the pH of the lysis buffer on the HO activity. RAW264.7 cells were stimulated with 10 μ M of curcumin for 24 h and HO activity was determined via the ELISA based HO-1 assay in whole cell lysate. Lysis buffers (lysis buffer 2, Table 7) were prepared using lysis buffers stock solutions with different pH as indicated. The amount of bilirubin was determined using a linear regression analysis of the bilirubin standard curve ($5\text{--}50 \cdot 10^{-9}$ M) measured in lysis buffer. Data represents the mean \pm SD of 3 independent experiments carried out in triplicates.

Taken together, an optimized lysis buffer system using a lysis buffer stock solution with an initial pH of 8.0 to give the necessary pH of 7.4 in the lysis buffer solutions, improved the conditions of the enzymatic reaction and also of the entire assay.

Reaction mixture additives: BVR, hemin and NADPH

Whole cell lysates were directly incubated with the HO/BVR reaction mixture, containing hemin, NADPH and a BVR source. In the beginning of the assay development the HO/BVR reaction was conducted with a liver cytosol fraction as a BVR source in order to convert biliverdin into bilirubin. The liver cytosol, a microsomal fraction received by ultracentrifugation, contained also HO-1 and/or HO-2 proteins and bilirubin that can overcompensate the measured HO activity present in the whole cell lysate sample, which was quickly prepared in the 96-well plate without prior or later centrifugation step. In a control experiment, the amount of liver cytosol usually added to the whole cell lysate (98 μ g/well) for the enzymatic HO/BVR reaction was assayed for its HO activity. The liver cytosol fraction was incubated with 3 mM NADPH and 25 μ M hemin in lysis

buffer pH 7.4 and for control the liver cytosol was assayed in lysis buffer alone, as described in section 2.2.6.9. The liver cytosol contained $7.66 \pm 1.1 \text{ nmol L}^{-1}$ of bilirubin and the amount increased to $29.2 \pm 2.6 \text{ nmol L}^{-1}$ of bilirubin when NADPH and hemin were added to the liver extract. A fourfold increase in the bilirubin concentration implicated a HO and BVR activity in the liver extract. With a protein amount of $98 \text{ }\mu\text{g}$ a HO activity of $38.7 \pm 3.4 \text{ pmol bilirubin h}^{-1} \text{ mg}^{-1}$ protein of the liver cytosol fraction could be determined. To avoid a overcompensation of the bilirubin and HO activity detection in the whole cell lysates when liver cytosol extract is used in the HO-1 assay, a purified BVR source was chosen. A commercial BVR recombinant rat protein was used for the HO enzymatic reaction in the assay with a specific activity of $>180 \text{ nmol biliverdin mg}^{-1} \text{ min}^{-1}$ for pH 8.5 at 37°C . Under the HO-1 assay conditions with pH 7.4 and 37°C a 4 fold decrease in BVR activity can be estimated²²³ and gives for a reaction time of 60 min a specific activity for BVR of $2700 \text{ nmol mg}^{-1} \text{ h}^{-1}$ or $2.7 \text{ pmol ng}^{-1} \text{ h}^{-1}$.

The necessary excess amount of hemin, NADPH and recombinant BVR in the HO reaction mixture was screened, to insure an accurate HO activity present in the whole cell lysate samples especially in higher induced cells. Initially, 1.0 ng BVR, 0.3 mM NADPH and $2.5 \text{ }\mu\text{M}$ hemin were added to the HO reaction mixture. A more concentrated reaction mixture containing 3.0 mM NADPH, $25 \text{ }\mu\text{M}$ hemin and 3.7 ng of BVR was also tested. Additionally, combinations of both preparations were screened: 3.7 ng BVR, 0.3 mM NADPH, $2.5 \text{ }\mu\text{M}$ hemin and 1.0 ng BVR, 3.0 mM NADPH, $25 \text{ }\mu\text{M}$ hemin. The HO/BVR reaction mixtures were incubated with whole cell lysates of control and stimulated RAW264.7 cells (with $10 \text{ }\mu\text{M}$ of the chalcone DHDMCH, for structure see Figure 11, section 1.6) and results are shown in Figure 24.

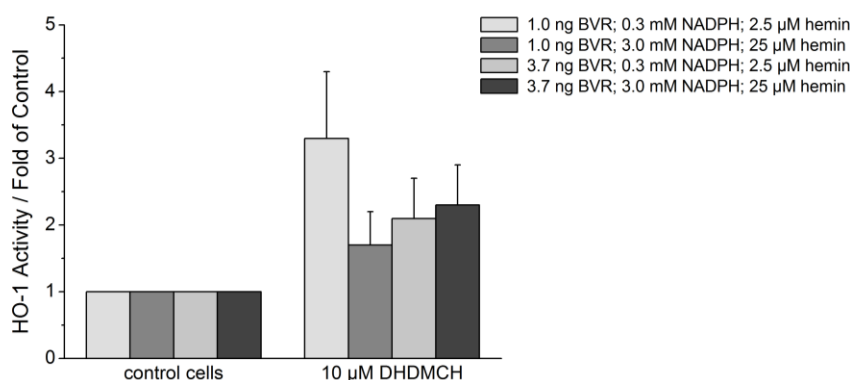


Figure 24. Effect of low and high concentrations of the HO reaction mixture, containing BVR, NADPH and hemin on the HO-1 activity measured by the ELISA-based HO-1 assay in RAW264.7 cells stimulated with $10 \text{ }\mu\text{M}$ of chalcone DHDMCH for 6 h. The amount of bilirubin was determined using a four parameter logistic equation fit of the sigmoidal bilirubin standard curve ($0.5\text{-}2500 \cdot 10^{-9} \text{ M}$) measured in whole cell lysates.. Data represents the mean \pm SD of 2-4 independent experiments carried out in triplicates.

The highest HO activity could be observed in the presence of the reaction mixture containing 1.0 ng BVR, 0.3 mM NADPH and $2.5 \text{ }\mu\text{M}$ hemin, while higher concentrations of each component

decreased the HO activity, which can be explained by feedback-inhibition of the substrate. Also the combinations of both preparations showed no increase in HO activity. Taken together, the results suggest that 1.0 ng BVR, 0.3 mM NADPH and 2.5 μ M hemin were sufficient to cover the HO activity in the whole cell lysates.

3.1.1.4 Optimization of the ELISA-bilirubin standard curve

In the early stages of the HO-1 assay development the bilirubin amount in the sample was quantified based on a linear regression analysis of the bilirubin standard curve measured in lysis buffer or cell lysate at concentrations between 5 to 50 $\cdot 10^{-9}$ M of bilirubin.

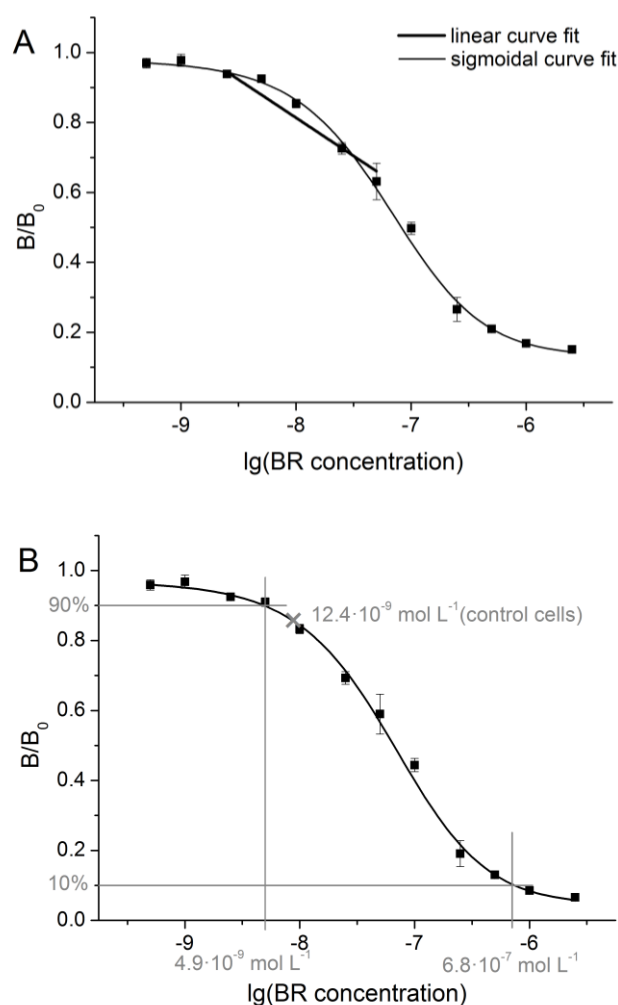


Figure 25. Representative bilirubin (BR) standard curve for the ELISA-based bilirubin quantification. Bilirubin standards ($0.5\text{--}2500 \cdot 10^{-9}$ M) were measured in whole cell lysates of RAW264.7 control cells and a sigmoidal calibration curve was plotted as the ratio of B/B_0 (B = mean absorbance for each 'bilirubin standard', B_0 = mean absorbance for 'zero control') against the bilirubin concentrations expressed as $\lg(\text{BR concentration})$. Unknown bilirubin concentrations in samples were determined by a four parameter logistic equation. For more details see section 2.2.6.6. A, Comparison between the sigmoidal curve fitting (slim line) as indicated above and the less exact linear curve fitting in the range of $2.5\text{--}50 \cdot 10^{-9}$ M bilirubin (thick line). B, Detection range of bilirubin in the assay is presented together with the average bilirubin content in unstimulated control cells incubated for 24 h.

Later on during assay development and new optimized parameters the range of the bilirubin standard curve was extended to $0.5\text{--}2500 \cdot 10^{-9}$ M in order to create the full, for ELISA measure-

ments typical sigmoidal response curve, which was fitted by a four parameter logistic equation in order to quantify the unknown bilirubin in the sample (Figure 25). The typical sigmoidal bilirubin standard curve is shown in Figure 25 A, where the added bilirubin amounts (0.5-2500 nM) were analyzed in presence of whole cell lysates of unstimulated RAW264.7 cells, where the sigmoidal and linear curve fit are compared. With the more precise sigmoidal curve fitting analysis the quantification of the bilirubin was more accurate, since the bilirubin amount detected in unstimulated control cells was near the non-linear range of the standard curve (Figure 25 B). The detection range of the ELISA-based HO activity assay was calculated from the bilirubin standard curves (which were gained within two years) to be 0.567 ± 0.301 (90% B/B₀) to 82.1 ± 25.0 (10% B/B₀) pmol bilirubin in 120 μ L assayed sample (compare with Figure 25 B). The average bilirubin content in unstimulated control cells was 1.49 ± 0.76 pmol. The average total protein content in whole cell lysates (control cells incubated for 24 h) was 0.284 ± 0.067 mg mL⁻¹, corresponding to 25.6 μ g per sample.

3.1.1.5 Quantification of bilirubin and HO-1 activity determination in RAW264.7 macrophages

Bilirubin concentrations for the standard curve were measured in the whole cell lysate to mimic the composition of the unknown samples as well as possible, since bilirubin is present in the cells. Endogenous bilirubin originates from general HO activity, where both HO-2 and HO-1 activity would be included. According to the data obtained by western blot analysis, HO-1 protein was present in non-stimulated control cells (see Figure 26 A). Thus, the comparison of the normalized data for control and stimulated cells gave the increase in HO-1 activity. Table 9 describes an example for the calculation of the HO-1 activity in RAW264.7 cells stimulated with 25 μ M of rosiglic acid for 6 h. The bilirubin content in the samples was estimated by the four parameter logistic curve fit equation (Equation 2) of the bilirubin standard curve measured in whole cell lysate as described in Figure 25. The total protein content in the whole cell lysate was determined for each sample using a protein assay kit (Bio Rad). The HO activity was determined as pmol bilirubin h⁻¹ mg⁻¹ total protein and HO-1 activity was expressed as fold HO-1 activity compared to control cells.

Table 9. Calculation of the HO-1 activity in RAW264.7 cells stimulated with 25 μ M of rosiglic acid for 6 h.

	Control cells	Stimulated RAW264.7 cells with 25 μ M rosiglic acid for 6 h
Bilirubin [nmol L ⁻¹]	11.3 ± 3.6	30.6 ± 10.5
Total protein [μ g per 90 μ L of sample]	19.0 ± 7.4	20.5 ± 7.3
HO activity [pmol h ⁻¹ mg ⁻¹ protein]	80.9 ± 33.5	205.8 ± 94.8
x-fold HO-1 activity	1.00 ± 0.0	2.56 ± 0.41

The data represent the mean \pm SD of 4 independent experiments carried out in triplicates.

3.1.2 Time course of HO-1 protein expression and HO-1 activity in RAW264.7 macrophages exposed to chalcone DHDMCH

In an initial screening 2',4'-dihydroxy-3,4-dimethoxychalcone (DHDMCH) was identified as a potent inducer of HO-1 activity in RAW264.7 cells (see section 3.3, Figure 39). 10 μ M of DHDMCH was used to investigate the time-dependent HO-1 protein expression and HO-1 activity in RAW264.7 macrophages (Figure 26).

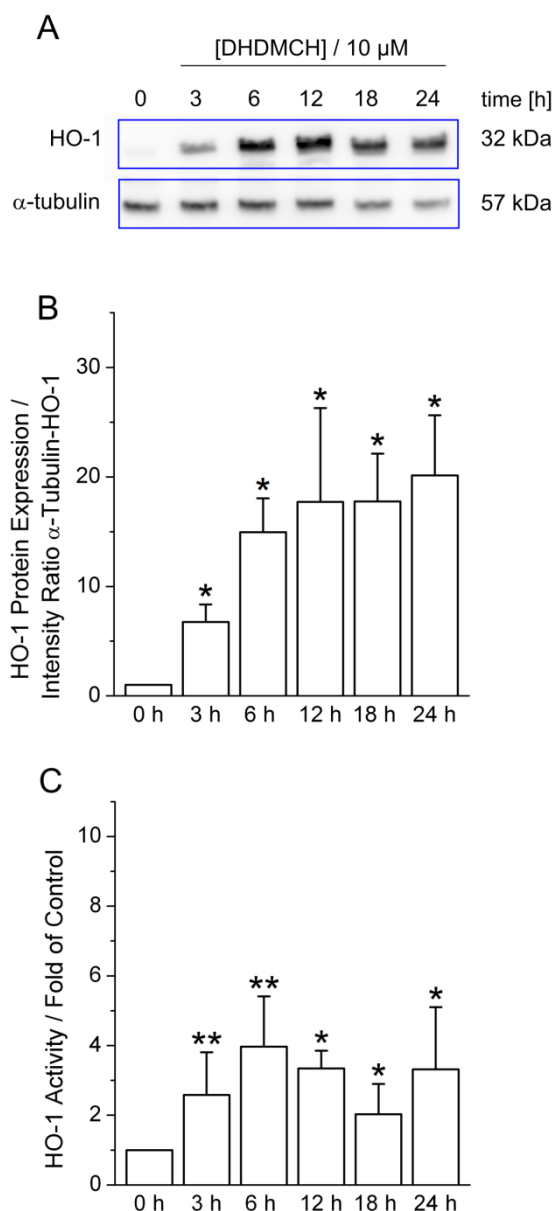


Figure 26. Time-dependent induction of HO-1 by the chalcone DMDHCH (10 μ M) in RAW264.7 cells for the incubation time indicated. A, HO-1 protein expression (Western blotting), a representative blot of 3 independent experiments is shown. B, Relative intensity of HO-1 protein expression, ratio of α -tubulin to HO-1 expressed as fold of control (0 h). Relative density of protein bands from Western blots was analyzed by the software Multi Gauge 3.0 (Fujifilm Life Science) and data is expressed as mean \pm SD of three independent blots. C, Induction of HO-1 activity. Cells were treated with DHDMCH for the indicated periods and HO-1 activity was examined by the HO-1 activity assay via ELISA. Data is expressed as mean \pm SD of at least 3 independent experiments.

Between 3 and 12 h the HO-1 protein levels increased over time, reached maximum HO-1 protein level at 12 h, remained elevated after 18 and slightly increased after 24 h (Figure 26, A, B). In comparison, the HO-1 activity maximum occurred after 6 h (4.0 fold) and decreased after 12 h (Figure 26, C). After 18 h HO-1 activity dropped to 2.0 fold but seemed to recover to 3.3 fold after 24 h. This result suggests that despite the fact that similar amounts of HO-1 are present at 12, 18 and 24 h, the HO-1 protein is not fully active after 18 h or that post-translational inhibition/inactivation occurs over time. The raise of HO-1 activity after 24 h may account for a general change in the lysate, which influences the HO activity assay or for newly synthesized active HO-1 which could be induced by alternative mechanisms or metabolites of DHDMCH.

3.1.2.1 HO-1 activity in different cell lysate fractions derived from RAW264.7 cells stimulated with 10 μM of DHDMCH

Whole cell lysates and crude extracts (supernatant fraction after centrifugation) prepared from RAW264.7 cells incubated with 10 μM of DHDMCH for 3-24 h were analyzed in parallel for HO-1 activity by the ELISA-based HO-1 activity assay. The HO-1 activity was compared to the HO-1 protein expression examined by Western blot analysis. Cell lysate samples were prepared and analyzed as described in Figure 27 and results are shown in Figure 28.

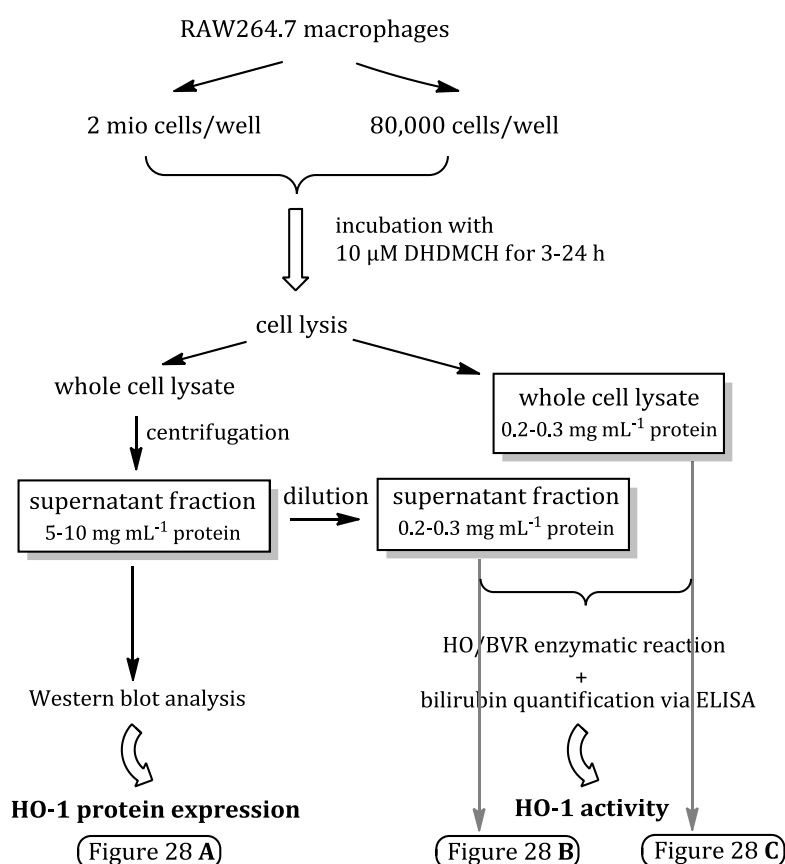
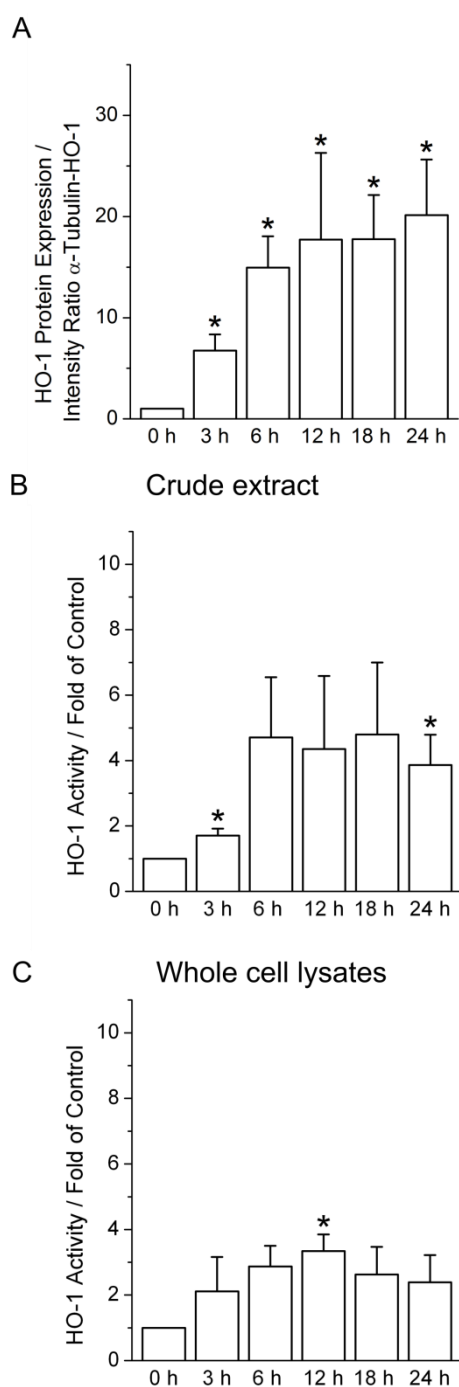


Figure 27. Sample preparation for the comparison of Western blot analysis to ELISA analysis of lysates from RAW264.7 cells incubated with 10 μM of the chalcone DHDMCH for 3-24 h (see Figure 28). A detailed procedure of the methods is given in chapters 2.2.7 and 2.2.6.

For Western blot analysis the supernatant fraction of the whole cell lysate (crude extract) was used. In comparison, whole cell lysates prepared in the 96-well plate were used for the HO-1 activity assay. Additionally, the crude extracts (Western blot samples) were diluted to a adequate total protein concentration of 200-300 $\mu\text{g ml}^{-1}$ and analyzed by the ELISA-based HO-1 activity assay. Three independent experiments were performed. HO-1 activity determined in the crude extracts reached a maximum after 6 h and remained elevated between 12 and 24 h



(Figure 28, B). The level of HO-1 activity follows the level of HO-1 protein expression (Figure 28, A) over time. A similar trend in HO-1 activity was observed with the whole lysate samples (Figure 28, C), which correlated quite good with the HO-1 protein expression. Furthermore, a difference in the HO-1 activity determined between the different fractions of cell lysates could be observed. In the partially purified, supernatant fraction of the cell lysate (crude extract) a higher HO-1 activity was found in comparison to the HO-1 activity detected in whole cell lysates. This result was expected, since the HO protein represents only a fraction of the total proteins present in the whole cell lysate prepared in the 96-well plate. The results suggest that a reasonable amount of HO protein can be 'detected' in the whole cell lysate in order to determine the HO-1 activity.

Figure 28. Comparison of HO-1 activity in different cell lysate fractions to HO-1 protein expression. RAW264.7 cells were treated with DMDHCH (10 μM) for the indicated incubation times. A, Relative intensity of HO-1 protein expression, ratio of α -tubulin to HO-1 expressed as fold of control (0 h). B, HO-1 activity of crude extracts. C, HO-1 activity of whole cell lysates determined by the ELISA-based HO-1 activity assay.

3.1.3 Inhibition of HO-1 activity in DHDMCH or LPS stimulated RAW264.7 macrophages by SnPPIX

In order to further validate the HO-1 assay RAW264.7 cells were exposed to DHDMCH and/or lipopolysaccharide (LPS) in presence and absence of the specific HO-1 activity inhibitor tin-protoporphyrin IX (SnPPIX).²²⁴ LPS is a known inducer of HO-1 in RAW264.7 cells,^{138, 225} which causes a proinflammatory response by induction of inducible NO synthase (iNOS)²²⁶ that in turn leads to an activation of HO-1.

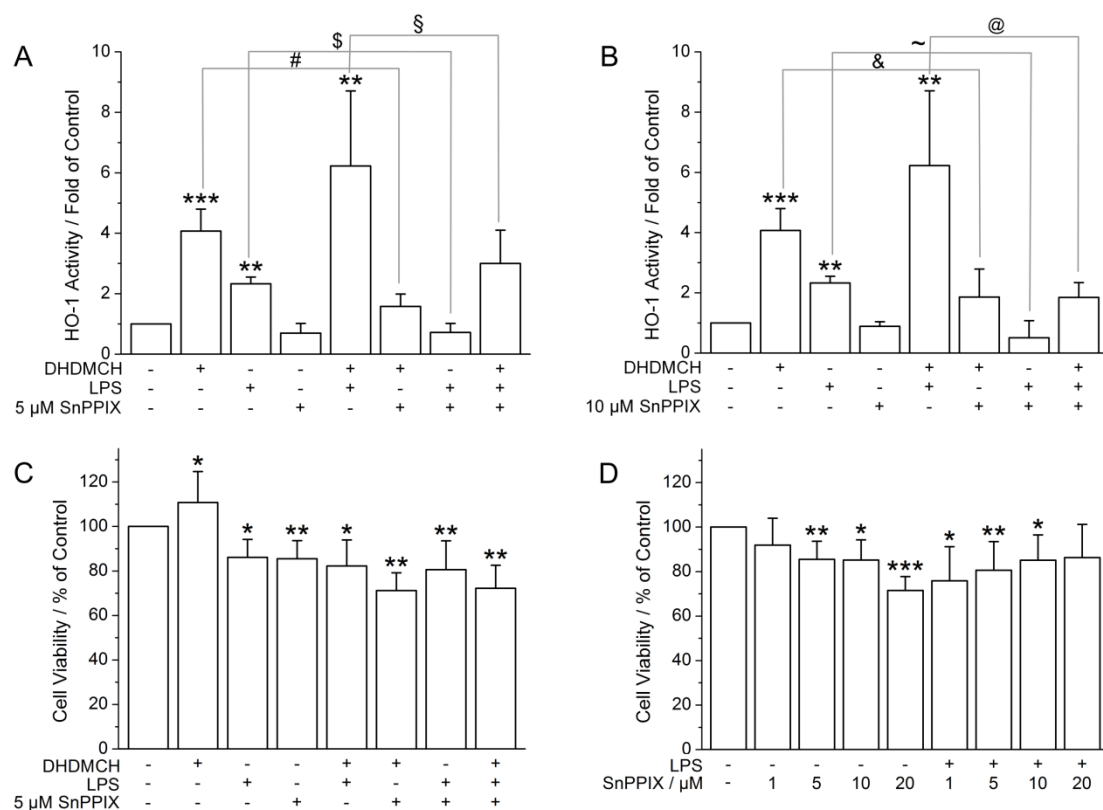


Figure 29. Influence of DHDMCH (10 μM), LPS (10 ng mL⁻¹) and SnPPIX on RAW264.7 cells in the indicated combinations when incubated for 24 h. A and B, induction of HO-1 activity; C and D, cell viability (MTT assay). Level of significance: ***, $p < 0.001$; **, $p < 0.01$; *, $p < 0.05$ versus control (cells were treated with medium alone); #, $p < 0.001$ versus DHDMCH; \$, $p < 0.001$ versus LPS; \$, $p < 0.05$ versus DHDMCH and LPS; &, $p < 0.01$ versus DHDMCH; ~, $p < 0.05$ versus LPS; @, $p < 0.01$ versus DHDMCH and LPS.

In LPS stimulated RAW264.7 cells HO-1 activity was induced (2.3 ± 0.2 fold) and was further elevated to 6.2 ± 2.5 fold in the presence of the chalcone DHDMCH. This induction was reduced by 52% to 70% when the cells were treated with 5 μM or 10 μM of SnPPIX, respectively (Figure 29 A and B). Together with LPS the induction of HO-1 activity was abolished by 5 μM of SnPPIX, while the induction by DHDMCH was only reduced by 61%. The observation that HO-1 induction is only reduced to half by 5 μM of SnPPIX in the presence of the highly active chalcone and even less by additional LPS suggests that the amount of HO-1 inhibitor with 5 μM is not quite sufficient to abolish the induced HO-1 activity. But, an equal observation for the HO-1 induction of the chalcone was also made when 10 μM of SnPPIX were used (Figure 29, B). Interestingly, with

10 μM of inhibitor, the combined HO-1 induction of DHMCH and LPS could be further inhibited but reached only the reduced HO-1 activity level of DHMCH alone. This suggests that there is still sufficient HO-1 activity left, which derives from the chalcone and cannot be abolished by the amount of 10 μM of SnPPIX inhibitor. Cell viability tests only allowed for a maximum concentration of 10 μM SnPPIX, since SnPPIX in absence of LPS revealed cytotoxicity of at 20 μM (Figure 29, D). No cytotoxic effect was observed in the range of 1 to 20 μM of SnPPIX in the presence of LPS. Noteworthy is the moderate cytotoxic effect of the chalcone with 5 μM SnPPIX in absence and presence of LPS (Figure 29, C), which should be kept in mind the HO-1 activity is evaluated when under these conditions.

3.1.4 Heme oxygenase-1 activity in human dendritic cells (DC)

As part of the innate immune system dendritic cells (DC) play a key role providing a crucial link between the innate and the adaptive immune response.²²⁷ DC are able to recognize and capture antigens, carrying them to the next lymphoid organ and present them to native T-cells thus activating the adaptive immune defense system. The activated dendritic cells exert also a variety of cytokines that influence the activity of T cells. The cells are used in DC-based immunotherapy against cancer and infectious diseases.²²⁸⁻²²⁹ It is known that HO-1 is expressed in human DC derived from monocytes and that upon HO-1 induction the function of the dendritic cells can be altered regarding the maturation state of the cells and their ability to exert the anti-inflammatory cytokine IL-10.²³⁰ Furthermore, the involvement of the Nrf2-ARE pathway leading to HO-1 gene expression was elucidated in DC after treatment with several electrophiles and pro-oxidative agents.²³¹

Dendritic cells derived from human monocytes obtained from blood samples of healthy donors (kindly provided by the Department of Internal Medicine III, University Hospital of Regensburg) were investigated for their heme oxygenase activity in presence of the $\alpha\text{-CF}_3$ -substituted tetrametoxychalcone (TMCH) derivative $\alpha\text{-CF}_3\text{-TMCH}$ (for structure see Figure 12). The adherent dendritic cells were stimulated with 0.5 and 1 μM of $\alpha\text{-CF}_3\text{-TMCH}$ in presence of 100 ng mL^{-1} LPS for 24 h and the HO-1 activity in the whole cell lysate was determined. For this test the HO-1 activity assay was slightly modified. Due to the limited amount of samples the bilirubin standards were prepared only in lysis buffer instead of the usual cell lysate. This assay modification allowed to determine the basal bilirubin level in the cell lysate of untreated DC stimulated with LPS together with the HO activity in control DC and DC treated with the chalcone in presence of LPS. The results are displayed in Figure 30.

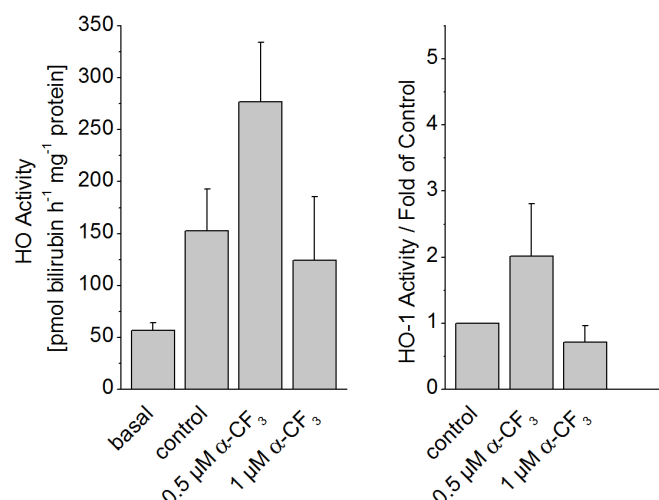


Figure 30. Heme oxygenase-1 activity of α -CF₃-substituted TMCH (α -CF₃) determined in human dendritic cells (DC). Cells were treated with α -CF₃-TMCH at the indicated concentration in presence of 100 ng mL⁻¹ LPS for 24 h. From the HO activity determined by the ELISA-based HO-1 activity assay (left diagram), the fold induction of HO-1 activity for α -CF₃-TMCH compared to control cells was calculated (right diagram). Data represent the mean \pm SD of 4 independent experiments carried out in triplicates. $p > 0.05$, Student's t-test.

The heme oxygenase activity in DC stimulated with LPS could be elevated in presence of the chalcone derivative α -CF₃ at a nanomolar concentration (500 nM) from 153 ± 40 to 277 ± 57 pmol bilirubin h⁻¹ mg⁻¹ total protein. Thus the HO-1 activity was induced by 2.0 ± 0.8 fold by α -CF₃-TMCH at 0.5 μ M. This inductive effect was not observed at a higher concentration, although at 1 μ M no cytotoxic effects occurred (confirmed by microscopic analysis), suggesting a alternative pathway in DC consuming the chalcone. However, the results were statistically not significant, suggesting that 24 h may not be an optimal time to stimulate the DC and that rather a shorter incubation time with the chalcone is required. This observation was made in murine macrophages RAW264.7, where the α -CF₃-TMCH showed a significant inductive effect on HO-1 protein expression and activity after 6 h of stimulation. However no effect on HO-1 activity was observed in RAW264.7 cells after an incubation time of 24 h with 0.5 μ M α -CF₃-TMCH, see section 3.4.2. Taken together these results confirm the applicability of the HO-1 activity assay in primary human cells.

3.2 Screening of natural products and drugs towards their HO-1 activity in RAW264.7 macrophages

A structurally diverse group of 18 natural products and synthetic compounds with pharmacologically interesting activity were screened for their HO-1 induction behavior using the ELISA-based HO-1 activity assay in the model cell line RAW264.7. The structures are given in Figure 9. The cytotoxicity of compounds in RAW264.7 cells was determined prior to the HO-1 activity screen and toxic concentrations were excluded from further testing.

3.2.1 Influence of natural products and drugs on the viability of RAW264.7 macrophages

The viability of RAW264.7 cells exposed to test compounds for a period of 24 h was determined by the MTT assay. Most of the natural products and the synthetic drugs showed a cytotoxic effect at 25 or 50 μ M (Figure 31 and Figure 32). The natural compounds chlorogenic acid, caffeic acid, (-)-epicatechin and 3-hydroxycoumarin revealed no cytotoxicity ≤ 100 μ M. Interestingly, a moderate but significant proliferative effect on RAW264.7 cells exposed to 1 and 5 μ M of zerumbone was observed. The most toxic compound was the synthetic drug dexamethasone at 500 nM followed by CAPE (5 μ M) and sulforaphane (10 μ M). In preliminary experiments dexamethasone was found to be toxic in the range of 100-0.5 μ M, displaying a cell viability of 60-70%.

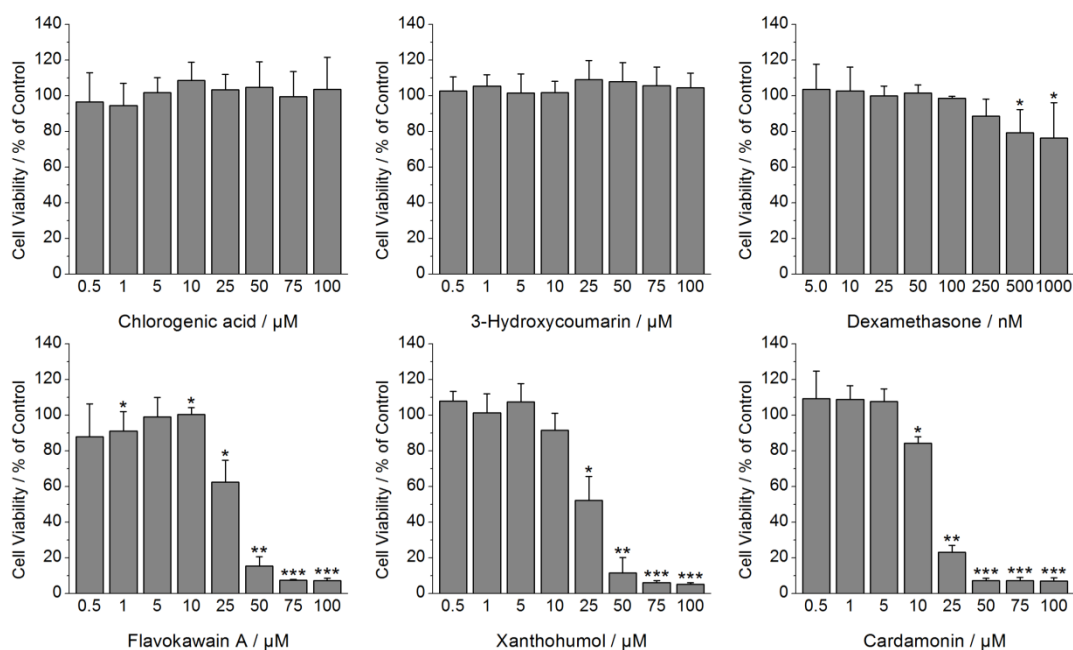


Figure 31. Influence of natural products and synthetic drugs on the viability of RAW264.7 macrophages. Cells were incubated with the test compounds at the indicated concentrations for 24 h and cell viability was determined by the MTT assay.

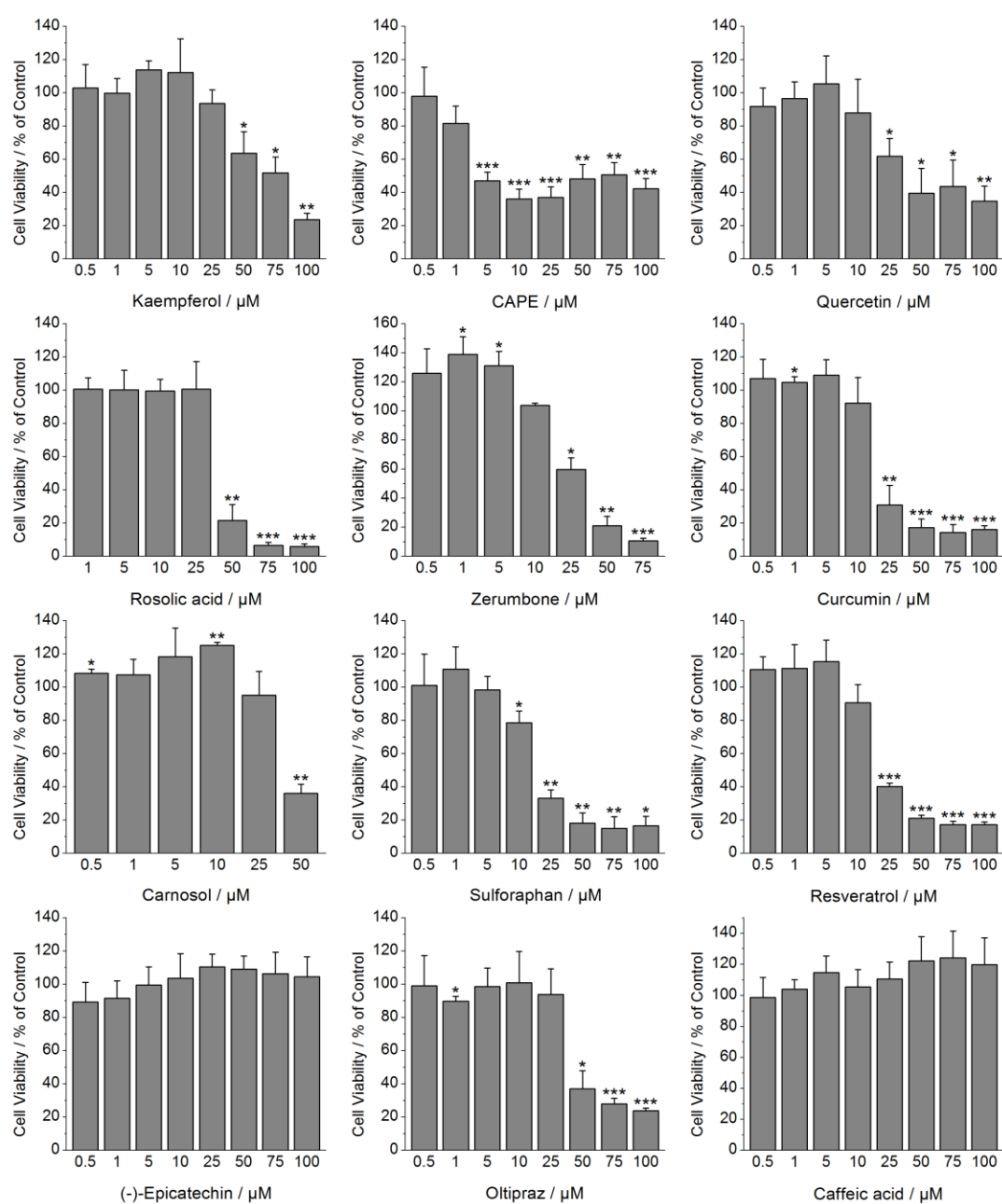


Figure 32. Influence of natural products and synthetic drugs on the viability of RAW264.7 macrophages. Cells were incubated with the test compounds at the indicated concentrations for 24 h and cell viability was determined by the MTT assay.

3.2.2 Effect of natural products as well as the two drugs oltipraz and dexamethasone on HO-1 activity in RAW264.7 macrophages

The HO-1 inducer activity of a diverse group of compounds was estimated in RAW264.7 murine macrophages using the ELISA-based HO-1 activity assay. The compounds were tested at 4 concentrations after 6 and 24 h of stimulation (Figure 33-Figure 35). The indicated test concentrations had no effect on the cell viability after an incubation of 24 h as determined by the MTT assay, see Figure 31 and Figure 32.

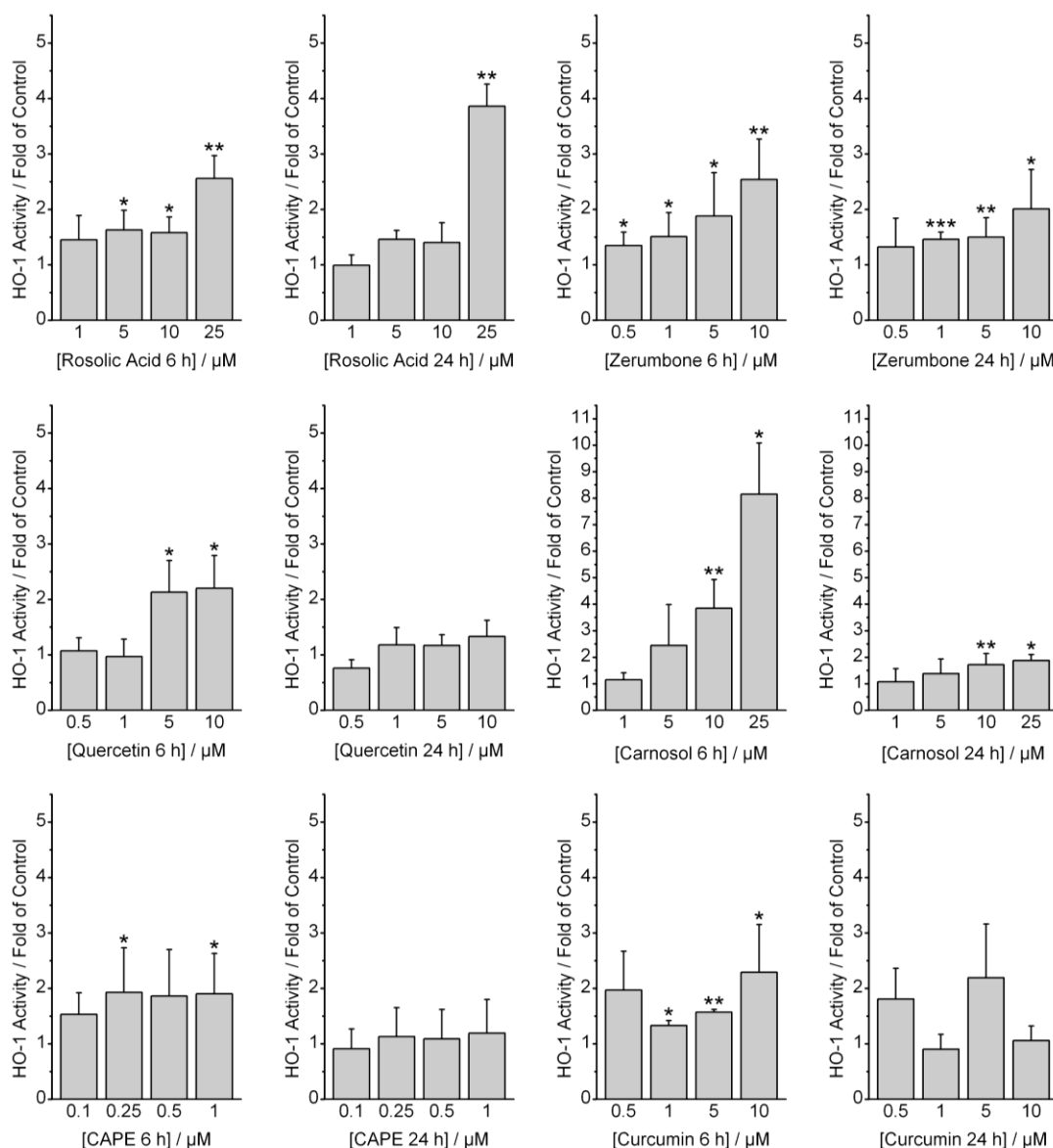


Figure 33. HO-1 activity was determined in whole cell lysates via the ELISA-based HO-1 activity assay. RAW264.7 cells were incubated with test compounds in several concentrations as indicated for 6 and 24 h.

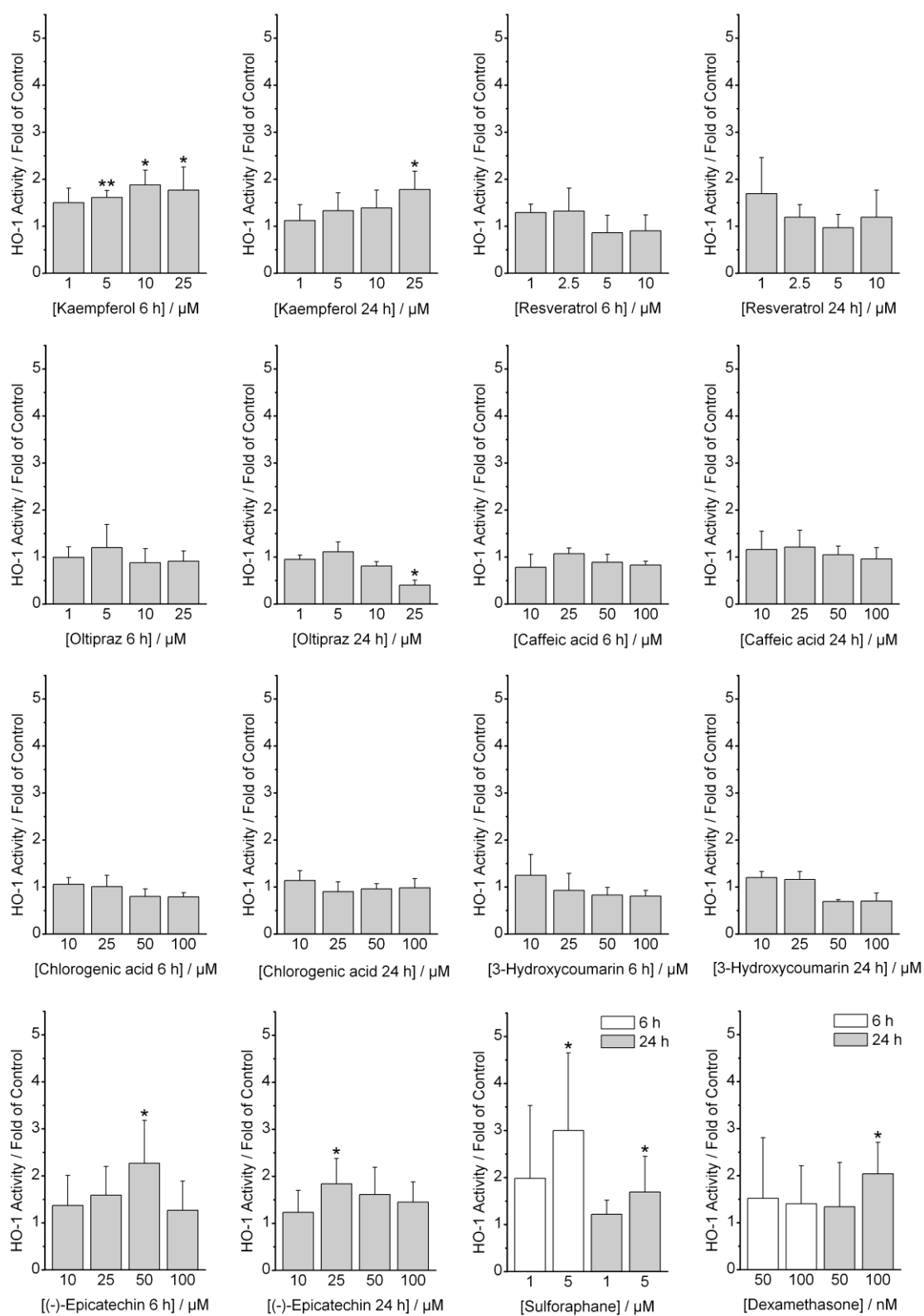


Figure 34. HO-1 activity was determined in whole cell lysates via the ELISA-based HO-1 activity assay. RAW264.7 cells were incubated with test compounds in several concentrations as indicated for 6 and 24 h.

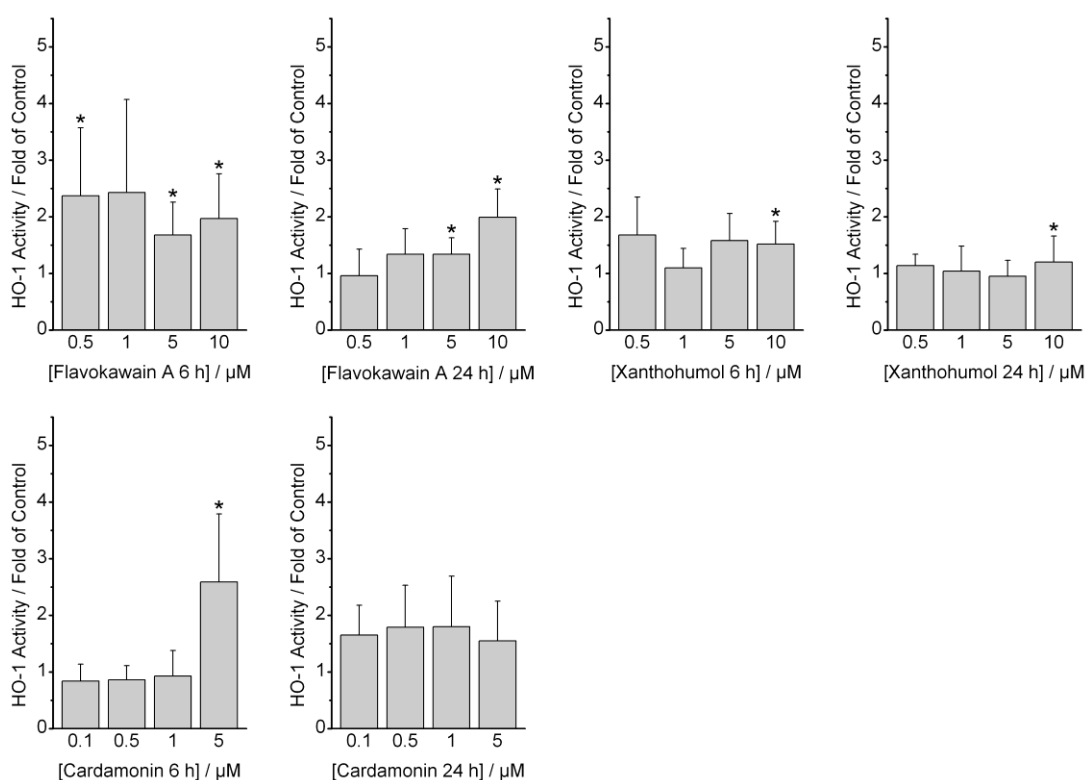


Figure 35. HO-1 activity was determined in whole cell lysates via the ELISA-based HO-1 activity assay. RAW264.7 cells were incubated with test compounds in several concentrations as indicated for 6 and 24 h.

From the 18 compounds tested, 13 proved to induce HO-1 activity in RAW264.7 cells (Table 10) with carnosol (8.2 fold at 25 μM) and sulforaphane (3.0 fold at 5 μM) showing the highest induction after 6 h. The chalcones flavokawain A and cardamonin as well as rosolic acid and zerumbone gave a 2.7-2.5 fold induction after 6 h. A lower, but clear induction of 2.3-1.5 fold was determined for curcumin, (-)-epicatechin, quercetin, CAPE, kaempferol and xanthohumol after the same incubation time. While the majority of the tested compounds showed a higher inductive power after 6 h compared to 24 h, rosolic acid revealed a higher HO-1 activity after 24 h (3.9 fold at 25 μM). The same applies to dexamethasone, which was inactive after 6 h but showed an HO-1 activity induction of 2.0 fold at 0.1 μM. After 24 h only 9 compounds were significantly active. A comparison of all compounds at 10 μM follows the same general trend as alluded before. Chlorogenic acid, caffeic acid and 3-hydroxycoumarin could not induce HO-1 in RAW264.7 cells, which was also found for the known HO-1 inducer resveratrol and the phase II protein inducer oltipraz.

Table 10. Influence of tested compounds on induction of HO-1 activity in RAW264.7 cells together with their toxicity limit (highest non-toxic concentration) determined by the MTT test.

Compound	Toxicity ^a limit [μ M]	Fold induction of HO-1 activity ^b			
		Maximum 6 h (conc [μ M])	Maximum 24 h (conc [μ M])	6 h at 10 μ M	24 h at 10 μ M
3-Hydroxycoumarin	> 100	ns	ns	ns	ns
Caffeic acid	> 100	ns	ns	ns	ns
CAPE	1.0	1.93 \pm 0.80 (0.25)	ns	- ^c	- ^c
Carnosol	25	8.15 \pm 1.93 (25)	1.88 \pm 0.22 (25)	3.85 \pm 1.08	1.72 \pm 0.42
Chlorogenic acid	> 100	ns	ns	ns	ns
(-)-Epicatechin	> 100	2.27 \pm 0.91 (50)	1.84 \pm 0.54 (25)	ns	ns
Curcumin	10	2.29 \pm 0.86 (10)	ns	2.29 \pm 0.86	ns
Kaempferol	25	1.88 \pm 0.31 (10)	1.78 \pm 0.39 (25)	1.88 \pm 0.31	ns
Quercetin	10	2.20 \pm 0.59 (10)	ns	2.20 \pm 0.59	ns
Resveratrol	10	ns	ns	ns	ns
Rosolic acid	25	2.56 \pm 0.41 (25)	3.86 \pm 0.40 (25)	1.58 \pm 0.28	ns
Zerumbone	10	2.54 \pm 0.73 (10)	2.01 \pm 0.71 (10)	2.54 \pm 0.73	2.01 \pm 0.71
Sulforaphane	5.0	3.00 \pm 1.65 (5)	1.69 \pm 0.76 (5)	- ^c	- ^c
Dexamethasone	0.25	ns	2.04 \pm 0.67 (0.10)	- ^c	- ^c
Oltipraz	25	ns	ns	ns	ns
Cardamonin	5.0	2.59 \pm 1.20 (5)	ns	- ^c	- ^c
Xanthohumol	10	1.52 \pm 0.40 (10)	1.20 \pm 0.46 (10)	1.52 \pm 0.40	1.20 \pm 0.46
Flavokawain A	10	2.73 \pm 1.20 (0.5)	1.99 \pm 0.50 (10)	1.97 \pm 0.79	1.99 \pm 0.50

^aCytotoxicity of test compounds was measured via MTT assay and the highest non-toxic concentrations are presented for an incubation time of 24 h (toxicity limit). ^bSignificant stimulation of maximum HO-1 activity is shown as fold of induction at concentrations, which were not toxic (cell viability > 80%). Cells were incubated for 6 and 24 h with compounds at the indicated concentrations and HO-1 activity (fold of control, $p \leq 0.05$) was determined in whole cell lysates via the ELISA-based HO-1 activity assay. ns, not significant, ^c no data was gained due to toxicity at this concentration.

The ability of CAPE, curcumin and rosolic acid to induce HO-1 activity in RAW264.7 cells determined with the HO-1 activity assay is in line with previous studies where these compounds were found to induce HO-1 activity in other cell lines (see Table 1). Our findings are also in agreement with the literature for xanthohumol, (-)-epicatechin, zerumbone, sulforaphane and carnosol, since their inductive potential on HO-1 mRNA and/or protein level was determined in other cell models (see Table 1). The two flavonoids quercetin and kaempferol were reported to induce HO-1 protein expression in RAW264.7 cells at concentrations of 100 μ M,^{139, 232} which we found to be cytotoxic in our assay. Nevertheless, the group reports an increase of HO-1 protein expression after 8 h with a maximum peak at 12 h which decreases after 24 h in the presence of 100 μ M of flavonoid, which is similar to our findings showing a higher activity of the compounds after 6 h rather than 24 h. In a recent study quercetin was found to increase the HO-1 protein level in a concentration-dependent manner (0.5-10 μ M) after 24 h of stimulation in RAW264.7 cells. Here

the group found a cytotoxic effect of quercetin in the range of 25-100 μM .²³³ For caffeic acid and chlorogenic acid our finding is in line with the literature, where they were found to be inactive. Moreover, 3-hydroxycoumarin which induced the phase II protein NQO1 in murine hepatocytes¹¹⁹ did not increase HO-1 activity in RAW264.7 cells.

The activation of the Nrf2 signaling pathway was shown to be essential for the chemopreventive actions of oltipraz,¹¹⁶ therefore a possible induction of HO-1 activity by oltipraz was assumed. Also induction of HO-1 on protein and activity level was shown for the structurally related dithiolethiones in hepatocytes.²³⁴ The mechanism by which Nrf2 is induced by dithiolethiones is an increase of the intracellular H_2O_2 production upon reductive cleavage of the S-S bond of dithiolethiones leading to generation of O_2^\bullet radicals.²³⁵ However, in our HO-1 activity assay oltipraz showed no inductive activity after 6 and 24 h in RAW264.7 cells.

3.2.3 Effect of natural products and dexamethasone on the HO-1 protein expression in RAW264.7 macrophages

In addition to the HO-1 activity measurements, some selected compounds were also investigated towards their ability to increase the HO-1 protein expression in RAW264.7 cells in order to evaluate the results in the HO-1 activity assay. The results of the Western blot analysis are shown in Figure 36.

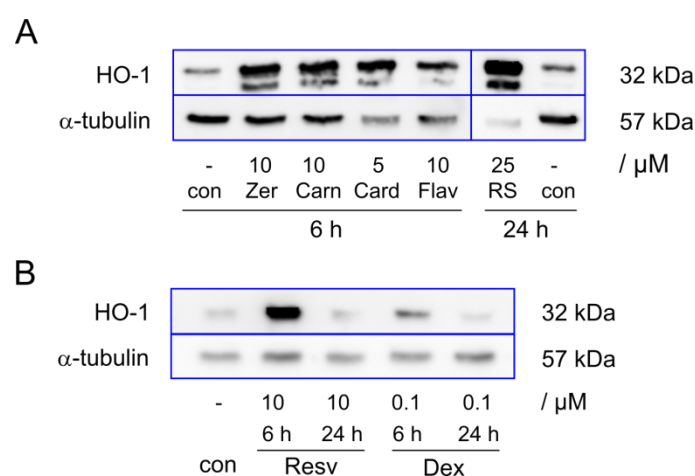


Figure 36. Effect of natural products and the drug dexamethasone on HO-1 protein expression. RAW264.7 macrophages were incubated with compounds at different concentration for 6 and 24 h as indicated and Western blot analysis was performed with 33 μg of protein. con, control; Res, resveratrol; Dex, dexamethasone; Zer, zerumbone; Carn, carnosol; Card, cardamomin; Flav, flavokawain A.

The most potent natural compounds found in the HO-1 activity screen, zerumbone, carnosol, cardamomin, flavokawain A and rosolic acid revealed also an inductive activity on the HO-1 protein level, confirming the results of the HO-1 activity assay. Resveratrol induced HO-1 protein expression after 6 h of incubation with RAW264.7 cells and decreased to control level after 24 h. Similar observations were made with dexamethasone.

Resveratrol was found to be inactive after 6 and 24 h in the HO-1 activity assay, suggesting that the HO-1 protein expressed after 6 h remains inactive in the RAW264.7 cells upon resveratrol treatment. One can assume that alternative pathways may be triggered by resveratrol that can suppress the activity of the expressed HO-1 protein, since it is known that resveratrol can activate multiple signaling pathways in the cell. Resveratrol has shown to stimulate HO-1 expression in human cells¹⁴³ as a response to the activation of the proinflammatory NF- κ B. On the contrary, it was also shown that in RAW264.7 macrophages resveratrol exerts anti-inflammatory activity by suppressing the NF- κ B signaling pathway.¹²³ These reports may suggest that HO-1 induction by resveratrol in RAW264.7 cells may be in parts mediated by the activation of the NF- κ B pathway. Another mechanism of action of resveratrol was found in rat cells, where the induction of HO-1 expression was triggered by activating the Nrf2/ARE pathway as well as the ERK pathway.¹³⁰ Beside this, resveratrol could not induce HO-1 protein expression or enzyme activity⁶⁷ in rat astrocytes, only an increase in mRNA level could be observed.¹⁴⁶ In conclusion these reports suggest that HO-1 induction by resveratrol relies on activation of multiple signaling pathways and that its activity can be cell type specific.

The glucocorticosteroid dexamethasone could elevate the HO-1 protein expression after 6 h while after 24 h the expression level of HO-1 decreased to control level in RAW264.7 cells at a concentration of 100 nM. On the contrary, no significant HO-1 activity was determined in RAW264.7 cells after 6 h, although some non significant induction of HO-1 activity was observed (Figure 34). Unexpectedly, HO enzyme activity doubled after 24 h upon dexamethasone treatment of RAW264.7 cells, which cannot be fully explained, since no HO-1 protein expression was detected after 24 h. In HeLa cells dexamethasone could induce HO-2 mRNA and protein level by activating the GRE (glucocorticoid response element) present in the promoter region of the HO-2 gene, while HO-1 mRNA was not detected. Also a increase in HO activity was observed in HeLa cells upon treatment with dexamethasone.¹⁵⁰ These findings may explain our observations of the increase in HO activity without an increase in HO-1 protein expression after 24 h. The detected HO activity may derive in this case from HO-2 induction in RAW264.7 cells by dexamethasone. These findings are interesting and need to be further investigated concerning the influence of dexamethasone on HO-2 in RAW264.7 cells.¹⁵¹

3.3 Characterization of chalcones towards their anti-inflammatory, antioxidative and cytoprotective activity

A group of natural and synthetic hydroxy and methoxychalcones (Figure 11) was characterized towards their anti-inflammatory and antioxidant behavior in RAW264.7 murine macrophages. Furthermore, a cell-free ORAC-fluorescein assay performed under physiological conditions was used to determine the radical scavenging properties of the chalcones and establish an antioxidant capacity compared to the vitamin E derivative Trolox.

3.3.1 Effect of chalcones on the viability of RAW264.7 macrophages

The cytotoxicity of chalcones in RAW264.7 cells was determined and toxic concentrations (< 80% viability) were excluded from further testing. Most of the chalcones showed cytotoxic effects at 25 μM , however ISL, THMCH and 2'-hydroxychalcone were toxic at 50 μM . The most toxic chalcone found, was calythrpsin at 5 μM . Calythrpsin is known for its cytotoxic effects.¹⁸²⁻

183

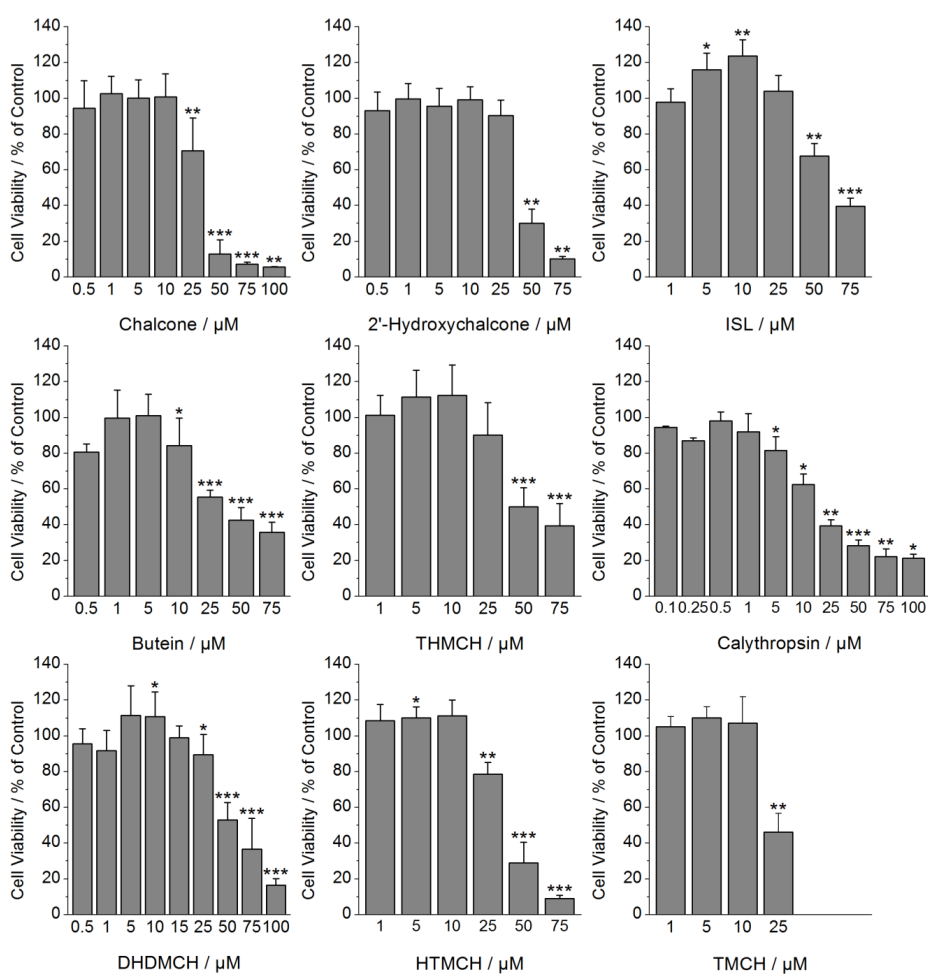


Figure 37. Influence of chalcones on the viability of RAW264.7. Cells were treated with the test compounds at the indicated concentrations for 24 h and cell viability was determined by the MTT assay.

Interestingly, ISL showed a significant proliferative effect up to 20% on RAW264.7 cells at 5 and 10 μM (Figure 37). The potential cytotoxic effect of these chalcones was further investigated in LPS-stimulated RAW264.7 macrophages, where the compounds were incubated together with 10 ng mL^{-1} LPS for 24 h and viability was assessed by the MTT-LPS test (Figure 38). Here, the cytotoxic concentrations were eliminated from further testing, relevant in the iNOS inhibition assay, were LPS-stimulated RAW264.7 cells were used to determine the influence of chalcones on the NO production. The chalcones were tested in the same concentration range as in the MTT assay without LPS addition except for 2'-hydroxychalcone and calythrpsin, where their influence in presence of LPS was tested at lower concentrations. All chalcones show a similar toxicity pattern, but a higher toxicity level in the presence of LPS when compared with their influence on RAW264.7 cells without LPS stimulation. This can be explained by a minor effect of LPS on the cell viability of RAW264.7 cells (> 80% viability, see Figure 29, C), which could influence the toxicity of the chalcones. LPS is a cell wall component of gram-negative bacteria, acting as a bacterial endotoxin and inducing an inflammatory state in cells.²³⁶⁻²³⁷

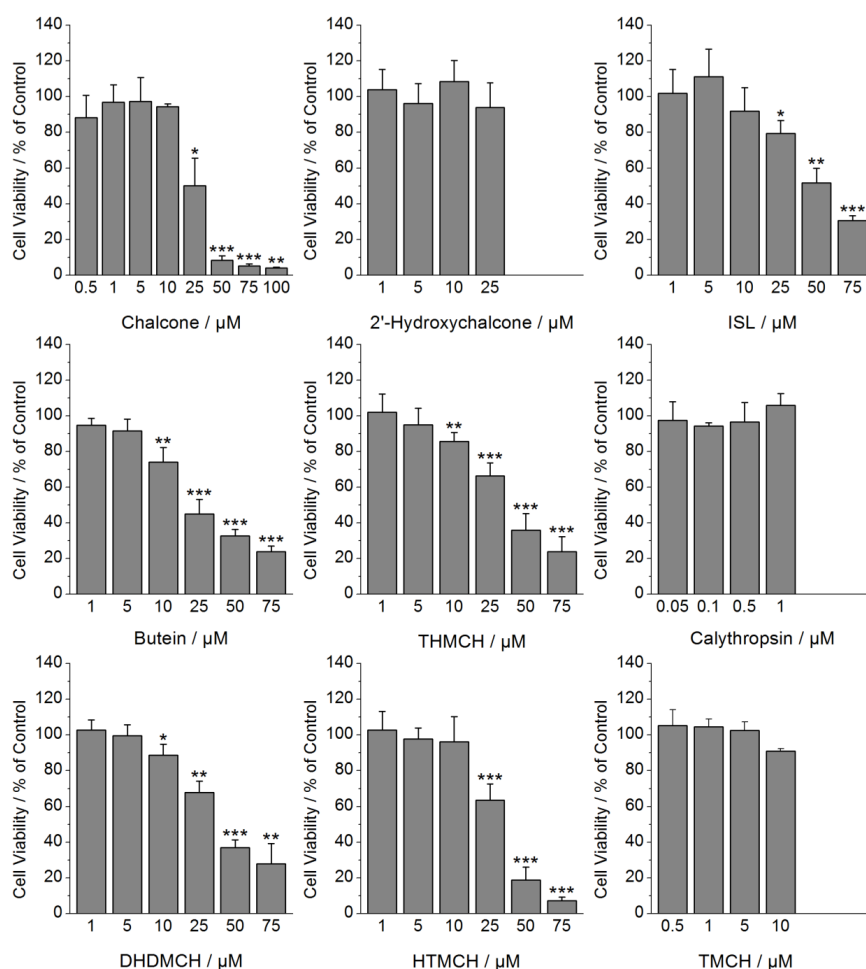


Figure 38. Influence of chalcones on the viability of LPS-stimulated RAW264.7. Cells were treated with the test compounds at the indicated concentrations and in the presence of 10 ng mL^{-1} LPS for 24 h and cell viability was determined by the MTT-LPS assay.

3.3.2 Influence of chalcones on HO-1 activity and HO-1 protein expression

The natural and synthetic chalcones were screened for their HO-1 induction behavior (Table 11) using the ELISA-based HO-1 activity assay. The compounds were tested typically at 4 concentrations that had no strong influence on the cell viability (> 80%) after 6 and 24 h of stimulation, which were found to be good time points for DHDMCH (see Figure 26). All of the 9 tested chalcones proved to induce HO-1 activity in RAW264.7 cells (Figure 39 and Figure 40) with DHDMCH showing the highest induction after 6 h of incubation (6.1 fold at 10 μ M), which could still be observed after 24 h (3.8 fold). Interestingly, all tested chalcones showed a significant HO-1 activity induction after 6 h, a relatively short incubation time. While ISL, butein, DHDMCH and TMCH showed a prolonged inductive activity after 24 h, the other chalcones displayed a significant activity only after 6 h and were inactive after 24 h.

Table 11. Influence of chalcones on induction of HO-1 activity in RAW264.7 cells together with their toxicity limit (highest non-toxic concentration) determined by the MTT test.

Compound	Toxicity ^a limit [μ M]	Fold induction of HO-1 activity ^b			
		Maximum 6 h (conc [μ M])	Maximum 24 h (conc [μ M])	6 h at 10 μ M	24 h at 10 μ M
DHDMCH	15	6.05 \pm 2.31 (10)	3.84 \pm 1.47 (10)	6.05 \pm 2.31	3.84 \pm 1.47
ISL	25	3.43 \pm 1.53 (25)	1.93 \pm 0.70 (25)	2.00 \pm 0.71	1.40 \pm 0.38
Butein	10	3.07 \pm 1.79 (10)	1.91 \pm 0.31 (10)	3.07 \pm 1.79	1.91 \pm 0.31
TMCH	10	2.96 \pm 0.23 (10)	2.35 \pm 0.32 (10)	2.96 \pm 0.23	2.35 \pm 0.32
THMCH	10	2.91 \pm 1.05 (10)	ns	2.91 \pm 1.05	ns
2'-Hydroxychalcone	25	2.38 \pm 0.57 (5.0)	ns	2.05 \pm 0.84	ns
Chalcone	10	2.15 \pm 0.67 (10)	ns	2.15 \pm 0.67	ns
Calythropsin	1	2.17 \pm 0.63 (0.1)	ns	- ^c	- ^c
HTMCH	10	1.52 \pm 0.17 (1.0)	ns	ns	ns

^a Cytotoxicity of test compounds was measured via MTT assay and the highest non-toxic concentrations are presented for an incubation time of 24 h (toxicity limit). ^b Significant stimulation of maximum HO-1 activity is shown as fold of induction at concentrations, which were not toxic (cell viability > 80%). Cells were incubated for 6 and 24 h with compounds at the indicated concentrations and HO-1 activity (fold of control, $p < 0.05$) was determined in whole cell lysates via the ELISA-based HO-1 activity assay. ns, not significant, ^c no data was gained due to toxicity at this concentration.

A concentration dependent induction of HO-1 activity was observed for ISL (6 h), butein (24 h) and DHDMCH (6 and 24 h), whereas for calythropsin and 2'-hydroxychalcone an indirect concentration dependence was found, for both after 6 h. A hormetic-like dose response was detected for THMCH at 6 h, where at a lower dose the activity was higher than at higher concentrations. A slight tendency to hormesis was observed for chalcone (6 h) and butein (6 h), although at low concentration the data was not significant, due to a high deviation of these data points. The chalcone HTMCH showed no concentration dependent HO-1 activity.

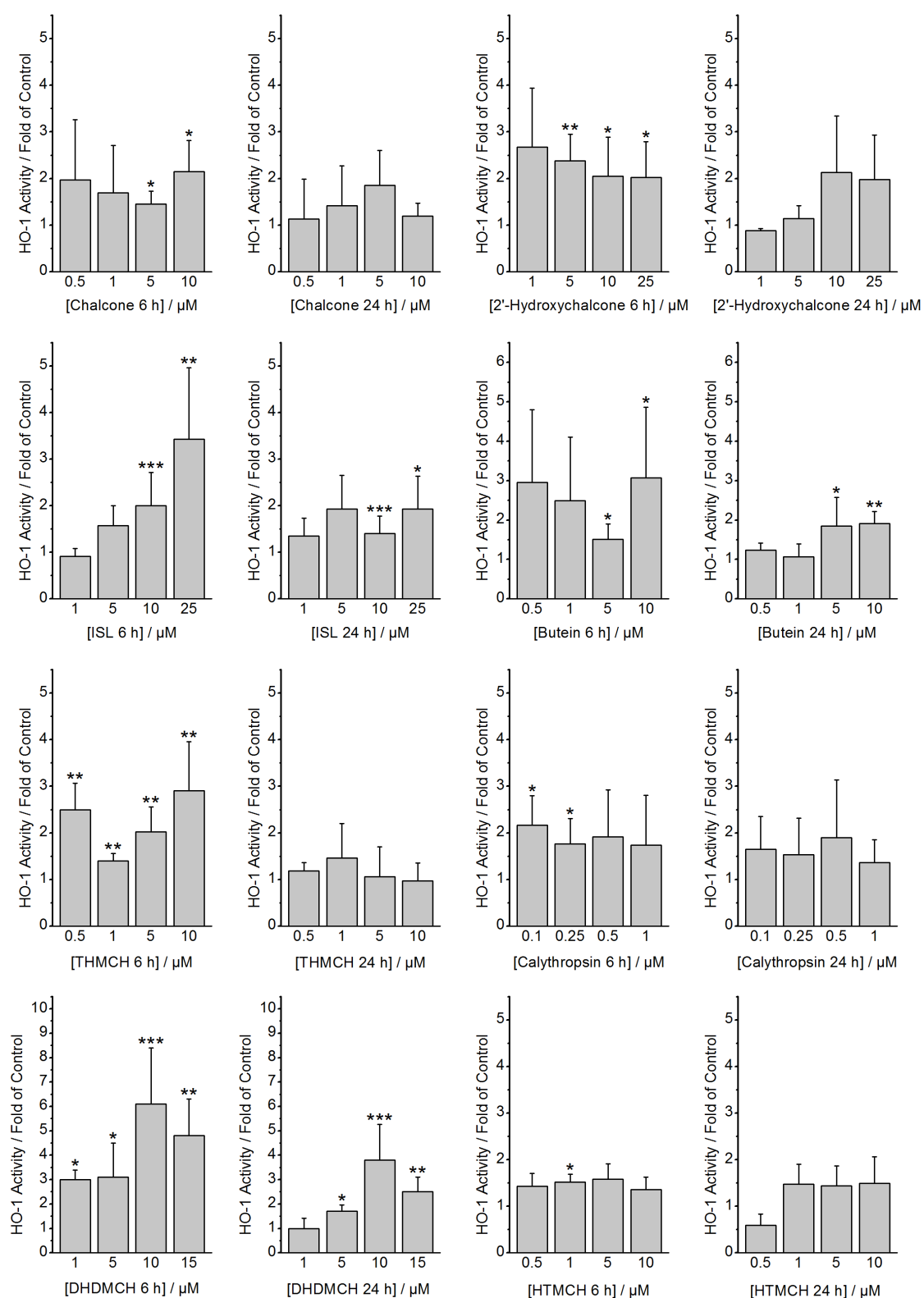


Figure 39. HO-1 activity was determined in whole cell lysates via the ELISA-based HO-1 activity assay. RAW264.7 cells were incubated with test compounds in several concentrations as indicated for 6 and 24 h.

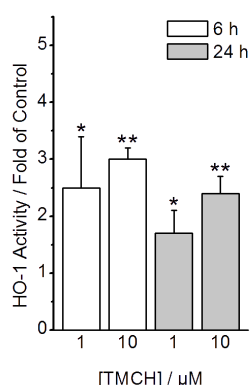


Figure 40. RAW264.7 cells were incubated with the chalcone TMCH at 1 and 10 μM as indicated for 6 and 24 h and HO-1 activity was determined in whole cell lysates via the ELISA-based HO-1 activity assay.

The data in the HO-1 activity screen showed that hydroxy-rich chalcones, such as ISL and butein, are in favor for a high induction of HO-1 activity, suggesting a combination between antioxidant activation mechanisms and Michael acceptor reactivity. The positive influence of the 2'-hydroxy group on the HO-1 activity was observed when comparing 2'-hydroxychalcone (2.4 fold) to chalcone (1.4 fold) at 5 μM . However, this effect could not be observed in the case of HTMCH compared to the tetramethoxychalcone TMCH, where the HO-1 activity decreased from 3.0 to 1.5 fold after 6 h, when the 2'-hydroxy group was present in the chalcone. Interestingly, the tetramethoxychalcone, TMCH showed a quite similar inductive activity as butein, suggesting different activation mechanisms of the chalcones, which come into play for HO-1 activation. The introduction of methoxy groups into the chalcone seems to retain the activity of these, when comparing the elevation of HO-1 activity from 2.2 fold in the case of chalcone to 3.1 and 3.0 fold for butein and TMCH, respectively after 6 h. The two regioisomers, concerning the methoxy groups, calythropsin and THMCH displayed a similar induction of HO-1 activity after 6 h in a nanomolar range of 2.2 fold at 100 nM and 2.5 fold 500 nM, respectively. A strong inducer in our screen was DHDMCH, the most potent chalcone in the HO-1 assay with a 6.1 fold increase of HO-1 activity at 10 μM after 6 h, which showed also an induction on HO-1 protein expression (Figure 26 A). The specific substitution motif on both aromatic rings, the two less electron donating methoxy groups on the B-ring and the two stronger electron donating hydroxy groups on the A-ring, seems to retain the reactivity of the α,β -unsaturated carbonyl moiety, since its double bond can be regarded as a push-pull double bond. Together with DHDMCH, butein and TMCH displayed the highest inductive HO-1 activity after a prolonged incubation time of 24 h, making these compounds most promising for parent chalcones for further investigations concerning the HO-1 activity *in vitro*.

For the most chalcones tested our data on HO-1 activity is in line with literature results. Similar to our results, butein was found to induce HO-1 activity in a concentration and time dependent

fashion in human dental pulp cells between 2.5 and 20 μM with a maximum induction after 18 h of stimulation.¹⁶⁶ Motterlini *et al.* showed that 2'-hydroxychalcone (2'-HOC) induces heme oxygenase activity in RAW264.7 after 6 h at a concentration of 15 and 30 μM (2 fold induction compared to control level). But they also showed that at concentrations ≥ 30 μM 2'-HOC decreased the cellular metabolism of macrophages,⁶⁹ which means that data gained at 30 μM of 2'-HOC has to be interpreted carefully. ISL showed in the HO-1 activity assay a high inductive activity of HO-1 after 6 h (3.4 fold), which decreases after 24 h to a 1.9 fold induction compared to control cells. This data supports the findings of the group of Lee *et al.*,¹⁷⁸ where in the presence of 10 μM ISL an increase of HO-1 protein was detected after 4 h and reached a maximum level after 12 h of incubation in RAW264.7 cells. However, the effect of ISL after 24 h of stimulation was not reported.

3.3.3 Effect of chalcones on nitrite production

The inhibitory influence of chalcones on the NO production, and thus iNOS activity in RAW264.7 macrophages stimulated with LPS for a period of 24 h was investigated. The NO production was determined by the nitrite level in LPS-stimulated RAW264.7 cells via the Griess assay. Amongst the tested compounds, 7 out of 9 displayed a significant inhibitory activity on the nitrite production, only chalcone and calythropsin were inactive (Figure 41). The selected test concentrations had no cytotoxic effect (viability > 80%, see Figure 38) on RAW264.7 macrophages that could influence the results. All active chalcones showed a concentration dependent reduction of NO generation. Table 12 summarizes the observed maximum inhibition of NO production for the chalcones, which was for the most potent to the less active ones at their toxicity limit.

Table 12. Inhibition of NO production in LPS-stimulated RAW264.7 macrophages determined by the Griess assay. Significant maximum NO inhibition values are given together with the toxicity limit (highest non-toxic concentration) determined by the MTT assay in presence of 10 ng mL⁻¹ LPS after an incubation time of 24 h.

Compound	Toxicity limit [μM]	Maximum inhibition of NO production, % (conc. [μM])
TMCH	10	96.9 \pm 11.9 (10)
DHDMCH	10	72.9 \pm 7.7 (10)
Butein	5	54.5 \pm 4.3 (5.0)
HTMCH	10	52.2 \pm 16.5 (10)
THMCH	10	42.7 \pm 3.1 (10)
ISL	10	38.0 \pm 7.4 (10)
2'-Hydroxychalcone	25	43.6 \pm 8.7 (25) ^a
Chalcone	10	ns
Calythropsin	1	ns

ns, not significant (no significant NO inhibition observed). ^a 2'-Hydroxychalcone gave at 10 μM a NO inhibition of 19.6 \pm 8.4%.

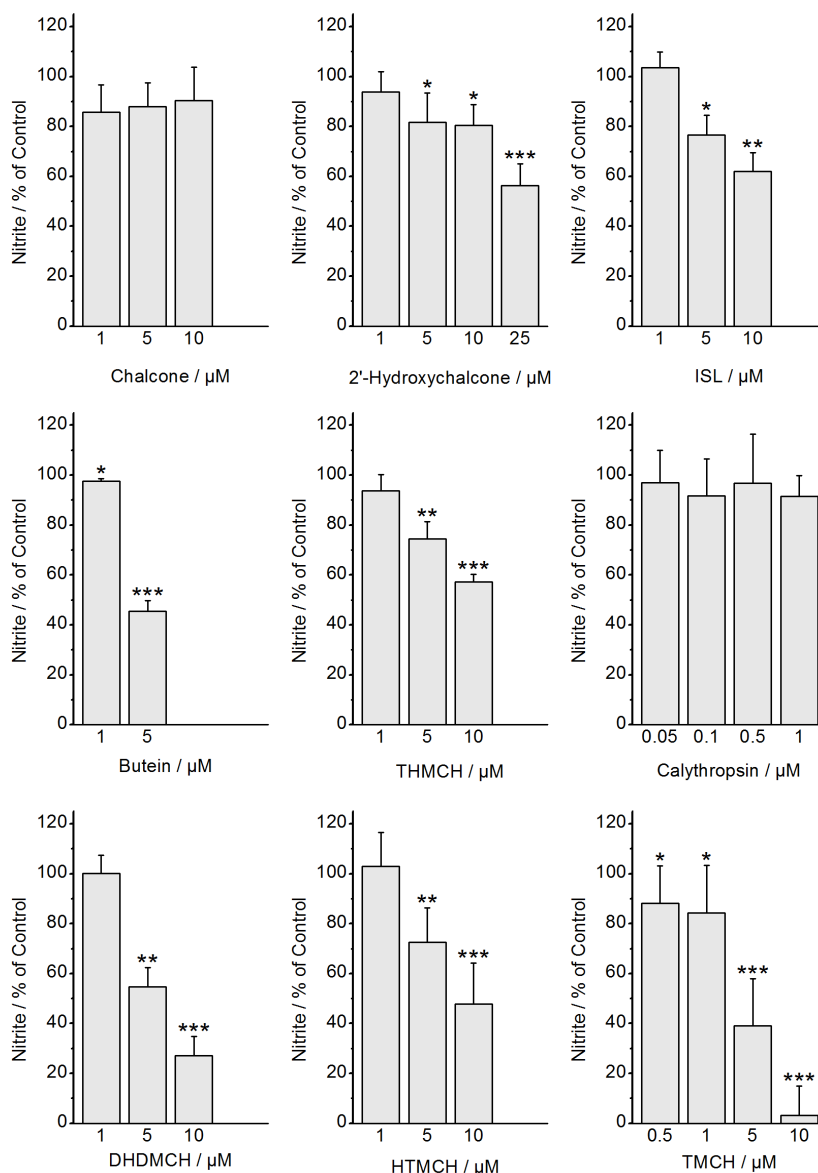


Figure 41. Influence of chalcones on NO production. RAW264.7 cells were exposed to 10 ng mL⁻¹ LPS alone (control) and LPS in presence of chalcones in the indicated concentrations for 24 h and the accumulated nitrite concentration present in the culture media was determined by the Griess assay.

Interestingly, the fully methoxylated chalcone TMCH was found to be the most active compound (97 ± 12% inhibition of NO release at 10 μM) followed by the A-ring dihydroxylated chalcone DHDMCH (73 ± 7.7% NO inhibition at 10 μM). The chalcone HTMCH, with three methoxy groups, however, showed a slightly decreased NO inhibition of 52 ± 17% at 10 μM, which was similar to the activity of butein (four OH groups) with 55 ± 4.3% measured at 5 μM, due to higher cytotoxicity of butein. This points to a particularly important influence of the OH group in 2'-position. Also THMCH and ISL (three OH groups) displayed similar inhibitory activity of NO production at 10 μM with 43 ± 3.1% and 38 ± 7.4%, respectively. The importance of the 2'-OH group becomes again clear, when the active 2'-hydroxychalcone (20 ± 8.4%, 10 μM) is compared to the inactive unsubstituted chalcone. On the other hand, this effect could not be observed on HTMCH, when compared with the tetramethoxychalcone TMCH. The regioisomers calythropsin and THMCH

differ in their cytotoxicity in LPS-stimulated RAW264.7, but are quite similar in their lack of inhibitory activity against NO release at 1 μM . Calythropsin displayed a higher cytotoxicity (toxicity limit 1 μM) and was inactive in decreasing the NO production, whereas THMCH was found to be a good inhibitory agent at higher concentrations ($43 \pm 3.1\%$, 10 μM) and less cytotoxic (toxicity limit 25 μM). In this case the *para*-position of the methoxy group on the B-ring is more activating than in the *para*-position on the A-ring. Taken together, two observations concerning the SAR of the chalcones can be made: i) the inhibition of the NO production is increasing from chalcone to butein, with an increased number of hydroxy groups on the chalcone, which can be explained by a higher antioxidant activity of the hydroxychalcones (as seen in Figure 42) and ii) an higher number of methoxy groups on the chalcone leads also to an increased inhibitory activity of NO production, were a combination of antioxidant activity and Michael acceptor activity can be assumed.

Similar to the findings of Lee *et al.*,¹⁶⁴ butein showed in the present study a concentration dependent inhibition of NO production with a 54% inhibition at 5 μM and a small activity at 1 μM . But in our study higher concentrations of butein were excluded, because it showed a cytotoxic effect on RAW264.7 cells in presence of 10 ng L⁻¹ LPS at 10 μM , a concentration that was reported to have no influence on cell viability. Abuarqoub *et al.* reported a high inhibition of NO production in the presence of 5-30 μM of 2'-hydroxychalcone in RAW264.7 cells treated with 1000 ng mL⁻¹ of LPS.⁶⁹ In contrast, our results showed only a moderate inhibitory activity of 44% at 25 μM , despite the fact that at higher concentration the 2'-hydroxychalcone was cytotoxic. One possible explanation is that in the other study⁶⁹ a 100 fold higher LPS concentration was used to stimulate the inflammatory state of the macrophages, which increases the iNOS induction and may thus influence the outcome of the assay. Lee *et al.* reported a concentration dependent inhibition of NO production in LPS-stimulated RAW264.7 cell for ISL,¹⁷⁸ which was much higher (86% at 10 μM) than in our observations (38% at 10 μM). An explanation could be the fact, that the group used a natural derived sample of ISL in their biological tests, which was extracted from dried heartwoods of *D. odorifera* compared to the synthetic ISL used in the present study. It is hypothesized that bioactive compounds retain a residual complexity after extraction and depending on the assay conditions, they can display a different biological result than the chemically pure compound. This was exemplified by a recent study with ISL.¹⁵⁸

3.3.4 Antioxidant capacity of chalcones

The antioxidant activity of the chalcones was investigated by the cell-free ORAC-fluorescein assay, where the radical scavenging activity was determined over time and compared to the antioxidant agent Trolox, a water-soluble vitamin E derivative.

Two structure characteristics contribute to the radical scavenging and reduction potential of chalcones: i) the α,β -unsaturated carbonyl moiety, reacting in a Michael addition-like reaction

with the radical and stabilizing the radical species by the conjugated π -electron system and ii) the hydroxy groups on the aromatic rings, which can in some cases oxidized to quinones²³⁸ (see Scheme 4). According to this, the results of the ORAC-fluorescein assay summarized in Table 13 clearly show that hydroxy groups are the key to antioxidant behavior. ISL and THMCH bearing three hydroxy groups reached 3 Trolox equivalents followed by butein with four hydroxy groups displays 2.6 Trolox equivalents. As expected, the simple chalcone, lacking any additional groups with radical scavenging or antioxidant functionality, showed no significant antioxidant capacity. Instead, the addition of one OH group in 2'-position increased the antioxidant activity more than twice to reach almost Trolox activity, as for 2'-hydroxychalcone.

Table 13. Antioxidant activity of chalcones and the positive control ascorbic acid.

Compound	Trolox equivalents (conc [μ M])
ISL	3.18 \pm 0.52 (0.5-10)
THMCH	3.08 \pm 0.26 (0.1-2.0)
Butein	2.63 \pm 0.15 (0.5-5.0)
Calythropsin	1.40 \pm 0.11 (0.1-5.0)
DHDMCH	1.36 \pm 0.23 (0.5-2.0)
2'-Hydroxychalcone	0.961 \pm 0.196 (0.5-10)
Chalcone	0.390 \pm 0.136 (0.5-10)
HTMCH	0.292 \pm 0.114 (0.5-10)
TMCH	0.241 \pm 0.099 (0.5-10)
Ascorbic acid (Vit. C)	0.642 \pm 0.164 (0.5-10)
The ORAC-fluorescein assay was carried out in 75 mM phosphate buffer pH 7.4 at 37 °C and antioxidant capacity is expressed as Trolox equivalents in the indicated concentration range.	

A subsequent substitution of the hydroxy groups by methoxy groups in the 2',3,4'-substituted chalcones leads to a decrease of antioxidant capacity (Figure 42). In the chalcone screen the best antioxidant activities were found as expected for the most hydroxy-rich compounds, ISL, butein and THMCH. The loss of activity in the case of calythropsin compared to its regioisomer THMCH was not expected, since the catechol group on the calythropsin is expected to contribute significantly to the antioxidant capacity. The results indicate that the position of the hydroxy group has an influence on the radical scavenging and antioxidant activity, which is in this case higher when the OH group is present on the A-ring rather than on the B-ring of the chalcone.

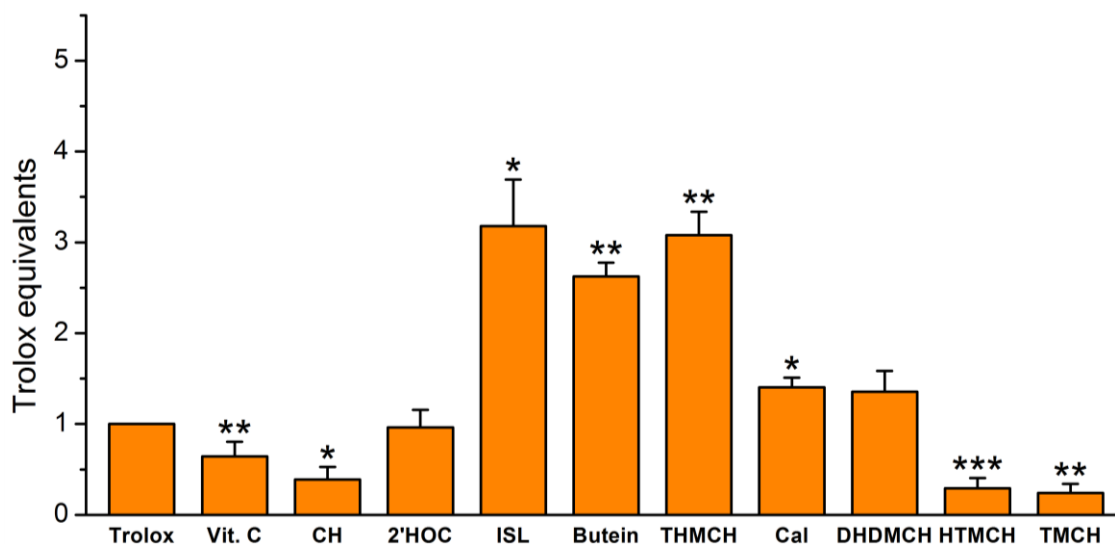


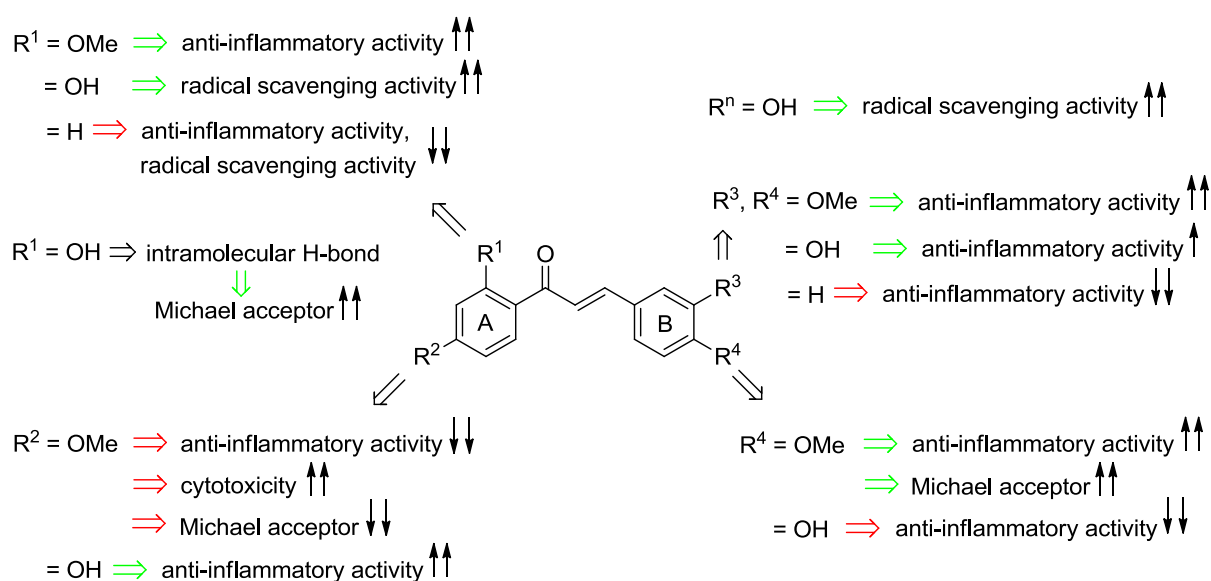
Figure 42. Antioxidant capacity of chalcones and vitamin C measured by the ORAC-fluorescein assay and expressed as Trolox equivalents. The assay was carried out in 75 mM phosphate buffer pH 7.4 at 37 °C. The antioxidant capacity values are depicted in order of the less substituted compound chalcone to the fully methoxylated chalcone TMCH. Levels of significance: ***, $p < 0.001$; **, $p < 0.01$; *, $p < 0.05$ versus Trolox.

3.3.5 Structure-activity relationship (SAR) of hydroxy- and methoxychalcones

Table 14 summarizes the results of the biological and chemical characterization of the chalcones. The table was extended by the results of the kinetic measurements in the thiol assay, performed by Nafisah Al-Rifai and Sabine Amslinger.¹⁵⁹ The calculated reaction rates of the thia-Michael addition between the chalcones and cysteamine were displayed as k_2 values in $M^{-1} s^{-1}$. The tested chalcones gave quite different reactivities in the Michael additions of thiols, displaying k_2 values from 5.08 to $0.193 M^{-1} s^{-1}$, demonstrating an overall good to very good electrophilicity.

A structure-activity relationship (Scheme 13) can be established to a certain extent regarding the anti-inflammatory and antioxidant activities of the chalcones.

An increased antioxidant activity of hydroxychalcones was observed with an increasing number of hydroxy groups present on the chalcone, demonstrated by their radical scavenging activity in the ORAC assay. Furthermore, the results show that antioxidant behavior and anti-inflammatory activity of hydroxychalcones are closely related. The well known natural chalcones ISL and butein, both containing 3 and 4 hydroxy groups, respectively, showed a high inductive effect on HO-1 activity (3 fold) and were good antioxidants as expected, due to their high potential of scavenging free oxygen radicals (3 Trolox equiv.). They showed also similar k_2 values and moderate inhibitory activity on NO production. Therefore ISL, butein and also THMCH can be regarded as bifunctional antioxidants. The correlation of potencies as phase II protein inducer and radical scavengers is known for hydroxychalcones and other Michael acceptors and was associated, at least amongst the natural occurring Michael acceptors, with their overall chemoprotective properties.¹¹⁹



Scheme 13. Structure-activity relationship of 2',3,4,4'-substituted hydroxy and methoxychalcones regarding their anti-inflammatory and antioxidant activity, as well as their Michael acceptor reactivity based on the k_2 values. Relative increase (\uparrow) or decrease (\downarrow) of activity/reactivity is given.

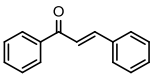
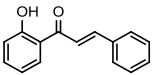
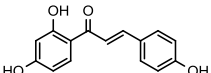
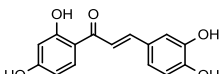
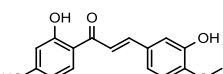
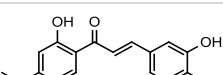
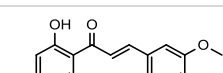
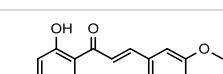
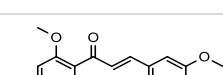
A subsequent methylation of the hydroxy groups on butein enhanced the Michael acceptor reactivity, demonstrated by increasing k_2 values. In comparison, the induction of HO-1 activity doubled from 3 to 6 fold, when the B-ring was fully methylated (DHDMCH) and HO-1 activity was reduced to 3 fold in the presence of the fully methylated chalcone (TMCH). A methylation on the 4'-position on the A-ring however caused a loss of inductive activity towards HO-1 (HTMCH) or high cytotoxicity (calythropsin). A similar trend for the methylation pattern could be also observed for the inhibitory activity towards NO production, where a methylation on the B-ring favors a higher anti-inflammatory activity than a substitution in 4'-position on the A-ring. In this case TMCH showed a higher activity compared to DHDMCH.

A change in the position of a methyl group, either on the B- or the A-ring as in the case of the two regioisomers THMCH and calythropsin, can have a great influence on the Michael acceptor reactivity. Calythropsin showed a weaker reactivity (k_2 value) compared to THMCH. This can be explained by the fact, that the double bond of the α,β -unsaturated carbonyl moiety may be regarded as a push-pull double bond. Here the less electron donating methoxy group compared to a hydroxy group on the C-4 on the B-ring restores more reactivity in the Michael acceptor system than the methoxy group in the A-ring. Regarding the biological activity however, both chalcones differ rather in their cytotoxicity than in their anti-inflammatory activity, with calythropsin being the more toxic chalcone (toxicity limit at 1 μM). Their activity towards HO-1 induction was quite similar in the nanomolar range, and they were also inactive in the inhibition of NO production, when compared at 1 μM . Only at higher concentrations of THMCH a significant inhibition of NO production could be observed.

Generally, a 2'-OH substitution compared to the non-substituted or methoxy substituted chalcone leads to an increased Michael acceptor reactivity, demonstrated by higher k_2 values. In the case of 2'-HOC compared to chalcone, the overall anti-inflammatory activity is increased, which can be contributed to the 2'-hydroxy group. For the chalcones HTMCH and TMCH, however, the effect of the 2'-OH group could not be observed concerning their biological activity. TMCH showed a higher anti-inflammatory potential compared to HTMCH, demonstrated by a higher induction of HO-1 activity and suppression of the inflammatory NO production. This can be explained by the fact, that both methoxychalcones are moderate electrophiles (k_2 values) due to the higher electron density in the molecule, which influences their anti-inflammatory activity compared to the non-substituted chalcone. It seems that a certain reactivity threshold must be hit for an increased anti-inflammatory activity, which is the case for weak to moderate electrophiles such as TMCH.

The importance of the α,β -unsaturated carbonyl moiety has been demonstrated to be crucial for the biological activity of chalcones.²³⁹ Our findings conclude that the overall biological activity of chalcones depends on the Michael acceptor reactivity of chalcones and that electronic effects due to different substitution patterns on the chalcone can influence the reactivity of the Michael acceptor and thus their biological activity. The observed correlations demonstrate that the electrophilicity of the chalcones is a major factor determining their potency as inducers of the cytoprotective HO-1 activity and as inhibitors of inflammatory NO production. Here, a rather moderate Michael acceptor reactivity is needed for a more efficient anti-inflammatory activity, in the chalcone screen this was found to be in the range of 0.4 to 0.2 $\text{M}^{-1} \text{s}^{-1}$. Strong electrophilic chalcones can be consumed by other metabolic pathways, such as a reaction with the cellular electrophile sensor GSH, without reaching their target protein. Therefore moderate electrophiles are in favor, because they can bypass such cellular traps and react with the target thiols on Keap-1 or NF- κ B in order to promote their anti-inflammatory activity. Despite of the crucial α,β -unsaturated carbonyl functionality, also alternative mechanisms of chalcones such as non-covalent interactions, isomerization or the potential activity of metabolites should be considered.

Table 14. Evaluation of chalcones towards their biological (anti-inflammatory and antioxidant) and chemical activity.

Name	Structure	Toxicity limit [μM]	Maximum HO-1 activ- ity, fold of control (conc. [μM])	Maximum inhibition of NO production, % (conc. [μM])	Trolox equivalents	k ₂ [M ⁻¹ s ⁻¹] values with cysteamine ^b
Chalcone		10	2.15 ± 0.67 (10)	ns	0.390 ± 0.136	3.04 ± 0.10
2'-Hydroxychalcone		25	2.38 ± 0.57 (5.0)	43.6 ± 8.68 (25)	0.961 ± 0.196	5.08 ± 0.04
ISL		25/10 ^a	3.43 ± 1.53 (25)	38.0 ± 7.41 (10)	3.18 ± 0.52	0.258 ± 0.010
Butein		10/5.0 ^a	3.07 ± 1.79 (10)	54.5 ± 4.27 (5.0)	2.63 ± 0.15	0.271 ± 0.027
THMCH		10	2.91 ± 1.05 (10)	42.7 ± 3.05 (10)	3.08 ± 0.26	0.417 ± 0.008
Calythropsin		1.0	2.17 ± 0.63 (0.1)	ns	1.40 ± 0.11	0.325 ± 0.011
DHDMCH		15	6.05 ± 2.31 (10)	72.9 ± 7.68 (10)	1.36 ± 0.23	0.464 ± 0.039
HTMCH		10	1.52 ± 0.17 (1.0)	52.2 ± 16.5 (10)	0.292 ± 0.114	0.717 ± 0.041
TMCH		10	2.96 ± 0.23 (10)	96.9 ± 11.9 (10)	0.241 ± 0.099	0.193 ± 0.019

Toxicity of chalcones was measured with the MTT assay in presence or absence of LPS, in the case of the concentrations marked with ^a, different toxicity limits were found in presence of LPS. ^b, k₂ values were determined via the kinetic thiol assay, at a chalcone concentration of 40 μM, by N. Al-Rifai and S. Amslinger.

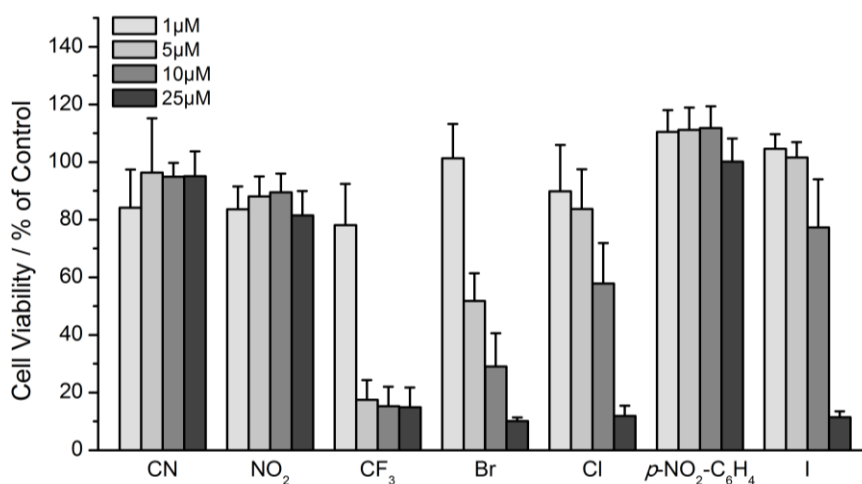
3.4 Characterization of α -X-TMCHs towards their anti-inflammatory, antioxidative and cytoprotective activity

3.4.1 Effect of α -X-TMCHs on the viability of RAW264.7 macrophages

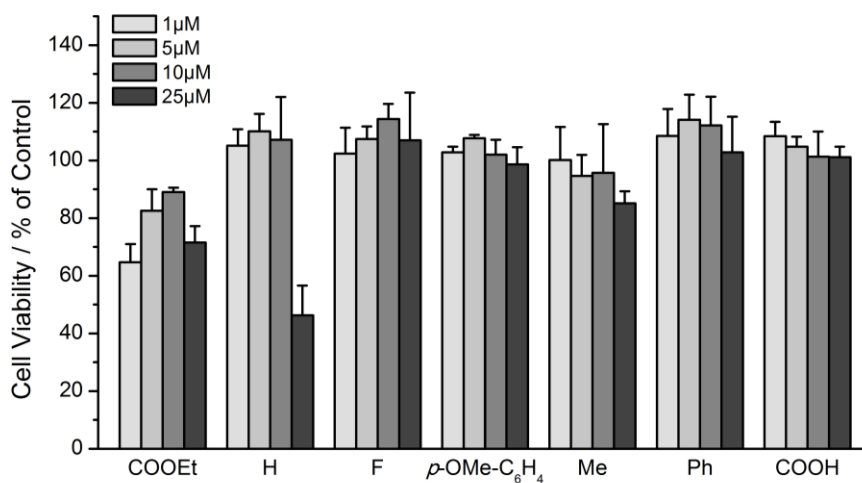
The cytotoxicity of the α -X-chalcones (α -X modified 2',3,4,4'-tertramethoxychalcones, α -X-TMCHs, Figure 12) was determined in a concentration range of 1-25 μ M in RAW264.7 cells via the MTT assay. The results are summarized in Figure 43. The influence of the α -X-TMCHs was also tested in the presence of LPS-stimulated RAW264.7 macrophages with the MTT-LPS assay, see Figure 44, in order to exclude an influence of LPS on the cytotoxicity of the compounds. Here again, only at non-toxic concentrations the α -X-TMCHs were used for further testing.

The α -CF₃-TMCH was found to be the most toxic compound in the α -X-TMCH series, here a lower test concentration range was required (Figure 43 C and Figure 44 C), with the highest non-toxic concentration in the nanomolar range (500 nM). The halogens displayed a cytotoxic effect above 1-5 μ M, except for the barely active α -F-TMCH, showing no cytotoxic effect even at 25 μ M. The α -X-TMCHs follow the rule that the more reactive/electrophilic the compounds, the more toxic they are. However, the two most reactive chalcones α -CN-TMCH and α -NO₂-TMCH had no major toxic influence on the cells at 25 and 10 μ M, respectively, suggesting that these relatively potent electrophiles could be neutralized in the cell before exerting toxicity. In the α -X-TMCH sequence the chalcones α -COOEt-TMCH to α -COOH-TMCH (Figure 43 B and Figure 44 B) had a toxic influence on RAW264.7 viability above 10 or 25 μ M, similar to the most chalcones tested, see Figure 37 and Figure 38 in the previous chapter 3.3.1. α -COOEt-TMCH showed an interesting cytotoxic behavior, displaying a bell-shaped dose-response curve, which was not observed when LPS was present in the assay. Here, one has to be careful evaluating the data of its biological activity, since a reduced viability (< 80%) was gained at 1 μ M of α -COOEt-TMCH. If one compares the results of the cell viability of the α -X-TMCHs in absences or presence of LPS, only α -Cl-TMCH and the aromatic α -*p*-NO₂-C₆H₄-TMCH and α -*p*-OMe-C₆H₄-TMCH showed a higher toxicity in the presence of LPS. For the other α -X-TMCHs the addition of LPS had no influence on their cytotoxic behavior.

A



B

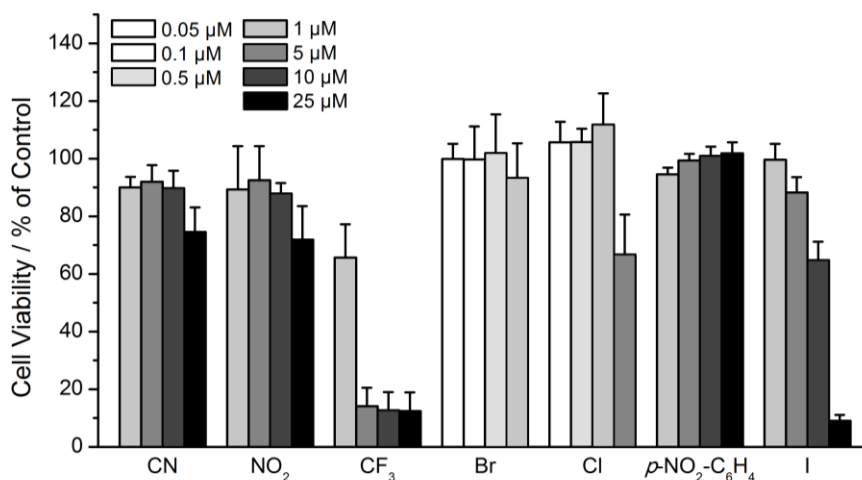


C

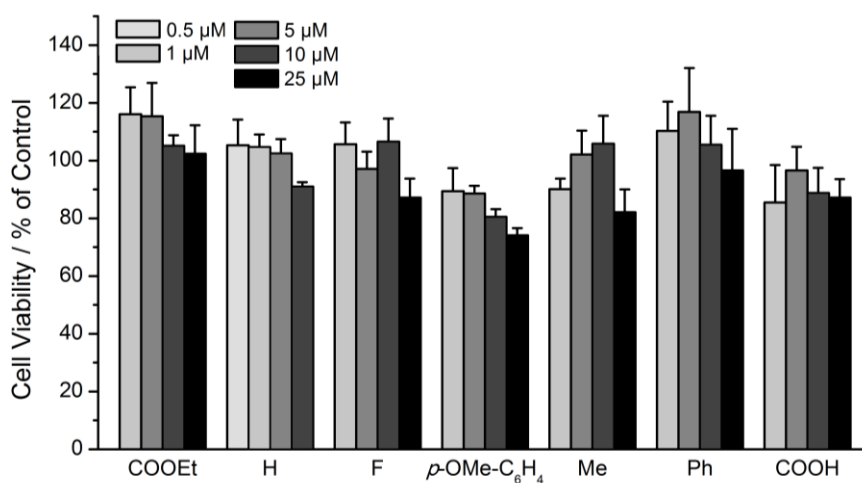
α -CF ₃ TMCH [μ M]	0.01	0.05	0.1	0.25	0.5	1
Viability [% of control]	94.8 \pm 13.5	105.6 \pm 12.6	111.7 \pm 11.0	104.1 \pm 6.5	100.3 \pm 9.4	78.1 \pm 13.3

Figure 43. Influence of α -X-TMCHs on the viability of RAW264.7 murine macrophages. Cells were treated with chalcones at the indicated concentrations (1-25 μ M) for 24 h and cell viability was determined by the MTT assay. A, B: Labels on the x-axis indicate the substituent X in the α -position of the α,β -unsaturated carbonyl moiety of the TMCH. C: The influence on cell viability of the α -CF₃-TMCH was determined at concentrations below 1 μ M as shown in the table. The level of significance was left out for a better overview. Viability \leq 80% of control were considered as cytotoxic.

A



B



C

α -CF ₃ -TMCH [μ M]	0.01	0.05	0.1	0.25	0.5	1
Viability [% of control]	89.7 \pm 0.8	102.5 \pm 13.7	97.9 \pm 14.4	87.3 \pm 5.2	86.3 \pm 11.4	65.7 \pm 10.6

Figure 44. Influence of α -X-TMCHs on the viability of LPS-stimulated RAW264.7 murine macrophages. Cells were treated with chalcones at the indicated concentrations in the presence of 10 ng mL⁻¹ LPS for 24 h and cell viability was determined by the MTT-LPS assay. A, B: Labels on the x-axis indicate the substituent X in the α -position of the α,β -unsaturated carbonyl moiety of the TMCH. The influence on cell viability of the α -CF₃-TMCH was determined at concentrations below 1 μ M as shown in table C. The level of significance was left out for a better overview. Viability \leq 80% of control were considered as cytotoxic.

3.4.2 Influence of α -X-TMCHs on HO-1 activity and HO-1 protein expression

The α -X-TMCHs were tested for their ability to induce the heme oxygenase-1 (HO-1) activity using the ELISA-based HO-1 assay as well as the protein expression using Western blot analysis in RAW264.7 macrophages. The results of the screen on HO-1 activity are depicted in Figure 45.

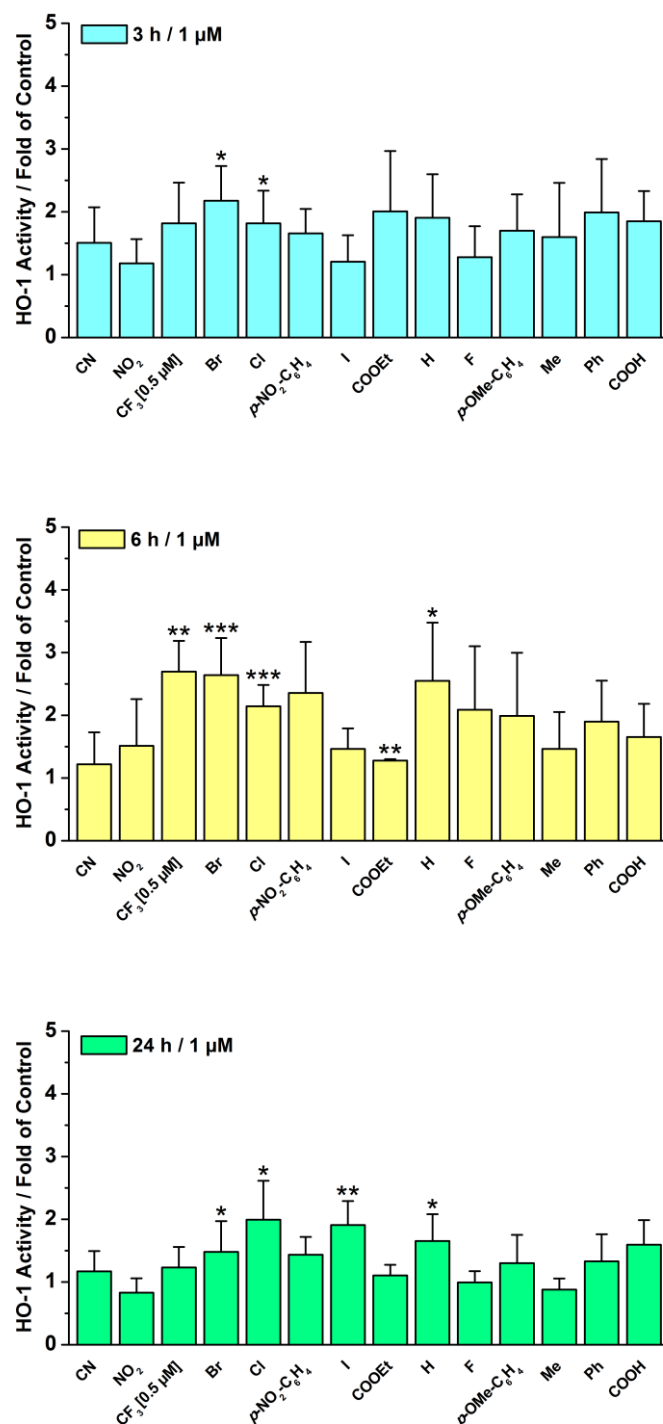


Figure 45. Influence of α -X-TMCHs on HO-1 activity in RAW264.7 macrophages. Cells were treated with different α -X-TMCHs at 1 μ M for the indicated periods. Labels on the x-axis indicate the substituent X in the α -position of the α,β -unsaturated carbonyl moiety of the 2',3,4,4'-tetramethoxychalcone (TMCH).

Here the series of α -X-TMCHs was tested at 1 μ M in order to compare their different inductive behavior on HO-1 activity. α -CF₃-TMCH was tested at 0.5 μ M due to cytotoxicity at higher concentrations. The HO-1 activity was determined after different stimulation times of the RAW264.7 cells with the chalcones for 3, 6 and 24 h. As shown in Figure 45 the inductive effect of the α -X-TMCHs was time dependent, reaching their maximum inductive activity after 6 h of incubation. While after a very short stimulation time of 3 h, only α -Br-TMCH and α -Cl-TMCH showed a significant 2 fold induction of HO-1 activity, more compounds were able to induce HO-1 activity after 6 h. Here, α -CF₃-TMCH (0.5 μ M) together with α -Br-TMCH and α -Cl-TMCH induced HO-1 activity in the range of 2.7-2.1 fold. Also the unsubstituted α -H-TMCH chalcone displayed a 2.6 fold induction of HO-1 activity. No significant activity showed α -COOEt-TMCH, α -F-TMCH, α -Me-TMCH, the α -aromatic -TMCHs and α -COOH-TMCH at 1 μ M. For most α -X-TMCHs the activity decreased after 24 h, only α -I-TMCH displayed a 1.9 fold inductive activity towards HO-1 after this prolonged stimulation time.

The observation that α -COOH-TMCH showed no activity against HO-1 correlates very well with its chemical reactivity (Table 2), since at pH 7.4 the deprotonated carboxylate group present in α -position deactivated the Michael acceptor reactivity of the chalcone. Interestingly, the most chemically reactive electrophiles found in Table 2, α -CN-TMCH and α -NO₂-TMCH, showed no activity at all at 1 μ M. This suggests that the chalcones are too strong electrophiles and might rather be consumed by GSH, which is present in cells in a relatively high concentration, before reaching their target, in this case the SH-groups on the surface of Keap1.

In Figure 46 the influence of the α -X-TMCHs on the HO-1 protein expression is shown at 1 μ M (0.5 μ M for α -CF₃-TMCH) after 6 h of stimulation. α -CF₃-TMCH, α -Br-TMCH and α -Cl-TMCH were able to induce HO-1 protein expression in RAW264.7 cells to a high level, whereas α -I-TMCH and α -H-TMCH displayed a moderate inductive effect compared to the level of HO-1 in unstimulated control cells. The other α -substituted TMCHs showed no inductive effect according to the results of the HO-1 activity assay.

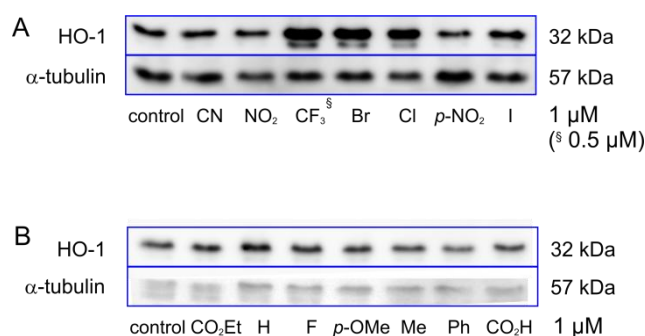


Figure 46. Influence of α -X-TMCHs on HO-1 protein expression. RAW264.7 cells were treated for 6 h with TMCHs at 1 μ M (0.5 μ M for α -CF₃-TMCH) and HO-1 was detected in cell lysates by Western blot analysis.

To a certain level there is a correlation between the inductive effect of the α -X-TMCHs on protein level and the activity of HO-1. But, although the protein level of HO-1 was elevated in the case of α -I-TMCH after 6 h, the enzymatic activity could be observed only after 24 h. An explanation for this time shift could be, that the expressed HO-1 native protein is in this case not fully folded to the enzymatic active protein. The α -X-TMCHs, which displayed at 1 μ M no induction of HO-1 protein expression, α -COOEt-TMCH and α -F-TMCH showed also no significant induction of HO-1 activity. For the most potent TMCHs, α -CF₃-TMCH, α -Br-TMCH, α -Cl-TMCH, but also α -H-TMCH, the induced protein expression leads also to an enhanced HO-1 activity after 6 h in RAW264.7 cells. The most chemically potent electrophiles in the α -X-TMCH series, α -CN-TMCH and α -NO₂-TMCH showed also on protein level no inductive effect of HO-1, suggesting an alternative pathway of the chalcones in the cell, such as a reaction with GSH.

3.4.3 Effect of α -X-TMCHs on nitrite production

The inhibitory effect of the α -X-TMCH series on the proinflammatory pathway regulated by NF- κ B was examined. For this, the amount of NO produced by the proinflammatory protein iNOS was determined in LPS-stimulated RAW264.7 macrophages via the Griess assay. The inhibition of NO production was examined at different non-toxic concentrations of the α -X-TMCHs and the result of the Griess assay is shown in Figure 47. All α -X-TMCHs showed an inhibitory activity against NO generation in LPS-stimulated macrophages, except for the α -aromatic *p*-OMe-C₆H₄-TMCH and α -Me-TMCH, which displayed a significant increase in NO production of $35 \pm 15\%$, suggesting a proinflammatory activity of this chalcone. Most of the active compounds revealed a concentration dependent inhibitory effect on iNOS activity, only α -CN-TMCH seemed not to follow this observation. While the strongest reduction of NO release was detected in the presence of 10 μ M α -H-TMCH (Table 15), the most active chalcone in our screening was α -CF₃-TMCH with a $85 \pm 9\%$ inhibition of NO production at 0.5 μ M. For the active α -X-TMCHs it was possible to calculate the IC₅₀ values of their NO inhibition and the values are given in Table 15. α -CF₃-TMCH showed an IC₅₀ value of NO production of 120 nM, followed by α -Br-TMCH with 640 nM.

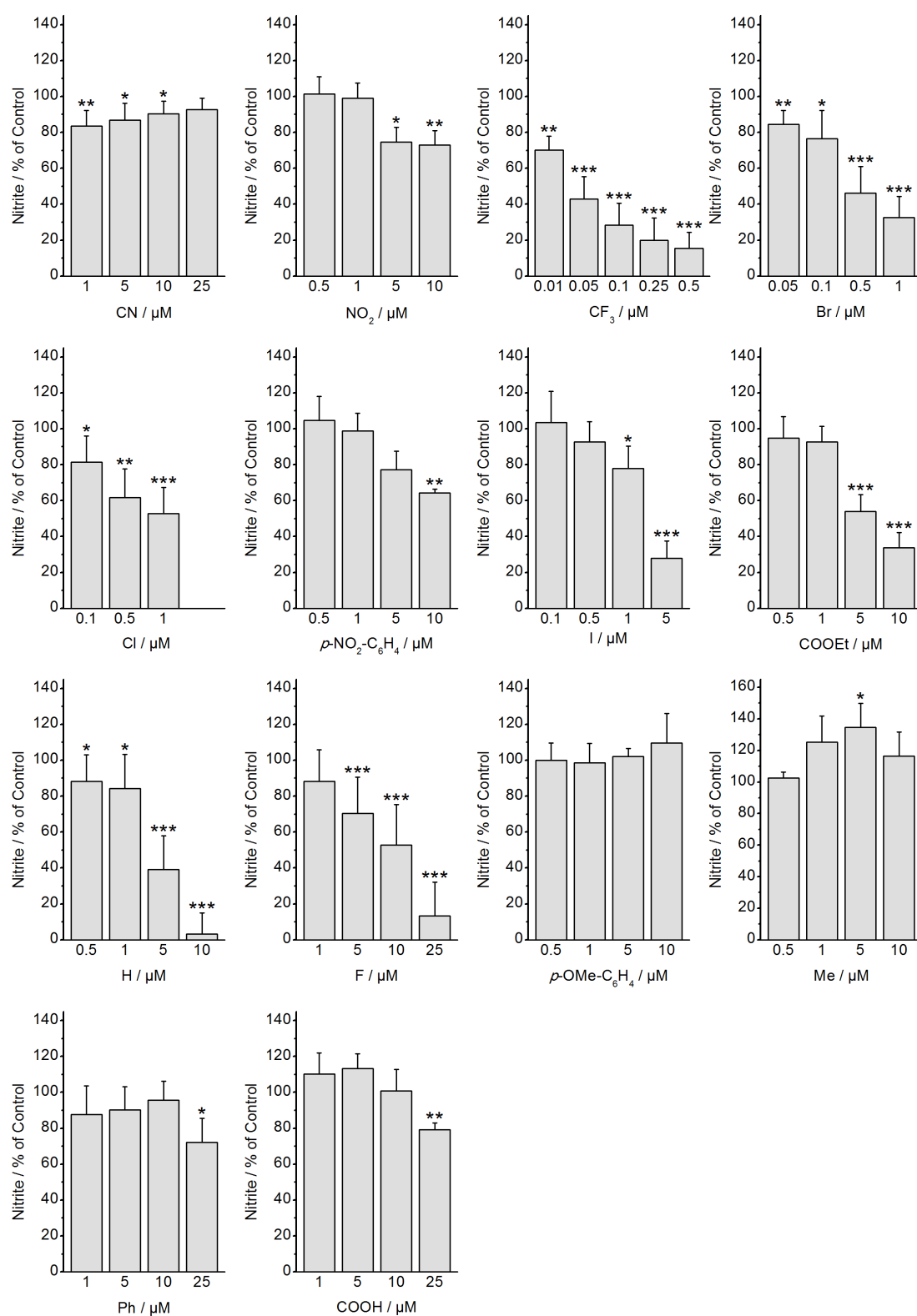


Figure 47. Influence of α -X-TMCHs on NO production. RAW264.7 cells were exposed to 10 ng mL^{-1} LPS alone (control) or in presence of TMCHs in the indicated concentrations for 24 h and the accumulated nitrite concentration present in the culture medium was determined by the Griess assay.

Table 15. Inhibition of NO production in LPS-stimulated RAW264.7 macrophages by α -X-TMCHs determined by the Griess assay. Significant maximum NO inhibition and IC₅₀ values are given together with the toxicity limit (highest non-toxic concentration) determined by the MTT assay in presence of 10 ng mL⁻¹ LPS after an incubation time of 24 h.

α -X-TMCH	Toxicity limit (μ M)	Inhibition of NO production % maximum (conc [μ M])	IC ₅₀ , NO production [μ M]
CN	25	16.4 \pm 8.7 (1.0)	nd
NO ₂	10	26.9 \pm 7.9 (10)	nd
CF ₃	0.5	84.6 \pm 8.9 (0.5)	0.120 \pm 0.062
Br	1	67.4 \pm 11.7 (1.0)	0.640 \pm 0.179
Cl	1	47.2 \pm 14.6 (1.0)	0.992 \pm 0.482
<i>p</i> -NO ₂ -C ₆ H ₄	10	35.8 \pm 2.3 (10)	nd
I	5	72.2 \pm 9.7 (5.0)	3.15 \pm 0.70
COOEt	10	66.8 \pm 8.5 (10)	6.65 \pm 0.53
H	10	96.9 \pm 11.9 (10)	4.44 \pm 1.29
F	25	86.6 \pm 18.9 (25)	12.9 \pm 5.6
<i>p</i> -OMe-C ₆ H ₄	10	ns	nd
Me	10	-34.7 \pm 15.2 (5.0)	nd
Ph	25	27.9 \pm 13.4 (25)	nd
COOH	25	20.8 \pm 3.7 (25)	nd

ns, not significant (no significant NO inhibition observed); nd, not determined due to low activity in the non-toxic concentration range.

In order to compare the quite different inhibitory influence of the α -substituent on the NO production in RAW264.7 cells, the activities of the α -X-TMCHs are summarized in Figure 48 at 1 and 5 μ M in order of their chemical reactivity according to Table 2. A clear trend in activity is apparent, beginning with α -CF₃-TMCH, the inhibitory activity of the α -X-TMCHs follows directly the order of their chemical reactivity as electrophiles: at 1 μ M CF₃ > Br > Cl > I and at 5 μ M I > H > F. Due to their low electrophilic reactivity towards thiols in the thia-Michael addition reactions (see k_2 values in Table 2), α -*p*-OMe-C₆H₄-TMCH, α -Me-TMCH, α -Ph-TMCH and α -COOH-TMCH showed no activity, in case of α -Ph-TMCH and α -COOH-TMCH a small inhibition only at higher concentrations was observed. α -*p*-NO₂-C₆H₄-TMCH does not follow the reactivity-activity relationship, as it remained inactive compared to the chalcones α -I-TMCH, α -COOEt-TMCH and α -H-TMCH, which show all together a similar chemical reactivity. Nevertheless in the series of the α -aromatic chalcones, *p*-NO₂-C₆H₄-TMCH displayed a higher NO inhibition of 36 \pm 2% at 10 μ M compared to α -Ph-TMCH (28 \pm 13% at 25 μ M) and the completely inactive α -aromatic *p*-OMe-C₆H₄-TMCH, which are more electron-rich derivatives. Similar to the results of the HO-1 assay, both chalcones α -CN-TMCH and α -NO₂-TMCH showed only low inhibitory activity of 13 \pm 9% and 25 \pm 8% at 5 μ M towards NO production, supporting the idea of a consumption by GSH in the cell.

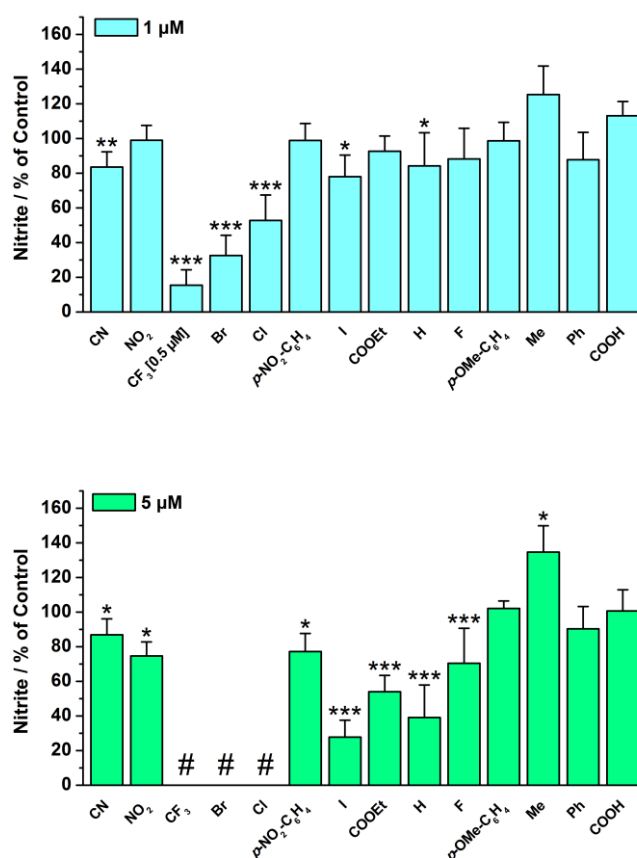


Figure 48. Comparison of α -X-TMCHs of their inhibition of NO production. RAW264.7 cells were exposed to 10 ng mL⁻¹ LPS in presence of 1 and 5 μ M α -X-TMCHs for 24 h. Accumulated nitrite concentration present in cell-culture medium was determined by the Griess assay. #, α -X-TMCHs were cytotoxic at 5 μ M and were therefore excluded from testing. Data was taken from Figure 47.

3.4.4 Conclusion

The influence of the different α -substituents on the α,β -unsaturated carbonyl unit in the 2',3,4,4'-tetramethoxychalcones (α -X-TMCHs) was investigated towards their *in vitro* anti-inflammatory activity based on their chemical reactivity estimated by the thiol assay in preliminary studies by Nafisah Al-Rifai and Sabine Amslinger.¹⁹⁵ The overall electronic and steric effects are of importance for the reactivity and thus the biological activity of α -X-TMCHs. The results of the biological studies showed that indeed the anti-inflammatory activity of 2',3,4,4'-tetramethoxychalcones can be modified by a simple substitution in α -position of the Michael acceptor moiety. A clear correlation can be established between their chemical reactivity and their biological activity, that is the inhibition of NO production as well as the induction of HO-1 on protein expression and activity, suggesting the involvement of the α -X-TMCHs in both inflammatory pathways, regulated by NF- κ B and Nrf2, respectively. Particularly, for the chalcones α -CF₃-TMCH, α -Br-TMCH, α -Cl-TMCH, α -I-TMCH and much less α -H-TMCH a direct correlation between their chemical reactivity and biological activities could be observed. α -H-TMCH displayed a much higher anti-inflammatory activity than expected from its chemical reactivity, suggesting the activation

of several pathways leading to an increase in the anti-inflammatory response. More limitations to the reactivity-activity relationship could play a role, such as off-target reactions like H-bonding of the ester group or π -interactions with the additional aryl unit of p -NO₂-C₆H₄-TMCH, that overwrite their intermediate electrophilic behavior. This is also true for the two most potent electrophiles in the α -X-TMCH series, α -CN-TMCH and α -NO₂-TMCH, that may be consumed by alternative pathways, such as a reaction with the electrophile sensitive peptide GSH. With our α -X-TMCHs we created a library of chalcones with a distinct chemical reactivity and biological activity, where a small reactivity window has to be hit to reach an effective biological response of the chalcone. In this regard a clear reactivity-activity relationship of the α -X-TMCHs can be concluded:

(Michael acceptor reactivity) vs. (anti-inflammatory activity)*



*inhibition of NO production and induction of HO-1 protein expression and activity

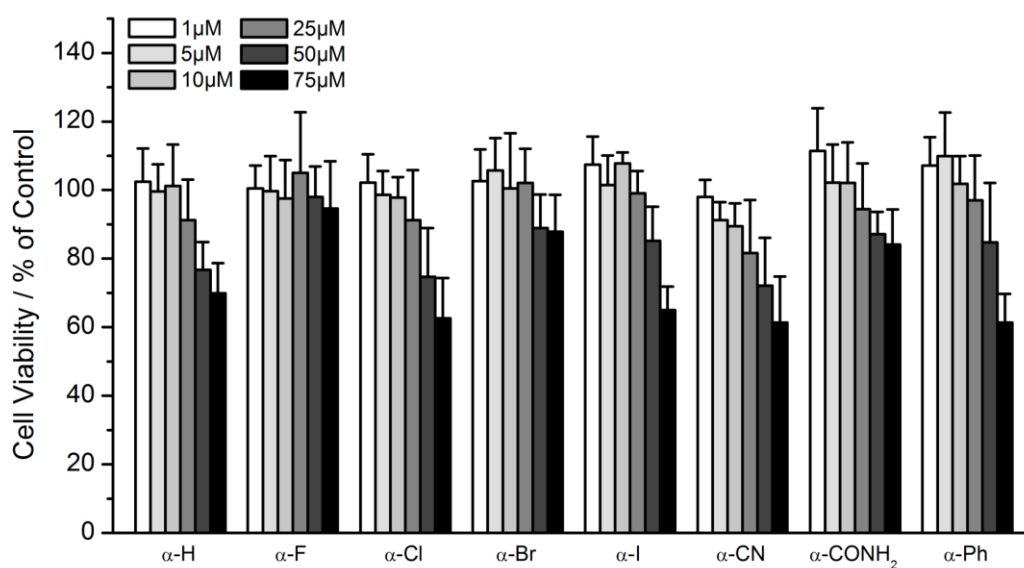
With these promising results in hand further tests will be needed to investigate the mechanism of action of these chalcones *in vitro*, which will also benefit further studies on structure-activity relationship, i.e. which particular targets are aimed by the chalcones on inflammation pathways regulated by Keap1-Nrf2 and NF- κ B and which role plays GSH on their biological response. The α -CF₃-TMCH seems particularly attractive for such studies because it exerts anti-inflammatory activity in the nanomolar range.

3.5 Characterization of α -X-Limno-CP derivatives (5-aryl-3(2H)-furanones) towards their anti-inflammatory and antioxidative activity

3.5.1 Effect of α -X-Limno-CPs on cell viability and nitrite production of RAW264.7 macrophages

The viability of LPS-induced RAW264.7 macrophages was determined in the presence of the α -X-Limno-CP and *i*-Pr- α -X-Limno-CP compounds (for structure see Figure 13) and cytotoxic concentrations were excluded from further testing (Figure 49).

A



B

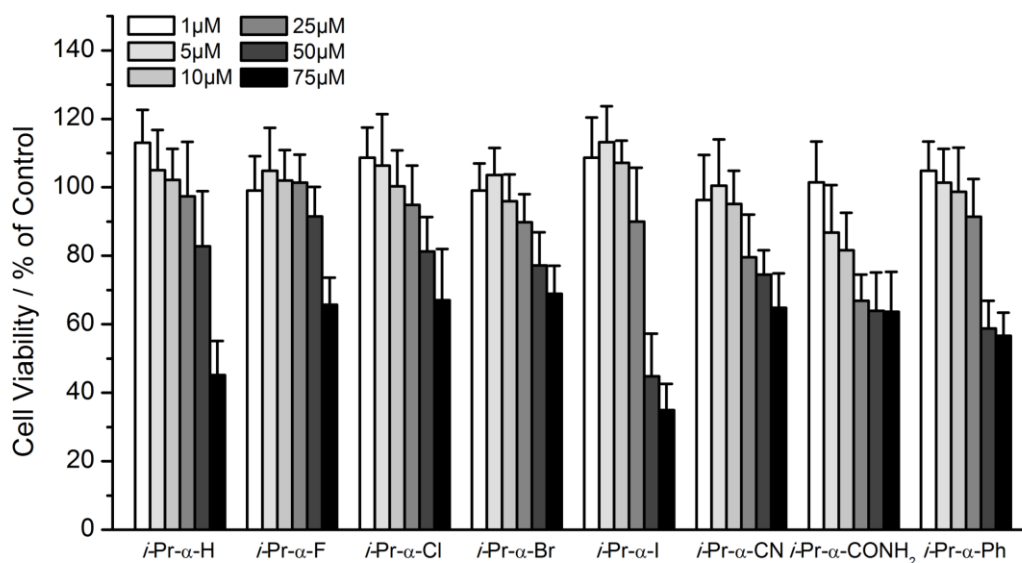


Figure 49. Influence of α -X-Limno-CPs on RAW264.7 macrophage viability. Cells were exposed to 10 ng mL⁻¹ LPS alone (control) and LPS in presence of α -X-Limno-CP (α -X, A) or *i*-Pr- α -X-Limno-CP (*i*-Pr- α -X, B) in the indicated concentrations for 24 h and cell viability was determined by the MTT-LPS assay.

The α -X-Limno-CPs displayed a moderate cytotoxicity against RAW264.7 cells in the range of 60-70% viability at 75 μ M. While α -F-Limno-CP and α -Br-Limno-CP showed no significant toxicity, α -H-Limno-CP, α -Cl-Limno-CP, α -I-Limno-CP, α -CN-Limno-CP, α -CONH₂-Limno-CP and α -Ph-Limno-CP had a negative effect on cell viability in the range of 50-75 μ M. In contrast, the protected *i*-Pr- α -X-Limno-CPs revealed a higher cytotoxic effect, except for *i*-Pr- α -Cl-Limno-CP, which showed the same cytotoxic pattern.

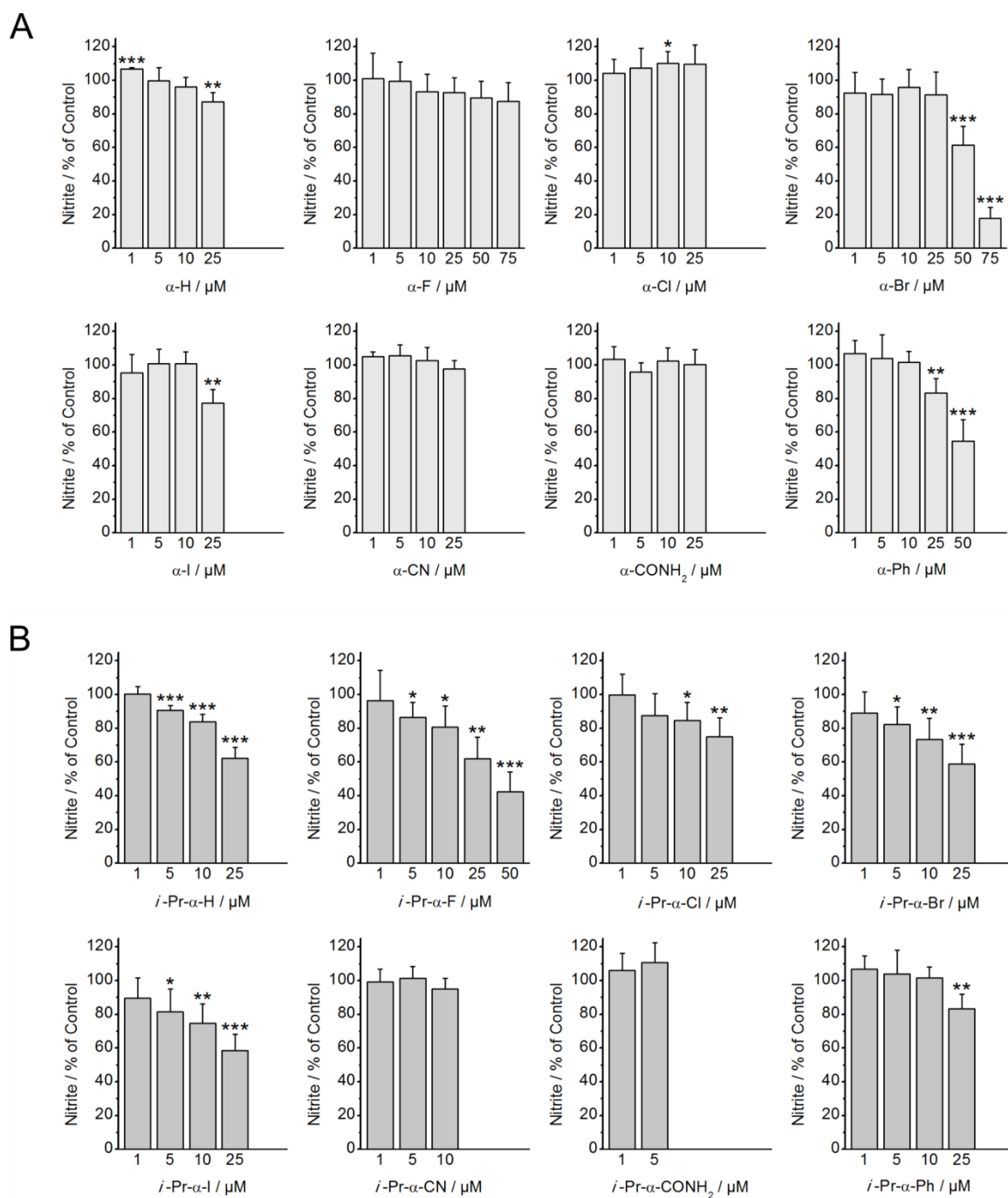


Figure 50. Effect of α -X-Limno-CP on the NO production. RAW264.7 cells were exposed to 10 ng mL⁻¹ LPS alone (control) and LPS in presence of α -X-Limno-CP (α -X, A) or *i*-Pr- α -X-Limno-CP (*i*-Pr- α -X, B) in the indicated concentrations for 24 h and the accumulated nitrite concentration present in the culture media was determined by the Griess (nitrite) assay.

i-Pr- α -I-Limno-CP and *i*-Pr- α -H-Limno-CP exerted an intermediate cytotoxicity and reached 40% of cell viability at 75 μ M. *i*-Pr- α -CONH₂-Limno-CP followed by *i*-Pr- α -CN-Limno-CP showed the lowest cytotoxicity level at a concentration of 5 μ M and 10 μ M, respectively. The halogenated *i*-Pr- α -X-Limno-CPs and the *i*-Pr- α -Ph-Limno-CP exerted their moderate toxic effect at 50 and 75 μ M. In order to estimate the anti-inflammatory activity of the α -X-Limno-CPs, their influence on the NO production by iNOS in LPS-stimulated RAW264.7 macrophages was investigated (Figure 50) using the Griess (nitrite) assay. Amongst the eight investigated *i*-Pr- α -X-Limno-CPs, *i*-Pr- α -F-Limno-CP was the most active inhibitor of NO production, with a suppression of $58 \pm 12\%$ of LPS induced NO formation at 50 μ M. When compared at 25 μ M *i*-Pr- α -Br-Limno-CP and *i*-Pr- α -I-Limno-CP were the most potent inhibitors of NO production followed by *i*-Pr- α -F-Limno-CP and *i*-Pr- α -H-Limno-CP and finally by *i*-Pr- α -Cl-Limno-CP and *i*-Pr- α -Ph-Limno-CP. *i*-Pr- α -CN-Limno-CP and *i*-Pr- α -CONH₂-Limno-CP remained inactive in the non-toxic concentration range (Table 16). Beside the fact that the protected *i*-Pr- α -X-Limno-CPs displayed in general a higher inhibitory activity than the α -X-Limno-CPs, the α -Br-Limno-CP exhibited the highest inhibition of NO release in this screen of $82 \pm 7\%$ at 75 μ M followed by a inhibition of $38 \pm 11\%$ at 50 μ M.

Table 16. Inhibition of NO production of Limno CPs in LPS-stimulated RAW264.7 cells determined by the Griess assay. Significant NO inhibition values at 25 μ M are given together with the toxicity limit (highest non-toxic concentration) determined by the MTT-LPS assay.

Limno-CP	Toxicity limit (μ M)	Inhibition of NO production, % of control at 25 μ M	Maximum inhibition of NO production, %, (conc. [μ M])
<i>i</i> -Pr- α -H	25	37.8 ± 6.5	37.8 ± 6.5 (25)
<i>i</i> -Pr- α -F	50	38.2 ± 12.8	57.6 ± 11.6 (50)
<i>i</i> -Pr- α -Cl	25	25.0 ± 11.3	25.0 ± 11.3 (25)
<i>i</i> -Pr- α -Br	25	41.3 ± 11.8	41.3 ± 11.8 (25)
<i>i</i> -Pr- α -I	25	41.6 ± 9.7	41.6 ± 9.7 (25)
<i>i</i> -Pr- α -CN	10	– ^a	– ^a
<i>i</i> -Pr- α -CONH ₂	5	– ^a	– ^a
<i>i</i> -Pr- α -Ph	25	22.3 ± 9.6	22.3 ± 9.6 (25)
α -H	25	12.7 ± 5.5	12.7 ± 5.5 (25)
α -F	75	ns	ns
α -Cl	25	ns	ns
α -Br	75	ns	82.2 ± 6.5 (75)
α -I	25	22.8 ± 8.1	22.8 ± 8.1 (25)
α -CN	25	ns	ns
α -CONH ₂	25	ns	ns
α -Ph	50	16.6 ± 8.6	45.3 ± 12.6 (50)
ns, not significant (no significant NO inhibition observed); ^a , not determined, due to toxicity at this concentration.			

However, at 25 μM $\alpha\text{-Br-Limno-CP}$ remained unreactive, whereas $\alpha\text{-I-Limno-CP}$, $\alpha\text{-Ph-Limno-CP}$ and $\alpha\text{-H-Limno-CP}$ inhibited NO production to $23 \pm 8\%$, $17 \pm 9\%$ and $13 \pm 6\%$, respectively. Even more, $\alpha\text{-Ph-Limno-CP}$ showed a higher inhibitory activity up to $45 \pm 13\%$ at 50 μM . The compounds $\alpha\text{-F-Limno-CP}$, $\alpha\text{-Cl-Limno-CP}$, $\alpha\text{-CN-Limno-CP}$ and $\alpha\text{-CONH}_2\text{-Limno-CP}$ showed no significant inhibition of NO production.

In summary, the isopropyl protecting group on the phenolic unit in the Limno-CPs enhances the anti-inflammatory activity. The isopropyl protected *i*-Pr- $\alpha\text{-X-Limno-CP}$ revealed a higher toxicity against LPS-induced RAW264.7 cells, but also an increased inhibition of NO production compared to the $\alpha\text{-X-Limno-CPs}$ with the free OH group. This can be explained by an electron-poorer β -position activating the Michael acceptor reactivity, when the free phenolic hydroxy group is alkylated. Also a higher lipophilicity may be assumed, leading to a better uptake of the isopropyl protected compounds by the cell membrane. In both cases $\alpha\text{-CN-Limno-CP}$ and $\alpha\text{-CONH}_2\text{-Limno-CP}$, which were expected to activate the Michael acceptor reactivity, remained inactive. The results of the NO inhibition screening showed that a modulation of the α -position of the α,β -unsaturated carbonyl moiety in the 3(2*H*)-furanone unit is not clearly influencing the inhibitory activity on the NO production. The Limno-CP derivatives exert only a moderate anti-inflammatory activity compared for example to the $\alpha\text{-X-TMCHs}$, which may not only derive from NF- κB inactivation but also from alternative activation on off-set targets, such as certain kinases, which may indirectly lead to an inhibition of NO production.

3.5.2 Antioxidant capacity of $\alpha\text{-X-Limno-CPs}$

The antioxidant capacities of the Limno-CPs were investigated by the cell free ORAC-fluorescein assay by determining the radical scavenging activity over time towards peroxy radicals generated from AAPH and compare it to the antioxidant standard Trolox, a water soluble vitamin E derivative. Two structure characteristics contribute to the radical scavenging property: i) the α,β -unsaturated carbonyl moiety, reacting in a Michael addition-like reaction with the radical and stabilizing the radical species by the conjugated π -electron system and ii) the phenolic hydroxy group on the 5-aryl-3(2*H*)-furanone unit which can be oxidized.

The results summarized in Figure 51 clearly show an antioxidant activity of the $\alpha\text{-X-Limno-CPs}$, due to the free hydroxy group on the phenolic moiety on the 3(2*H*)-furanone, with $\alpha\text{-H-Limno-CP}$ displaying the highest Trolox equivalents (3.78 ± 0.69). When the hydroxy group is masked by the isopropyl protecting group, the antioxidant capacity of the *i*-Pr- $\alpha\text{-X-Limno-CPs}$ is abolished, independent of the α -substituent.

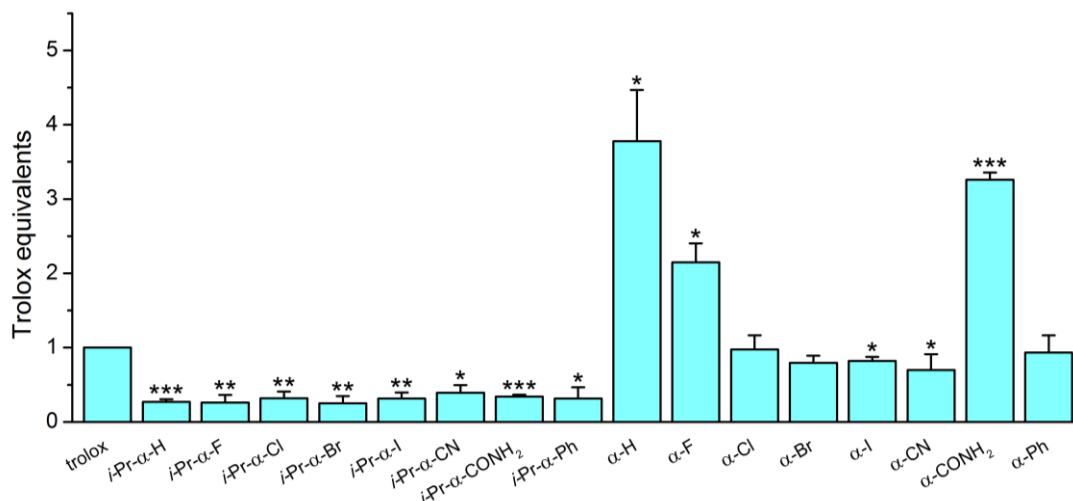


Figure 51. Antioxidant capacity of α -X-Limno-CPs measured by the ORAC-fluorescein assay and expressed as Trolox equivalents at 1 μ M. The assay was carried out in 75 mM phosphate buffer pH 7.4 at 37 °C. Level of significance: *, $p < 0.001$; **, $p < 0.01$; *, $p < 0.05$ versus Trolox.**

α -CONH₂-Limno-CP showed a high antioxidant capacity value (3.26 ± 0.10), suggesting that the amide group itself reacts as a H-atom donor, stabilizing the radical species by the conjugated π -electron system, without necessarily influencing the Michael system. On the other hand, the influence of the α -substituent on the radical scavenging activity of the Michael acceptor system could be observed in the case of α -F-Limno-CP (2.15 ± 0.26), where α -F acts in this system as a π -electron donor (β -C: 167 ppm vs. 183 ppm for α -H) due to a positive resonance effect, which also contributes to the stabilization of the radical species in the conjugated π -system. This can explain the decreased activity of α -F-Limno-CP compared to α -H-Limno-CP, but also why α -F-Limno-CP displayed the highest activity in the halogen series of α -X-Limno-CP. The halogenated as well as α -CN-Limno-CP and α -Ph-Limno-CP displayed similar antioxidant capacities as Trolox, which may be only connected to the free phenolic hydroxy group, since no clear influence of the α -modification on the radical scavenging reactivity could be observed.

3.5.3 Conclusion

In order to predict biological activity by manipulating the chemical reactivity through α -modifications, ¹³C NMR studies can be useful to determine the relative electrophilicity of the β -carbon as the reactive center of the Michael system. This approach was used to study the chemical implications of antitumor and antiviral activities of prostaglandins.²⁴⁰ However, concerning the Limno-CP model compounds a modulation of their anti-inflammatory activity based only on ¹³C NMR characterization of the β -carbon seems not sufficient. The Limno-CP derivatives have been considered as atypical and moderate electrophiles, due to their overall electron rich α,β -unsaturated carbonyl system. Typically, enone systems with chemical shifts of 120–170 ppm show intermediate to high reactivities in 1,4-additions. Especially, exomethylenic enone entities like in helenalin with a ¹³C NMR value of 122 ppm are very reactive.²⁴¹ Also for the α -X-TMCHs,

which showed a broad spectrum of very high to moderate reactivities in thia-Michael additions, the chemical shifts of the β -carbon were in the range of 120 to 153 ppm.¹⁹⁵ In the case of the Limno-CP system, more low-field shifted values of 167 to 185 ppm for the β -carbon were achieved. Moreover, in kinetic measurement of the 1,4-addition with cysteamine in the thiol assay performed by Katrin Winter²⁴² the Limno-CP derivatives showed no reaction, due to their poor electrophilicity. Also the steric hindrance of the double-substituted β -carbon hampers a possible attack of reactive thiols of target proteins. In comparison to the α -X-TMCHs, the Limno-CPs exerted a lower cytotoxicity but also a rather poor anti-inflammatory activity. On the other hand, the α -X-Limno-CPs, at least α -H-Limno-CP, α -F-Limno-CP and α -CONH₂-Limno-CP displayed a good antioxidant activity, namely radical scavenging activity, rather than a distinguished Michael acceptor reactivity, demonstrated by the ORAC-fluorescein assay. Taken together, pivotal for the approach of introducing α -modifications in an α,β -unsaturated carbonyl system in order to reach a high specificity of their biological activity, a reliable scaffold with a moderate but sufficient electrophilicity is needed.

3.6 Characterization of both enantiomers of arteludovicinolide A towards their anti-inflammatory activity

3.6.1 Influence on the viability and nitrite production of RAW264.7 macrophages

Both enantiomers of arteludovicinolide A and a derivative, *de-exo*-methylated-(+)-arte A (Figure 14), were tested for their cytotoxic effect and their ability to inhibit the production of NO in RAW264.7 macrophages stimulated with lipopolysaccharide (LPS, 10 ng mL⁻¹) for 24 h. The results are depicted in Figure 52.

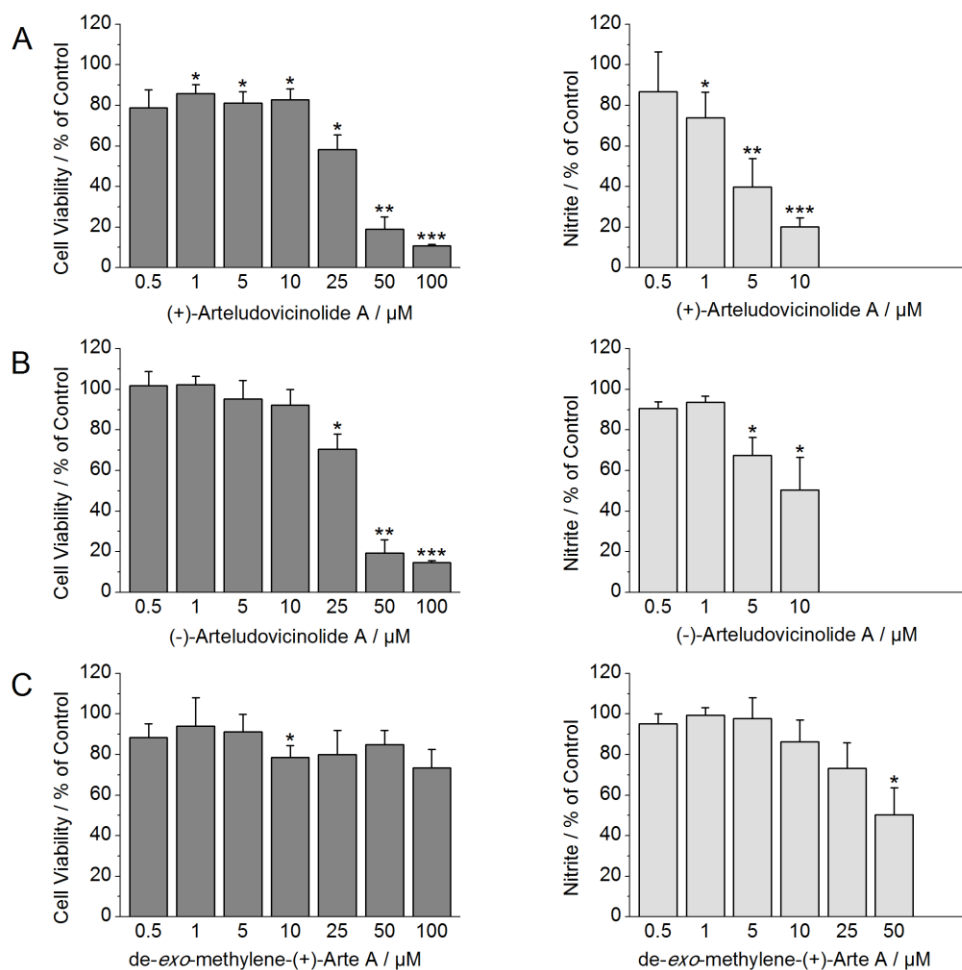


Figure 52. Influence of test compounds on the viability (left column) and the nitrite production (right column) of RAW264.7 cells stimulated with 10 ng mL⁻¹ of LPS. Cell viability of was determined by the MTT assay in presence of 10 ng mL of LPS for the indicated concentrations of the compounds at an incubation time of 24 h (left side of chart). The NO production (Griess assay) was measured under the same conditions at non-toxic concentrations as indicated (right side of the chart).

Additionally, IC₅₀ values (inhibition of 50%) of the cell viability (without LPS stimulation) and the NO production could be determined and are summarized in Table 17.

While (+)- and (-)-arteludovicinolide A displayed a similar cytotoxic pattern, with IC₅₀ values of 49.3 ± 2.7 and 45.3 ± 2.6 μM, their inhibitory influence on NO production differed significantly. The (+)-enantiomer exhibited a significantly higher inhibitory effect on NO production with a IC₅₀ value of 4.87 ± 1.07 μM compared to the unnatural (-)-enantiomer with an IC₅₀ value of

10.3 ± 5.7 µM. In order to investigate the contribution of the second Michael acceptor on the cyclopentenone moiety to the biological activity, besides the *exo*-methylene group on the lactone, the derivative compound was also tested. However, the derivative showed no cytotoxic effect between the concentration range of 0.5-100 µM and displayed a weak inhibition of NO release (IC₅₀ values of 50.2 ± 18.3 µM).

Table 17. IC₅₀ values of compounds tested for viability and NO production in RAW264.7 stimulated with LPS.

	IC ₅₀ [µM], cell viability	IC ₅₀ [µM], NO production
(+)-Arteludovicinolide A	49.3 ± 2.7 µM	4.87 ± 1.07 µM
(-)-Arteludovicinolide A	45.3 ± 2.6 µM	10.3 ± 5.7 µM
de- <i>exo</i> -methylene-(+)-Arte A	> 100 µM	50.2 ± 18.3 µM
Inhibition of cell viability and NO production in RAW264.7 macrophages in presence of test compounds for 24 h.		

These results clearly disagree with the data previously reported on the anti-inflammatory activity of (+)-arteludovicinolide A, demonstrated by the inhibition of NO production in RAW264.7 macrophages. Our results show a 15 times higher anti-inflammatory activity compared to the previous report on an IC₅₀ value of 70.4 µM.²⁰² Moreover, the measurements were in a much higher concentration range of the compound (≥ 45 µM), which is according to our results already in the cytotoxic range. One has to mention that the data reported previously was taken with RAW264.7 cells stimulated with a higher concentration of LPS (1 µg mL⁻¹, 100 times concentrated than our LPS), which can influence the biological readout.

3.6.2 Influence of both enantiomers of arteludovicinolide A on the heme oxygenase-1 (HO-1) activity in murine macrophages RAW264.7

The two more active compounds (+)-and (-)-arteludovicinolide A were further tested for their ability to induce heme oxygenase-1 in RAW264.7 macrophage cells by the ELISA-based HO-1 activity assay at a non-cytotoxic concentration of 10 µM (preliminary MTT results) at two different stimulation times for 6 and 24 h (Table 18). After 6 h of stimulation only the naturally occurring (+)-arteludovicinolide A displayed a 2.1 fold induction of HO-1 activity in RAW264.7 cells, while (-)-arteludovicinolide A remained inactive. However, both enantiomers could induce HO-1 activity after 24 h to 2 fold activity compared to control cells. An epimerization of the (-)-enantiomer into a more active form after a prolonged incubation time in the cell culture media may be considered.

Table 18. Influence of both enantiomers of arteludovicinolide A [10 μ M] on the induction of HO-1 activity in RAW264.7 cells measured via the HO-1 activity assay together with their influence on the cell viability determined by the MTT test.

	Cell viability at 10 μ M, % of control	Fold induction of HO-1 activity at 10 μ M	
		6 h	24 h
(+)-Arteludovicinolide A	97.3 \pm 8.2	2.14 \pm 0.70	1.91 \pm 0.28
(-)-Arteludovicinolide A	97.9 \pm 17.8	ns	2.03 \pm 0.16

Cytotoxicity of test compounds was measured at 10 μ M after 24 h via MTT assay and cell viability is presented. Significant stimulation of HO-1 activity ($p \leq 0.05$) is shown as fold of induction when cells were incubated for 6 and 24 h with compounds at 10 μ M and HO-1 activity was determined in whole cell lysates via the ELISA-based HO-1 activity assay. ns, not significant.

3.6.3 Summary

The naturally occurring (+)-arteludovicinolide A and its synthetic enantiomer (-)-arteludovicinolide A were shown to display anti-inflammatory activity at non-cytotoxic concentration in RAW264.7 murine macrophages. Both enantiomers were able to inhibit the production of NO, regulated by the proinflammatory NF- κ B pathway and on the other hand to induce the activity of the anti-inflammatory and cytoprotective enzyme HO-1, which is activated by the Nrf2/Keap1/ARE signaling pathway. In both cases, the (+)-arteludovicinolide A displayed a higher activity than the (-)-enantiomer, with a 2.14 fold induction of HO-1 activity after 6 h and an IC_{50} value of 4.87 μ M in NO inhibition compared to an insignificant modulation of HO-1 activity and an IC_{50} value of 10.3 μ M, respectively. Interestingly after a longer incubation time of 24 h both compounds were able to induce the HO-1 activity (2 fold) compared to control cells. This observation may suggest an epimerization of the (-)-enantiomer under cell culture conditions leading to a more active form of the compound. This remains to be investigated. Additionally, it was shown that the *exo*-methylene group in the lactone ring is crucial for the anti-inflammatory activity of the natural product.

3.7 The anti-inflammatory activity of iron dienyolphosphate tri-carbonyl complexes as enzyme-triggered CO-releasing molecules (ET-CORMs)

The biological activity of two phosphorester-based ET-CORMs, *rac-17* and *rac-18* (Figure 16) was investigated in the murine macrophage cell line RAW264.7 by determining their influence on the cell viability and the LPS induced production of NO. Both racemic ET-CORMs were synthesized by Steffen Romanski (research group of H.-G. Schmalz, Universität zu Köln). The synthesis of these water soluble ET-CORMs and the biological evaluation of some selected compounds were recently published.²¹³ The phosphate ester complexes *rac-17* and *rac-18* differ in their cytotoxicity and also in their inhibitory activity on NO production in RAW264.7 cells stimulated with 10 ng mL⁻¹ LPS (Figure 53). The compound *rac-17* was found to be the more active compound, displaying an IC₂₀ value of 252 ± 39 µM and an inhibition of NO production of 31 ± 8% at 100 µM, whereas *rac-18* was inactive in the test concentration range of 1-100 µM without displaying a significant toxicity even at 1.0 mM (Table 19).

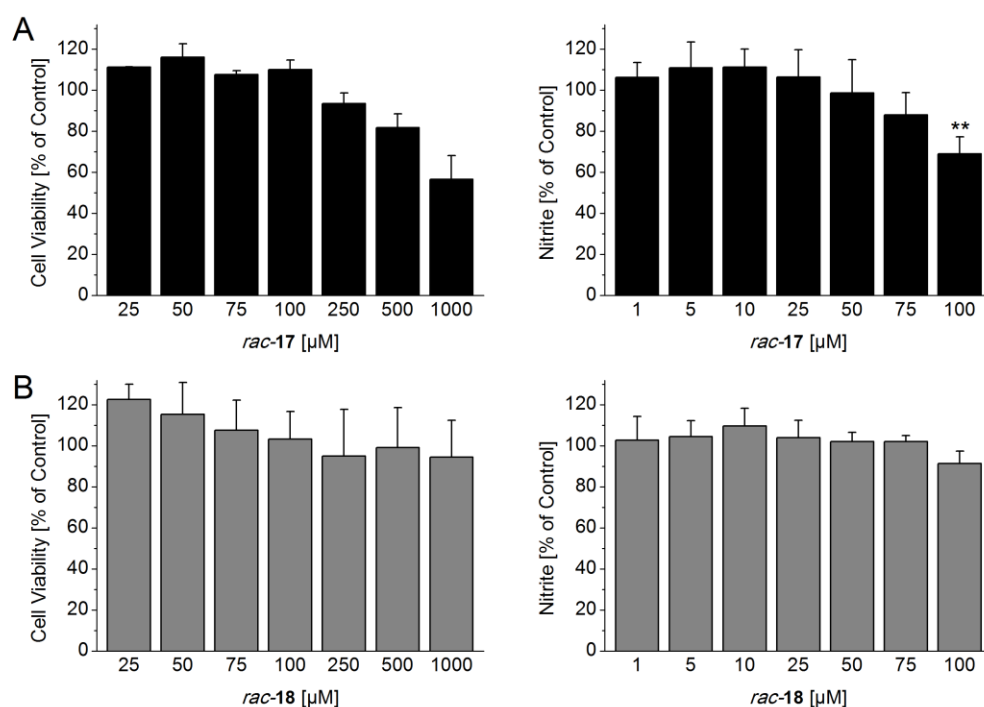


Figure 53. Influence of ET-CORMs *rac-17* and *rac-18* on the viability (left column) and the nitrite production (right column) of RAW264.7 cells stimulated with 10 ng mL⁻¹ of LPS. Cell viability of was determined by the MTT assay for the indicated concentrations of the compounds at an incubation time of 24 h. The NO production (Griess assay) was measured under the same conditions at non-toxic concentrations. Data represent at least three independent experiments performed in quadruplicates.

Table 19. Evaluation of the cytotoxic and anti-inflammatory activity of two water-soluble ET-CORMs in RAW264.7 murine macrophages.

ET-CORM	IC ₂₀ [μ M], cell viability	Inhibition of NO production at 100 μ M [%]
<i>rac-17</i>	252 \pm 39	31.0 \pm 8.3
<i>rac-18</i>	> 1000 ^a	- ^b

Inhibition of cell viability and NO production in RAW264.7 macrophages stimulated with 10 ng mL⁻¹ LPS in presence of test compounds for 24 h. ^aAn IC₅₀ value for *rac-17* could not be determined due to the overall low toxicity. ^bNo significant NO inhibition compared to control cells was found.

Upon enzymatic triggered CORMs degradation free Fe³⁺ ions are released, which could also influence the anti-inflammatory activity of ET-CORMs.²¹⁴ For this purpose the free ions Fe²⁺ and Fe³⁺ were assessed towards their effect on the viability and on the NO production in RAW264.7 cells (Figure 54). Both FeCl₂ and FeCl₃ proved to be cytotoxic with IC₂₀ values of 33.7 \pm 17.2 μ M for FeCl₂ and 39.8 \pm 15.3 μ M for FeCl₃ and an IC₅₀ value > 100 μ M for both compounds. However, no inhibitory influence on the NO production in RAW264.7 cells was observed for Fe²⁺ and Fe³⁺ at non-toxic concentrations (1-25 μ M).

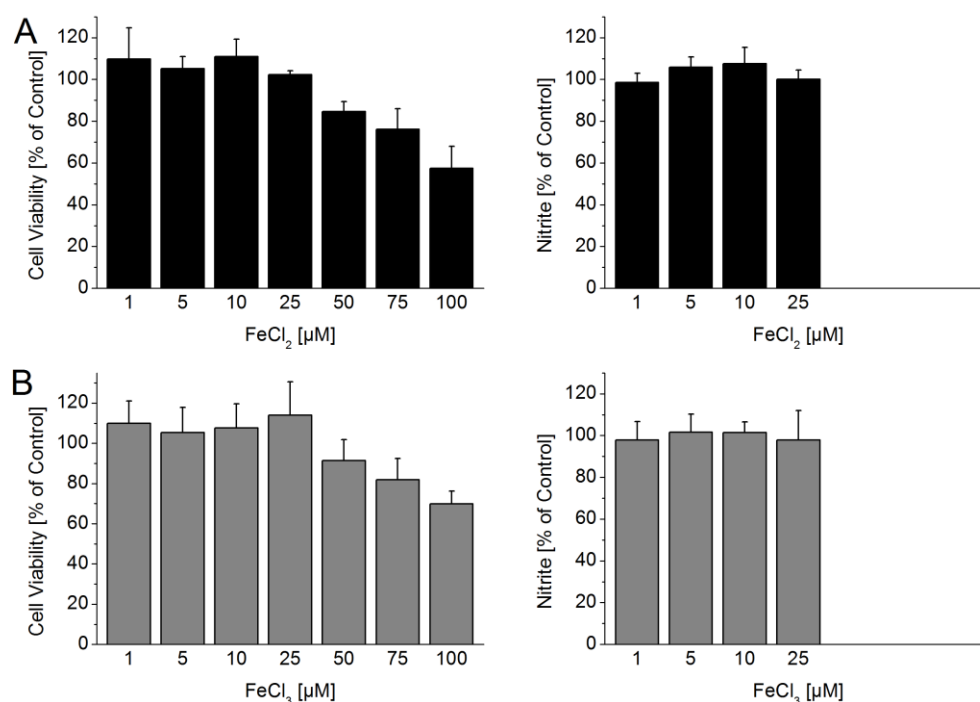


Figure 54. Results of the *in vitro* assays performed with RAW264.7 cells stimulated with 10 ng mL⁻¹ of LPS together with FeCl₂ and FeCl₃. Charts on the left side refer to MTT tests after an incubation time of 24 h at different concentrations. Charts to the right display the influence on NO production (Griess assay) of the iron chlorides at non-toxic concentrations. Data represent at least three independent experiments performed in quadruplicate.

Furthermore, the degradation products obtained upon decomposition of acyloxycyclohexadiene-Fe(CO)₃ complexes can also contribute to the biological activity of ET-CORMs, since it was shown for cyclohexenones to strongly contribute to the overall activity of the monoester complexes of ET-CORMs.²¹² Therefore, some phenolic and cyclohexanone derivatives, as possible decomposition products of the ligand released from structurally different acyloxycyclohexadiene-Fe(CO)₃ complexes (Figure 55) were investigated towards their cytotoxic activity and their influence on the NO production in RAW264.7 macrophages (Figure 54 and Table 20).

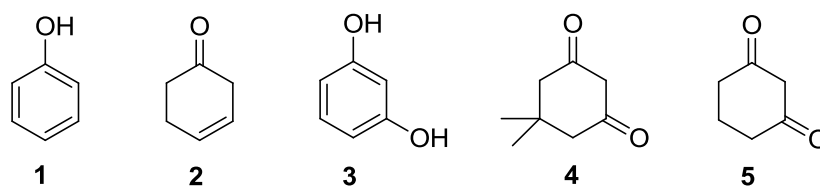


Figure 55. Structures of tested potential decomposition products of ET-CORMs.

The potential ET-CORM decomposition products showed overall low cytotoxicity, except for the 3-cyclohexenone **2**, which displayed an IC₅₀ value of 43.1 ± 6 µM, followed by compound **5** with an IC₂₀ value of 66.2 ± 30 µM. All compounds revealed a concentration dependent inhibitory effect on the NO production in RAW264.7 cells at non-toxic concentrations. Whereas compounds **1**, **3**, **4** and **5** displayed a similar maximum inhibitory activity in the range of 39-42%, compound **2** was found to be the most potent inhibitor with a 70 ± 16% inhibition of NO production at 10 µM. The IC₅₀ value for the NO inhibition was calculated at non-toxic concentrations and gave 6.6 ± 3.3 µM for compound **2**.

Table 20. Evaluation of the cytotoxic and anti-inflammatory activity of potential ET-CORMs decomposition products in LPS-stimulated RAW264.7 macrophages.

Compound	Cytotoxicity		Inhibition of NO production [%]		
	Toxicity limit [µM]	IC ₅₀ [µM]	Maximum inhibition	Inhibition at 10 µM	IC ₅₀ [µM]
1	100	>100 ^a	39.4 ± 15.6	24.4 ± 11.9	>100 ^a
2	10	43.1 ± 5.5	70.0 ± 16.2	70.0 ± 16.2	6.6 ± 3.3
3	100	>100 ^a	40.3 ± 13.5	26.8 ± 11.0	>100 ^a
4	100	>100 ^a	42.2 ± 7.8	33.1 ± 5.2	>100 ^a
5	75	IC ₂₀ = 66.2 ± 30.2	39.5 ± 11.2	26.9 ± 4.4	>100 ^a

Cytotoxicity of test compounds was measured via MTT-LPS assay and the NO production was determined by the Griess assay in RAW264.7 cells stimulated with 10 ng mL⁻¹ of LPS for an incubation time of 24 h. The toxicity limit determines the highest non-toxic concentrations. ^aIC₅₀ value was not determined due to a low toxicity or activity.

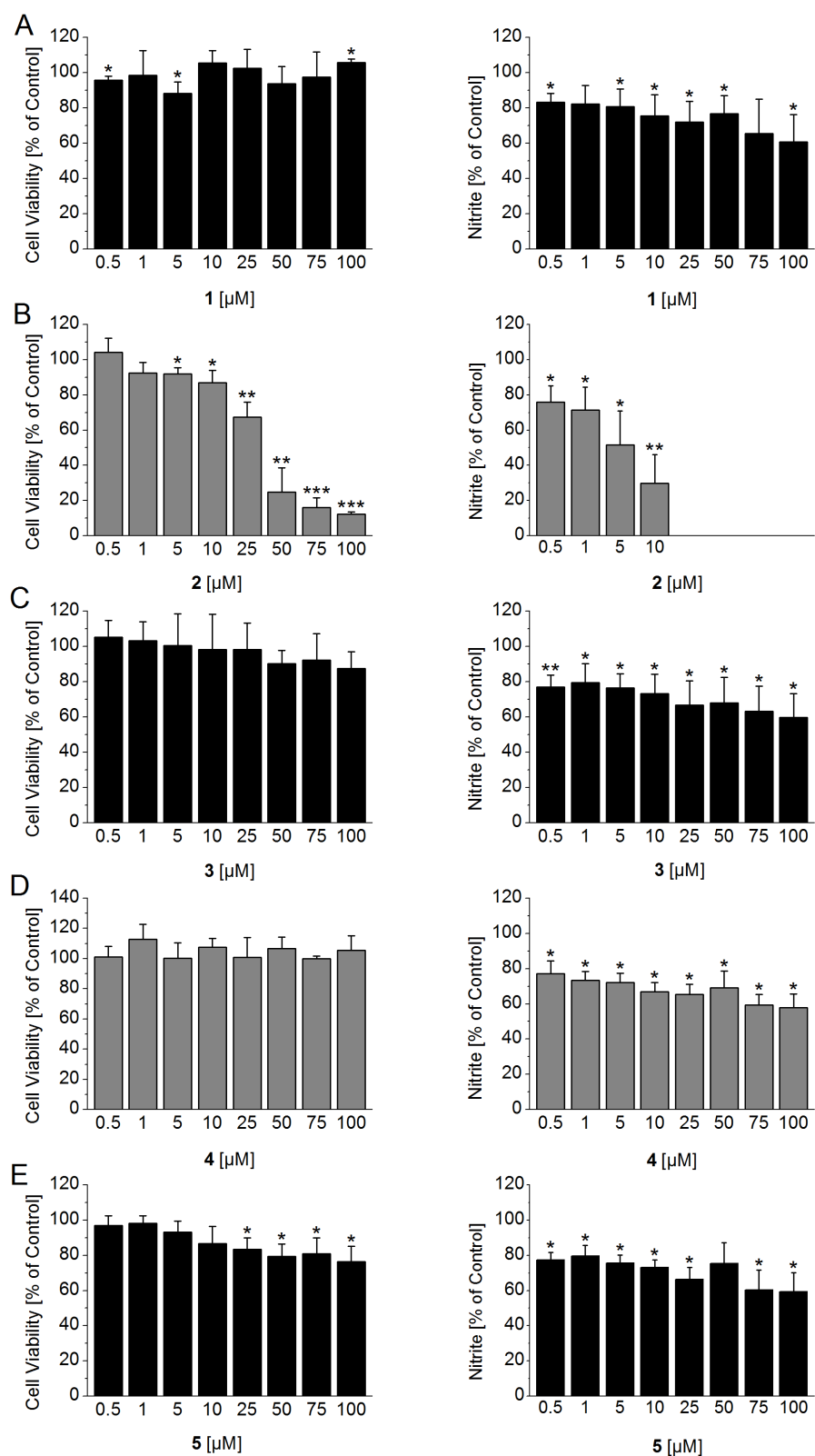


Figure 56. Results of the *in vitro* assays performed with RAW264.7 cells stimulated with 10 ng mL⁻¹ of LPS together with possible ET-CORM decomposition products 1-5 (see Figure 17). Chart on the left side refer to MTT tests after an incubation time of 24 h at different concentrations. Chart to the right display their influence on NO production (Griess assay). Data represent at least three independent experiments performed in quadruplicate.

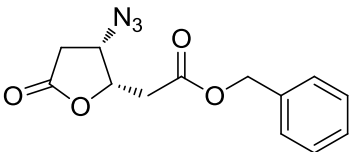
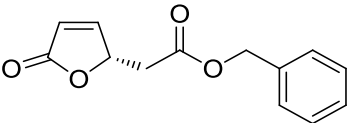
Interestingly, the effect of phenol **1** and its dihydroxy derivative **3** on the viability of the murine macrophages was very low, showing no relevant toxicity in the range of 0.5 to 100 μM . Surprisingly, the 3-cyclohexenone **2** exerted a relatively high toxic effect and a strong inhibitory effect on the NO production although no α,β -unsaturated unit is present in the system. This may suggest a potential isomerization of the 3-cyclohexenone under cell culture conditions to the active 2-cyclohexenone. Compounds **4** and **5**, which can derive from hydrolysis of the corresponding diester complexes (see Figure 17) showed relatively moderate anti-inflammatory activity and a weak cytotoxicity. This was also found for the aromatic compounds **1** and **3**, which could decompose from the corresponding hydroxycyclohexadiene- $\text{Fe}(\text{CO})_3$ complexes (see Figure 17). In conclusion, the determined activity of the possible decomposition products contribute significantly to the overall activity of the corresponding acyloxycyclohexadiene- $\text{Fe}(\text{CO})_3$ complexes and may even account for most of their activity.

3.8 Characterization of further compounds towards their cytotoxic, antioxidative and anti-inflammatory activity

3.8.1 Cytotoxic activity of two γ -butyrolactone derivatives on the human colon cancer cell line HT-29

Two functionalized γ -butyrolactones, GBL-1 and GBL-2, both bearing an acetic acid benzyl ester moiety, were tested for their cytotoxic effect in the human colon cancer cell line HT-29. The compounds were synthesized by Mohd Tajudin Mohd Ali (research group of O. Reiser, Universität Regensburg).²⁴³ The results of both γ -butyrolactones on their inhibitory effect on the cell viability of HT-29 cells is summarized in Table 21 and IC_{50} and IC_{20} values were calculated from nine different test concentrations in the range of 1-500 μ M. The γ -butyrolactone compounds showed only weak cytotoxicity against the human colon cancer cell line HT-29, whereas GBL-2, bearing a α,β -unsaturated moiety, displayed a slight toxicity with an IC_{50} value of 463 μ M compared to the azide GBL-1 with an IC_{50} value over 500 μ M.

Table 21. Effect of γ -butyrolactones on the viability of human colon cancer cells (HT-29). Cells were treated with test compounds (1-500 μ M) for an incubation time of 24 h and cell viability was determined by the MTT assay.

					
GBL-1			GBL-2		
IC_{20} [μ M]	241 \pm 92		IC_{20} [μ M]	184 \pm 41	
IC_{50} [μ M]	> 500		IC_{50} [μ M]	463 \pm 132	

3.8.2 Biological activity of different sesquiterpene lactone derivatives, γ -butyrolactones and 4-substituted cyclopentenones

Several compounds derived from sesquiterpene lactones, γ -butyrolactone derivatives and cyclopentenones with different substituents in 4-position were investigated towards their cytotoxic and anti-inflammatory activity in the murine macrophages RAW264.7 and the human colon cancer cells HT-29. Additionally, some compounds were also tested for their radical scavenging properties in the cell-free ORAC-fluorescein assay. The results of the activity screening together with the structures of the compounds is summarized in Table 22. The compounds were synthesized by different members of the research group of O. Reiser (Universität Regensburg) as indicated in the table. The compound **AB-1** derived from the anti-tumor²⁴⁴ and anti-inflammatory²⁴⁵⁻²⁴⁷ sesquiterpene lactone xanthatin (Figure 57) was investigated towards its anti-inflammatory activity in LPS-stimulated RAW264.7 macrophages by determining the inhibition of NO production, which gave an IC_{50} value of 7.1 \pm 1.2 μ M. Furthermore, its toxicity towards the macrophage cell line was estimated with an IC_{50} value of 46.3 \pm 1.7 μ M. The xanthatin deriva-

tive possesses two Michael acceptor moieties which may contribute to its anti-inflammatory activity, one at the side chain of the 7-membered ring and the second representing the α -methylene- γ -lactone unit. These structural requirements were reported to be essential for the anti-inflammatory activity of xanthatin, where an IC_{50} value of 5 μ M for the inhibition of NO production in RAW264.7 cells was reported.²⁴⁷

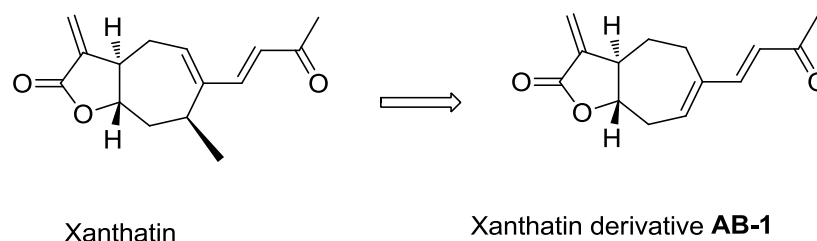


Figure 57. Structure of the sesquiterpene lactone xanthatin and its derivative AB-1, which was investigated towards its toxicity and anti-inflammatory activity in RAW264.7 macrophages.

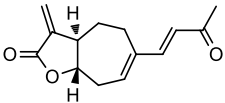
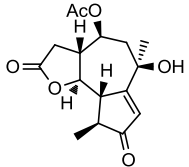
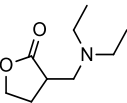
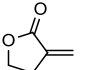
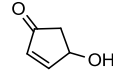
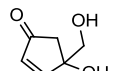
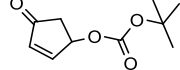
A derivative compound from the guaianolide family, **MS-342 F9-18**, bearing a γ -butyrolactone unit beside a cyclopentenone moiety, was screened for its toxicity in two cell lines. The guaianolide derivative showed no significant effect on the viability of human colon cancer cells HT-29 in the concentration range of 10-50 μ M and also no relevant cytotoxic effect at concentrations up to 75 μ M towards the murine macrophages RAW264. A weak effect on the viability of RAW264.7 cells was detected at 100 μ M ($73.6 \pm 8.9\%$). Furthermore, since the compound consists of several moieties that can also act as antioxidant and radical scavenger, the antioxidant capacity in the cell-free ORAC-fluorescein assay was determined. Compared to the vitamin E derivative Trolox, **MS-342 F9-18** revealed a third of the Trolox antioxidant capacity (0.30 ± 0.06 Trolox equivalents) in the range of 0.5-10 μ M, suggesting an overall weak radical scavenging-based antioxidant activity.

Two γ -butyrolactone derivatives were tested for their cytotoxicity in RAW264.7 murine macrophages and IC_{50} values could be estimated (entry 3 and 4 in Table 22). It is proposed, that the diethylamino-substituted γ -butyrolactone serves as a precursor for the α -methylene γ -butyrolactone, which once present in the cell can release the free active α -methylene unit upon elimination of diethylamine. The results of the screen showed that both compounds have weak cytotoxic effects on RAW264.7 cells. However, a higher toxicity was observed for the α -methylene lactone with an IC_{50} value of 236 ± 14 μ M compared to the precursor ($IC_{50} = 315 \pm 22$ μ M). The potential decomposition product of the precursor, diethylamine, was found to have no effect on the cell viability.

The 4-hydroxy-2-cyclopentenone molecule is a versatile scaffold and its application in the synthesis towards divers drug target molecules is very broad.²⁴⁸ The distinct chemical property of cyclopentenones, i.e. the α,β -unsaturated carbonyl moiety, by which they can react as a Michael acceptor with thiols on regulatory proteins makes them to a key functional unit for the biological

activity of natural products.²⁴⁹ Eight derivatives of 4-hydroxy-2-cyclopenteneone (**KU 1-KU 8**),²⁵⁰ with several substituents in 4-position were screened towards their cytotoxic and anti-inflammatory activity in RAW264.7 cells at concentration of 100/10/1 μM . Also the 4-hydroxy-2-cyclopenteneone was tested for its toxicity towards both cell lines, displaying an IC_{50} value of $39.7 \pm 5.7 \mu\text{M}$ against RAW264.7 cells and a similar toxicity limit (non-toxic concentration) of 10 μM towards HT-29 colon carcinoma cell. The MTT viability assay of the eight cyclopentenone derivatives with the RAW264.7 cell line stimulated with 10 ng mL^{-1} of LPS revealed a concentration dependent toxicity of the compounds in the range of 100-1 μM and IC_{50} values could be calculated. While all compounds showed a nearly complete toxicity at 100 μM , except for **KU 6** ($64.0 \pm 7.8\%$ cell viability at 100 μM), all compounds had no effect on cell viability at 1 μM . The concentration of the compounds needed to reduce the cell viability to 50% (IC_{50}) was determined in the range of 33-47 μM , whereas **KU 5** was found to be the most toxic compound in the screen (IC_{50} value of $33.1 \pm 3.6 \mu\text{M}$). Subsequently, the test compounds were tested at 1 μM for their ability to inhibit the production of NO in RAW264.7 cells. Here, **KU 1** and **KU 6** were inactive at 1 μM and revealed only at higher concentrations of 10 μM an inhibition of NO production. Compounds **KU 2**, **KU 3**, **KU 4**, **KU 7** and **KU 8** showed a weak to moderate inhibition of NO production at 1 μM . The most active derivative was the TBS-protected 4-hydroxy-2-cyclohexenone (**KU 5**) displaying an inhibition of NO production of $72 \pm 7\%$ at 1 μM . In contrast, the 4-hydroxy-2-cyclopentenone showed no relevant inhibition of NO production at the non-toxic concentration of 1 μM ($3.4 \pm 2.7\%$). These results suggest, that a substitution in 4-position of the 4-hydroxy-2-cyclopentenone has a weak effect on the inhibition of NO production in the case of the carbonates (**KU 2** and **KU 4**), the naphthoate (**KU 3**) or the acetate (**KU 8**). Their weak effect may be explained by a possible hydrolysis in the culture medium/cell, which leads to the less active 4-hydroxy-2-cyclopentenone. However, the activity could be enhanced in the case of the *tert*-butyldimethylsilyl (TBS) protecting group (**KU 5**). That is important to note for potential variations in the substitution pattern of future cyclopentenone compounds tested for their biological activity.

Table 22. Overview of data gained from screening for biological activity and radical scavenging and antioxidant properties (ORAC assay) of different compounds.^a

Name	Structure	Cytotoxicity				Anti-inflammatory activity	Antioxidant activity
		Cell line	IC ₅₀ value [μM]	Viability, % of control (conc. [μM]) ^c	Toxicity limit	Inhibition of NO production (%)	Trolox equivalents
Xanthatin derivative AB-1 , Andreas Bergmann		RAW264.7	46.3 ± 1.7	8.5 ± 1.0 (100)	10 μM	IC ₅₀ = 7.11 ± 1.22 μM ^d	nd
MS-342 F9-F18 , Michael Schwarz		RAW264.7	nd	73.6 ± 8.9 (100) ^b	75 μM	nd	0.300 ± 0.061 (0.5-10 μM)
		HT-29	nd	94.0 ± 12.4 (50) ^b	> 50 μM	-	
Diethylaminomethyl-GBL, Sabrina Fürst		RAW264.7	315 ± 22 ^b	4.95 ± 0.96 (1000) ^b	250 μM	nd	nd
α-methylene-GBL, Sabrina Fürst		RAW264.7	236 ± 14 ^b	5.29 ± 1.18 (1000) ^b	100 μM	nd	nd
4-Hydroxy-2-cyclopentenone, Peter Kreitmeier		RAW264.7	39.7 ± 5.7 ^b	20.1 ± 2.5 (100) ^b	10 μM	3.39 ± 2.65 (1 μM)	0.287 ± 0.023 (0.5-7 μM)
		HT-29	nd	74.3 ± 10.6 (25) ^b	10 μM	-	
(±)-4-Hydroxy-4-(hydroxymethyl) cyclopent-2-enone, Kathrin Ulbrich 1		RAW264.7	47.0 ± 6.4	9.37 ± 0.62 (100)	10 μM	-16.0 ± 25.1 (1 μM) 59.8 ± 20.0 (10 μM)	nd
(±)- <i>tert</i> -Butyl(4-oxo-cyclopent-2-en-1-yl) carbonate, Kathrin Ulbrich 2		RAW264.7	35.5 ± 7.3	8.22 ± 1.43 (100)	1 μM	16.3 ± 13.5 (1 μM)	nd

Name	Structure	Cytotoxicity			Toxicity limit	Anti-inflammatory activity	Antioxidant activity
		Cell line	IC ₅₀ value [μM]	Viability, % of control (conc. [μM]) ^c		Inhibition of NO production (%)	Trolox equivalents
(S)-4-Oxocyclopent-2-en-1-yl 1-naphthoate, Kathrin Ulbrich 3		RAW264.7	46.0 ± 4.3	8.35 ± 1.14 (100)	1 μM	8.19 ± 15.4 (1 μM)	nd
(±)-Methyl(4-oxocyclopent-2-en-1-yl) carbonate, Kathrin Ulbrich 4		RAW264.7	36.7 ± 6.2	8.30 ± 1.32 (100)	1 μM	15.0 ± 7.6 (1 μM)	nd
(±)-4-((<i>tert</i> -Butyldimethylsilyl)oxy)-cyclopent-2-enone, Kathrin Ulbrich 5		RAW264.7	33.1 ± 3.6	8.20 ± 1.46 (100)	1 μM	72.1 ± 7.2 (1 μM)	nd
(S)-2-(4-Oxocyclopent-2-en-1-yl)isoindoline-1,3-dione, Kathrin Ulbrich 6		RAW264.7	> 100	64.0 ± 7.8 (100)	10 μM	5.77 ± 15.5 (1 μM) 75.4 ± 11.1 (10 μM)	nd
(S)-4-(6-Chloro-9H-purin-9-yl)cyclopent-2-enone, Kathrin Ulbrich 7		RAW264.7	36.1 ± 5.7	8.13 ± 1.44 (100)	1 μM	34.2 ± 13.7 (1 μM)	nd
(±)-4-Oxocyclopent-2-en-1-yl acetate, Kathrin Ulbrich 8		RAW264.7	38.0 ± 5.0	8.39 ± 1.55 (100)	1 μM	21.8 ± 13.3 (1 μM)	nd

^aThe compounds used in the biological testing were synthesized by different group members of O. Reiser (Universität Regensburg) as indicated. Cytotoxicity with RAW264.7 cells was determined via the MTT-LPS assay in the presence of 10 ng mL⁻¹ of LPS. ^b Cytotoxicity in the cell lines HT-29 and RAW264.7 was determined by the MTT assay after an incubation time of 24 h, no LPS was added here. ^c Cell viability at highest test concentration of the compound. The toxicity limit refers to the non-toxic concentration of compounds (viability > 80%). The NO production was determined by the Griess assay in RAW264.7 cells stimulated with 10 ng mL⁻¹ of LPS at non-toxic concentrations of compounds. ^d Here, an IC₅₀ value could be calculated. Antioxidant capacity of compounds was measured by the ORAC-fluorescein assay and expressed as Trolox equivalents. nd, not determined.

3.8.3 Biological activity of chalcone-analogs

Three different chalcone derivatives and one flavone derivative (**SU-F-01**) synthesized by Mihai Surducan (visiting PhD student in the group of B. König, Universität Regensburg) were tested for their anti-inflammatory activity in RAW264.7 murine macrophages (Table 23). All chalcone analogs possess instead of the A-ring a thiazol unit bearing a phenyl ring in 2-position of the thiazol ring. Two *para*-substituted chalcone derivatives on the B-ring of the **MS-C-01** scaffold were investigated towards their influence on the anti-inflammatory activity, namely **SU-CT-03** with a more activating NO₂ group and **SU-C-02** with a deactivating OMe group towards a possible Michael addition with SH-groups on target proteins regulating inflammatory pathways. In order to exclude cytotoxic effect of the compounds, their influence on the viability of RAW264.7 cells in presence of 10 ng mL⁻¹ of LPS after 24 h was determined via the MTT-LPS assay. Subsequently, the compounds were tested for their ability to inhibit the NO production in RAW264.7 macrophages at non-toxic concentrations. Due to the poor solubility of the compounds in the cell culture medium, a high dilution was necessary to overcome this problem. The chalcone derivatives showed an overall weak toxicity. A moderate but significant reduction of cell viability was observed for **MS-C-01** and **SU-CT-03** at 1 and 0.5 μM. At non-toxic test concentrations compounds showed no relevant inhibition of the NO production in RAW264.7 macrophages.

Table 23. Evaluation of different chalcone analogs^a towards their toxicity and anti-inflammatory activity.

Name	Structure	Cytotoxicity	Anti-inflammatory activity	
		Viability ^b , % of control (conc. [μM])	Toxicity limit ^c	Maximum inhibition of NO production ^d (%), (conc.)
MS-C-01		79.8 ± 7.44 (1)	250 nM	-5.74 ± 5.56 (250 nM)
SU-F-01		88.9 ± 11.1 (5)	5 μM	-4.14 ± 17.2 (5 μM)
SU-C-02		92.5 ± 15.8 (5)	5 μM	10.8 ± 14.5 (5 μM)
SU-CT-03		73.4 ± 8.64 (1)	250 nM	1.39 ± 4.12 (250 nM)

^a The compounds used in the biological testing were synthesized by Mihai Surducan, a visiting PhD student in the group of B. König (Universität Regensburg). ^b Cytotoxicity was determined via the MTT-LPS assay in the presence of 10 ng mL⁻¹ of LPS and cell viability is given for the highest test concentration of the compound. ^c The toxicity limit refers to the non-toxic concentration of compounds. ^d The NO production was determined by the Griess assay in LPS-stimulated RAW264.7 macrophages at non-toxic concentrations of compounds.

4 Summary

To fight chronic inflammation in autoimmune diseases such as rheumatic arthritis and multiple sclerosis or cancer is an exigency. Therefore the inhibition of proinflammatory proteins such as inducible NO-synthase (iNOS) and the activation of anti-inflammatory proteins such as heme oxygenase-1 (HO-1) are important measures to be addressed. Many natural products and synthetic compounds with an α,β -unsaturated carbonyl moiety reveal a variety of biological properties, including antioxidant, anti-inflammatory and cytoprotective properties. α,β -Unsaturated carbonyl compounds possess Michael acceptor activity and can react with nucleophilic sulfhydryl groups on key cysteins to regulate the inhibition of NF- κ B and the activation of Nrf2, which are the transcriptional factors needed for the expression of iNOS and HO-1, respectively.

Heme oxygenase-1 is a redox sensitive, inducible stress protein converting heme to CO, Fe²⁺ and biliverdin, which is further reduced to bilirubin by biliverdin reductase (BVR). Thereby, the overall anti-inflammatory, chemopreventive and chemoprotective effect connected to the HO-1 activity is a result of the heme degradation. An ELISA-based HO-1 assay was developed and proved to be a reliable and easy cell line-based assay in order to screen compound libraries to find new HO-1 inducers, which could be used as lead structures for drug development. The HO-1 activity assay combines the HO enzyme reaction in presence of recombinant BVR with the quantification of the reaction product bilirubin by an indirect sandwich enzyme-linked immunosorbent assay (ELISA) using the murine macrophage cell line RAW264.7. The detection of the total bilirubin level in whole cell lysates requires only a fraction of the total protein amount, that is 10-30 μ g per sample. By comparing the bilirubin levels in stimulated cells and control cells, the HO-1 activity can be expressed as 'fold of control' based on pmol bilirubin h⁻¹mg⁻¹ total protein. The reliable HO-1 activity assay was developed in a 96-well plate format allowing the screening of multiple compounds in parallel. 18 small molecules, mainly natural products with an α,β -unsaturated carbonyl unit as well as the drugs dexamethasone and oltipraz were tested and the activity of most known HO-1 inducers was confirmed. The diterpene carnosol was found the most potent HO-1 inducer in the screen of HO-1 activity (8.2 ± 1.9 fold after 6 h) followed by rosolic acid with an induction of HO-1 activity of 3.9 ± 0.4 fold after 24 h. Amongst the natural chalcones, cardamonin and flavokawain A were identified as new potent HO-1 inducers. The most potent HO-1 activity inducer was found to be the 2',4'-dihydroxy-3,4-dimethoxychalcone (DHDMCH), with a maximum induction of HO-1 activity of 6.1 ± 2.3 fold. Moreover, the time dependence of HO-1 protein expression for DHDMCH was compared to its enzyme activity, which was further evaluated in presence of lipopolysaccharide (LPS) and the specific HO-1 inhibitor tin protoporphyrin IX (SnPPiX). Furthermore, the HO-1 activity assay was successfully applied on human primary dendritic cells, where the HO-1 activity of the α -CF₃-TMCH was determined.

Natural and synthetic hydroxy- and methoxychalcones were characterized towards their anti-inflammatory and antioxidant behavior in RAW264.7 murine macrophages. Particularly, their influence on the induction of the anti-inflammatory and cytoprotective protein HO-1 and the inhibition of the proinflammatory protein iNOS, more specifically the reduction of NO production was investigated. Additionally, a cell-free assay performed under physiological conditions was used to determine the radical scavenging properties of the chalcones and establish an antioxidant capacity compared to the vitamin E derivative Trolox. The overall biological activity of chalcones depends on their Michael acceptor reactivity, which can be influenced by different substitution patterns on the aromatic rings, as well as on the presence of free hydroxy groups on the aromatic rings of the chalcone. By these means, introducing methoxy groups in 2',4'-position on the A-ring or in 3,4-positions on the B-ring enhances the anti-inflammatory activity, while an increasing number of hydroxy groups leads to a higher radical scavenging activity of chalcones. The observations demonstrate that an indirect influence on the electrophilicity of Michael acceptors can indeed determine the potency of chalcones as inducers of HO-1 activity and as inhibitors of inflammatory NO production. On the other hand, a hydroxy-rich chalcone like butein, which is a relatively weak Michael acceptor, can act as a powerful antioxidant determined by its radical scavenging properties.

A direct change at the Michael system can also alter the reactivity and thus the biological activity of enones. The approach of modifying the α -position of the α,β -unsaturated carbonyl system is a promising concept, because it should lead to a direct and straightforward influence on its reactivity. The chemical reactivity of α -X-enones depends on the nature of the α -substituent, thus activating or deactivating the Michael acceptor reactivity toward thiols responsible for a biological response. The influence of different α -X-substituted 2',3,4,4'-tetramethoxychalcones (α -X-TMCHs) on the induction of HO-1 protein expression and HO-1 enzymatic activity and on the other hand the inhibition of NO production, regulated by iNOS was determined in RAW264.7 murine macrophages. A clear correlation could be established between the reactivity of α -X-TMCHs, demonstrated by their thia-Michael addition reaction with cysteamine (k_2 values) and their biological activity. The results demonstrate that a rather moderate electrophilicity of α -X-TMCHs is a crucial factor determining their potency to induce HO-1 activity or inhibit NO production. This could be observed for the most electrophilic TMCHs in our screen, α -CN-TMCH and α -NO₂-TMCH, displaying relatively high k_2 values in the thia-Michael addition reaction. Both TMCHs were only weak inhibitors of iNOS activity and showed no induction of HO-1 activity or protein expression, which may suggest an alternative pathway of the chalcones in the cell, such as a consumption by GSH, thus preventing them to reach their target SH-groups. The more intermediate electrophiles (with lower k_2 values), α -CF₃-TMCH, α -Br-TMCH and α -Cl-TMCH however, displayed a high activity in the biological screening of the α -X-TMCHs. Here, α -CF₃-TMCH was the most active chalcone, with an IC₅₀ value of NO production of 120 ± 62 nM and a 2.7 ± 0.5

fold induction of HO-1 activity in RAW264.7 macrophages. The importance of a sufficient Michael acceptor activity of α -X-modified enones required for a reasonable biological activity was demonstrated by the model compounds α -X-Limno-CPs, derived from the natural product limnophilaspiroketone. The α -X-Limno-CPs exerted a weak anti-inflammatory activity in inhibiting the NO production in RAW264.7 macrophages, due to their overall electron rich enone system making them weak electrophiles compared to the α -X-TMCHs.

A water soluble phosphorester-based enzyme-triggered CO-releasing molecule (ET-CORMs) was found to moderately inhibit the NO production ($31 \pm 8\%$ at $100 \mu\text{M}$ for rac-**17**) in RAW264.7 macrophages. Thereby, an expected influence of the iron ions Fe^{2+} and Fe^{3+} , which can derive upon oxidative decomposition of the ester (cyclohexadiene) $\text{Fe}(\text{CO})_3$ complex, on the inhibitory activity of the ET-CORMs was not found. In contrary, for some possible decomposition products of acyloxy(cyclohexadiene) $\text{Fe}(\text{CO})_3$ complexes as ET-CORMs, such as phenolic and cyclohexanone derivatives, a significant activity was determined, which can contribute to the activity of the corresponding ET-CORMs. These results confirm previous findings that cyclohexenones, especially 2-cyclohexenone, may strongly contribute to the overall activity of such ET-CORMs as the acyloxy(cyclohexadiene) $\text{Fe}(\text{CO})_3$ complexes.

The naturally occurring (+)-arteludovicinolide A and its synthetic enantiomer (-)-arteludovicinolide A were shown to display anti-inflammatory activity, demonstrated by their ability to inhibit the NO production and induce HO-1 activity in RAW264.7 macrophages. (+)-Arteludovicinolide A was the more active enantiomer, displaying an inhibitory effect of the NO production with an IC_{50} value of $4.9 \pm 1.1 \mu\text{M}$ and an induction of HO-1 activity of 2.1 ± 0.7 fold after 6 h of incubation. The functional groups on these sesquiterpenes, a α -methylene group and a cyclopentenone ring may be involved in their biological activity, since it was shown that the α -methylene group in the lactone ring is crucial for the anti-inflammatory activity of the natural product. Furthermore, a diverse group of synthetic compounds and natural product derivatives bearing the cyclopentenone ring or a γ -butyrolactone moiety were found to exert weak to moderate cytotoxicity in RAW264.7 macrophages or HT-29 colon cells and weak to moderate anti-inflammatory activity in RAW264.7 cells.

In conclusion, the Michael acceptor functionality of electrophilic enones proved to be crucial for their biological activity, regarding their potency as inducers of the cytoprotective and anti-inflammatory HO-1 activity and protein expression and as inhibitors of proinflammatory iNOS activity. α,β -Unsaturated carbonyl compounds are a very useful class of substances. A systematic manipulation of the Michael acceptor reactivity by modifying the α -position of the enone system leads to a fine-tuned biological activity in chalcone scaffolds. This approach might be highly valuable for drug design in order to predict the biological activity.

5 References

1. Gersch, M.; Kreuzer, J.; Sieber, S. A., Electrophilic natural products and their biological targets. *Nat. Prod. Rep.* **2012**, *29*, 659-682.
2. Buelna-Chontal, M.; Zazueta, C., Redox activation of Nrf2 & NF-kappaB: A double end sword? *Cell. Signal.* **2013**, *25*, 2548-57.
3. Talalay, P.; De Long, M. J.; Prochaska, H. J., Identification of a common chemical signal regulating the induction of enzymes that protect against chemical carcinogenesis. *Proc. Natl. Acad. Sci. USA* **1988**, *85*, 8261-8265.
4. Amslinger, S., The Tunable Functionality of α,β -Unsaturated Carbonyl Compounds Enables Their Differential Application in Biological Systems. *ChemMedChem* **2010**, *5*, 351-356.
5. Itoh, K.; Mochizuki, M.; Ishii, Y.; Ishii, T.; Shibata, T.; Kawamoto, Y.; Kelly, V.; Sekizawa, K.; Uchida, K.; Yamamoto, M., Transcription factor Nrf2 regulates inflammation by mediating the effect of 15-deoxy-Delta(12),(14)-prostaglandin J(2). *Mol. Cell. Biol.* **2004**, *24*, 36-45.
6. Dinkova-Kostova, A. T.; Liby, K. T.; Stephenson, K. K.; Holtzclaw, W. D.; Gao, X. Q.; Suh, N.; Williarri, C.; Risingsong, R.; Honda, T.; Gribble, G. W.; Sporn, M. B.; Talalay, P., Extremely potent triterpenoid inducers of the phase 2 response: Correlations of protection against oxidant and inflammatory stress. *Proc. Natl. Acad. Sci. USA* **2005**, *102*, 4584-4589.
7. Dinkova-Kostova, A. T.; Talalay, P.; Sharkey, J.; Zhang, Y.; Holtzclaw, W. D.; Wang, X. J.; David, E.; Schiavoni, K. H.; Finlayson, S.; Mierke, D. F.; Honda, T., An Exceptionally Potent Inducer of Cytoprotective Enzymes. *J. Biol. Chem.* **2010**, *285*, 33747-33755.
8. Zheng, S. Q.; Laxmi, Y. R. S.; David, E.; Dinkova-Kostova, A. T.; Schiavoni, K. H.; Ren, Y. Q.; Zheng, Y.; Trevino, I.; Bumeister, R.; Ojima, I.; Wigley, W. C.; Bliska, J. B.; Mierke, D. F.; Honda, T., Synthesis, Chemical Reactivity as Michael Acceptors, and Biological Potency of Monocyclic Cyanoenones, Novel and Highly Potent Anti-inflammatory and Cytoprotective Agents. *J. Med. Chem.* **2012**, *55*, 4837-4846.
9. Liby, K.; Hock, T.; Yore, M. M.; Suh, N.; Place, A. E.; Risingsong, R.; Williams, C. R.; Royce, D. B.; Honda, T.; Honda, Y.; Gribble, G. W.; Hill-Kapturczak, N.; Agarwal, A.; Sporn, M. B., The Synthetic Triterpenoids, CDDO and CDDO-Imidazolide, Are Potent Inducers of Heme Oxygenase-1 and Nrf2/ARE Signaling. *Cancer Res.* **2005**, *65*, 4789-4798.
10. Holland, R.; Fishbein, J. C., Chemistry of the Cysteine Sensors in Kelch-Like ECH-Associated Protein 1. *Antioxid. Redox. Signal.* **2010**, *13*, 1749-1761.
11. Tkachev, V.; Menshchikova, E.; Zenkov, N., Mechanism of the Nrf2/Keap1/ARE signaling system. *Biochemistry (Mosc)* **2011**, *76*, 407-422.
12. Kobayashi, M.; Yamamoto, M., Molecular mechanisms activating the Nrf2-Keap1 pathway of antioxidant gene regulation. *Antioxid. Redox. Sign.* **2005**, *7*, 385-394.
13. Surh, Y.-J.; Kundu, J. K.; Na, H.-K., Nrf2 as a Master Redox Switch in Turning on the Cellular Signaling Involved in the Induction of Cytoprotective Genes by Some Chemopreventive Phytochemicals. *Planta Med.* **2008**, *74*, 1526-1539.
14. Kobayashi, M.; Li, L.; Iwamoto, N.; Nakajima-Takagi, Y.; Kaneko, H.; Nakayama, Y.; Eguchi, M.; Wada, Y.; Kumagai, Y.; Yamamoto, M., The Antioxidant Defense System Keap1-Nrf2 Comprises a Multiple Sensing Mechanism for Responding to a Wide Range of Chemical Compounds. *Mol. Cell. Biol.* **2009**, *29*, 493-502.
15. Negi, G.; Kumar, A.; Joshi, R. P.; Sharma, S. S., Oxidative stress and Nrf2 in the pathophysiology of diabetic neuropathy: Old perspective with a new angle. *Biochem. Biophys. Res. Commun.* **2011**, *408*, 1-5.

16. Scapagnini, G.; Sonya, V.; Nader, A. G.; Calogero, C.; Zella, D.; Fabio, G., Modulation of Nrf2/ARE Pathway by Food Polyphenols: A Nutritional Neuroprotective Strategy for Cognitive and Neurodegenerative Disorders. *Mol. Neurobiol.* **2011**, *44*, 192-201.
17. Lee, J.-S.; Surh, Y.-J., Nrf2 as a novel molecular target for chemoprevention. *Cancer Lett.* **2005**, *224*, 171-184.
18. Pahl, H. L., Activators and target genes of Rel/NF-kappa B transcription factors. *Oncogene* **1999**, *18*, 6853-6866.
19. Lawrence, T.; Gilroy, D. W.; Colville-Nash, P. R.; Willoughby, D. A., Possible new role for NF-kappa B in the resolution of inflammation. *Nat. Med.* **2001**, *7*, 1291-1297.
20. Kumar, A.; Takada, Y.; Boriek, A.; Aggarwal, B., Nuclear factor- κ B: its role in health and disease. *J. Mol. Med.* **2004**, *82*, 434-448.
21. Yamamoto, Y.; Gaynor, R. B., Therapeutic potential of inhibition of the NF- κ B pathway in the treatment of inflammation and cancer. *J. Clin. Invest.* **2001**, *107*, 135-142.
22. Otterbein, L. E.; Soares, M. P.; Yamashita, K.; Bach, F. H., Heme oxygenase-1: unleashing the protective properties of heme. *Trends Immunol.* **2003**, *24*, 449-455.
23. Maines, M. D.; Gibbs, P. E. M., 30 some years of heme oxygenase: From a "molecular wrecking ball" to a "mesmerizing" trigger of cellular events. *Biochem. Biophys. Res. Commun.* **2005**, *338*, 568-577.
24. Immenschuh, S.; Ramadori, G., Gene regulation of heme oxygenase-1 as a therapeutic target. *Biochem. Pharmacol.* **2000**, *60*, 1121-1128.
25. Soares, M. P.; Bach, F. H., Heme oxygenase-1: from biology to therapeutic potential. *Trends Mol. Med.* **2009**, *15*, 50-58.
26. Keyse, S. M.; Tyrrell, R. M., Heme Oxygenase Is The Major 32-Kda Stress Protein-Induced In Human-Skin Fibroblasts By Uva Radiation, Hydrogen-Peroxide, And Sodium Arsenite. *Proc. Natl. Acad. Sci. USA* **1989**, *86*, 99-103.
27. Dinkova-Kostova, A. T.; Massiah, M. A.; Bozak, R. E.; Hicks, R. J.; Talalay, P., Potency of Michael reaction acceptors as inducers of enzymes that protect against carcinogenesis depends on their reactivity with sulfhydryl groups. *Proc. Natl. Acad. Sci. USA* **2001**, *98*, 3404-3409.
28. Dinkova-Kostova, A. T.; Holtzclaw, W. D.; Cole, R. N.; Itoh, K.; Wakabayashi, N.; Katoh, Y.; Yamamoto, M.; Talalay, P., Direct evidence that sulfhydryl groups of Keap1 are the sensors regulating induction of phase 2 enzymes that protect against carcinogens and oxidants *Proc. Natl. Acad. Sci. USA* **2002**, *99*, 11908-11913.
29. Kyriakis, J. M.; Avruch, J., Mammalian mitogen-activated protein kinase signal transduction pathways activated by stress and inflammation. *Physiol. Rev.* **2001**, *81*, 807-869.
30. Li, C.; Hossieny, P.; Wu, B. J.; Qawasmeh, A.; Beck, K.; Stocker, R., Pharmacologic induction of heme oxygenase-1. *Antioxid. Redox. Signal.* **2007**, *9*, 2227-2239.
31. Alam, J.; Cook, J. L., How many transcription factors does it take to turn on the heme oxygenase-1 gene? *Am. J. Respir. Cell Mol. Biol.* **2007**, *36*, 166-174.
32. Ryter, S. W.; Alam, J.; Choi, A. M. K., Heme oxygenase-1/carbon monoxide: From basic science to therapeutic applications. *Physiol. Rev.* **2006**, *86*, 583-650.
33. Poss, K. D.; Tonegawa, S., Heme oxygenase 1 is required for mammalian iron reutilization. *Proc. Natl. Acad. Sci. U. S. A.* **1997**, *94*, 10919-10924.
34. Poss, K. D.; Tonegawa, S., Reduced stress defense in heme oxygenase 1-deficient cells. *Proc. Natl. Acad. Sci. U. S. A.* **1997**, *94*, 10925-10930.

35. Yachie, A.; Niida, Y.; Wada, T.; Igarashi, N.; Kaneda, H.; Toma, T.; Ohta, K.; Kasahara, Y.; Koizumi, S., Oxidative stress causes enhanced endothelial cell injury in human heme oxygenase-1 deficiency. *J. Clin. Invest.* **1999**, *103*, 129-135.
36. Vreman, H. J.; Stevenson, D. K., Heme oxygenase activity as measured by carbon monoxide production. *Anal. Biochem.* **1988**, *168*, 31-38.
37. Suttner, D. M.; Sridhar, K.; Lee, C. S.; Tomura, T.; Hansen, T. N.; Dennery, P. A., Protective effects of transient HO-1 overexpression on susceptibility to oxygen toxicity in lung cells. *Am. J. Physiol. Lung Cell Mol. Physiol.* **1999**, *276*, L443-L451.
38. Maines, M. D., Heme Oxygenase - Function, Multiplicity, Regulatory Mechanisms, and Clinical-Applications. *FASEB J.* **1988**, *2*, 2557-2568.
39. Tenhunen, R.; Marver, H. S.; Schmid, R., Enzymatic Conversion Of Heme To Bilirubin By Microsomal Heme Oxygenase. *Proc. Natl. Acad. Sci. USA* **1968**, *61*, 748-755.
40. Maines, M. D.; Kappas, A., Cobalt Induction of Hepatic Heme Oxygenase; with Evidence That Cytochrome P-450 Is Not Essential for This Enzyme Activity. *Proc. Natl. Acad. Sci. U. S. A.* **1974**, *71*, 4293-4297.
41. Tenhunen, R., Method for microassay of microsomal heme oxygenase activity. *Anal. Biochem.* **1972**, *45*, 600-607.
42. Lincoln, B. C.; Mayer, A.; Bonkovsky, H. L., Microassay of heme oxygenase by high-performance liquid chromatography: Application to assay of needle biopsies of human liver. *Anal. Biochem.* **1988**, *170*, 485-490.
43. Ryter, S.; Kvam, E.; Richman, L.; Hartmann, F.; Tyrrell, R. M., A chromatographic assay for heme oxygenase activity in cultured human cells: Application to artificial heme oxygenase overexpression. *Free Radic. Biol. Med.* **1998**, *24*, 959-971.
44. Bian, W.; Zhang, N.; Jiang, C., Spectrofluorimetric determination of bilirubin in serum samples. *Luminescence* **2011**, *26*, 54-8.
45. Nagaoka, S.; Cowger, M. L., A novel method to determine total and free serum bilirubin. *Anal. Biochem.* **1979**, *96*, 364-77.
46. Wells, R.; Drew, J. H.; Hammond, K. B., Bilirubin binding capacity and free bilirubin concentration: fluorescence quenching compared with peroxidase oxidation and sephadex column elution techniques. *Clin. Chim. Acta* **1981**, *116*, 69-79.
47. Klemz, R.; Mashreghi, M.-F.; Spies, C.; Volk, H.-D.; Kotsch, K., Amplifying the fluorescence of bilirubin enables the real-time detection of heme oxygenase activity. *Free Radic. Biol. Med.* **2009**, *46*, 305-311.
48. Huber, A. H.; Zhu, B.; Kwan, T.; Kampf, J. P.; Hegyi, T.; Kleinfeld, A. M., Fluorescence sensor for the quantification of unbound bilirubin concentrations. *Clin. Chem.* **2012**, *58*, 869-76.
49. Kumagai, A.; Ando, R.; Miyatake, H.; Greimel, P.; Kobayashi, T.; Hirabayashi, Y.; Shimogori, T.; Miyawaki, A., A Bilirubin-Inducible Fluorescent Protein from Eel Muscle. *Cell* **2013**, *153*, 1602-1611.
50. Neugebauer, U.; März, A.; Henkel, T.; Schmitt, M.; Popp, J., Spectroscopic detection and quantification of heme and heme degradation products. *Anal. Bioanal. Chem.* **2012**, *404*, 2819-2829.
51. Sigala, P. A.; Crowley, J. R.; Hsieh, S.; Henderson, J. P.; Goldberg, D. E., Direct tests of enzymatic heme degradation by the malaria parasite Plasmodium falciparum. *J Biol Chem* **2012**, *287*, 37793-807.
52. Izumi, Y.; Yamazaki, M.; Shimizu, S.; Shimizu, K.; Yamaguchi, T.; Nakajima, H., Anti-bilirubin monoclonal antibody II. Enzyme-linked immunosorbent assay for bilirubin fractions by combination of two monoclonal antibodies. *Biochim. Biophys. Acta* **1988**, *967*, 261-266.

53. Doumas, B. T.; Perry, B. W.; Sasse, E. A.; Straumfjord, J. V., Standardization in Bilirubin Assays: Evaluation of Selected Methods and Stability of Bilirubin Solutions. *Clin. Chem.* **1973**, *19*, 984-993.
54. Andreu, Y.; Galban, J.; de Marcos, S.; Castillo, J. R., Determination of direct-bilirubin by a fluorimetric-enzymatic method based on bilirubin oxidase. *Fresenius. J. Anal. Chem.* **2000**, *368*, 516-21.
55. Kohashi, K.; Date, Y.; Morita, M.; Tsuruta, Y., Fluorescence reaction of bilirubin with zinc ion in dimethyl sulfoxide and its application to assay of total bilirubin in serum. *Anal. Chim. Acta* **1998**, *365*, 177-182.
56. Tenhunen, R.; Marver, H. S.; Schmid, R., Microsomal Heme Oxygenase - Characterization of Enzyme. *J. Biol. Chem.* **1969**, *244*, 6388-6394.
57. Kitchin, K. T.; Anderson, W. L.; Suematsu, M., An ELISA assay for heme oxygenase (HO-1). *J. Immunol. Methods* **2001**, *247*, 153-161.
58. Balla, G.; Jacob, H. S.; Balla, J.; Rosenberg, M.; Nath, K.; Apple, F.; Eaton, J. W.; Vercellotti, G. M., Ferritin: a cytoprotective antioxidant strategem of endothelium. *J. Biol. Chem.* **1992**, *267*, 18148-18153.
59. Motterlini, R.; Foresti, R.; Intaglietta, M.; Winslow, R. M., NO-mediated activation of heme oxygenase: Endogenous cytoprotection against oxidative stress to endothelium. *Am. J. Physiol.-Heart Circ. Physiol.* **1996**, *39*, H107-H114.
60. Maines, M. D.; Kappas, A., Cobalt stimulation of heme degradation in the liver. Dissociation of microsomal oxidation of heme from cytochrome P-450. *J. Biol. Chem.* **1975**, *250*, 4171-7.
61. Tenhunen, R.; Ross, M. E.; Marver, H. S.; Schmid, R., Reduced Nicotinamide-Adenine Dinucleotide Phosphate Dependent Biliverdin Reductase . Partial Purification and Characterization. *Biochemistry* **1970**, *9*, 298-303.
62. Kutty, R. K.; Maines, M. D., Purification and characterization of biliverdin reductase from rat liver. *J. Biol. Chem.* **1981**, *256*, 3956-3962.
63. Motterlini, R.; Foresti, R.; Vandegriff, K.; Intaglietta, M.; Winslow, R. M., Oxidative-Stress Response in Vascular Endothelial-Cells Exposed to Acellular Hemoglobin-Solutions. *Am. J. Physiol.-Heart Circ. Physiol.* **1995**, *38*, H648-H655.
64. Motterlini, R.; Foresti, R.; Bassi, R.; Calabrese, V.; Clark, J. E.; Green, C. J., Endothelial heme oxygenase-1 induction by hypoxia - Modulation by inducible nitric-oxide synthase and S-nitrosothiols. *J. Biol. Chem.* **2000**, *275*, 13613-13620.
65. Motterlini, R.; Foresti, R.; Bassi, R.; Green, C. J., Curcumin, an antioxidant and anti-inflammatory agent, induces heme oxygenase-1 and protects endothelial cells against oxidative stress. *Free Radic. Biol. Med.* **2000**, *28*, 1303-1312.
66. Foresti, R.; Hoque, M.; Monti, D.; Green, C. J.; Motterlini, R., Differential activation of heme oxygenase-1 by chalcones and rosolic acid in endothelial cells. *J. Pharmacol. Exp. Ther.* **2005**, *312*, 686-693.
67. Scapagnini, G.; Foresti, R.; Calabrese, V.; Stella, A. M. G.; Green, C. J.; Motterlini, R., Caffeic acid phenethyl ester and curcumin: A novel class of heme oxygenase-1 inducers. *Mol. Pharmacol.* **2002**, *61*, 554-561.
68. Balogun, E.; Hoque, M.; Gong, P.; Killeen, E.; Green, C. J.; Foresti, R.; Alam, J.; Motterlini, R., Curcumin activates the haem oxygenase-1 gene via regulation of Nrf2 and the antioxidant-responsive element. *Biochem. J.* **2003**, *371*, 887-895.
69. Abuarqoub, H.; Foresti, R.; Green, C. J.; Motterlini, R., Heme oxygenase-1 mediates the anti-inflammatory actions of 2'-hydroxychalcone in RAW264.7 murine macrophages. *Am. J. Physiol. Cell Physiol.* **2006**, *290*, C1092-C1099.

70. Sawle, P.; Moulton, B. E.; Jarzykowska, M.; Green, C. J.; Foresti, R.; Fairlamb, I. J. S.; Motterlini, R., Structure-Activity Relationships of Methoxychalcones as Inducers of Heme Oxygenase-1. *Chem. Res. Toxicol.* **2008**, *21*, 1484-1494.
71. Shimizu, S.; Izumi, Y.; Yamazaki, M.; Shimizu, K.; Yamaguchi, T.; Nakajima, H., Anti-bilirubin monoclonal antibody I. Preparation and properties of monoclonal antibodies to covalently coupled bilirubin-albumin. *Biochim. Biophys. Acta* **1988**, *967*, 255-260.
72. Izumi, Y.; Yamazaki, M.; Shimizu, S.; Shimizu, K.; Yamaguchi, T.; Nakajima, H., Anti-bilirubin monoclonal antibody II. Enzyme-linked immunosorbent assay for bilirubin fractions by combination of two monoclonal antibodies. *Biochim. Biophys. Acta* **1988**, *967*, 261-266.
73. Nakayama, M.; Takahashi, K.; Komaru, T.; Fukuchi, M.; Shioiri, H.; Sato, K.; Kitamuro, T.; Shirato, K.; Yamaguchi, T.; Suematsu, M.; Shibahara, S., Increased expression of heme oxygenase-1 and bilirubin accumulation in foam cells of rabbit atherosclerotic lesions. *Arterioscler. Thromb. Vasc. Biol.* **2001**, *21*, 1373-1377.
74. Huang, E.; Ong, W.-Y.; Go, M.-L.; Garey, L. J., Heme oxygenase-1 activity after excitotoxic injury: immunohistochemical localization of bilirubin in neurons and astrocytes and deleterious effects of heme oxygenase inhibition on neuronal survival after kainate treatment. *J. Neurosci. Res.* **2005**, *80*, 268-278.
75. Kimpara, T.; Takeda, A.; Yamaguchi, T.; Arai, H.; Okita, N.; Takase, S.; Sasaki, H.; Itoyama, Y., Increased bilirubins and their derivatives in cerebrospinal fluid in Alzheimer's disease. *Neurobiol. Aging* **2000**, *21*, 551-554.
76. Kozaki, N.; Shimizu, S.; Chijiwa, K.; Yamaguchi, K.; Kuroki, S.; Shimoharada, K.; Yamaguchi, T.; Nakajima, H.; Tanaka, M., Bilirubin as an anti-oxidant for surgical stress: a preliminary report of bilirubin oxidative metabolites. *HPB Surg.* **1999**, *11*, 241-248.
77. Yamada, N.; Yamaya, M.; Okinaga, S.; Lie, R.; Suzuki, T.; Nakayama, K.; Takeda, A.; Yamaguchi, T.; Itoyama, Y.; Sekizawa, K.; Sasaki, H., Protective Effects of Heme Oxygenase-1 against Oxidant-Induced Injury in the Cultured Human Tracheal Epithelium. *Am. J. Respir. Cell Mol. Biol.* **1999**, *21*, 428-435.
78. Rücker, H. Diploma thesis, University of Regensburg, 2009.
79. Garthwaite, J., Concepts of neural nitric oxide-mediated transmission. *Eur. J. Neurosci.* **2008**, *27*, 2783-2802.
80. Rees, D. D.; Palmer, R. M.; Moncada, S., Role of endothelium-derived nitric oxide in the regulation of blood pressure. *PNAS* **1989**, *86*, 3375-3378.
81. Kleinert, H.; Schwarz, P. M.; Förstermann, U., Regulation of the Expression of Inducible Nitric Oxide Synthase. *Biol. Chem.* **2005**, *384*, 1343-1364.
82. Alderton, W. K.; Cooper, C. E.; Knowles, R. G., Nitric oxide synthases: structure, function and inhibition. *Biochem. J.* **2001**, *357*, 593-615.
83. Förstermann, U.; Sessa, W. C., Nitric oxide synthases: regulation and function. *Eur. Heart J.* **2012**, *33*, 829-837.
84. Vallance, P.; Leiper, J., Blocking NO synthesis: How, where and why? *Nat. Rev. Drug Discov.* **2002**, *1*, 939-950.
85. Aktan, F., iNOS-mediated nitric oxide production and its regulation. *Life Sci.* **2004**, *75*, 639-653.
86. Tsikas, D., Analysis of nitrite and nitrate in biological fluids by assays based on the Griess reaction: Appraisal of the Griess reaction in the L-arginine/nitric oxide area of research. *J. Chromatogr. B Analyt. Technol. Biomed. Life Sci.* **2007**, *851*, 51-70.

87. Stuehr, D. J.; Marletta, M. A., Mammalian Nitrate Biosynthesis: Mouse Macrophages Produce Nitrite and Nitrate in Response to Escherichia coli Lipopolysaccharide. *Proc. Natl. Acad. Sci. U. S. A.* **1985**, *82*, 7738-7742.
88. Davalos, A.; Gomez-Cordoves, C.; Bartolome, B., Extending Applicability of the Oxygen Radical Absorbance Capacity (ORAC-Fluorescein) Assay. *J. Agric. Food Chem.* **2003**, *52*, 48-54.
89. Israf, D. A.; Khaizurin, T. A.; Syahida, A.; Lajis, N. H.; Khozirah, S., Cardamonin inhibits COX and iNOS expression via inhibition of p65NF-kappaB nuclear translocation and Ikappa-B phosphorylation in RAW 264.7 macrophage cells. *Mol. Immunol.* **2007**, *44*, 673-679.
90. Qin, Y.; Sun, C.-Y.; Lu, F.-R.; Shu, X.-R.; Yang, D.; Chen, L.; She, X.-M.; Gregg, N. M.; Guo, T.; Hu, Y., Cardamonin exerts potent activity against multiple myeloma through blockade of NF-κB pathway in vitro. *Leuk. Res.* **2012**, *36*, 514-520.
91. Park, S.; Gwak, J.; Han, S. J.; Oh, S., Cardamonin Suppresses the Proliferation of Colon Cancer Cells by Promoting β-Catenin Degradation. *Biol. Pharm. Bull.* **2013**, *36*, 1040-1044.
92. Folmer, F.; Blasius, R.; Morceau, F.; Tabudravu, J.; Dicato, M.; Jaspars, M.; Diederich, M., Inhibition of TNFα-induced activation of nuclear factor κB by kava (Piper methysticum) derivatives. *Biochem. Pharmacol.* **2006**, *71*, 1206-1218.
93. Stevens, J. F.; Page, J. E., Xanthohumol and related prenylflavonoids from hops and beer: to your good health! *Phytochemistry* **2004**, *65*, 1317-1330.
94. Gerhäuser, C.; Alt, A.; Heiss, E.; Gamal-Eldeen, A.; Klimo, K.; Knauf, J.; Neumann, I.; Scherf, H. R.; Frank, N.; Bartsch, H.; Becker, H., Cancer chemopreventive activity of Xanthohumol, a natural product derived from hop. *Mol. Cancer Ther.* **2002**, *1*, 959-969.
95. Dietz, B. M.; Kang, Y. H.; Liu, G.; Eggler, A. L.; Yao, P.; Chadwick, L. R.; Pauli, G. F.; Farnsworth, N. R.; Mesecar, A. D.; van Breemen, R. B.; Bolton, J. L., Xanthohumol isolated from *Humulus lupulus* Inhibits menadione-induced DNA damage through induction of quinone reductase. *Chem. Res. Toxicol.* **2005**, *18*, 1296-305.
96. Damianaki, A.; Bakogeorgou, E.; Kampa, M.; Notas, G.; Hatzoglou, A.; Panagiotou, S.; Gemetzi, C.; Kouroumalis, E.; Martin, P. M.; Castanas, E., Potent inhibitory action of red wine polyphenols on human breast cancer cells. *J. Cell. Biochem.* **2000**, *78*, 429-441.
97. Kampa, M.; Hatzoglou, A.; Notas, G.; Damianaki, A.; Bakogeorgou, E.; Gemetzi, C.; Kouroumalis, E.; Martin, P. M.; Castanas, E., Wine antioxidant polyphenols inhibit the proliferation of human prostate cancer cell lines. *Nutr. Cancer* **2000**, *37*, 223-33.
98. Wang, L.; Tu, Y.-C.; Lian, T.-W.; Hung, J.-T.; Yen, J.-H.; Wu, M.-J., Distinctive Antioxidant and Antiinflammatory Effects of Flavonols. *J. Agric. Food Chem.* **2006**, *54*, 9798.
99. Munoz-Espada, A. C.; Watkins, B. A., Cyanidin attenuates PGE2 production and cyclooxygenase-2 expression in LNCaP human prostate cancer cells. *J. Nutr. Biochem.* **2006**, *17*, 589-96.
100. Liang, Y. C.; Huang, Y. T.; Tsai, S. H.; Lin-Shiau, S. Y.; Chen, C. F.; Lin, J. K., Suppression of inducible cyclooxygenase and inducible nitric oxide synthase by apigenin and related flavonoids in mouse macrophages. *Carcinogenesis* **1999**, *20*, 1945-1952.
101. Sloley, B. D.; Urichuk, L. J.; Morley, P.; Durkin, J.; Shan, J. J.; Pang, P. K. T.; Coutts, R. T., Identification of kaempferol as a monoamine oxidase inhibitor and potential neuroprotectant in extracts of Ginkgo biloba leaves. *J. Pharm. Pharmacol.* **2000**, *52*, 451-459.
102. Hämäläinen, M.; Nieminen, R.; Vuorela, P.; Heinonen, M.; Moilanen, E., Anti-Inflammatory Effects of Flavonoids: Genistein, Kaempferol, Quercetin, and Daidzein Inhibit STAT-1 and NF-κB Activations, Whereas Flavone, Isorhamnetin, Naringenin, and Pelargonidin Inhibit only NF-κB Activation along with

Their Inhibitory Effect on iNOS Expression and NO Production in Activated Macrophages. *Mediators Inflamm.* **2007**, 2007, 45673-45683.

103. Lee, K. W.; Kang, N. J.; Heo, Y. S.; Rogozin, E. A.; Pugliese, A.; Hwang, M. K.; Bowden, G. T.; Bode, A. M.; Lee, H. J.; Dong, Z., Raf and MEK protein kinases are direct molecular targets for the chemopreventive effect of quercetin, a major flavonol in red wine. *Cancer Res.* **2008**, 68, 946-55.

104. Chen, J. H.; Ho, C. T., Antioxidant activities of caffeic acid and its related hydroxycinnamic acid compounds. *J. Agric. Food Chem.* **1997**, 45, 2374-2378.

105. Rice-Evans, C. A.; Miller, N. J.; Paganga, G., Structure-antioxidant activity relationships of flavonoids and phenolic acids. *Free Radic. Biol. Med.* **1996**, 20, 933-956.

106. Kasai, H.; Fukada, S.; Yamaizumi, Z.; Sugie, S.; Mori, H., Action of chlorogenic acid in vegetables and fruits as an inhibitor of 8-hydroxydeoxyguanosine formation in vitro and in a rat carcinogenesis model. *Food Chem. Toxicol.* **2000**, 38, 467-471.

107. Miller, N. J.; Rice-Evans, C.; Davies, M. J.; Gopinathan, V.; Milner, A., A novel method for measuring antioxidant capacity and its application to monitoring the antioxidant status in premature neonates. *Clin. Sci.* **1993**, 84, 407-412.

108. Chen, Y. J.; Shiao, M. S.; Wang, S. Y., The antioxidant caffeic acid phenethyl ester induces apoptosis associated with selective scavenging of hydrogen peroxide in human leukemic HL-60 cells. *Anticancer Drugs* **2001**, 12, 143-9.

109. Natarajan, K.; Singh, S.; Burke, T. R.; Grunberger, D.; Aggarwal, B. B., Caffeic acid phenethyl ester is a potent and specific inhibitor of activation of nuclear transcription factor NF-kappa B. *PNAS* **1996**, 93, 9090-9095.

110. Michaluart, P.; Masferrer, J. L.; Carothers, A. M.; Subbaramaiah, K.; Zweifel, B. S.; Koboldt, C.; Mestre, J. R.; Grunberger, D.; Sacks, P. G.; Tanabe, T.; Dannenberg, A. J., Inhibitory Effects of Caffeic Acid Phenethyl Ester on the Activity and Expression of Cyclooxygenase-2 in Human Oral Epithelial Cells and in a Rat Model of Inflammation. *Cancer Res.* **1999**, 59, 2347-2352.

111. Huang, M.-T.; Ma, W.; Yen, P.; Xie, J.-G.; Han, J.; Frenkel, K.; Grunberger, D.; Conney, A. H., Inhibitory effects of caffeic acid phenethyl ester (CAPE) on 12-O-tetradecanoylphorbol-13-acetate-induced tumor promotion in mouse skin and the synthesis of DNA, RNA and protein in HeLa cells. *Carcinogenesis* **1996**, 17, 761-765.

112. Zhang, Y. S.; Talalay, P.; Cho, C. G.; Posner, G. H., A Major Inducer Of Anticarcinogenic Protective Enzymes From Broccoli - Isolation And Elucidation Of Structure. *Proc. Natl. Acad. Sci. U. S. A.* **1992**, 89, 2399-2403.

113. Gamet-Payraastre, L.; Li, P. F.; Lumeau, S.; Cassar, G.; Dupont, M. A.; Chevolleau, S.; Gasc, N.; Tulliez, J.; Terce, F., Sulforaphane, a naturally occurring isothiocyanate, induces cell cycle arrest and apoptosis in HT29 human colon cancer cells. *Cancer Res.* **2000**, 60, 1426-1433.

114. Gao, X.; Dinkova-Kostova, A. T.; Talalay, P., Powerful and prolonged protection of human retinal pigment epithelial cells, keratinocytes, and mouse leukemia cells against oxidative damage: The indirect antioxidant effects of sulforaphane. *Proc. Natl. Acad. Sci. USA* **2001**, 98, 15221-15226.

115. Kang, K. W.; Cho, I. J.; Lee, C. H.; Kim, S. G., Essential Role of Phosphatidylinositol 3-Kinase-Dependent CCAAT/Enhancer Binding Protein β Activation in the Induction of Glutathione S-Transferase by Oltipraz. *J. Natl. Cancer Inst.* **2003**, 95, 53-66.

116. Kensler, T. W.; Qian, G.-S.; Chen, J.-G.; Groopman, J. D., Translational strategies for cancer prevention in liver. *Nat. Rev. Cancer* **2003**, 3, 321-329.

117. Kensler, T. W.; Groopman, J. D.; Sutter, T. R.; Curphey, T. J.; Roebuck, B. D., Development of cancer chemopreventive agents: Oltipraz as a paradigm. *Chem. Res. Toxicol.* **1999**, 12, 113-126.

118. Esatbeyoglu, T.; Huebbe, P.; Ernst, I. M. A.; Chin, D.; Wagner, A. E.; Rimbach, G., Curcumin - From Molecule to Biological Function. *Angew. Chem. Int. Ed.* **2012**, *51*, 5308-5332.
119. Dinkova-Kostova, A. T.; Abeygunawardana, C.; Talalay, P., Chemoprotective properties of phenylpropenoids, bis(benzylidene)cycloalkanones, and related Michael reaction acceptors: Correlation of potencies as phase 2 enzyme inducers and radical scavengers. *J. Med. Chem.* **1998**, *41*, 5287-5296.
120. Ohnishi, K.; Irie, K.; Murakami, A., In Vitro Covalent Binding Proteins of Zerumbone, a Chemopreventive Food Factor. *Biosci., Biotechnol., Biochem.* **2009**, *73*, 1905-1907.
121. Ozaki, Y.; Kawahara, N.; Harada, M., ANTIINFLAMMATORY EFFECT OF ZINGIBER-CASSUMUNAR ROXB AND ITS ACTIVE PRINCIPLES. *Chem. Pharm. Bull.* **1991**, *39*, 2353-2356.
122. Rahman, I., Regulation of nuclear factor- κ B, activator protein-1, and glutathione levels by tumor necrosis factor- α and dexamethasone in alveolar epithelial cells. *Biochem. Pharmacol.* **2000**, *60*, 1041-1049.
123. Cagiralla, H.; Vingtdeux, V.; Zhao, H.; Sankowski, R.; Al-Abed, Y.; Davies, P.; Marambaud, P., Resveratrol mitigates lipopolysaccharide- and $\text{A}\beta$ -mediated microglial inflammation by inhibiting the TLR4/NF- κ B/STAT signaling cascade. *J. Neurochem.* **2012**, *120*, 461-472.
124. Kode, A.; Rajendrasozhan, S.; Caito, S.; Yang, S.-R.; Megson, I. L.; Rahman, I., Resveratrol induces glutathione synthesis by activation of Nrf2 and protects against cigarette smoke-mediated oxidative stress in human lung epithelial cells. *Am. J. Physiol. Lung Cell Mol. Physiol.* **2008**, *294*, L478-88.
125. Chan, M. M. Y.; Ho, C. T.; Huang, H. I., EFFECTS OF 3 DIETARY PHYTOCHEMICALS FROM TEA, ROSEMARY AND TURMERIC ON INFLAMMATION-INDUCED NITRITE PRODUCTION. *Cancer Lett.* **1995**, *96*, 23-29.
126. Singletary, K.; MacDonald, C.; Wallig, M., Inhibition by rosemary and carnosol of 7,12 dimethylbenz alpha anthracene (DMBA)-induced rat mammary tumorigenesis and in vivo DMBA-DNA adduct formation. *Cancer Lett.* **1996**, *104*, 43-48.
127. Dinkova-Kostova, A. T.; Holtzclaw, W. D.; Cole, R. N.; Itoh, K.; Wakabayashi, N.; Katoh, Y.; Yamamoto, M.; Talalay, P., Direct evidence that sulfhydryl groups of Keap1 are the sensors regulating induction of phase 2 enzymes that protect against carcinogens and oxidants *PNAS* **2002**, *99*, 11908-11913.
128. Shin, J. W.; Ohnishi, K.; Murakami, A.; Lee, J. S.; Kundu, J. K.; Na, H. K.; Ohigashi, H.; Surh, Y. J., Zerumbone Induces Heme Oxygenase-1 Expression in Mouse Skin and Cultured Murine Epidermal Cells through Activation of Nrf2. *Cancer Prev. Res.* **2011**, *4*, 860-870.
129. Luo, Y.; Egger, A. L.; Liu, D.; Liu, G.; Mesecar, A. D.; van Breemen, R. B., Sites of alkylation of human Keap1 by natural chemoprevention agents. *J. Am. Soc. Mass Spectrom.* **2007**, *18*, 2226-32.
130. Chen, C.-Y.; Jang, J.-H.; Li, M.-H.; Surh, Y.-J., Resveratrol upregulates heme oxygenase-1 expression via activation of NF-E2-related factor 2 in PC12 cells. *Biochem. Biophys. Res. Commun.* **2005**, *331*, 993-1000.
131. Rushworth, S. A.; Ogborne, R. M.; Charalambos, C. A.; O'Connell, M. A., Role of protein kinase C delta in curcumin-induced antioxidant response element-mediated gene expression in human monocytes. *Biochem. Biophys. Res. Commun.* **2006**, *341*, 1007-1016.
132. Martin, D.; Rojo, A. I.; Salinas, M.; Diaz, R.; Gallardo, G.; Alam, J.; de Galarreta, C. M. R.; Cuadrado, A., Regulation of Heme Oxygenase-1 Expression through the Phosphatidylinositol 3-Kinase/Akt Pathway and the Nrf2 Transcription Factor in Response to the Antioxidant Phytochemical Carnosol. *J. Biol. Chem.* **2004**, *279*, 8919-8929.
133. Krajka-Kuzniak, V.; Paluszczak, J.; Baer-Dubowska, W., Xanthohumol induces phase II enzymes via Nrf2 in human hepatocytes in vitro. *Toxicol. in Vitro* **2013**, *27*, 149-156.

134. Wang, X.; Stavchansky, S.; Kerwin, S. M.; Bowman, P. D., Structure-activity relationships in the cytoprotective effect of caffeic acid phenethyl ester (CAPE) and fluorinated derivatives: Effects on heme oxygenase-1 induction and antioxidant activities. *Eur. J. Pharmacol.* **2010**, *635*, 16-22.
135. Martin, D.; Rojo, A. I.; Salinas, M.; Diaz, R.; Gallardo, G.; Alam, J.; de Galarreta, C. M. R.; Cuadrado, A., Regulation of Heme Oxygenase-1 Expression through the Phosphatidylinositol 3-Kinase/Akt Pathway and the Nrf2 Transcription Factor in Response to the Antioxidant Phytochemical Carnosol. *J. Biol. Chem.* **2004**, *279*, 8919-8929.
136. Hanneken, A.; Lin, F.-F.; Johnson, J.; Maher, P., Flavonoids protect human retinal pigment epithelial cells from oxidative-stress-induced death. *Invest. Ophthalmol. Vis. Sci.* **2006**, *47*, 3164-3177.
137. Farombi, E. O.; Shrotriya, S.; Na, H.-K.; Kim, S.-H.; Surh, Y.-J., Curcumin attenuates dimethylnitrosamine-induced liver injury in rats through Nrf2-mediated induction of heme oxygenase-1. *Food Chem. Toxicol.* **2008**, *46*, 1279-1287.
138. Lin, H.-Y.; Juan, S.-H.; Shen, S.-C.; Hsu, F.-L.; Chen, Y.-C., Inhibition of lipopolysaccharide-induced nitric oxide production by flavonoids in RAW264.7 macrophages involves heme oxygenase-1. *Biochem. Pharmacol.* **2003**, *66*, 1821-1832.
139. Choi, I. S.; Choi, E. Y.; Jin, J. Y.; Park, H. R.; Choi, J. I.; Kim, S. J., Kaempferol Inhibits P. intermedia Lipopolysaccharide-Induced Production of Nitric Oxide Through Translational Regulation in Murine Macrophages: Critical Role of Heme Oxygenase-1-Mediated ROS Reduction. *J. Periodontol.* **2013**, *84*, 545-555.
140. Gao, S.; Choi, B.-M.; Chen, X.; Zhu, R.; Kim, Y.; So, H.; Park, R.; Sung, M.; Kim, B.-R., Kaempferol Suppresses Cisplatin-Induced Apoptosis Via Inductions of Heme Oxygenase-1 and Glutamate-Cysteine Ligase Catalytic Subunit in HEI-OC1 cells. *Pharm. Res.* **2010**, *27*, 235-245.
141. Chen, J.-C.; Ho, F.-M.; Chao, P.-D. L.; Chen, C.-P.; Jeng, K.-C. G.; Hsu, H.-B.; Lee, S.-T.; Wu, W.-T.; Lin, W.-W., Inhibition of iNOS gene expression by quercetin is mediated by the inhibition of I κ B kinase, nuclear factor-kappa B and STAT1, and depends on heme oxygenase-1 induction in mouse BV-2 microglia. *Eur. J. Pharmacol.* **2005**, *521*, 9-20.
142. Yao, P.; Nussler, A.; Liu, L.; Hao, L.; Song, F.; Schirmeier, A.; Nussler, N., Quercetin protects human hepatocytes from ethanol-derived oxidative stress by inducing heme oxygenase-1 via the MAPK/Nrf2 pathways. *J. Hepatol.* **2007**, *47*, 253-261.
143. Juan, S.-H.; Cheng, T.-H.; Lin, H.-C.; Chu, Y.-L.; Lee, W.-S., Mechanism of concentration-dependent induction of heme oxygenase-1 by resveratrol in human aortic smooth muscle cells. *Biochem. Pharmacol.* **2005**, *69*, 41-48.
144. Zhuang, H.; Kim, Y.-S.; Koehler, R. C.; Dore, S., Potential mechanism by which resveratrol, a red wine constituent, protects neurons. *Ann. N. Y. Acad. Sci.* **2003**, *993*, 276.
145. Scapagnini, G.; Butterfield, D. A.; Colombrita, C.; Sultana, R.; Pascale, A.; Calabrese, V., Ethyl Ferulate, a Lipophilic Polyphenol, Induces HO-1 and Protects Rat Neurons Against Oxidative Stress. *Antioxid. Redox Signal.* **2004**, *6*, 811-818.
146. Scapagnini, G.; Butterfield, D. A.; Colombrita, C.; Sultana, R.; Pascale, A.; Calabrese, V., Ethyl ferulate, a lipophilic polyphenol, induces HO-1 and protects rat neurons against oxidative stress. *Antioxid. Redox Sign.* **2004**, *6*, 811-818.
147. Nakamura, Y.; Yoshida, C.; Murakami, A.; Ohigashi, H.; Osawa, T.; Uchida, K., Zerumbone, a tropical ginger sesquiterpene, activates phase II drug metabolizing enzymes. *FEBS Lett.* **2004**, *572*, 245-250.
148. Wu, L. Y.; Juurlink, B. H. J., The impaired glutathione system and its up-regulation by sulforaphane in vascular smooth muscle cells from spontaneously hypertensive rats. *J. Hypertens.* **2001**, *19*, 1819-1825.

149. Keum, Y. S.; Yu, S. W.; Chang, P. P. J.; Yuan, X. L.; Kim, J. H.; Xu, C. J.; Han, J. H.; Agarwal, A.; Kong, A. N. T., Mechanism of action of sulforaphane: Inhibition of p38 mitogen-activated protein kinase isoforms contributing to the induction of antioxidant response element-mediated heme oxygenase-1 in human hepatoma HepG2 cells. *Cancer Res.* **2006**, *66*, 8804-8813.
150. Raju, V. S.; McCoubrey Jr, W. K.; Maines, M. D., Regulation of heme oxygenase-2 by glucocorticoids in neonatal rat brain: characterization of a functional glucocorticoid response element. *Biochim. Biophys. Acta Gene Struct. Expression* **1997**, *1351*, 89-104.
151. Mehindate, K.; Sahlas, D. J.; Frankel, D.; Mawal, Y.; Liberman, A.; Corcos, J.; Dion, S.; Schipper, H. M., Proinflammatory cytokines promote glial heme oxygenase-1 expression and mitochondrial iron deposition: implications for multiple sclerosis. *J. Neurochem.* **2001**, *77*, 1386-1395.
152. Mores, N.; Errico, S.; Pusateri, A.; Barone, E.; Mancuso, C., Heme oxygenase expression and activity in immortalized hypothalamic neurons GT1-7. *Neurosci. Lett.* **2008**, *444*, 106-108.
153. Huang, Y.; Li, J.; Cao, Q.; Yu, S.-C.; Lv, X.-W.; Jin, Y.; Zhang, L.; Zou, Y.-H.; Ge, J.-F., Anti-oxidative effect of triterpene acids of *Eriobotrya japonica* (Thunb.) Lindl. leaf in chronic bronchitis rats. *Life Sci.* **2006**, *78*, 2749-2757.
154. Kweon, M.-H.; Jung, M.-J.; Sung, H.-C., Cytoprotective effects of heme oxygenase-1 induction by 3-O-caffeoyl-1-methylquinic acid. *Free Radic. Biol. Med.* **2004**, *36*, 40-52.
155. Tavares, E. M.; Carvalho, A. M.; Goncalves, L. M.; Valente, I. M.; Moreira, M. M.; Guido, L. F.; Rodrigues, J. A.; Doneux, T.; Barros, A. A., Chemical sensing of chalcones by voltammetry: trans-Chalcone, cardamomin and xanthohumol. *Electrochim. Acta* **2013**, *90*, 440-444.
156. Dinkova-Kostova, A. T.; Talalay, P., Direct and indirect antioxidant properties of inducers of cytoprotective proteins. *Mol. Nutr. Food Res.* **2008**, *52*, S128-S138.
157. Jin, F.; Jin, X. Y.; Jin, Y. L.; Sohn, D. W.; Kim, S. A.; Sohn, D. H.; Kim, Y. C.; Kim, H. S., Structural requirements of 2',4',6'-tris(methoxymethoxy) chalcone derivatives for anti-inflammatory activity: The importance of a 2'-hydroxy moiety. *Arch. Pharm. Res.* **2007**, *30*, 1359-1367.
158. Simmler, C.; Hajirahimkhan, A.; Lankin, D. C.; Bolton, J. L.; Jones, T.; Soejarto, D. D.; Chen, S. N.; Pauli, G. F., Dynamic Residual Complexity of the Isoliquiritigenin-Liquiritigenin Interconversion During Bioassay. *J. Agric. Food Chem.* **2013**, *61*, 2146-2157.
159. Amslinger, S.; Al-Rifai, N.; Winter, K.; Wörmann, K.; Scholz, R.; Baumeister, P.; Wild, M., Reactivity assessment of chalcones by a kinetic thiol assay. *Org. Biomol. Chem.* **2013**, *11*, 549.
160. Batovska, D. I.; Todorova, I. T., Trends in utilization of the pharmacological potential of chalcones. *Current clinical pharmacology* **2010**, *5*, 1-29.
161. Bukhari, S. N. A.; Jantan, I.; Jasamai, M., Anti-Inflammatory Trends of 1, 3-Diphenyl-2-propen-1-one Derivatives. *Mini-Rev. Med. Chem.* **2013**, *13*, 87-94.
162. Alcaraz, M. J.; Vicente, A. M.; Araico, A.; Dominguez, J. N.; Terencio, M. C.; Ferrándiz, M. L., Role of nuclear factor- κ B and heme oxygenase-1 in the mechanism of action of an anti-inflammatory chalcone derivative in RAW 264.7 cells. *Br. J. Pharmacol.* **2004**, *142*, 1191-1199.
163. Pandey, M. K.; Sandur, S. K.; Sung, B.; Sethi, G.; Kunnumakkara, A. B.; Aggarwal, B. B., Butein, a Tetrahydrochalcone, Inhibits Nuclear Factor NF- κ B and NF- κ B-regulated Gene Expression through Direct Inhibition of I κ B α Kinase β on Cysteine 179 Residue. *J. Biol. Chem.* **2007**, *282*, 17340-17350.
164. Lee, S. H.; Seo, G. S.; Sohn, D. H., Inhibition of lipopolysaccharide-induced expression of inducible nitric oxide synthase by butein in RAW 264.7 cells. *Biochem. Biophys. Res. Commun.* **2004**, *323*, 125-132.

165. Yang, Y. C.; Lii, C. K.; Lin, A. H.; Yeh, Y. W.; Yao, H. T.; Li, C. C.; Liu, K. L.; Chen, H. W., Induction of glutathione synthesis and heme oxygenase 1 by the flavonoids butein and phloretin is mediated through the ERK/Nrf2 pathway and protects against oxidative stress. *Free Radic. Biol. Med.* **2011**, *51*, 2073-2081.
166. Lee, D. S.; Li, B.; Kim, K. S.; Jeong, G. S.; Kim, E. C.; Kim, Y. C., Butein protects human dental pulp cells from hydrogen peroxide-induced oxidative toxicity via Nrf2 pathway-dependent heme oxygenase-1 expressions. *Toxicol. in Vitro* **2013**, *27*, 874-881.
167. Cai, Y.-Z.; Mei, S.; Jie, X.; Luo, Q.; Corke, H., Structure–radical scavenging activity relationships of phenolic compounds from traditional Chinese medicinal plants. *Life Sci.* **2006**, *78*, 2872-2888.
168. Liu, Y.-C.; Hsieh, C.-W.; Wu, C.-C.; Wung, B.-S., Chalcone inhibits the activation of NFκB and STAT3 in endothelial cells via endogenous electrophile. *Life Sci.* **2007**, *80*, 1420-1430.
169. Wattenberg, L. W.; Coccia, J. B.; Galbraith, A. R., INHIBITION OF CARCINOGEN-INDUCED PULMONARY AND MAMMARY CARCINOGENESIS BY CHALCONE ADMINISTERED SUBSEQUENT TO CARCINOGEN EXPOSURE. *Cancer Lett.* **1994**, *83*, 165-169.
170. Maggiolini, M.; Statti, G.; Vivacqua, A.; Gabriele, S.; Rago, V.; Loizzo, M.; Menichini, F.; Amdò, S., Estrogenic and antiproliferative activities of isoliquiritigenin in MCF7 breast cancer cells. *J. Steroid Biochem. Mol. Biol.* **2002**, *82*, 315-322.
171. Jang, E. Y.; Choe, E. S.; Hwang, M.; Kim, S. C.; Lee, J. R.; Kim, S. G.; Jeon, J.-P.; Buono, R. J.; Yang, C. H., Isoliquiritigenin suppresses cocaine-induced extracellular dopamine release in rat brain through GABA_B receptor. *Eur. J. Pharmacol.* **2008**, *587*, 124-128.
172. Kim, Y. M.; Kim, T. H.; Kim, Y. W.; Yang, Y. M.; Ryu, D. H.; Hwang, S. J.; Lee, J. R.; Kim, S. C.; Kim, S. G., Inhibition of liver X receptor-α-dependent hepatic steatosis by isoliquiritigenin, a licorice antioxidant flavonoid, as mediated by JNK1 inhibition. *Free Radic. Biol. Med.* **2010**, *49*, 1722-1734.
173. Takahashi, T.; Baba, M.; Nishino, H.; Okuyama, T., Cyclooxygenase-2 plays a suppressive role for induction of apoptosis in isoliquiritigenin-treated mouse colon cancer cells. *Cancer Lett.* **2006**, *231*, 319-325.
174. Chen, G.; Hu, X.; Zhang, W.; Xu, N.; Wang, F.-Q.; Jia, J.; Zhang, W.-F.; Sun, Z.-J.; Zhao, Y.-F., Mammalian target of rapamycin regulates isoliquiritigenin-induced autophagic and apoptotic cell death in adenoid cystic carcinoma cells. *Apoptosis* **2012**, *17*, 90-101.
175. Hsu, Y.-L.; Chia, C.-C.; Chen, P.-J.; Huang, S.-E.; Huang, S.-C.; Kuo, P.-L., Shallot and licorice constituent isoliquiritigenin arrests cell cycle progression and induces apoptosis through the induction of ATM/p53 and initiation of the mitochondrial system in human cervical carcinoma HeLa cells. *Mol. Nutr. Food Res.* **2009**, *53*, 826-835.
176. Kim, J.-Y.; Park, S. J.; Yun, K.-J.; Cho, Y.-W.; Park, H.-J.; Lee, K.-T., Isoliquiritigenin isolated from the roots of *Glycyrrhiza uralensis* inhibits LPS-induced iNOS and COX-2 expression via the attenuation of NF-κB in RAW 264.7 macrophages. *Eur. J. Pharmacol.* **2008**, *584*, 175-184.
177. Feldman, M.; Santos, J.; Grenier, D., Comparative Evaluation of Two Structurally Related Flavonoids, Isoliquiritigenin and Liquiritigenin, for Their Oral Infection Therapeutic Potential. *J. Nat. Prod.* **2011**, *74*, 1862-1867.
178. Lee, S.; Kim, J.; Seo, G.; Kim, Y. C.; Sohn, D., Isoliquiritigenin, from *Dalbergia odorifera*, up-regulates anti-inflammatory heme oxygenase-1 expression in RAW264.7 macrophages. *Inflamm. Res.* **2009**, *58*, 257-262.
179. Lee, T.-S.; Tsai, H.-L.; Chau, L.-Y., Induction of Heme Oxygenase-1 Expression in Murine Macrophages Is Essential for the Anti-inflammatory Effect of Low Dose 15-Deoxy-Δ^{12,14}-prostaglandin J₂. *J. Biol. Chem.* **2003**, *278*, 19325-19330.

180. Cuendet, M.; Oteham, C. P.; Moon, R. C.; Pezzuto, J. M., Quinone reductase induction as a biomarker for cancer chemoprevention. *J. Nat. Prod.* **2006**, *69*, 460-463.
181. Zhan, C.; Yang, J., Protective effects of isoliquiritigenin in transient middle cerebral artery occlusion-induced focal cerebral ischemia in rats. *Pharmacol. Res.* **2006**, *53*, 303-309.
182. Beutler, J. A.; Cardellina, J. H.; Gray, G. N.; Prather, T. R.; Shoemaker, R. H.; Boyd, M. R.; Lin, C. M.; Hamel, E.; Cragg, G. M., Two New Cytotoxic Chalcones from *Calythropsis aurea*. *J. Nat. Prod.* **1993**, *56*, 1718-1722.
183. Ross, S. A.; Zagloul, A.; Nimrod, A. C.; Mehmedic, Z.; ElSohly, H. N., A cytotoxic chalcone from *Faramea salicifolia*. *Planta Med.* **1999**, *65*, 194-194.
184. L. de Almeida, M. E.; Filho, R. B.; von Bülow, M. V.; Corrêa, J. J. L.; Gottlieb, O. R.; S. Maia, J. G.; da Silva, M. S., Diarylpropanoids from *Iryanthera polyneura*. *Phytochemistry* **1979**, *18*, 1015-1016.
185. Rao, Y. K.; Fang, S.-H.; Tzeng, Y.-M., Differential effects of synthesized 2'-oxygenated chalcone derivatives: modulation of human cell cycle phase distribution. *Bioorganic & Medicinal Chemistry* **2004**, *12*, 2679-2686.
186. Honda, T.; Gribble, G. W.; Suh, N.; Finlay, H. J.; Rounds, B. V.; Bore, L.; Favalaro, F. G.; Wang, Y.; Sporn, M. B., Novel Synthetic Oleanane and Ursane Triterpenoids with Various Enone Functionalities in Ring A as Inhibitors of Nitric Oxide Production in Mouse Macrophages. *J. Med. Chem.* **2000**, *43*, 1866-1877.
187. Honda, T.; Honda, Y.; Favalaro, F. G.; Gribble, G. W.; Suh, N.; Place, A. E.; Rendi, M. H.; Sporn, M. B., A novel dicyanotriterpenoid, 2-cyano-3,12-dioxooleana-1,9(11)-dien-28-onitrile, active at picomolar concentrations for inhibition of nitric oxide production. *Bioorg. Med. Chem. Lett.* **2002**, *12*, 1027-1030.
188. Lawrence, N. J.; Patterson, R. P.; Ooi, L.-L.; Cook, D.; Ducki, S., Effects of α -substitutions on structure and biological activity of anticancer chalcones. *Bioorg. Med. Chem. Lett.* **2006**, *16*, 5844-5848.
189. Edwards, M. L.; Stemerick, D. M.; Sunkara, P. S., Chalcones: a new class of antimitotic agents. *J. Med. Chem.* **1990**, *33*, 1948-1954.
190. Kerr, D. J.; Hamel, E.; Jung, M. K.; Flynn, B. L., The concise synthesis of chalcone, indanone and indenone analogues of combretastatin A4. *Biorg. Med. Chem.* **2007**, *15*, 3290-3298.
191. Ducki, S.; Mackenzie, G.; Greedy, B.; Armitage, S.; Chabert, J. F. D.; Bennett, E.; Nettles, J.; Snyder, J. P.; Lawrence, N. J., Combretastatin-like chalcones as inhibitors of microtubule polymerisation. Part 2: Structure-based discovery of alpha-aryl chalcones. *Biorg. Med. Chem.* **2009**, *17*, 7711-7722.
192. Ducki, S.; Forrest, R.; Hadfield, J. A.; Kendall, A.; Lawrence, N. J.; McGown, A. T.; Rennison, D., Potent antimitotic and cell growth inhibitory properties of substituted chalcones. *Bioorg. Med. Chem. Lett.* **1998**, *8*, 1051-1056.
193. Ducki, S.; Rennison, D.; Woo, M.; Kendall, A.; Chabert, J. F. D.; McGown, A. T.; Lawrence, N. J., Combretastatin-like chalcones as inhibitors of microtubule polymerization. Part 1: Synthesis and biological evaluation of antivasular activity. *Biorg. Med. Chem.* **2009**, *17*, 7698-7710.
194. Wang, S.-J.; Yan, J.-F.; Hao, D.; Niu, X.-W.; Cheng, M.-S., Synthesis and Activity of a New Series of (Z)-3-Phenyl-2-benzoylpropenoic Acid Derivatives as Aldose Reductase Inhibitors. *Molecules* **2007**, *12*, 885-895.
195. Al-Rifai, N.; Rücker, H.; Amslinger, S., Opening or Closing the Lock? When Reactivity Is the Key to Biological Activity. *Chem. Eur. J.* **2013**, *19*, 15384-15395.
196. Jang, D. S.; Su, B. N.; Pawlus, A. D.; Jones, W. P.; Kleps, R. A.; Bunyapraphatsara, N.; Fong, H. H. S.; Pezzuto, J. M.; Kinghorn, A. D., Limnophilaspiroketone, a highly oxygenated phenolic derivative from *Limnophila geoffrayi*. *J. Nat. Prod.* **2005**, *68*, 1134-1136.

197. Smith, A. B.; Levenberg, P. A.; Jerris, P. J.; Scarborough, R. M.; Wovkulich, P. M., Synthesis and reactions of simple 3(2H)-furanones. *J. Am. Chem. Soc.* **1981**, *103*, 1501-1513.
198. Amslinger, S.; Lindner, S. K., Limno-CP: A Natural-Product-Inspired 5-Aryl-3(2H)-furanone as Scaffold for a Library of α -Modified Enones. *Synthesis* **2011**, 2671-2683.
199. Lindner, S. Dissertation, University of Regensburg, 2011.
200. Huang, Z.-S.; Pei, Y.-H.; Liu, C.-M.; Lin, S.; Tang, J.; Huang, D.-S.; Song, T.-F.; Lu, L.-H.; Gao, Y.-P.; Zhang, W.-D., Highly Oxygenated Guaianolides from *Artemisia dubia*. *Planta Med.* **2010**, *76*, 1710-1716.
201. Jakupovic, J.; Tan, R. X.; Bohlmann, F.; Boldt, P. E.; Jia, Z. J., Sesquiterpene lactones from *Artemisia ludoviciana*. *Phytochemistry* **1991**, *30*, 1573-1577.
202. Hegazy, M. E. F.; Abdel-Lateff, A.; Gamal-Eldeen, A. M.; Turkey, F.; Hirata, T.; Pare, P. W.; Karchesy, J.; Kamel, M. S.; Ahmed, A. A., Anti-inflammatory activity of new guaiane acid derivatives from *Achillea coarctata*. *Nat. Prod. Commun.* **2008**, *3*, 851-856.
203. Schmidt, T. J.; Lyß, G.; Pahl, H. L.; Merfort, I., Helenanolide type sesquiterpene lactones. Part 5: The role of glutathione addition under physiological conditions. *Biorg. Med. Chem.* **1999**, *7*, 2849-2855.
204. Kreuzer, A. Dissertation, University of Regensburg, 2014.
205. Kreuzer, A.; Kerres, S.; Ertl, T.; Rücker, H.; Amslinger, S.; Reiser, O., Asymmetric Synthesis of Both Enantiomers of Arteludovicinolide A. *Org. Lett.* **2013**, *15*, 3420-3423.
206. Motterlini, R.; Otterbein, L. E., The therapeutic potential of carbon monoxide. *Nat. Rev. Drug Discov.* **2010**, *9*, 728-743.
207. Kim, H. S.; Loughran, P. A.; Billiar, T. R., Carbon monoxide decreases the level of iNOS protein and active dimer in IL-1 β -stimulated hepatocytes. *Nitric Oxide* **2008**, *18*, 256-265.
208. Watts, R. N.; Ponka, P.; Richardson, D. R., Effects of nitrogen monoxide and carbon monoxide on molecular and cellular iron metabolism: mirror-image effector molecules that target iron. *Biochem. J.* **2003**, *369*, 429-440.
209. Johnson, T. R.; Mann, B. E.; Clark, J. E.; Foresti, R.; Green, C. J.; Motterlini, R., Metal Carbonyls: A New Class of Pharmaceuticals? *Angew. Chem. Int. Ed.* **2003**, *42*, 3722-3729.
210. Clark, J. E.; Naughton, P.; Shurey, S.; Green, C. J.; Johnson, T. R.; Mann, B. E.; Foresti, R.; Motterlini, R., Cardioprotective actions by a water-soluble carbon monoxide-releasing molecule. *Circ. Res.* **2003**, *93*, E2-E8.
211. Romanski, S.; Kraus, B.; Schatzschneider, U.; Neudörfl, J.-M.; Amslinger, S.; Schmalz, H.-G., Acyloxybutadiene Iron Tricarbonyl Complexes as Enzyme-Triggered CO-Releasing Molecules (ET-CORMs). *Angew. Chem. Int. Ed.* **2011**, *50*, 2392-2396.
212. Romanski, S.; Kraus, B.; Guttentag, M.; Schlundt, W.; Rücker, H.; Adler, A.; Neudörfl, J.-M.; Alberto, R.; Amslinger, S.; Schmalz, H.-G., Acyloxybutadiene tricarbonyl iron complexes as enzyme-triggered CO-releasing molecules (ET-CORMs): a structure-activity relationship study. *Dalton Trans.* **2012**, *41*, 13862-13875.
213. Romanski, S.; Rücker, H.; Stamellou, E.; Guttentag, M.; Neudörfl, J.-M.; Alberto, R.; Amslinger, S.; Yard, B.; Schmalz, H.-G., Iron Dienylphosphate Tricarbonyl Complexes as Water-Soluble Enzyme-Triggered CO-Releasing Molecules (ET-CORMs). *Organometallics* **2012**, *31*, 5800-5809.
214. Weiss, G.; Werner-Felmayer, G.; Werner, E. R.; Grünewald, K.; Wachter, H.; Hentze, M. W., Iron regulates nitric oxide synthase activity by controlling nuclear transcription. *J. Exp. Med.* **1994**, *180*, 969-976.

215. Bhalla, P.; Singh, N. P.; Ravi, K., Attenuation of angiotensin converting enzyme inhibitor induced cough by iron supplementation: role of nitric oxide. *J. Renin-Angiotensin-Aldosterone Syst.* **2011**, *12*, 491-497.
216. Raschke, W. C.; Baird, S.; Ralph, P.; Nakoinz, I., Functional macrophage cell lines transformed by abelson leukemia-virus. *Cell* **1978**, *15*, 261-267.
217. Fogh, J.; Fogh, J. M.; Orfeo, T., One Hundred and Twenty-Seven Cultured Human Tumor Cell Lines Producing Tumors in Nude Mice. *J. Natl. Cancer Inst.* **1977**, *59*, 221-226.
218. Mosmann, T., Rapid colorimetric assay for cellular growth and survival: Application to proliferation and cytotoxicity assays. *J. Immunol. Methods* **1983**, *65*, 55-63.
219. Lowry, O. H.; Rosebrough, N. J.; Farr, A. L.; Randall, R. J., Protein measurement with the folin phenol reagent. *J. Biol. Chem.* **1951**, *193*, 265-275.
220. Dudley, R. A.; Edwards, P.; Ekins, R. P.; Finney, D. J.; McKenzie, I. G.; Raab, G. M.; Rodbard, D.; Rodgers, R. P., Guidelines for immunoassay data processing. *Clin. Chem.* **1985**, *31*, 1264-71.
221. Bradford, M. M., A rapid and sensitive method for the quantitation of microgram quantities of protein utilizing the principle of protein-dye binding. *Anal. Biochem.* **1976**, *72*, 248-254.
222. Gottfried, E.; Kunz-Schughart, L. A.; Ebner, S.; Mueller-Klieser, W.; Hoves, S.; Andreesen, R.; Mackensen, A.; Kreutz, M., Tumor-derived lactic acid modulates dendritic cell activation and antigen expression. *Blood* **2006**, *107*, 2013-21.
223. Maines, M. D.; Plevoda, B. V.; Huang, T.-J.; McCoubrey, W. K., Human Biliverdin IX α Reductase is a Zinc-Metalloprotein. *Eur. J. Biochem.* **1996**, *235*, 372-381.
224. Drummond, G. S.; Kappas, A., Prevention of neonatal hyperbilirubinemia by tin protoporphyrin IX, a potent competitive inhibitor of heme oxidation. *Proc Natl Acad Sci U S A* **1981** *78*, 6466-6470.
225. Wijayanti, N.; Huber, S.; Samoylenko, A.; Kietzmann, T.; Immenschuh, S., Role of NF-kappa B and p38 MAP kinase signaling pathways in the lipopolysaccharide-dependent activation of heme oxygenase-1 gene expression. *Antioxid. Redox Sign.* **2004**, *6*, 802-810.
226. Noda, T.; Amano, F., Differences in Nitric Oxide Synthase Activity in a Macrophage-Like Cell Line, RAW264.7 Cells, Treated with Lipopolysaccharide (LPS) in the Presence or Absence of Interferon- γ (IFN- γ): Possible Heterogeneity of iNOS Activity. *J. Biochem. (Tokyo)*. **1997**, *121*, 38-46.
227. Banchereau, J.; Briere, F.; Caux, C.; Davoust, J.; Lebecque, S.; Liu, Y.-J.; Pulendran, B.; Palucka, K., Immunobiology of Dendritic Cells. *Annu. Rev. Immunol.* **2000**, *18*, 767-811.
228. Berger, T. G.; Schultz, E. S., Dendritic cell-based immunotherapy. *Curr. Top. Microbiol. Immunol.* **2003**, *276*, 163-97.
229. Gottfried, E.; Kreutz, M.; Mackensen, A., Tumor-induced modulation of dendritic cell function. *Cytokine Growth Factor Rev.* **2008**, *19*, 65-77.
230. Chauveau, C.; Rémy, S.; Royer, P. J.; Hill, M.; Tanguy-Royer, S.; Hubert, F.-X.; Tesson, L.; Brion, R.; Beriou, G.; Gregoire, M.; Josien, R.; Cuturi, M. C.; Anegón, I., Heme oxygenase-1 expression inhibits dendritic cell maturation and proinflammatory function but conserves IL-10 expression. *Blood* **2005**, *106*, 1694-1702.
231. Migdal, C.; Botton, J.; El Ali, Z.; Azoury, M.-E.; Guldemann, J.; Giménez-Arnau, E.; Lepoittevin, J.-P.; Kerdine-Römer, S.; Pallardy, M., Reactivity of Chemical Sensitizers Toward Amino Acids In Cellulo Plays a Role in the Activation of the Nrf2-ARE Pathway in Human Monocyte Dendritic Cells and the THP-1 Cell Line. *Toxicol. Sci.* **2013**, *133*, 259-274.

232. Lin, H. Y.; Juan, S. H.; Shen, S. C.; Hsu, F. L.; Chen, Y. C., Inhibition of lipopolysaccharide-induced nitric oxide production by flavonoids in RAW264.7 macrophages involves heme oxygenase-1. *Biochem. Pharmacol.* **2003**, *66*, 1821-1832.
233. Boesch-Saadatmandi, C.; Loboda, A.; Wagner, A. E.; Stachurska, A.; Jozkowicz, A.; Dulak, J.; Doring, F.; Wolfram, S.; Rimbach, G., Effect of quercetin and its metabolites isorhamnetin and quercetin-3-glucuronide on inflammatory gene expression: role of miR-155. *J. Nutr. Biochem.* **2011**, *22*, 293-299.
234. Primiano, T.; Kensler, T. W.; Kuppusamy, P.; Zweier, J. L.; Sutter, T. R., Induction of hepatic heme oxygenase-1 and ferritin in rats by cancer chemopreventive dithiolethiones. *Carcinogenesis* **1996**, *17*, 2291-2296.
235. Holland, R.; Navamal, M.; Velayutham, M.; Zweier, J. L.; Kensler, T. W.; Fishbein, J. C., Hydrogen Peroxide Is a Second Messenger in Phase 2 Enzyme Induction by Cancer Chemopreventive Dithiolethiones. *Chem. Res. Toxicol.* **2009**, *22*, 1427-1434.
236. Palsson-McDermott, E. M.; O'Neill, L. A. J., Signal transduction by the lipopolysaccharide receptor, Toll-like receptor-4. *Immunology* **2004**, *113*, 153-162.
237. Ulevitch, R. J.; Tobias, P. S., RECEPTOR-DEPENDENT MECHANISMS OF CELL STIMULATION BY BACTERIAL-ENDOTOXIN. *Annu. Rev. Immunol.* **1995**, *13*, 437-457.
238. Nishida, J.; Kawabata, J., DPPH Radical Scavenging Reaction of Hydroxy- and Methoxychalcones. *Biosci. Biotechnol. Biochem.* **2006**, *70*, 193-202.
239. Srinivasan, B.; Johnson, T. E.; Lad, R.; Xing, C., Structure–Activity Relationship Studies of Chalcone Leading to 3-Hydroxy-4,3',4',5'-tetramethoxychalcone and Its Analogues as Potent Nuclear Factor κ B Inhibitors and Their Anticancer Activities. *J. Med. Chem.* **2009**, *52*, 7228-7235.
240. Suzuki, M.; Mori, M.; Niwa, T.; Hirata, R.; Furuta, K.; Ishikawa, T.; Noyori, R., Chemical implications for antitumor and antiviral prostaglandins: Reaction of Delta(7)-prostaglandin A(1) and prostaglandin A(1) methyl esters with thiols. *J. Am. Chem. Soc.* **1997**, *119*, 2376-2385.
241. Schmidt, T. J., Helenanolide-type sesquiterpene lactones .3. Rates and stereochemistry in the reaction of helenalin and related helenanolides with sulfhydryl containing biomolecules. *Biorg. Med. Chem.* **1997**, *5*, 645-653.
242. Winter, K. Zulassungsarbeit, University of Regensburg, 2012.
243. Ali, M. T. M. Dissertation, University of Regensburg, 2011.
244. Li, W. D.; Wu, Y.; Zhang, L.; Yan, L. G.; Yin, F. Z.; Ruan, J. S.; Chen, Z. P.; Yang, G. M.; Yan, C. P.; Zhao, D.; Lu, Y.; Cai, B. C., Characterization of xanthatin: Anticancer properties and mechanisms of inhibited murine melanoma in vitro and in vivo. *Phytomedicine* **2013**, *20*, 865-873.
245. Nibret, E.; Youns, M.; Krauth-Siegel, R. L.; Wink, M., Biological Activities of Xanthatin from *Xanthium strumarium* Leaves. *Phytother. Res.* **2011**, *25*, 1883-1890.
246. Yoon, J. H.; Lim, H. J.; Lee, H. J.; Kim, H. D.; Jeon, R.; Ryu, J. H., Inhibition of lipopolysaccharide-induced inducible nitric oxide synthase and cyclooxygenase-2 expression by xanthanolides isolated from *Xanthium strumarium*. *Biorg. Med. Chem. Lett.* **2008**, *18*, 2179-2182.
247. Dirsch, V. M.; Stuppner, H.; Ellmerer-Müller, E. P.; Vollmar, A. M., Structural requirements of sesquiterpene lactones to inhibit LPS-induced nitric oxide synthesis in RAW 264.7 macrophages. *Biorg. Med. Chem.* **2000**, *8*, 2747-2753.
248. Roche, S. P.; Aitken, D. J., Chemistry of 4-Hydroxy-2-cyclopentenone Derivatives. *Eur. J. Org. Chem.* **2010**, *2010*, 5339-5358.

249. Hall, I. H.; Lee, K.-H.; Mar, E. C.; Starnes, C. O.; Waddell, T. G., Antitumor agents. 21. A proposed mechanism for inhibition of cancer growth by tenulin and helenalin and related cyclopentenones. *J. Med. Chem.* **1977**, *20*, 333-337.
250. Ulbrich, K.; Kreitmeier, P.; Vilaivan, T.; Reiser, O., Enantioselective Synthesis of 4-Heterosubstituted Cyclopentenones. *J. Org. Chem.* **2013**, *78*, 4202-4206.

Acknowledgements

Ganz herzlich möchte ich mich bei **PD Dr. Sabine Amslinger** für die Möglichkeit, an diesem interessanten Thema zu arbeiten, sowie Ihre wohlwollende Unterstützung während der Durchführung dieser Arbeit bedanken.

Zunächst bedanke ich mich bei allen Beteiligten, die in zahlreichen Kollaborationen einen Großteil der in dieser Arbeit getesteten Verbindungen bereitgestellt haben und dadurch zu einer vielfältigen Arbeit beigetragen haben, **Nafisah Al-Rifai, Sabine Amslinger, Paul Baumeister, Simon Lindner, Andreas Kreuzer, Kathrin Ulbrich, Sabrina Fürst, Andreas Bergmann, Peter Kreitmeier, Michael Schwarz, Mihai Surducan** und **Steffen Romanski**.

Bei meinen ehemaligen und jetzigen Arbeitskollegen, **Simon Lindner, Paul Baumeister, Petr Jirasek, Anas Rasras, Nafisah Al-Rifai, Janina Gonschor, Sonay Kasikci** und **Monika Enzinger** möchte ich mich für eine sehr angenehme Arbeitsatmosphäre bedanken, sowie für die moralische Unterstützung und den zahlreichen Ratschlägen während der Doktorarbeit. Ganz besonders danke ich **Dita Fritsch** für ihre Unterstützung im Laboralltag und für eine sehr gute Zusammenarbeit.

Auch bei den Kollegen in den Arbeitsgruppen von **Prof. Dr. Oliver Reiser** und von **Prof. Dr. Burkhard König** möchte ich mich für eine gute Zusammenarbeit und eine tolle Zeit auch außerhalb des Labors bedanken.

Ebenso möchte ich mich ganz herzlich bei **Prof. Dr. Jörg Heilmann** bedanken für die Möglichkeit an seinem Lehrstuhl die zellbiologischen Arbeiten durchzuführen. Ich danke auch allen Mitarbeiter des Lehrstuhls für die sehr gute Zusammenarbeit, ihre freundliche Unterstützung und Beratung. Ganz herzlich möchte ich mich bei **Dr. Birgit Kraus** und **Gabi Brunner** bedanken, die immer ein offenes Ohr für mich hatten.

Besonders danken möchte ich meinen **Freunden** und meiner **Familie**. Ich danke euch für eure Unterstützung, Motivation und vielen hilfreichen Ratschlägen und für die tollen Momente während dieser Zeit, die unvergesslich bleiben.